ASERC
4. ULUSLARARASI SAĞLIK, MÜHENDİSLİK, MİMARLIK ve MATEMATİK KONGRESİ

23 - 29 Temmuz 2026
St. Petersburg

YÜZYÜZE ve ONLINE

Son başvuru : 19 Temmuz
Kitap yayın tarihi : 28 Ağustos

aserc.org

ASERC 4th INTERNATIONAL CONGRESS ON HEALTH, ENGINEERING, ARCHITECTURE and MATHEMATICS

JULY 23 – 29, 2026
ST. PETERSBURG

Edited By
ASSOS. PROF. DR. NURKAN YILMAZ

Issued: 20.08.2026
ISBN: 978-625-8795-33-2

ASSOCIATION & ACADEMIC INCENTIVES :
In the conference 22 papers have been presented by Turkish participants and 31 papers by international participants.
Members of the organizing committees of the conference perform their duties with an "official assignment letter"

Web: www.aserckongresi.org Contact: aserckongresi@gmail.com

CONFERENCE ID

ASERC 4TH INTERNATIONAL CONGRESS ON HEALTH, ENGINEERING, ARCHITECTURE AND MATHEMATICS

DATE – PLACE
JULY 23 – 29, 2026
ST. PETERSBURG

ORGANIIZATION
ACADEMY GLOBAL CONFERENCES & JOURNALS

EVALUATION PROCESS
All applications have undergone a double-blind peer review process.

PARTICIPATING COUNTRIES
Turkey – Kazakhstan – Malaysia- Italy- Nigeria – Iran - China- Kenya- Ghana- South Korea- Kyrgyzstan- Indonesia- Egypt -

PRESENTATION
Oral presentation

CONGRESS ORGANIZING BOARD

Scientific & Review Committee

Prof. Dr. Hülya Çiçek – Turkiye

Prof. Dr. Emine Koca – Turkiye

Prof. Dr. Fatma Koç – Turkiye

Prof. Dr. Valide Paşayeva - Türkiye

Prof. Dr. Ali Bilgili - Turkiye

Prof. Dr. Naile Bilgili - Turkiye

Prof. Dr. Başak Hanedan – Turkiye

Prof. Dr. Aysel Güven - Turkiye

Prof Dr. Bülent Kurtişoğlu – Turkiye

Prof. Dr. Hajar Huseynova – Azerbaijan

Prof. Dr. Dwi Sulisworo – Indonesia

Prof. Dr. Natalia Latygina – Ukraina

Prof. Dr. Yunir Abdrahimov – Russia

Prof. Muntazir Mehdi – Pakistan

Prof. Dr. T.Venkat Narayana Rao – India

Prof. Dr. İzzet Gümüş – Turkiye

Prof. Dr. Mustafa Bayram – Turkiye

Prof. Dr. Saim Zeki Bostan – Turkiye

Prof. Dr. Hyeonjin Lee – China

Prof. Yakup Babayev - Azerbaijan

Prof. Dr. Suyatno – Indonesia

Prof. Dr. Zain Musa – Cambodia

Prof. Dr. Sameer Jain – India

Prof. Mehdi Mohammadzade – Iran

Prof. Dr. Ika Maryani – Indonesia

Prof. Dr. Guler Yenice – Turkiye

Prof. Dr. Elif Akpınar Külekçi – Turkiye

Prof. Dr. Mavlonova Ugiloy Khamdamovna – Uzbekistan

	Number of paper	*%*
Papers by Turkish Participants	22	41,50
Papers by International Participants (12 Countries)	31	58,50

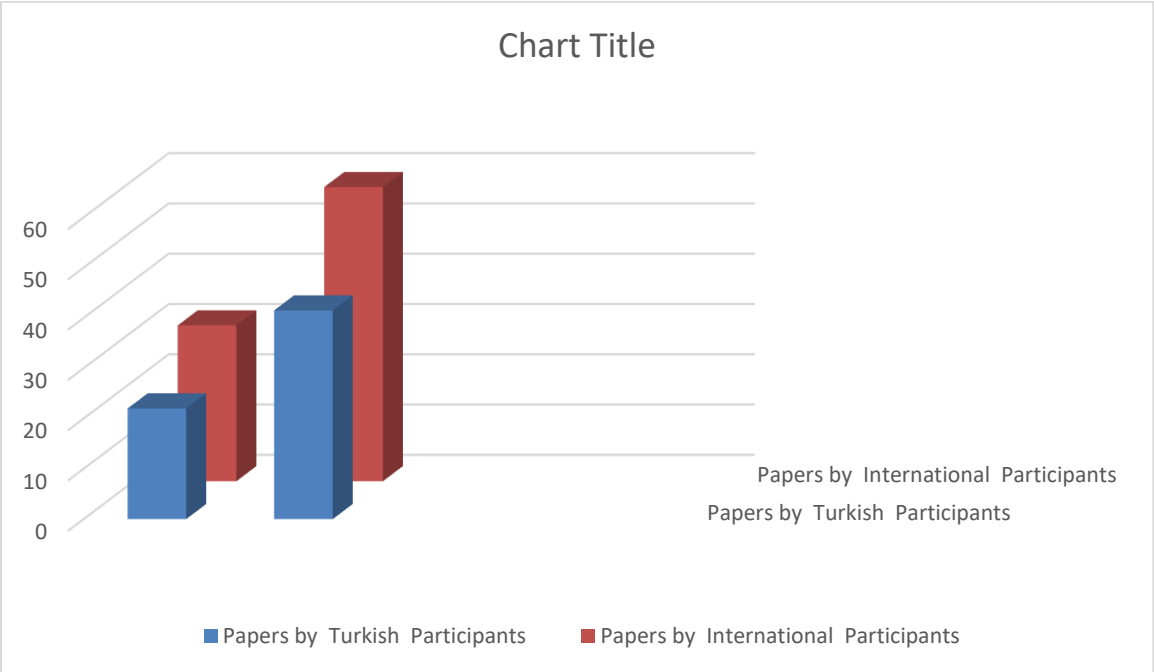

ASERC 4TH INTERNATIONAL CONGRESS ON HEALTH, ENGINEERING, ARCHITECTURE AND MATHEMATICS
JULY 23 – 29, 2026
ST. PETERSBURG

NO : **AC- 4A - 2026. 350M– 3857**
Konu : Akademik Teşvik Uygunluk Belgesi 20/08/2026

İLGİLİ MAKAMA

Academy Global Conferences tarafından düzenlenen **ASERC 4TH INTERNATIONAL CONGRESS ON HEALTH, ENGINEERING, ARCHITECTURE AND MATHEMATICS** kongresi 23-29 Temmuz 2026 tarihlerinde ST. PETERSBURG 'da 12 farklı ülkeden akademisyenin katılımıyla gerçekleştirilmiştir. Kongre kapsamında sunulan 53 bildirinin 22'si Türkiye'den, 31'i ise farklı 11 ülkeden katılan akademisyenler tarafından sunulmuştur. Kongre, 16 Ocak 2020 Akademik Teşvik Ödeneği Yönetmeliğine getirilen "Tebliğlerin sunulduğu yurt içinde veya yurt dışındaki etkinliğin uluslararası olarak nitelendirilebilmesi için Türkiye dışında en az beş farklı ülkeden sözlü tebliğ sunan konuşmacının katılım sağlaması ve tebliğlerin yarıdan fazlasının Türkiye dışından katılımcılar tarafından sunulması esastır." değişikliğine uygun olarak düzenlenmiştir.

Bilgilerinize arz ederiz

Saygılarımızla

Doç. Dr. Nurkan Yılmaz

Evrak Tarih ve Sayısı: 23/06/2025-606980

T.C.
İNÖNÜ ÜNİVERSİTESİ REKTÖRLÜĞÜ
Spor Bilimleri Fakültesi Dekanlığı

Sayı : E-21619327-900-606980 23/06/2025
Konu : Kurum İzin Talebi

Sayın Doç.Dr. Nurkan YILMAZ
Beden Eğitimi ve Spor Öğretmenliği Bölüm Başkanlığı - Öğretim Üyesi

"Academy Global Conferences & Publishing (https://www.akademikongre.org/registration)" tarafından önümüzdeki tarihlerde düzenlenecek olan uluslararası kongrelerde; kongre başkanı, kongre düzenleme ve bilim kurulu üyesi olarak görev alabilmenize yönelik talebiniz Dekanlığımızca uygun bulunmuştur.

Gereğini bilgilerinize rica ederim.

Prof.Dr. Cemal GÜNDOĞDU
Dekan

Ek:Dilekçe

Adres:Spor Bilimleri Fakültesi/Malatya
Telefon:04223774940 Faks:0 422 341 00 32
e-Posta:spor.bilimleri@inonu.edu.tr Web:http://www.inonu.edu.tr/sporbilimleri
Kep Adresi:inonuuniversitesi@hs03.kep.tr

Bilgi için: Güler CANPOLAT
Unvanı: Bilgisayar İşletmeni
Tel No: 04223774974

ISBN NR. : 978-625-8795-33-2

Contents

ISBN NR. : 978-625-8795-33-2

ISBN NR. : 978-625-8795-33-2

KARANLIK FERMANTASYONLA BİYOHİDROJEN ÜRETİMİNDE ANAEROBİK AŞI ÇAMURUNUN ISIL ÖN İŞLEMİNİN OPTİMİZASYONU

Candan UÇARKUŞ

T.C EGE ÜNİVERSİTESİ

Fen Bilimleri Enstitüsü, Biyoteknoloji Ana Bilim Dalı

ucarkuscandan@gmail.com - 0009-0003-1216-3667

Prof. Dr. Nuri AZBAR

T.C EGE ÜNİVERSİTESİ

Mühendislik Fakültesi, Biyomühendislik Bölümü

nuri.azbar@gmail.com - 0000-0003-4463-0197

ÖZET

Aşı çamuruna uygulanan ön işlemin optimize edilmesi, hidrojen tüketen metanojenik mikroorganizmaların baskılanması ve hidrojen üreten bakterilerin metabolik aktivitelerinin korunması açısından karanlık fermantasyonla biyohidrojen üretiminde kritik bir öneme sahiptir. Bu çalışmada, modifiye Yukarı Akışlı Anaerobik Çamur Yataklı (UASB) reaktörün işletimine başlamadan önce anaerobik aşı çamuruna uygulanacak en uygun ısıl ön işlem koşulları belirlenmiştir. Bu kapsamda aşı çamuruna 80, 90 ve 110°C sıcaklıklarda 20 dakika süreyle ısıl ön işlem uygulanmış ve farklı sıcaklıkların etkileri Biyokimyasal Hidrojen Potansiyeli (BHP) testleri ile değerlendirilmiştir. En uygun ön işlem koşulunun belirlenmesi amacıyla toplam gaz üretimi, net gaz üretimi ve gaz kompozisyonları karşılaştırılmıştır. Elde edilen sonuçlar, 90°C'de 20 dakika uygulanan ön işlemin 362,7 mL net gaz üretimi ile en yüksek biyohidrojen üretim performansını sağladığını göstermiştir. Bu koşulun metanojenik mikroorganizmaları etkin şekilde inhibe ederken hidrojen üreten bakterilerin metabolik aktivitelerini koruduğu belirlenmiştir. Buna karşın 80°C'de uygulanan ön işlemin metanojenleri tamamen baskılamak için yetersiz kaldığı, 110°C'de uygulanan ön işlemin ise mikrobiyal canlılığı olumsuz etkileyerek hidrojen üretimini azalttığı görülmüştür. Optimum olarak belirlenen ön işlem koşulu daha sonra Fe_3O_4 manyetit nanopartiküllerinin biyohidrojen üretimine etkisinin araştırıldığı sürekli çalışan UASB reaktör deneylerinde uygulanmıştır. Elde edilen bulgular, ısıl ön işlemin uygun şekilde optimize edilmesinin aşı çamurunun performansını önemli ölçüde artırdığını ve karanlık fermantasyonla biyohidrojen üretiminde güvenilir ve tekrarlanabilir bir işletme altyapısı sağladığını göstermektedir. Sonuç olarak, aşı çamuruna uygulanan ısıl ön işlemin optimizasyonu, anaerobik fermantasyon sistemlerinde hidrojen veriminin ve proses performansının artırılması açısından önemli bir işletme parametresidir.

Anahtar Kelimeler: Biyohidrojen, Karanlık Fermantasyon, Isıl Ön İşlem, Biyokimyasal Hidrojen Potansiyeli, UASB Reaktörü

ISBN NR. : 978-625-8795-33-2

OPTIMIZATION of THERMAL PRETREATMENT of ANAEROBIC INOCULUM SLUDGE for BIOHYDROGEN PRODUCTION VIA DARK FERMENTATION

ABSTRACT

The optimization of the pretreatment applied to the inoculum sludge is of critical importance for dark fermentative biohydrogen production, as it suppresses hydrogen-consuming methanogenic microorganisms while preserving the metabolic activity of hydrogen-producing bacteria. In this study, the optimum thermal pretreatment conditions for anaerobic inoculum sludge were determined prior to the operation of a modified Upflow Anaerobic Sludge Blanket (UASB) reactor. For this purpose, the inoculum sludge was subjected to thermal pretreatment at 80, 90, and 110°C for 20 min, and the effects of different temperatures were evaluated using Biochemical Hydrogen Potential (BHP) tests. Total gas production, net gas production, and gas composition were compared to determine the optimum pretreatment condition. The results demonstrated that thermal pretreatment at 90°C for 20 min provided the highest biohydrogen production performance, yielding a net gas production of 362.7 mL. This condition effectively inhibited methanogenic microorganisms while maintaining the metabolic activity of hydrogen-producing bacteria. In contrast, pretreatment at 80°C was insufficient to completely suppress methanogens, whereas pretreatment at 110°C adversely affected microbial viability, resulting in reduced hydrogen production. The optimum pretreatment condition was subsequently applied in continuous modified UASB reactor experiments investigating the effect of Fe_3O_4 magnetite nanoparticles on biohydrogen production. The findings demonstrated that appropriate optimization of the thermal pretreatment significantly enhanced the performance of the inoculum sludge and provided a reliable and reproducible operational basis for biohydrogen production through dark fermentation. Consequently, optimization of the thermal pretreatment applied to inoculum sludge is an important operational parameter for improving hydrogen yield and overall process performance in anaerobic fermentation systems.

Keywords: Biohydrogen, Dark Fermentation, Thermal Pretreatment, Biochemical Hydrogen Potential, UASB Reactor

1. GİRİŞ

Artan dünya nüfusu, sanayileşme ve teknolojik gelişmeler, enerji talebinin her geçen yıl yükselmesine neden olmaktadır. Günümüzde enerji ihtiyacının büyük bölümü fosil yakıtlardan karşılanmakta olup, bu kaynakların sınırlı rezervlere sahip olması ve sera gazı emisyonları nedeniyle çevresel sorunlara yol açması, sürdürülebilir enerji teknolojilerine yönelik araştırmaları hızlandırmıştır. Bu kapsamda yenilenebilir enerji kaynaklarından elde edilen çevre dostu yakıtlar, enerji arz güvenliğinin sağlanması ve karbon emisyonlarının azaltılması açısından önemli bir alternatif olarak değerlendirilmektedir.

Hidrojen (H_2), birim kütle başına yüksek enerji içeriğine sahip olması ve kullanım sırasında yalnızca su oluşturması nedeniyle geleceğin temiz enerji taşıyıcılarından biri olarak kabul edilmektedir. Ancak hidrojenin çevresel açıdan sürdürülebilir olabilmesi, üretim

ISBN NR. : 978-625-8795-33-2

yöntemine doğrudan bağlıdır. Fosil yakıt temelli hidrojen üretim prosesleri yüksek karbon emisyonlarına neden olurken, biyolojik yöntemlerle gerçekleştirilen biyohidrojen üretimi daha düşük enerji gereksinimi ve çevresel etkileri nedeniyle son yıllarda önemli ölçüde ilgi görmektedir (Albuquerque ve ark., 2024; Talapko ve ark., 2023).

Biyohidrojen üretiminde kullanılan biyolojik yöntemler arasında karanlık fermantasyon, ışığa ihtiyaç duymadan gerçekleştirilebilmesi, kısa hidrolik bekleme süreleri (HRT), üretiminde farklı organik substratların kullanılabilmesi ve nispeten düşük işletme maliyetleri gibi avantajları nedeniyle öne çıkmaktadır (Yadav ve ark., 2023; Kumar ve ark., 2024). Bununla birlikte karanlık fermantasyon sistemlerinde hidrojen verimini sınırlandıran en önemli sorunlardan biri, aşı çamurunda doğal olarak bulunan hidrojen tüketici metanojenik mikroorganizmaların faaliyet göstermesidir. Bu mikroorganizmalar oluşan hidrojeni metana dönüştürerek proses verimini düşürebilmektedir.

Bu nedenle karanlık fermantasyon öncesinde uygulanan ön işlem yöntemleri, hidrojen üreten sporlu bakterilerin korunması ve metanojenlerin baskılanması açısından kritik bir işletme basamağıdır. Fiziksel, kimyasal ve biyolojik ön işlem yöntemleri arasında yer alan ısıl ön işlem, uygulama kolaylığı, kimyasal kullanımını gerektirmemesi ve seçici mikrobiyal zenginleşme sağlayabilmesi nedeniyle en yaygın kullanılan yöntemlerden biridir. Bununla birlikte uygulanan sıcaklık ve sürenin yetersiz veya aşırı olması, hidrojen üretim performansını olumsuz etkileyebileceğinden optimum ön işlem koşullarının deneysel olarak belirlenmesi gerekmektedir (Ledakowicz ve ark., 2024; de Almeida ve ark., 2024).

Isıl ön işlem koşullarının değerlendirilmesinde yaygın olarak kullanılan yöntemlerden biri biyokimyasal hidrojen potansiyeli (BHP) testleridir. BHP testleri, farklı işletme koşullarının hidrojen üretim kapasitesi üzerindeki etkisini laboratuvar ölçeğinde karşılaştırmaya olanak sağlamasının yanı sıra, sürekli reaktör çalışmalarından önce uygun işletme parametrelerinin belirlenmesine de katkı sunmaktadır (Ramos ve ark., 2020; Kovalev ve ark., 2023). Gaz kromatografisi (GC) analizleri ile birlikte değerlendirildiğinde ise yalnızca üretilen gaz miktarı değil, gazın bileşimi de belirlenebilmekte ve hidrojen üretim performansı daha kapsamlı biçimde değerlendirilebilmektedir.

Bu çalışma kapsamında, ileriki çalışmalarda modifiye UASB reaktöründe yürütülecek sürekli biyohidrojen üretim deneyleri öncesinde anaerobik aşı çamuru için en uygun ısıl ön işlem koşulunun belirlenmesi amaçlanmıştır. Bu doğrultuda 80°C, 90°C ve 110°C'de 20 dakika uygulanan ısıl ön işlemler biyokimyasal hidrojen potansiyeli (BHP) testleri ile karşılaştırılmış; toplam gaz üretimi, net gaz üretimi ve gaz kompozisyonu birlikte değerlendirilerek optimum ön işlem sıcaklığı belirlenmiştir. Böylece sürekli reaktör çalışmalarında kullanılacak aşı çamurunun hidrojen üretim performansının artırılmasına yönelik deneysel bir temel oluşturulmuştur.

ISBN NR. : 978-625-8795-33-2

2. DENEYSEL ÇALIŞMALAR

2.1. Aşı Çamuru, Karbon Kaynağı ve Besiyeri

Deneylerde kullanılan anaerobik aşı çamuru, İzmir'de yer alan, mezofilik koşullarda çalışan tam ölçekli bir biyogaz tesisinden temin edilmiştir. Numuneler laboratuvara getirildikten sonra hava ile temas etmeyecek şekilde kapalı kaplarda muhafaza edilmiş ve deneyler öncesinde homojen hale getirilmiştir.

Bu çalışmada karbon kaynağı olarak, hızlı metabolize olan, erişimi kolay, maliyeti düşük olan glukoz kullanılmıştır. BHP deneylerinde mikroorganizmaların besinsel gereksinimlerini karşılamak amacıyla gerekli makro ve mikro besin elementlerini içeren sentetik besi ortamı hazırlanmıştır. Besin içeriği olarak karbon kaynağı glukoz (2 g/L) ve iz elementler (1,25 mg/L $NaHCO_3$; 0,5 mg/L NH_4Cl; 0,25 mg/L KH_2PO_4; 0,25 mg/L $CaCl_2$, 0,032 mg/L $NiSO_4$; 0,32 mg/L $MgSO_4 \cdot 7H_2O$; 0,02 mg/L $FeCl_2$; 0.0144 mg/L $Na_2MoO_4 \cdot 2H_2O$; 0.023 mg/L $ZnCl_2$; 0.021 mg/L $CoCl_2 \cdot 6H_2O$; 0,01 mg/L $CuCl_2 \cdot 6H_2O$ ve 0,03 mg/L $MnCl_2 \cdot 4H_2O$ (Abubackar vd., 2019). Aşı çamurunun pH'sının ayarlanmasında %10'luk hidroklorik asit (HCl) çözeltisinden yararlanılmıştır.

2.2. Analitik Ölçümler

Aşı çamurunun başlangıç karakterizasyonu kapsamında toplam katı madde (TKM) ve uçucu askıda katı madde (UAKM) analizleri Standard Methods (APHA, 2017)'ye göre gerçekleştirilmiştir. TKM tayini için önceden kurutulup tartılan krozelere belirli miktarda numune alınmış ve 105 °C'de sabit ağırlığa ulaşıncaya kadar kurutulmuştur. Kurutma sonrası elde edilen ağırlıklar kullanılarak toplam katı madde miktarı hesaplanmıştır. Daha sonra aynı numuneler 550 °C'de kül fırınında 1 saat yakılmış, desikatörde soğutulduktan sonra tekrar tartılmıştır. Yakma işlemi sonrasında meydana gelen ağırlık kaybı esas alınarak uçucu askıda katı madde miktarı belirlenmiştir. Daha sonra biyohidrojen üretim deneylerinde kullanılmak üzere uygun ön işlemlere tabi tutulmuştur.

$$\%\text{TKM} = \frac{[(105°\text{C sonras kroze} + \text{örnek}) - \text{kroze ağırlığı}]\text{x } 100}{(\text{Başlangıç kroze ağırlığı} + \text{örnek}) - \text{kroze}}$$

$$\%\text{UAKM} = \frac{[(105\ °\text{C sonrası kroze} + \text{örnek}) - (\ 550\ °\text{C sonrası kroze} + \text{örnek})]\text{x}100}{(105\ °\text{C sonrası kroze} + \text{örnek}) - \text{kroze ağırlığı}}$$

2.3. Anaerobik Aşı Çamuru ve Isıl Ön İşlem Optimizasyonu

Karanlık fermantasyon sırasında hidrojen tüketen metanojenik mikroorganizmaların baskılanması amacıyla anaerobik aşı çamuruna farklı sıcaklıklarda ısıl ön işlem uygulanmıştır. Bu kapsamda aşı çamuru **80°C, 90°C ve 110°C** sıcaklıklarda **20 dakika** süreyle otoklavda tutulmuştur. Ön işlem sonrasında numuneler oda sıcaklığına kadar soğutulmuş ve biyokimyasal

ISBN NR. : 978-625-8795-33-2

hidrojen potansiyeli deneylerinde kullanılmadan önce pH değeri **%10'luk HCl çözeltisi** kullanılarak **5,5** seviyesine ayarlanmıştır. Böylece farklı sıcaklıklarda uygulanan ön işlemlerin biyohidrojen üretimi üzerindeki etkileri karşılaştırılmıştır.

2.4. Biyokimyasal Hidrojen Potansiyeli (BHP) Deneyleri

Isıl ön işlem koşullarının biyohidrojen üretimine etkisinin belirlenmesi amacıyla biyokimyasal hidrojen potansiyeli (BHP) deneyleri gerçekleştirilmiştir. Deneyler **100 mL hacmindeki amber renkli serum şişelerinde** yürütülmüş olup her şişede **50 mL çalışma hacmi** kullanılmıştır. Çalışma hacmi **40 mL ön işlem uygulanmış anaerobik aşı çamuru** ile **10 mL glukoz çözeltisinden** oluşturulmuştur. Deneyler üç paralel olarak yürütülmüş ve tüm şişeler anaerobik koşullar sağlandıktan sonra mezofilik sıcaklıkta (37**°C**) inkübasyona bırakılmıştır. Ön işlem uygulanan ancak besin ilavesi yapılmayan aşı çamuru kontrol grubu olarak değerlendirilmiştir. 21 gün boyunca oluşan gaz hacimleri düzenli aralıklarla şişelerin tepe boşluklarından ölçülmüş ve toplam gaz üretim değerleri kaydedilmiştir.

2.5. Gaz Kromatografisi (GC) Analizi

BHP deneyleri sırasında şişelerin içerisinde oluşan biyogazın bileşimi gaz kromatografisi (GC) kullanılarak analiz edilmiştir. Gaz analizleri **Agilent 6890N** gaz kromatografi cihazında **termal iletkenlik dedektörü (TCD)** kullanılarak gerçekleştirilmiştir. Ayırma işlemi **Hayesep D (80/100 mesh)** kolonda yapılmış, taşıyıcı gaz olarak **argon** kullanılmış ve taşıyıcı gaz akış hızı **20 mL dk^{-1}** olarak ayarlanmıştır. Enjektör ve dedektör sıcaklıkları **150°C**, kolon sıcaklığı ise **35°C** olarak uygulanmıştır. Gaz örnekleri serum şişelerinin tepe boşluğundan gaz geçirmez enjektör yardımıyla alınmış ve manuel olarak cihaza enjekte edilmiştir. Analizler sonucunda hidrojen (H_2), karbondioksit (CO_2) ve metan (CH_4) gazlarının yüzdesel dağılımları belirlenmiştir.

ISBN NR. : 978-625-8795-33-2

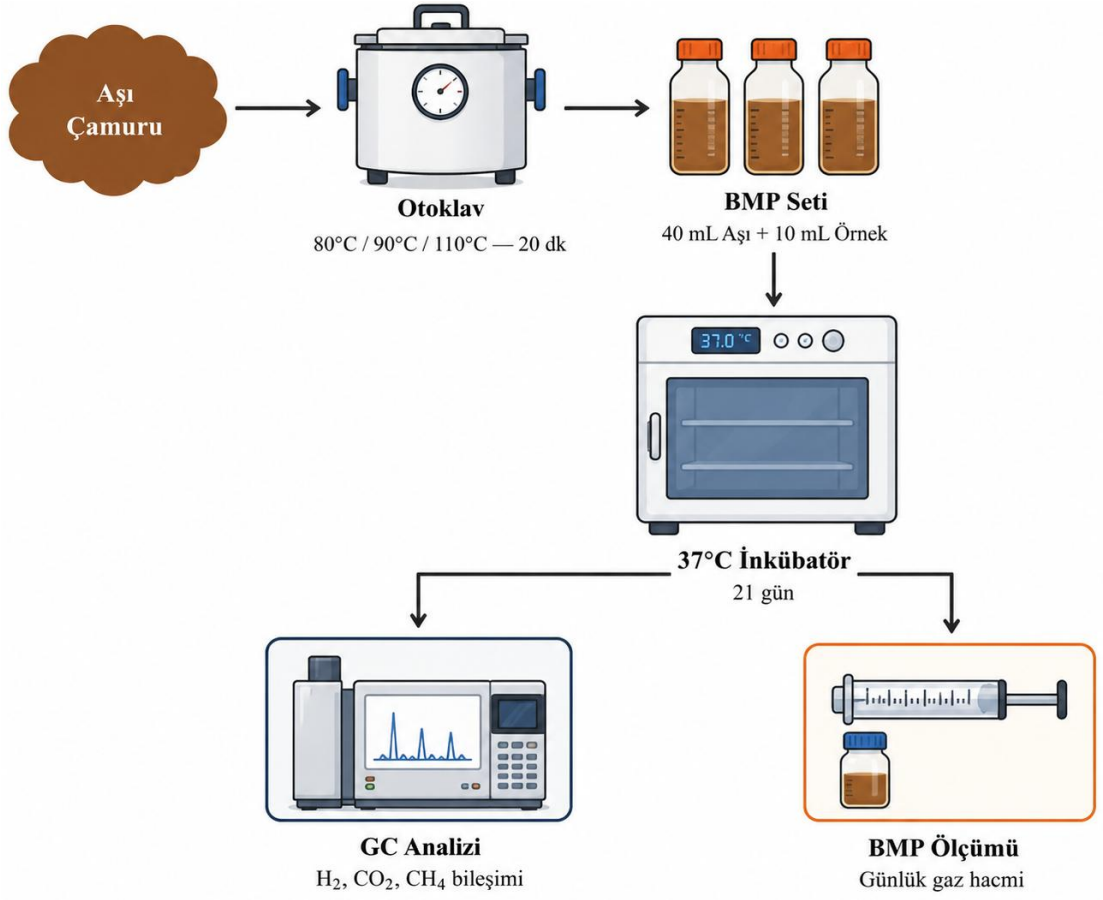

Görsel 1. BHP ve GC Analiz Şeması

2.6. İstatistiksel Analiz

Tüm deneysel çalışmalar üç paralel olarak gerçekleştirilmiştir. Sonuçlar ortalama ± standart sapma şeklinde ifade edilmiş ve farklı ısıl ön işlem koşullarının biyohidrojen üretimi üzerindeki etkileri tek yönlü varyans analizi (One-way ANOVA) ile değerlendirilmiştir. İstatistiksel anlamlılık düzeyi **p <0,05** olarak kabul edilmiştir.

3. SONUÇLAR VE DEĞERLENDİRME

3.1. Aşı Çamurunun Karakterizasyonu

BHP deneylerinde kullanılan anaerobik aşı çamurunun başlangıç karakterizasyonu yapılmıştır. Analiz sonuçlarına göre aşı çamurunun pH değeri 5,5, TKM oranı %6,86 ve UAKM miktarı ise TKM'nin %51,2'si olarak belirlenmiştir. UAKM/TKM oranı, aşı çamurunun biyolojik olarak parçalanabilir organik madde bakımından zengin olduğunu ve karanlık fermantasyon ile biyohidrojen üretimi için uygun özellikler taşıdığını göstermektedir.

ISBN NR. : 978-625-8795-33-2

3.2. Isıl Ön İşlem Koşullarının Biyokimyasal Hidrojen Üretim Potansiyeline Etkisi

Farklı sıcaklıklarda uygulanan ısıl ön işlemlerin biyohidrojen üretimine etkisi, biyokimyasal hidrojen potansiyeli (BHP) deneyleri ile değerlendirilmiş olup elde edilen toplam ve net gaz üretim değerleri **Görsel 2** ve **3**'te sunulmuştur. Üç farklı ön işlem sıcaklığı arasında belirgin farklılıklar gözlenmiş ve uygulanan sıcaklığın hidrojen üretim performansı üzerinde önemli bir etkisinin olduğu belirlenmiştir.

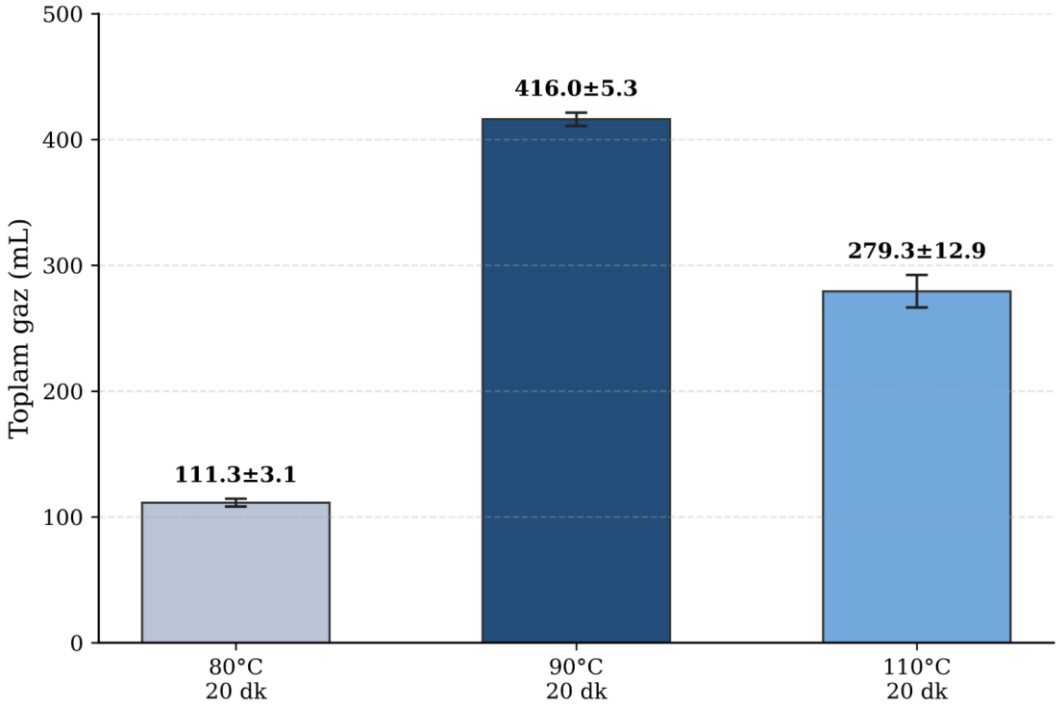

Görsel 2. BHP analiz toplam gaz (mL) sonuçları (ortalama ± standart sapma, n=3)

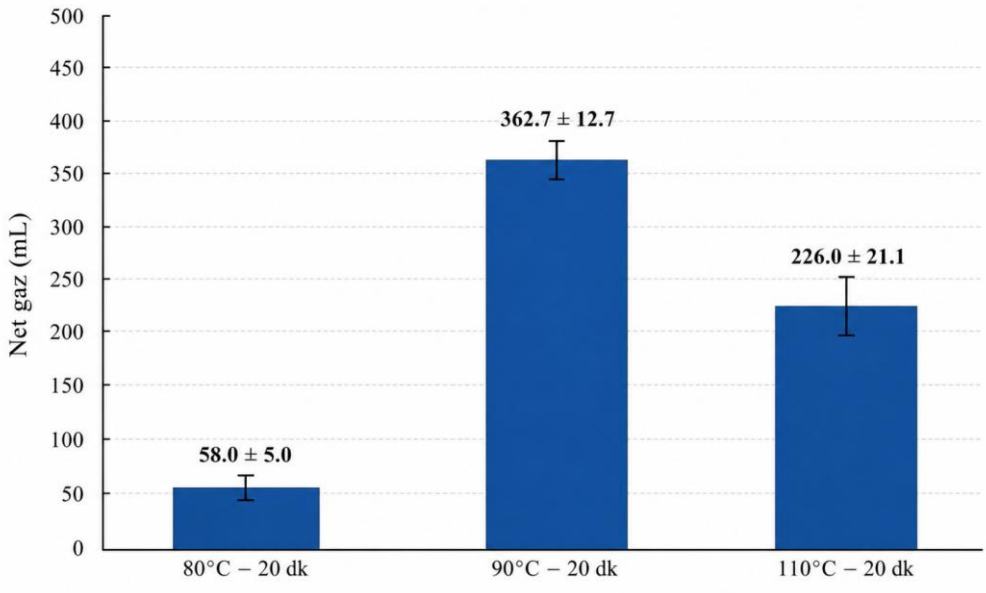

Görsel 3. BHP analizi net gaz (mL) sonuçları (ortalama ± standart sapma, n=3)

ISBN NR. : 978-625-8795-33-2

Deney sonuçlarına göre en yüksek toplam gaz üretimi **90°C'de 20 dakika** uygulanan ön işlem grubunda **416,0 ± 5,3 mL** olarak belirlenmiştir. Bu değeri **110°C'de 20 dakika** uygulanan grup **(279,3 ± 12,9 mL)** izlerken, en düşük gaz üretimi **80°C'de 20 dakika** uygulanan grupta **(111,3 ± 3,1 mL)** elde edilmiştir. Benzer eğilim net gaz üretiminde de gözlenmiş ve **90°C'de 20 dakika** uygulanan ön işlem, **362,7 mL** ile en yüksek net gaz üretimini sağlamıştır.

Bu sonuçlar, ön işlem sıcaklığının yalnızca toplam gaz miktarını değil, hidrojen üretim verimini de doğrudan etkilediğini göstermektedir. **80°C** uygulamasında metanojenik mikroorganizmaların yeterince baskılanamadığı düşünülmektedir. Buna karşılık **110°C** uygulamasında metanojenlerin baskılanmasına rağmen yüksek sıcaklığın hidrojen üreten sporlu bakterilerin bir kısmını da olumsuz etkilemiş olabileceği değerlendirilmektedir. Her iki durum birlikte ele alındığında, **90°C'de 20 dakika** uygulanan ön işlemin hidrojen üreten mikroorganizmaların aktivitesini korurken metanojenik popülasyonu etkin biçimde baskılayan optimum koşulu sağladığı görülmektedir. Bu değerlendirme, Woo ve Song (2010) tarafından bildirilen optimum ısıl ön işlem sıcaklığı ile de uyumludur. Ayrıca Kumar ve ark. (2016) da 90°C'de uygulanan ısıl ön işlemin, 70 ve 80°C uygulamalarına göre daha yüksek hidrojen üretim performansı sağladığını rapor etmişlerdir.

3.3. Gaz Kompozisyonunun Gaz Kromatografisi (GC) ile Değerlendirilmesi

Isıl ön işlem uygulamalarının biyohidrojen üretimine etkisini daha ayrıntılı değerlendirebilmek amacıyla BHP deneyleri sırasında oluşan gazların bileşimi gaz kromatografisi (GC) ile analiz edilmiş ve sonuçlar **Şekil 3,4 ve 5**'te verilmiştir. Gaz bileşimi incelendiğinde farklı ön işlem sıcaklıklarının H_2, CH_4 ve CO_2 oluşumu üzerinde belirgin etkiler oluşturduğu görülmüştür.

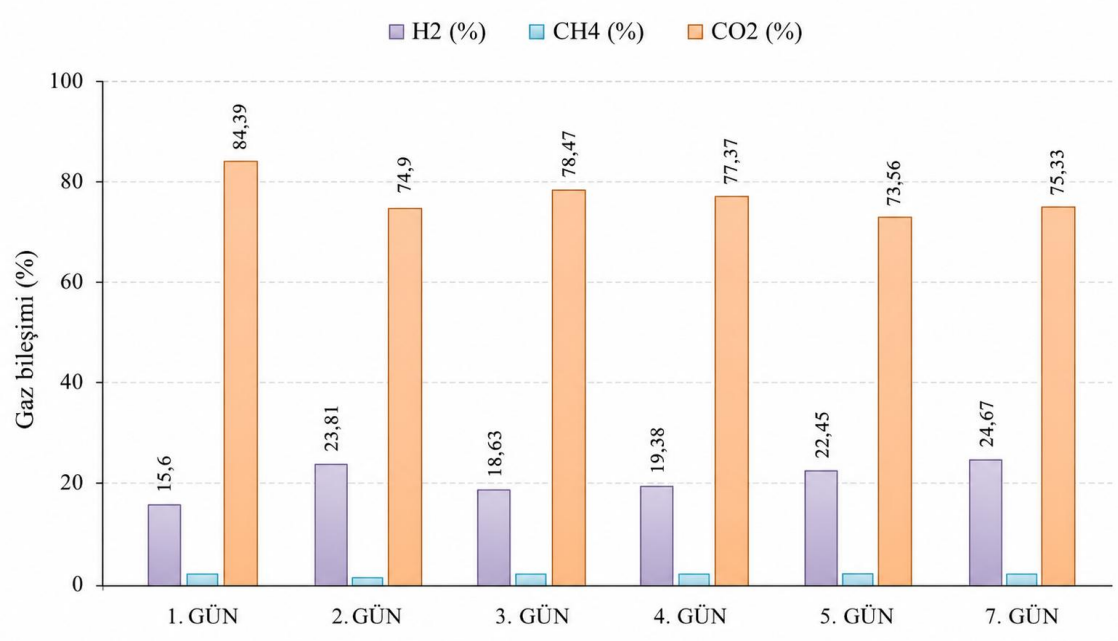

Görsel 4. 80 ºC 20 dk ön işlemiyle hazırlanan BHP deneylerinin gaz kromatografi (GC) sonuçları (%)

ISBN NR. : 978-625-8795-33-2

80°C uygulamasında metan gazının deney süresince baskın bileşen olarak kaldığı, CH_4 oranının yaklaşık **%74–84** aralığında değiştiği belirlenmiştir. Buna karşılık H_2 oranı oldukça düşük seviyelerde kalmış ve anlamlı bir artış göstermemiştir. Bu durum, uygulanan sıcaklığın metanojenik mikroorganizmaların aktivitesini tamamen baskılamak için yeterli olmadığını ve üretilen hidrojenin metan oluşumunda tüketilmeye devam ettiğini göstermektedir. Benzer şekilde, inokuluma uygulanan yetersiz ısıl ön işlemlerin metanojenik aktiviteyi tam olarak inhibe edemediği ve bunun hidrojen üretim performansını olumsuz etkilediği farklı çalışmalarda da rapor edilmiştir (Ledakowicz ve ark., 2024; Zhang ve ark., 2023).

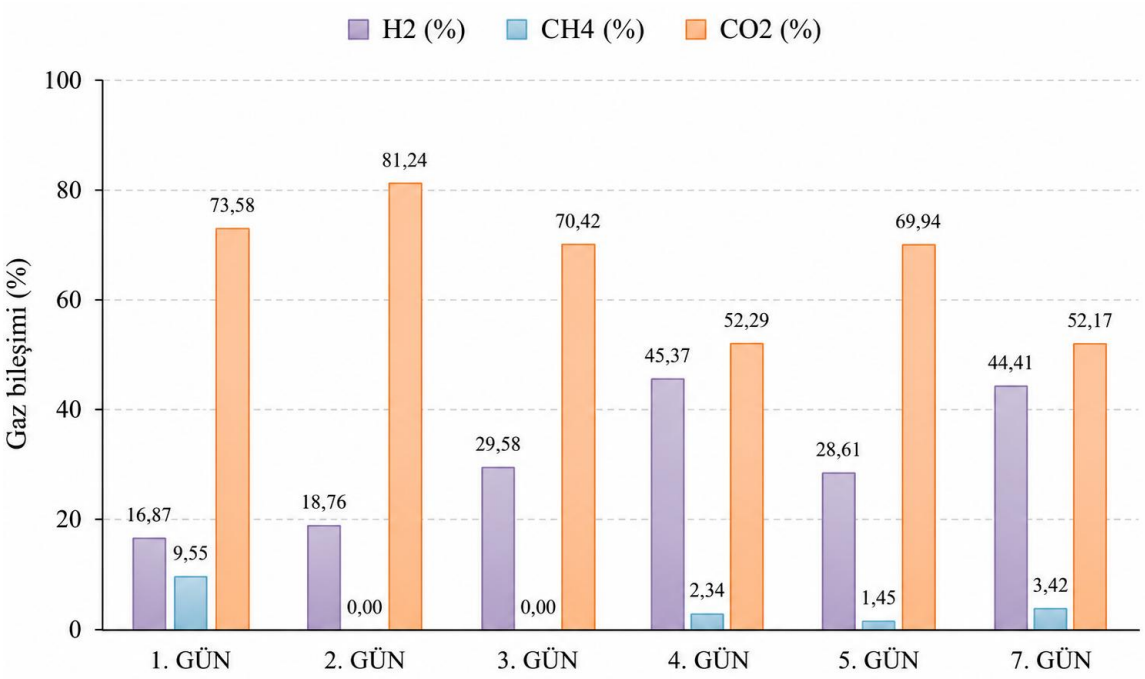

Görsel 5. 90 °C 20 dk ön işlemiyle hazırlanan BHP deneylerinin gaz kromatografi (GC) sonuçları (%)

90°C uygulamasında ise gaz kompozisyonunda belirgin bir değişim gözlenmiştir. H_2 oranı ilk günde yaklaşık **%9,14** olarak belirlenirken üçüncü günde **%29,68**'e ve dördüncü günde **%45,37**'ye yükselmiştir. Aynı süreçte CH_4 oranında azalma eğilimi gözlenmiştir. CO_2 oranındaki artış, karanlık fermantasyon sırasında organik maddenin asidojenik parçalanmasının devam ettiğini ve metanojenik yolakların baskılanmasıyla birlikte gaz fazının ağırlıklı olarak H_2 ve CO_2'den oluştuğunu göstermektedir (de Almeida ve ark., 2024). Bu gaz dağılımı, metanojenik aktivitenin önemli ölçüde baskılandığını ve hidrojen üreten fermantatif mikroorganizmaların sistemde daha etkin hâle geldiğini göstermektedir. Literatürde 90°C civarında uygulanan ısıl ön işlemin metanojenik popülasyonu etkin şekilde inhibe ederken *Clostridium* gibi sporlu hidrojen üretici bakterilerin gelişimini desteklediği ve hidrojen oranını önemli ölçüde artırdığı farklı araştırmalarda da belirtilmiştir (Woo ve Song, 2010; de Almeida ve ark., 2024).

ISBN NR. : 978-625-8795-33-2

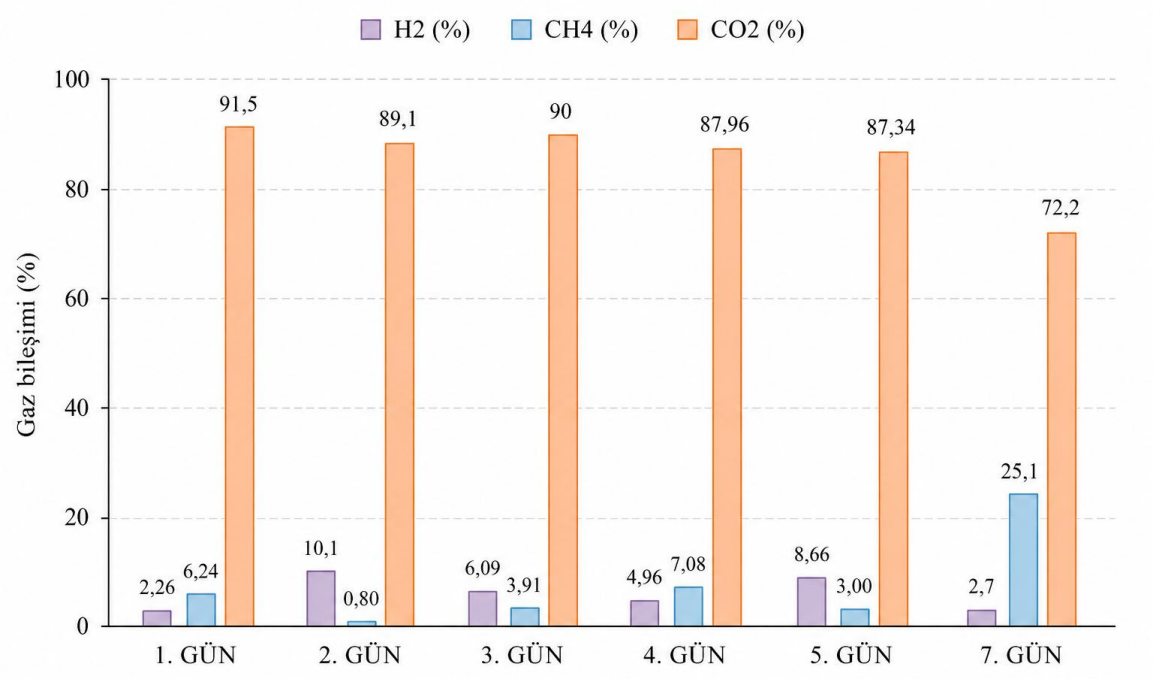

Görsel 6. 110 ºC 20 dk ön işlemiyle hazırlanan BHP deneylerinin gaz kromatografi (GC) sonuçları (%)

110°C uygulamasında CH_4 oluşumu büyük ölçüde baskılanmasına rağmen hidrojen üretiminin 90°C uygulamasına göre daha düşük olduğu belirlenmiştir. Bu durum, yüksek sıcaklığın yalnızca metanojenik mikroorganizmaları değil, hidrojen üretiminde görev alan bazı sporlu bakterileri de olumsuz etkilemiş olabileceğini düşündürmektedir. Dolayısıyla daha yüksek sıcaklık uygulanması her zaman daha yüksek hidrojen üretimi anlamına gelmemektedir. Farklı sıcaklıklarda gerçekleştirilen çalışmalarda da optimum değerin üzerindeki ısıl ön işlem sıcaklıklarının hidrojen üreten mikroorganizmaların canlılığını ve metabolik aktivitelerini olumsuz etkileyerek hidrojen veriminde azalmaya neden olduğu bildirilmiştir (Woo ve Song, 2010; Ledakowicz ve ark., 2024).

Genel olarak değerlendirildiğinde, BHP deneylerinden elde edilen gaz üretim verileri ile GC analizleri birbirini desteklemektedir. Toplam ve net gaz üretiminin en yüksek olduğu **90°C** uygulamasında aynı zamanda H_2 oranının da en yüksek değerlere ulaşması, seçilen ön işlem koşulunun hidrojen üretimi açısından en uygun sıcaklık olduğunu göstermektedir. Bu nedenle sonraki sürekli reaktör çalışmalarında **90°C'de 20 dakika** uygulanan ön işlem koşulu tercih edilmiştir.

4. GENEL DEĞERLENDİRME VE SONUÇLAR

Bu çalışmada, karanlık fermantasyonla biyohidrojen üretiminde kullanılacak anaerobik aşı çamuruna uygulanacak optimum ısıl ön işlem koşulları araştırılmıştır. Farklı sıcaklıklarda gerçekleştirilen BHP testleri sonucunda, ön işlem sıcaklığının hidrojen üretim performansı üzerinde belirleyici bir etkiye sahip olduğu ortaya konulmuştur. Toplam gaz üretimi, net gaz

ISBN NR. : 978-625-8795-33-2

üretimi ve gaz kompozisyonu birlikte değerlendirildiğinde, **90°C'de 20 dakika** uygulanan ısıl ön işlemin en yüksek biyohidrojen üretim performansını sağladığı belirlenmiştir.

80°C'de uygulanan ön işlemin metanojenik mikroorganizmaları yeterince baskılayamadığı ve bu nedenle hidrojen üretiminin sınırlı kaldığı görülürken, 110°C'de uygulanan ön işlemin ise hidrojen üreten bakterilerin metabolik aktivitelerini olumsuz etkileyerek biyohidrojen üretiminde azalmaya neden olduğu belirlenmiştir. Bu sonuçlar, uygulanan ön işlemin yalnızca metanojenlerin inhibisyonunu değil, aynı zamanda hidrojen üreten mikroorganizmaların canlılığının korunmasını da sağlayacak şekilde optimize edilmesi gerektiğini göstermektedir.

Çalışma kapsamında belirlenen optimum ön işlem koşulu, daha sonraki sürekli çalışan modifiye UASB reaktör deneylerinde uygulanmış ve sistem işletmesi için uygun bir başlangıç koşulu oluşturmuştur. Bu yönüyle çalışma, yalnızca kesikli sistemlerde ön işlem optimizasyonunu ortaya koymakla kalmamış, aynı zamanda sürekli biyohidrojen üretim proseslerinin işletilmesi için güvenilir bir temel sağlamıştır.

Sonuç olarak, anaerobik aşı çamuruna uygulanan **90°C'de 20 dakika** süreli ısıl ön işlemin, biyohidrojen üretim performansını artıran en uygun koşul olduğu belirlenmiştir. Elde edilen bulgular, karanlık fermantasyon proseslerinde aşı çamurunun uygun şekilde ön işleme tabi tutulmasının hidrojen veriminin artırılması ve proses performansının iyileştirilmesi açısından önemli bir işletme parametresi olduğunu göstermektedir. Bu çalışmanın, biyohidrojen üretimine yönelik gelecekte gerçekleştirilecek laboratuvar ve pilot ölçekli uygulamalara katkı sağlayacağı değerlendirilmektedir.

KAYNAKÇA

Abubackar, H. N., Keskin, T., Yazgin, O., Gunay, B., Arslan, K., & Azbar, N. (2019). Biohydrogen production from autoclaved fruit and vegetable wastes by dry fermentation under thermophilic condition. International Journal of Hydrogen Energy, 44(34), 18776-18784.

Albuquerque, M. M., Sartor, G. de B., Martinez-Burgos, W. J., Scapini, T., Edwiges, T., Soccol, C. R., & Medeiros, A. B. P. (2024). Biohydrogen produced via dark fermentation: A review. Methane, 3(3), 500–532. https://doi.org/10.3390/methane3030029

de Almeida, M. P. G., Mondini, C., Bruant, G., Tremblay, J., Weissbrodt, D. G., & Mockaitis, G. (2024). Thermal and alkaline pre-treatments of inoculum halt methanogenesis and enable cheese whey valorization by batch acidogenic fermentation. Journal of Chemical Technology & Biotechnology, 99(4), 989–1001. https://doi.org/10.1002/jctb.7607

Kovalev, A. A., Kovalev, D. A., Zhuravleva, E. A., Laikova, A. A., Shekhurdina, S. V., Vivekanand, V., & Litti, Y. V. (2023). Biochemical hydrogen potential assay for predicting the

patterns of the kinetics of semi-continuous dark fermentation. Bioresource Technology, 376, 128919. https://doi.org/10.1016/j.biortech.2023.128919

Kumar, G., Bakonyi, P., Kim, S. H., & diğerleri. (2016). The effects of heat-shock pretreatment conditions on dark hydrogen fermentation from glucose. International Journal of Ambient Energy, 38(6), 1–8. https://doi.org/10.1080/01430750.2016.1181566

Kumar, S., vd. (2024). Biohydrogen production through dark fermentation: Recent trends and advances in transition to a circular bioeconomy. International Journal of Hydrogen Energy, 52, 335–357. https://doi.org/10.1016/j.ijhydene.2023.05.161

Ledakowicz, S., vd. (2024). Influence of inoculum thermal pretreatment time on hydrogen production in dark fermentation. Energies, 17(4), 974. https://doi.org/10.3390/en17040974

Ledakowicz, S., ve ark. (2024). Influence of inoculum thermal pretreatment time on hydrogen production in dark fermentation. Energies, 17(4), 974. https://doi.org/10.3390/en17040974

Ramos, L. R., Klein, B. C., da Silva, V., Mantovani, H. C., Aquino, S. F., Chernicharo, C. A. L., & Mockaitis, G. (2020). Standardized protocol for determination of biohydrogen potential. MethodsX, 7, 100702. https://doi.org/10.1016/j.mex.2019.11.019

Talapko, D., Talapko, J., Erić, I., & Škrlec, I. (2023). Biological hydrogen production from biowaste using dark fermentation, storage and transportation. Energies, 16(8), 3321. https://doi.org/10.3390/en16083321

Woo, J. H., & Song, Y. C. (2010). Influence of temperature and duration of heat treatment used for anaerobic seed sludge on biohydrogen fermentation. KSCE Journal of Civil Engineering, 14(2), 141-147.

Yadav, M. D., Sohale, A. P., Janardanan, S., Dash, B., & Yadav, M. D. (2023). Dark fermentative biohydrogen production: Recent advances and challenges. Industrial & Engineering Chemistry Research, 62(37), 14755–14771. https://doi.org/10.1021/acs.iecr.3c01439

Zhang, X., vd. (2023). Comparative effect of acid and heat inoculum pretreatment on dark fermentative biohydrogen production. Environmental Research, 239, 117433. https://doi.org/10.1016/j.envres.2023.117433

ISBN NR. : 978-625-8795-33-2

CHATGPT'NİN İŞİTSEL İŞLEMLEME BOZUKLUĞU VE DUYUSAL İŞLEMLEME BOZUKLUĞUNU AYIRT ETME PERFORMANSININ DEĞERLENDİRİLMESİ

Doç. Dr. Banu BAŞ[1]

Ankara Yıldırım Beyazıt Üniversitesi, Sağlık Bilimleri Fakültesi, Odyoloji Bölümü, Ankara, Türkiye.

E-posta: bbas@aybu.edu.tr – **ORCID ID:** 0000-0002-2521-4545

İrem YILBAT[2]

Ankara Yıldırım Beyazıt Üniversitesi, Sağlık Bilimleri Enstitüsü, Odyoloji Yüksek Lisans Programı, Ankara, Türkiye.

E-posta: iremyilbat25@aybu.edu.tr – **ORCID ID:** 0009-0005-7844-3412

ÖZET

Çalışmanın amacı, ChatGPT'nin İşitsel İşlemleme Bozukluğu (Auditory Processing Disorder, APD) ile Duyusal İşlemleme Bozukluğu (Sensory Processing Disorder, SPD) kavramlarını tanımlama, karşılaştırma ve ayırt etme konusundaki performansını araştırmacı ve bağımsız iki odyolog puanlamaları doğrultusunda değerlendirmektir. Tanımlayıcı ve gözlemsel olarak tasarlanan bu çalışmada, araştırmacılar tarafından literatür doğrultusunda oluşturulan ve 7 tanım, 7 karşılaştırma ile 3 klinik vaka değerlendirme sorusundan oluşan toplam 17 soruluk bir soru seti kullanılmıştır. Aynı soru seti ChatGPT'ye ve alanında deneyimli iki bağımsız odyologa uygulanmıştır. İlk aşamada ChatGPT'nin yanıtları ile odyologların referans yanıtları karşılaştırılarak araştırmacı tarafından 0–2 puanlama sistemi ile değerlendirilmiştir. İkinci aşamada ise ChatGPT yanıtları iki bağımsız odyolog tarafından bilimsel doğruluk açısından 0–2 puanlama sistemi kullanılarak puanlanmıştır. Araştırmacı değerlendirmesi betimsel olarak analiz edilmiş; odyolog puanları için betimsel istatistikler, Sınıf İçi Korelasyon Katsayısı (ICC) analizi uygulanmıştır. Araştırmacı değerlendirmesine göre ChatGPT, toplam 34 puan üzerinden 30 puan almış ve genel başarı oranı %88,2 olarak bulunmuştur. Tanım ve karşılaştırma sorularında başarı oranı %92,9, klinik vaka sorularında ise %66,7 olarak hesaplanmıştır. Odyologların ChatGPT yanıtlarına verdikleri ortalama puan 1,82±0,39 olarak bulunmuştur. ICC analizinde değerlendiriciler arası uyum düşük düzeyde bulunmuştur (ICC=0,190). Sonuç olarak, ChatGPT'nin APD ve SPD'ye ilişkin temel kavramsal bilgileri yüksek doğrulukla sunabildiğini ve iki bozukluk arasındaki temel farklılıkları başarılı şekilde açıklayabildiği görülmüştür. Ayrıca, klinik vaka değerlendirmelerinde performansının görece daha düşük olduğu belirlenmiştir. ChatGPT'nin APD ve SPD konularında eğitim ve bilgiye erişimde yararlı bir araç olabileceği, ancak klinik karar verme ve ayırıcı tanı süreçlerinde uzman değerlendirmesinin yerini alamayacağı sonucuna varılmıştır.

ISBN NR. : 978-625-8795-33-2

Anahtar Kelimeler: ChatGPT, İşitsel İşlemleme Bozukluğu, Duyusal İşlemleme Bozukluğu, Yapay Zekâ, Odyoloji

1. GİRİŞ

İşitsel İşlemleme Bozukluğu (Auditory Processing Disorder, APD) ve Duyusal İşlemleme Bozukluğu (Sensory Processing Disorder, SPD), klinik belirtilerindeki benzerlik nedeniyle ayırıcı tanıda güçlük oluşturabilen iki önemli nörogelişimsel bozukluktur (Buffone ve Schochat, 2022; Mapholi ve ark., 2024). APD, bireyin normal periferik işitme eşiklerine sahip olmasına rağmen sesin zamansal özelliklerini çözümleme, gürültüde konuşmayı ayırt etme ve iki kulaktan gelen işitsel bilgiyi entegre etme gibi santral işitsel sinir sistemi işlevlerinde meydana gelen bozuklukları ifade eder (ASHA, 2005; Küçük Ceyhan ve ark., 2023). APD'li bireylerde özellikle gürültülü ortamlarda konuşmayı anlama güçlüğü, işitsel ayırt etme problemleri, ses lokalizasyonunda yetersizlikler, işitsel dikkat sorunları ve sözel yönergeleri takip etmede güçlük görülebilmektedir (ASHA, 2005; Bolulu ve Elkin, 2019; Elibol ve Pehlivanoğlu, 2024). Bu nedenle APD'nin doğru tanılanması ve yönetimi, multidisipliner bir yaklaşım gerektirmektedir (Küçükünal, 2025). SPD ise dokunsal, görsel, işitsel, vestibüler ve proprioseptif duyular aracılığıyla çevreden ve vücuttan alınan uyaranların merkezi sinir sisteminde koordine edilmesi, bütünleştirilmesi ve bu uyaranlara uygun motor veya davranışsal yanıtların oluşturulması sürecindeki aksaklıkları kapsayan daha geniş bir tablodur (Miller ve ark., 2007; Dunn, 1997). SPD'li bireyler duyusal modülasyon stratejilerindeki yetersizlikler nedeniyle sese karşı aşırı hassasiyet (hiperakuzi), düşük ses toleransı veya duyusal arayış gibi davranışlar sergileyebilirler. Bu durum otizm spektrum bozukluğu başta olmak üzere birçok nörogelişimsel süreçte de belirgin olarak kendini gösterebilir (Cevher ve Kurnaz, 2024; Türer ve Köse, 2023).

APD ve SPD farklı bozukluklar olarak tanımlanmasına rağmen bazı klinik belirtiler açısından benzerlik gösterebilmektedir. Her iki gruptaki çocuklar özellikle gürültülü ortamlarda zorlanma, işitsel uyaranlara olağandışı tepkiler verme, işitsel yönergeleri takip etmede güçlük yaşama veya çevre tarafından "duymuyor gibi" algılanma gibi benzer davranışlar sergileyebilmektedir (Krüger ve ark., 2001; Mapholi ve ark., 2024). Bu benzerlikler APD ve SPD'nin ayırıcı tanısını güçleştirebilmekte ve klinisyenlerin uygun değerlendirme ve müdahale planını belirlemesini zorlaştırabilmektedir (Buffone ve Schochat, 2022; Elibol ve Pehlivanoğlu, 2024).

Yapay zeka teknolojileri günümüzde tıp eğitimi, hasta bilgilendirme, klinik karar destek mekanizmaları ve sağlık hizmetlerinin dijital dönüşümü gibi birçok alanda önemli değişikliklere yol açmaktadır (Birden, 2025; Eriç ve ark., 2024; Yiğit ve ark., 2023). Bu teknolojiler arasında yer alan ChatGPT, sağlık profesyonelleri tarafından bilgiye erişim, hasta bilgilendirme ve klinik karar destek süreçlerinde giderek daha fazla kullanılmaktadır (Genç, 2023; Yiğit ve ark., 2023). Odyoloji ve otoloji alanında yapay zekanın objektif işitme testlerinin yorumlanmasından koklear implant rehabilitasyon süreçlerine, tinnitus yönetiminden işitme kaybının erken teşhisine kadar geniş bir klinik yelpazede yenilikçi çözümler sunduğu görülmektedir (AlSamhori ve ark., 2024; Bahng, 2025; Torun, 2024). Güncel literatürde

ISBN NR. : 978-625-8795-33-2

ChatGPT ve benzeri sistemlerin, uluslararası odyolog yeterlilik sınavlarında (Qi ve ark., 2025), saf ses odyogramlarının tanısal yorumlanmasında (Karaçaylı ve ark., 2025), pediatrik odyoloji vakalarında (Ratuszniak ve ark., 2025) ve koklear implant ameliyatı sonrası hasta bilgilendirme süreçlerindeki (Aliyeva ve ark., 2024; İçöz ve Kocabay, 2025) performansını değerlendiren çalışmalar giderek artmaktadır.

Bununla birlikte, ChatGPT gibi yapay zekâ sistemlerinin klinik ortamda karar destek aracı olarak kullanılabilmesi, ürettikleri bilgilerin doğruluğuna, kısa ve uzun dönemli tekrarlanabilirliğine (retest reliability) ve klinik kılavuzlarla olan uyumuna doğrudan bağlıdır (İçöz ve Kocabay, 2025; Jedrzejczak ve ark., 2024; Lin ve ark., 2025). Yapay zeka modellerinin zaman zaman "halüsinasyon" olarak adlandırılan bilimsel açıdan hatalı veya uydurma referanslar üretme eğilimi, tıp ve odyoloji gibi kritik alanlarda yanlış bilgilendirme riskini de beraberinde getirmektedir (Jedrzejczak ve ark., 2026; Kochanek ve ark., 2024). Pourhoseingholi ve ark. (2025) farklı yapay zekâ sohbet botlarının, işitme kaybına ilişkin sunduğu bilgilerin doğruluk ve güvenilirlik düzeylerinin değişkenlik gösterebildiği bildirmiştir. Bu nedenle, yapay zeka sistemlerinin klinik karar verme süreçlerinde kullanılmadan önce farklı klinik tablolar üzerindeki performanslarının değerlendirilmesi gerekmektedir (Caragli ve ark., 2026; Gaeta, 2025; Pastucha ve ark., 2025).

Mevcut literatürde yapay zekanın odyolojik test yorumlama, hasta bilgilendirme ve genel KBB konularındaki performansı çeşitli çalışmalarla değerlendirilmiş olsa da APD ve SPD gibi klinik olarak benzer özellikler gösterebilen iki bozukluğu ayırt etme yeterliliği henüz incelenmemiştir. Özellikle bu iki bozukluğa ait ortak ve ayırt edici semptomların değerlendirilmesi ile klinik vaka senaryolarının yorumlanmasında ChatGPT'nin performansına ilişkin bilgi sınırlıdır. Bu doğrultuda bu çalışmada ChatGPT'nin işitsel işlemleme bozukluğu (APD) ile duyusal işlemleme bozukluğu (SPD) kavramlarını tanımlama, karşılaştırma ve ayırt etme konusundaki doğruluk, tutarlılık ve kavramsal ayrım yapabilme yeterliliğinin değerlendirilmesi amaçlanmıştır.

2. YÖNTEM

2.1. Çalışma Tasarımı ve Etik Beyan

Bu çalışma, ChatGPT'nin işitsel işlemleme bozukluğu (APD) ile duyusal işlemleme bozukluğu (SPD) kavramlarını ayırt etme yeterliliğini değerlendirmeye yönelik tanımlayıcı ve gözlemsel bir araştırma olarak gerçekleştirilmiştir. Çalışmada ChatGPT'nin APD ve SPD ile ilgili tanım, karşılaştırma ve klinik vaka sorularına verdiği yanıtlar incelenmiş; yanıtların doğruluk düzeyi, kavramsal ayrım yapabilme yeterliliği değerlendirilmiştir. Çalışma kapsamında herhangi bir kişisel veri kullanılmamıştır ve tüm araştırma süreci bilimsel araştırma ve yayın etiği ilkelerine uygun olarak yürütülmüştür. Bu nedenle çalışma için etik kurul onayı gerekmemektedir.

2.2. Soru Setinin Oluşturulması

Araştırmada kullanılan soru seti, APD ve SPD'ye ilişkin literatürde yer alan tanım, klinik özellikler ve ayırt edici kriterler temel alınarak araştırmacılar tarafından geliştirilmiştir. Sorular

ISBN NR. : 978-625-8795-33-2

hazırlanırken APD ve SPD'nin ortak ve ayırt edici özelliklerini kapsayacak, tanısal ayrımı ortaya koyabilecek ve klinik muhakemeyi değerlendirebilecek içeriklere yer verilmesine dikkat edilmiştir.

Soru seti üç bölümden ve toplam 17 sorudan oluşmaktadır. 7 tanım sorusu, 7 karşılaştırma sorusu ve 3 klinik vaka değerlendirme sorusu şeklinde yapılandırılmıştır. Tanım soruları, ChatGPT'nin APD ve SPD ile ilişkili temel kavramları doğru tanımlama ve uygun bozuklukla eşleştirme becerisini değerlendirmek amacıyla hazırlanmıştır. Karşılaştırma soruları, ChatGPT'nin iki bozukluk arasındaki benzerlik ve farklılıkları açıklayabilme, ayırt edici özellikleri kullanabilme ve kavramsal ayrım yapabilme yeterliliğini değerlendirmek amacıyla oluşturulmuştur. Klinik vaka değerlendirme soruları ise APD, SPD ve her iki bozukluğun ortak özelliklerini içeren senaryolar üzerinden ChatGPT'nin klinik muhakeme ve ayırıcı tanı yaklaşımını değerlendirmek amacıyla hazırlanmıştır.

Araştırmada kullanılan soru seti aşağıdaki sorulardan oluşmaktadır:

Tanım Soruları

1. İşitmesi normal olan bireyde gürültüde konuşmayı anlamama hangi bozuklukla ilişkilidir?
2. Seslere aşırı hassasiyet hangi bozukluğu düşündürür?
3. İşitsel bilginin merkezi düzeyde işlenmesindeki güçlük hangi bozuklukla ilişkilidir?
4. Çoklu duyusal uyaranlara aşırı tepki hangi bozuklukta görülür?
5. Duyusal uyaranlara karşı regülasyon bozukluğu hangi durumu düşündürür?
6. İşitsel ayırt etmede güçlük hangi bozuklukla ilişkilidir?
7. Duyusal aşırı yüklenme (sensory overload) hangi bozuklukla daha uyumludur?

Karşılaştırma Soruları

8. APD ile SPD arasındaki temel fark nedir?
9. APD'de problem daha çok hangi düzeydedir (periferik/merkezi/duyusal)? SPD ile karşılaştırınız.
10. SPD hangi duyusal sistemleri kapsar? APD ile farkını açıklayınız.
11. İşitsel odaklı bir sorun ile genel duyusal düzenleme sorunu arasındaki fark nedir?
12. Sadece işitsel zorluk bulunması SPD tanısını dışlar mı?
13. Gürültüde konuşmayı anlamama hem APD hem de SPD'de görülebilir mi?
14. APD ve SPD'de dikkat sorunları nasıl farklı açıklanır?

Klinik Vaka Değerlendirme Soruları

15. **Vaka 1:** 8 yaşındaki bir çocuğun ailesi, çocuğun özellikle kalabalık sınıf ortamlarında öğretmeninin söylediklerini kaçırdığını, uzun cümleleri tekrar etmekte zorlandığını ve gürültülü ortamlarda konuşmaları anlamakta güçlük yaşadığını bildirmektedir. Ancak ev ortamında konuşmaları genellikle anladığı belirtilmiştir. Ayrıca seslerin geldiği yönü belirlemede zorlandığı ve bazen aynı kelimeyi farklı zamanlarda farklı şekilde anladığı ifade

ISBN NR. : 978-625-8795-33-2

edilmektedir. Sessiz ortamda daha iyi performans gösterdiği ancak dikkatini sürdüremediği gözlenmektedir. **Bu belirtiler göz önüne alındığında olası tanı nedir?**

Vaka 2: 7 yaşındaki bir çocuğun ailesi, çocuğun günlük yaşamda seslere karşı aşırı hassasiyet gösterdiğini, elektrik süpürgesi, kalabalık ortamlar ve yüksek sesli çevrelerde yoğun huzursuzluk yaşadığını belirtmektedir. Çocuk bazı sesleri diğer bireylerin fark etmediği şekilde fark ettiğini ifade etmekte ve bu durum karşısında rahatsızlık göstermektedir. Yoğun çevresel uyaranların olduğu sınıf gibi ortamlarda sürekli hareket etmekte ve ortamdan kaçmak istemektedir. **Bu belirtiler göz önüne alındığında olası tanı ne olabilir?**

16. **Vaka 3:** 9 yaşındaki bir çocuğun ailesi, çocuğun hem konuşmaları anlamada zorlandığını hem de gürültülü ortamlarda aşırı rahatsızlık yaşadığını bildirmektedir. Çocuk zaman zaman sessiz ortamlarda bile bazı sesleri yanlış algıladığını ifade etmekte, kalabalık ortamlarda ise çabuk yorulmakta ve dikkatini sürdürmekte zorlanmaktadır. Ayrıca grup aktivitelerinde kendisine seslenildiğinde duymuyormuş veya ilgisizmiş gibi görünmekte ve sosyal grup etkinliklerinden kaçınma eğilimi göstermektedir. **Bu belirtiler göz önüne alındığında olası tanı ne olabilir?**

2.3. Veri Toplama Süreci

Araştırma kapsamında oluşturulan soru seti aynı sohbet oturumunda ardışık olarak ChatGPT'ye yöneltilmiştir. Tanım, karşılaştırma ve klinik vaka kategorilerinde yer alan sorulara verilen yanıtlar kayıt altına alınmış ve değerlendirme sürecinde kullanılmak üzere belgelenmiştir. Aynı soru seti ayrıca alanında deneyimli iki bağımsız odyoloğa yöneltilmiş ve verdikleri yanıtlar referans yanıt olarak kayıt altına alınmıştır.

2.4. Değerlendirme Süreci ve Puanlama

ChatGPT ve iki odyolog aynı soru setini bağımsız olarak yanıtlamıştır. Odyologların yanıtları referans yanıt olarak kabul edilmiştir. İlk aşamada ChatGPT'nin yanıtları, referans yanıtlarla karşılaştırılarak araştırmacı tarafından 0–2 puanlama sistemi doğrultusunda değerlendirilmiştir.

Değerlendirmede aşağıdaki ölçütler dikkate alınmıştır:

- Doğru kavrama eşleştirme: ChatGPT'nin verilen belirti, durum veya vaka senaryosunu uygun bozukluk (APD veya SPD) ile ilişkilendirebilme başarısı.
- Ayırt edici özellik kullanımı: ChatGPT'nin APD ve SPD'yi birbirinden ayıran klinik özellikleri doğru tanımlayabilme ve açıklamalarında kullanabilme düzeyi.
- Açıklama derinliği: Yanıtın yalnızca doğru kavramı belirtmekle sınırlı kalmayıp klinik açıdan yeterli gerekçe ve açıklama içermesi.
- Klinik vaka yorumlama: Vaka senaryolarında sunulan bilgileri bütüncül olarak değerlendirerek uygun tanı veya ayırıcı tanı yaklaşımı geliştirebilme düzeyi.

Yanıtların doğruluk düzeyi üçlü puanlama sistemi kullanılarak değerlendirilmiştir.

ISBN NR. : 978-625-8795-33-2

0 puan (Yanlış): Yanıtın bilimsel olarak hatalı olması, APD ve SPD kavramlarının yanlış tanımlanması veya belirgin biçimde karıştırılması.

1 puan (Kısmen Doğru): Yanıtın genel olarak doğru kavrama işaret etmesi ancak açıklamanın eksik olması, ayırt edici özelliklerin yeterince vurgulanmaması veya kavramlar arasında kısmi karışıklık bulunması.

2 puan (Doğru): Yanıtın doğru kavramı içermesi, yeterli açıklama sunması ve APD ile SPD arasında açık ve doğru bir ayrım yapması.

İkinci aşamada ise ChatGPT tarafından oluşturulan yanıtlar, iki bağımsız odyoloğa bilimsel doğruluk açısından değerlendirmeleri amacıyla sunulmuştur. Odyologlar her bir yanıtı 0–2 puanlama sistemi kullanarak bağımsız olarak puanlamıştır. Elde edilen puanlar, odyologlar arası uyumun ve ChatGPT'nin performansının istatistiksel olarak değerlendirilmesinde kullanılmıştır.

2.5. İstatistiksel Analiz

Araştırmacı tarafından gerçekleştirilen karşılaştırmalı değerlendirme sonucunda elde edilen doğru, kısmen doğru ve yanlış yanıtların sayı ve yüzdeleri hesaplanarak betimsel olarak sunulmuştur. ChatGPT'nin tanım, karşılaştırma ve klinik vaka sorularındaki performansı kategori bazında değerlendirilmiş ve başarı oranları hesaplanmıştır.

Odyologlar tarafından ChatGPT yanıtlarına verilen puanlar IBM SPSS Statistics 22 programı kullanılarak analiz edilmiştir. Verilerin analizinde betimsel istatistikler (ortalama, standart sapma, minimum ve maksimum değerler) hesaplanmıştır. İki bağımsız odyoloğun puanlama uyumunu değerlendirmek amacıyla Sınıf İçi Korelasyon Katsayısı (Intraclass Correlation Coefficient, ICC) analizi uygulanmıştır. ICC analizinde Two-Way Mixed Effects modeli ve Absolute Agreement yaklaşımı kullanılmıştır. Tüm istatistiksel analizlerde anlamlılık düzeyi $p<0,05$ olarak kabul edilmiştir.

3. BULGULAR

3.1. Araştırmacının ChatGPT ve Odyolog Yanıtlarını Karşılaştırmalı Değerlendirmesi

ChatGPT'nin işitsel işlemleme bozukluğu (APD) ve duyusal işlemleme bozukluğu (SPD) kavramlarını ayırt etme performansı, tanım, karşılaştırma ve klinik vaka değerlendirme sorularından oluşan toplam 17 soru üzerinden araştırmacı tarafından değerlendirilmiştir. ChatGPT’nin yanıtları, aynı soru setini bağımsız olarak yanıtlayan iki odyoloğun referans yanıtları ile araştırmacı tarafından karşılaştırılmış ve bu karşılaştırma doğrultusunda her bir soru için 0–2 puan verilmiştir. Soru bazında elde edilen karşılaştırma sonuçları ve araştırmacı puanları Çizelge 1'de sunulmuştur.

Çizelge 1. ChatGPT ve Odyolog Yanıtları Karşılaştırılması ile Araştırmacı Değerlendirmesi

ISBN NR. : 978-625-8795-33-2

Soru No	Sorular	ChatGPT Yanıtı	1. Odyolog Yanıtı	2. Odyolog Yanıtı	Araştırmacı Puanı
1	İşitmesi normal olan bireyde gürültüde konuşmayı anlamama hangi bozuklukla ilişkilidir?	APD	APD	APD	2
2	Seslere aşırı hassasiyet hangi bozukluğu düşündürür?	Hiperakuzi	SPD	Hiperakuzi	1
3	İşitsel bilginin merkezi düzeyde işlenmesindeki güçlük hangi bozuklukla ilişkilidir?	APD	APD	APD	2
4	Çoklu duyusal uyaranlara aşırı tepki hangi bozuklukta görülür?	SPD	SPD	SPD	2
5	Duyusal uyaranlara karşı regülasyon bozukluğu hangi durumu düşündürür?	SPD	SPD	SPD	2
6	İşitsel ayırt etmede güçlük hangi bozuklukla ilişkilidir?	APD	APD	APD	2
7	Duyusal aşırı yüklenme (sensory overload) hangi bozuklukla daha uyumludur?	SPD	SPD	SPD	2
8	APD ile SPD arasındaki temel fark nedir?	APD-SPD ayrımını doğru açıklamıştır	Benzer	Benzer	2
9	APD'de problem daha çok hangi düzeydedir (periferik / merkezi / duyusal)? SPD ile karşılaştırınız.	APD merkezi, SPD çoklu duyusal işlemleme	Benzer	Kısmen benzer	2
10	SPD hangi duyusal sistemleri kapsar? APD ile farkını açıklayınız.	SPD'nin çoklu duyusal sistemleri kapsadığını açıklamıştır	Benzer	Benzer	2
11	İşitsel odaklı bir sorun ile genel duyusal düzenleme sorunu arasındaki fark nedir?	İşitsel odaklı sorun ile genel duyusal düzenleme sorununu ayırt etmiştir	Benzer	Yanıt vermedi	1
12	Sadece işitsel zorluk bulunması SPD tanısını dışlar mı?	SPD tanısını dışlamayacağını belirtmiştir	Benzer	Benzer	2
13	Gürültüde konuşmayı anlamama hem APD hem de SPD'de görülebilir mi?	Her iki bozuklukta da görülebileceğini belirtmiştir	Benzer	Benzer	2
14	APD ve SPD'de dikkat sorunları nasıl farklı açıklanır?	Dikkat sorunlarının nedenlerini ayırt etmiştir	Benzer	Benzer	2
15	**Vaka 1** – 8 yaşındaki bir çocuğun ailesi, çocuğun özellikle kalabalık sınıf ortamlarında öğretmeninin söylediklerini kaçırdığını, uzun cümleleri tekrar etmekte zorlandığını ve gürültülü ortamlarda konuşmaları anlamakta güçlük yaşadığını bildirmektedir. Ancak ev ortamında	APD	APD	APD	2

ISBN NR. : 978-625-8795-33-2

	konuşmaları genellikle anladığı belirtilmiştir. Ayrıca seslerin geldiği yönü belirlemede zorlandığı ve bazen aynı kelimeyi farklı zamanlarda farklı şekilde anladığı ifade edilmektedir. Sessiz ortamda daha iyi performans gösterdiği ancak dikkatini sürdüremediği gözlenmektedir. Bu belirtiler göz önüne alındığında olası tanı nedir?				
16	**Vaka 2** – 7 yaşındaki bir çocuğun ailesi, çocuğun günlük yaşamda seslere karşı aşırı hassasiyet gösterdiğini, elektrik süpürgesi, kalabalık ortamlar ve yüksek sesli çevrelerde yoğun huzursuzluk yaşadığını belirtmektedir. Çocuk bazı sesleri diğer bireylerin fark etmediği şekilde fark ettiğini ifade etmekte ve bu durum karşısında rahatsızlık göstermektedir. Yoğun çevresel uyaranların olduğu sınıf gibi ortamlarda sürekli hareket ediyor ve ortamdan kaçmak istiyor. Bu belirtiler göz önüne alındığında olası tanı ne olabilir?	SPD	APD+SPD	APD	1
17	**Vaka 3** – 9 yaşındaki bir çocuğun ailesi, çocuğun hem konuşmaları anlamada zorlandığını hem de gürültülü ortamlarda aşırı rahatsızlık yaşadığını bildirmektedir. Çocuk zaman zaman sessiz ortamlarda bile bazı sesleri yanlış algıladığını ifade etmekte, kalabalık ortamlarda ise çabuk yorulmakta ve dikkatini sürdürmekte zorlanmaktadır. Ayrıca grup aktivitelerinde kendisine seslenildiğinde duymuyormuş veya ilgisizmiş gibi görünmekte ve sosyal grup etkinliklerinden kaçınma eğilimi göstermektedir. Bu belirtiler göz önüne alındığında olası tanı ne olabilir?	APD+SPD	APD+SPD	SPD	1

Çizelge 1 incelendiğinde, araştırmacı değerlendirmesine göre ChatGPT'nin 17 sorunun 14'ünde tam uyum (2 puan), 3 soruda ise kısmi uyum (1 puan) gösterdiği belirlenmiştir. Kısmi uyum gösteren sorular, bir tanım sorusu (Soru 2), bir karşılaştırma sorusu (Soru 11) ve bir klinik vaka sorusundan (Soru 16) oluşmaktadır. Araştırmacı değerlendirmesi sonucunda elde edilen toplam puan ve kategori bazındaki başarı oranları Çizelge 2'de sunulmuştur.

Çizelge 2. Kategori Bazında Performans

ISBN NR. : 978-625-8795-33-2

Soru Kategorisi	Soru Numaraları	Soru Sayısı	Maksimum Puan	Elde Edilen Puan	Başarı Yüzdesi (%)
Tanım Soruları	1–7	7	14	13	%92,9
Karşılaştırma Soruları	8–14	7	14	13	%92,9
Klinik Vaka Soruları	15–17	3	6	4	%66,7
Toplam	1–17	17	34	30	%88,2

Çizelge 2 incelendiğinde, ChatGPT'nin araştırmacı değerlendirmesi sonucunda toplam 34 puan üzerinden 30 puan aldığı ve genel başarı oranının %88,2 olduğu görülmektedir. Kategori bazında değerlendirildiğinde, tanım ve karşılaştırma sorularında 14 puan üzerinden 13 puan elde edilmiş ve başarı oranı %92,9 olarak hesaplanmıştır. Klinik vaka değerlendirme sorularında ise 6 puan üzerinden 4 puan elde edilmiş ve başarı oranı %66,7 olarak bulunmuştur. Buna göre en yüksek başarı oranı tanım ve karşılaştırma sorularında (%92,9), en düşük başarı oranı ise klinik vaka sorularında (%66,7) elde edilmiştir.

3.2. ChatGPT Yanıtlarının Odyologlar Tarafından Değerlendirilmesi

Araştırmacı değerlendirmesinin ardından her iki odyolog, ChatGPT yanıtlarını birbirinden bağımsız olarak puanlanmıştır. Odyologların soru bazında verdikleri puanlar Çizelge 3'te sunulmuştur.

Çizelge 3. Odyologların ChatGPT yanıtlarına verdiği puanlar.

Soru No	Sorular	ChatGPT Yanıtı	1.Odyolog Puanlaması	2.Odyolog Puanlaması
1	İşitmesi normal olan bireyde gürültüde konuşmayı anlamama hangi bozuklukla ilişkilidir?	APD	2	2
2	Seslere aşırı hassasiyet hangi bozukluğu düşündürür?	Hiperakuzi	1	2
3	İşitsel bilginin merkezi düzeyde işlenmesindeki güçlük hangi bozuklukla ilişkilidir?	APD	2	2
4	Çoklu duyusal uyaranlara aşırı tepki hangi bozuklukta görülür?	SPD	2	2
5	Duyusal uyaranlara karşı regülasyon bozukluğu hangi durumu düşündürür?	SPD	2	2
6	İşitsel ayırt etmede güçlük hangi bozuklukla ilişkilidir?	APD	2	2
7	Duyusal aşırı yüklenme (sensory overload) hangi bozuklukla daha uyumludur?	SPD	2	2
8	APD ile SPD arasındaki temel fark nedir?	APD-SPD ayrımını doğru açıklamıştır	2	1
9	APD'de problem daha çok hangi düzeydedir (periferik / merkezi / duyusal)? SPD ile karşılaştırınız.	APD merkezi, SPD çoklu duyusal işlemleme	2	1

ISBN NR. : 978-625-8795-33-2

10	SPD hangi duyusal sistemleri kapsar? APD ile farkını açıklayınız.	SPD'nin çoklu duyusal sistemleri kapsadığını açıklamıştır	2	2
11	İşitsel odaklı bir sorun ile genel duyusal düzenleme sorunu arasındaki fark nedir?	İşitsel odaklı sorun ile genel duyusal düzenleme sorununu ayırt etmiştir	1	1
12	Sadece işitsel zorluk bulunması SPD tanısını dışlar mı?	SPD tanısını dışlamayacağını belirtmiştir	2	2
13	Gürültüde konuşmayı anlamama hem APD hem de SPD'de görülebilir mi?	Her iki bozuklukta da görülebileceğini belirtmiştir	2	2
14	APD ve SPD'de dikkat sorunları nasıl farklı açıklanır?	Dikkat sorunlarının nedenlerini ayırt etmiştir	2	2
15	**Vaka 1** – 8 yaşındaki bir çocuğun ailesi, çocuğun özellikle kalabalık sınıf ortamlarında öğretmeninin söylediklerini kaçırdığını, uzun cümleleri tekrar etmekte zorlandığını ve gürültülü ortamlarda konuşmaları anlamakta güçlük yaşadığını bildirmektedir. Ancak ev ortamında konuşmaları genellikle anladığı belirtilmiştir. Ayrıca seslerin geldiği yönü belirlemede zorlandığı ve bazen aynı kelimeyi farklı zamanlarda farklı şekilde anladığı ifade edilmektedir. Sessiz ortamda daha iyi performans gösterdiği ancak dikkatini sürdüremediği gözlenmektedir. Bu belirtiler göz önüne alındığında olası tanı nedir?	APD	2	2
16	**Vaka 2** – 7 yaşındaki bir çocuğun ailesi, çocuğun günlük yaşamda seslere karşı aşırı hassasiyet gösterdiğini, elektrik süpürgesi, kalabalık ortamlar ve yüksek sesli çevrelerde yoğun huzursuzluk yaşadığını belirtmektedir. Çocuk bazı sesleri diğer bireylerin fark etmediği şekilde fark ettiğini ifade etmekte ve bu durum karşısında rahatsızlık göstermektedir. Yoğun çevresel uyaranların olduğu sınıf gibi ortamlarda sürekli hareket ediyor ve ortamdan kaçmak istiyor. Bu belirtiler göz önüne alındığında olası tanı ne olabilir?	SPD	1	2
17	**Vaka 3 -**– 9 yaşındaki bir çocuğun ailesi, çocuğun hem konuşmaları anlamada zorlandığını hem de gürültülü ortamlarda aşırı rahatsızlık yaşadığını bildirmektedir. Çocuk zaman zaman sessiz ortamlarda bile bazı sesleri yanlış algıladığını ifade etmekte, kalabalık ortamlarda ise çabuk yorulmakta ve dikkatini sürdürmekte zorlanmaktadır. Ayrıca	APD+SPD	2	2

ISBN NR. : 978-625-8795-33-2

	grup aktivitelerinde kendisine seslenildiğinde duymuyormuş veya ilgisizmiş gibi görünmekte ve sosyal grup etkinliklerinden kaçınma eğilimi göstermektedir. Bu belirtiler göz önüne alındığında olası tanı ne olabilir?			

Çizelge 3 incelendiğinde, birinci odyoloğun ChatGPT yanıtlarının 14'üne 2 puan, 3'üne ise 1 puan verdiği; ikinci odyoloğun ise 13 yanıta 2 puan, 4 yanıta 1 puan verdiği görülmektedir. İki odyolog tarafından 13 soruda aynı puan verilmiş, dört soruda ise puan farklılığı gözlenmiştir.

Çizelge 4. Odyolog puanlarına ilişkin betimsel istatistikler

	Sayı	Minimum	Maximum	Ortalama	Standart sapma
ODY1	17	1	2	1,82	,393
ODY2	17	1	2	1,82	,393
Sayı	17				

Çizelge 4 incelendiğinde, her iki odyoloğun ChatGPT yanıtlarına verdiği ortalama puan 1,82±0,39 olarak hesaplanmıştır. Her iki odyoloğun puanları 1 ile 2 arasında değişmektedir.

Çizelge 5. Değerlendiriciler arası uyum (ICC) analizi sonuçları

ICC	95% GA Alt	95% GA Üst	p
0,190	-0,305	0,605	0,225

İki yönlü karma etki modeli ve tutarlılık (Consistency) yaklaşımı kullanılarak yapılan ICC analizi sonucunda, tekil ölçümler için ICC değeri 0,190 (95% GA:-0,305–0,605) olarak hesaplanmıştır. Bu sonuç, iki odyoloğun ChatGPT yanıtlarına verdikleri puanlar arasında düşük düzeyde uyum olduğunu göstermektedir.

4. TARTIŞMA

Bu çalışmada ChatGPT'nin işitsel işlemleme bozukluğu (APD) ve duyusal işlemleme bozukluğu (SPD) kavramlarını ayırt etme yeterliliği değerlendirilmiştir. Araştırmacı değerlendirmesi sonucunda ChatGPT'nin yanıtlarının büyük bölümünün odyologların referans yanıtlarıyla uyumlu olduğu, yalnızca üç soruda kısmi uyum gösterdiği belirlenmiştir. ChatGPT'nin özellikle tanım ve karşılaştırma sorularında yüksek performans sergilediği, klinik vaka sorularında ise görece daha düşük performans gösterdiği görülmüştür. Genel başarı oranının %88,2 olarak bulunması, ChatGPT'nin APD ve SPD'ye ilişkin temel kavramsal bilgileri büyük ölçüde doğru kullanabildiğini göstermektedir. Bu bulgu, ChatGPT'nin odyoloji alanındaki performansını değerlendiren önceki çalışmalarla uyumludur. Qi ve ark. (2025),

ISBN NR. : 978-625-8795-33-2

ChatGPT'nin standartlaştırılmış odyolog yeterlilik sınavında başarılı performans gösterdiğini bildirirken, Karaçaylı ve ark. (2025) odyogram yorumlamada, Ratuszniak ve ark. (2025) ise pediatrik odyoloji alanında benzer şekilde yüksek doğruluk düzeyleri rapor etmiştir.

Bu çalışmada araştırmacı değerlendirmesine ek olarak ChatGPT yanıtları iki bağımsız odyolog tarafından da puanlanmıştır. ICC analizi sonucunda iki odyoloğun puanları arasında düşük düzeyde uyum saptanmıştır. Bununla birlikte, iki odyoloğun puanlarının büyük ölçüde benzer olduğu görülmektedir. Nitekim iki odyolog toplam 17 sorunun 13'ünde aynı puanı vermiştir. Puan farklılıklarının yalnızca dört soruda görülmesi, örneklem büyüklüğünün sınırlı olması ve puanlama ölçeğinin dar olması ICC katsayısının düşük hesaplanmasına sebep olabilir. Bu bulgu, ChatGPT yanıtlarının genel olarak benzer biçimde değerlendirildiğini, ancak APD ve SPD gibi klinik olarak ayırıcı tanısı güç durumlarda uzmanlar arasında yorum farklılıklarının ortaya çıkabileceğini göstermektedir.

Tanım sorularında elde edilen %92,9'luk başarı oranı, ChatGPT'nin APD ve SPD ile ilişkili temel belirtileri ve kavramları doğru bozukluklarla eşleştirebildiğini göstermektedir. Bununla birlikte, tanım sorularından biri olan "Seslere aşırı hassasiyet hangi bozukluğu düşündürür?" sorusunda ChatGPT, beklenen APD-SPD ayrımı yerine hiperakuzi yanıtını vermiştir. Benzer şekilde iki odyologdan biri de aynı yanıtı vermiştir. Bu durum, seslere aşırı hassasiyet belirtisinin yalnızca SPD ile ilişkilendirilmeyip klinik uygulamada hiperakuzi gibi daha spesifik işitsel durumlar açısından da değerlendirilebildiğini göstermektedir. Bulgular, ChatGPT'nin bazı sorularda daha geniş bir klinik perspektif kullanarak alternatif açıklamalar üretebildiğini düşündürmektedir. Mapholi ve ark. (2024), duyusal işlemleme bozukluğu, işitsel işlemleme bozukluğu ve azalmış ses toleransı arasındaki ilişkinin karmaşık bir yapıya sahip olduğunu bildirmiştir. Bu nedenle söz konusu soruda ortaya çıkan görüş farklılığı, yalnızca yanlış bir eşleştirme olarak değil, farklı klinik yorumların bir yansıması olarak da değerlendirilebilir.

Karşılaştırma sorularında ChatGPT'nin APD ve SPD arasındaki temel farklılıkları başarılı şekilde açıklayabildiği görülmüştür. Özellikle APD'nin işitsel bilginin merkezi düzeyde işlenmesiyle, SPD'nin ise çoklu duyusal sistemlerden gelen bilgilerin düzenlenmesiyle ilişkili olduğunu doğru biçimde vurgulamıştır. Bu bulgu, ChatGPT'nin yalnızca tanı etiketlerini eşleştirmekle kalmayıp iki bozukluk arasındaki kavramsal ayrımı da büyük ölçüde koruyabildiğini göstermektedir.

Çalışmada en düşük başarı oranı klinik vaka değerlendirme sorularında elde edilmiştir (%66,7). Klinik vakalar, tanım ve karşılaştırma sorularından farklı olarak belirtilerin bütüncül şekilde değerlendirilmesini ve ayırıcı tanı yapılmasını gerektirmektedir. Özellikle ikinci ve üçüncü vakalarda ChatGPT ile odyologlar arasında görüş farklılıkları bulunmuştur. Bununla birlikte, aynı vakalarda odyologlar arasında da tam görüş birliği olmadığı görülmüştür. Bu durum, APD ve SPD arasındaki klinik ayrımın her zaman net olmadığını ve bazı olgularda belirtilerin birbiriyle örtüşebildiğini göstermektedir. Üçüncü vakada ChatGPT, APD ve SPD birlikteliği olasılığını vurgulamış ve iki odyologdan biri de benzer şekilde değerlendirme yapmıştır. Bu bulgu, ChatGPT'nin karmaşık klinik senaryolarda birden fazla olasılığı dikkate alabilme eğiliminde olduğunu göstermektedir. Ancak klinik karar verme süreçlerinde yalnızca semptom

ISBN NR. : 978-625-8795-33-2

temelli değerlendirmelerin yeterli olmadığı, ayrıntılı odyolojik ve duyusal değerlendirmelerin gerekli olduğu unutulmamalıdır. Bu durum, APD ve SPD belirtilerinin birlikte görülebileceğini bildiren önceki çalışmalarla uyumludur (Buffone ve Schochat, 2022; Krüger ve ark., 2001). Bu durum, yapay zekâ sistemlerinin temel kavramsal bilgileri doğru şekilde sunabilmesine karşın, klinik muhakeme gerektiren karmaşık senaryolarda dikkatli kullanılmasının gerektiğini düşündürmektedir.

Bu çalışmanın önemli bulgularından biri, bazı sorularda odyologlar arasında da görüş farklılıklarının bulunmasıdır. Bu durum, ChatGPT'nin verdiği her farklı yanıtın doğrudan hata olarak değerlendirilmemesi gerektiğini göstermektedir. Özellikle APD ve SPD gibi benzer semptomlarda farklı odyologların aynı olguyu farklı şekillerde yorumlayabilmesi mümkündür. Dolayısıyla ChatGPT'nin performansı değerlendirilirken yalnızca doğru-yanlış yaklaşımından ziyade odyolog görüşleriyle uyum düzeyi de dikkate alınmalıdır.

Çalışmanın bazı sınırlılıkları bulunmaktadır. Değerlendirme yalnızca iki odyoloğun görüşleri ile gerçekleştirilmiş olup farklı odyolog gruplarının dahil edilmesi farklı sonuçlar ortaya koyabilir. Gelecekte yapılacak çalışmalarda farklı yapay zekâ modellerinin karşılaştırılması ve daha geniş vaka örneklerinin kullanılması yararlı olabilir. Ayrıca çalışmada kullanılan soru sayısının sınırlı olması ve puanlamanın yalnızca üç basamaklı (0–2) bir ölçek üzerinden yapılmış olması, değerlendiriciler arası uyum analizini etkilemiş olabilir.

5. SONUÇ

Bu çalışmada ChatGPT'nin işitsel işlemleme bozukluğu (APD) ve duyusal işlemleme bozukluğu (SPD) kavramlarını tanımlama, karşılaştırma ve ayırt etme performansı araştırmacı değerlendirmesi ve bağımsız odyolog puanlamaları doğrultusunda değerlendirilmiştir. Elde edilen bulgular, ChatGPT'nin APD ve SPD'ye ilişkin temel kavramsal bilgileri doğru ve tutarlı biçimde sunabildiğini ve iki bozukluk arasındaki temel farklılıkları başarılı şekilde açıklayabildiğini göstermiştir. Bununla birlikte, klinik vaka değerlendirmelerinde performansın görece daha düşük olduğu ve bazı vakalarda odyolog görüşleriyle farklılıklar bulunduğu belirlenmiştir.

Bu sonuçlar, ChatGPT'nin APD ve SPD konularında bilgiye erişim, eğitim ve kavramsal destek amacıyla yararlı bir araç olarak kullanılabileceğini; ancak klinik karar verme ve ayırıcı tanı süreçlerinde uzman değerlendirmesinin yerini alamayacağını göstermektedir. Gelecekte yapılacak çalışmalarda farklı yapay zekâ modellerinin karşılaştırılması, daha fazla uzman görüşünün değerlendirme sürecine dahil edilmesi ve daha kapsamlı klinik vaka senaryolarının kullanılması önerilmektedir. Bu tür çalışmalar, yapay zekâ sistemlerinin odyoloji alanındaki potansiyel kullanım alanlarının ve sınırlılıklarının daha iyi anlaşılmasına katkı sağlayacaktır.

KAYNAKÇA

Aliyeva, A., Sari, E., Alaskarov, E., & Nasirov, R. (2024). Enhancing postoperative cochlear implant care with ChatGPT-4: A study on Artificial Intelligence (AI)-assisted patient education and support. *Cureus*, *16*(2), e53897. https://doi.org/10.7759/cureus.53897

AlSamhori, J. F., AlSamhori, A. R. F., Amourah, R. M., AlQadi, Y., Koro, Z. W., Haddad, T. R. A., AlSamhori, A. F., Kakish, D., Kawwad, M. J., Zuriekat, M., & Nashwan, A. J. (2024). Artificial intelligence for hearing loss prevention, diagnosis, and management. *Journal of Medicine, Surgery, and Public Health*, *3*, 100133. https://doi.org/10.1016/j.issn.2949-916X.2024.100133

American Academy of Audiology [AAA]. (2010). *Clinical practice guidelines: Diagnosis, treatment and management of children and adults with central auditory processing disorder*. American Academy of Audiology.

American Speech-Language-Hearing Association [ASHA]. (2005). *(Central) Auditory processing disorders* [Technical Report]. Working Group on Auditory Processing Disorders. https://doi.org/10.1044/policy.TR2005-00043

Aggarwal, K., Ravi, R., & Yerraguntla, K. (2025). Use of artificial intelligence tools by audiologists and speech-language therapists: An international survey of academicians. *Journal of Otology*, *20*(1), 20–25. https://doi.org/10.1016/j.joto.2024.11.002

Bahng, J. (2025). The potential and applications of artificial intelligence in the field of audiology. *Audiology and Speech Research*, *21*(3), 209–214. https://doi.org/10.21848/asr.250189

Birden, B. (2025). Tıp alanında ChatGPT kullanımının etik açıdan incelenmesi. *Lokman Hekim Journal*, *15*(2), 400–406. https://doi.org/10.46498/lhj.1430985

Bolulu, A., & Elkin, N. (2019). İşitsel işlemleme, bozuklukları ve potansiyeller. *İstanbul Gelişim Üniversitesi Sağlık Bilimleri Dergisi (IGUSABDER)*, *8*, 816–826.

Buffone, F. R. R. C., & Schochat, E. (2022). Sensory profile of children with Central Auditory Processing Disorder (CAPD). *CoDAS*, *34*(1), e20190282. https://doi.org/10.1590/2317-1782/20212019282

Caragli, V., Pellegrino, M., Pingani, L., Galeazzi, G. M., Soloperto, D., Genovese, E., de Filippis, C., Marioni, G., & Franz, L. (2026). Human versus AI in audiological practice: A comparative evaluation of ChatGPT and physician treatment decisions in idiopathic sudden sensorineural hearing loss. *PLOS ONE*, *21*(6), e0350549. https://doi.org/10.1371/journal.pone.0350549

Cevher, Z., & Kurnaz, E. (2024). Sensory processing disorders in children with autism spectrum disorders. *Cumhuriyet International Journal of Education*, *13*(3), 710–723. https://dx.doi.org/10.30703/cije.1437401

Çetinkaya, Ü. C., & Akyol, C. (2026). AI readiness in hearing care: Workforce attitudes, anxiety, and innovativeness from a policy perspective. *Health Policy and Technology*, *15*(1), 101219. https://doi.org/10.1016/j.hlpt.2025.101219

Dunn, W. (1997). The impact of sensory processing abilities on the daily lives of young children and their families: A conceptual model. *Infants & Young Children*, *9*(4), 23–35. https://doi.org/10.1097/00001163-199704000-00005

Elibol, F., & Pehlivanoğlu, Ş. (2024). İşitsel işlemleme bozukluğu olan çocuklar bağlamında müdahale yaklaşımları: Sistematik derleme. *Batı Anadolu Eğitim Bilimleri Dergisi*, *15*(3), 3411–3424.

Eriç, A., Özgür, E. G., Asker, Ö. F., & Bekiroğlu, N. (2024). ChatGPT ve sağlık bilimlerinde kullanımı. *Manisa Celal Bayar Üniversitesi Sağlık Bilimleri Enstitüsü Dergisi (MCBU SBED)*, *11*(1), 176–182.

Frosolini, A., Franz, L., Caragli, V., Genovese, E., de Filippis, C., & Marioni, G. (2024). Artificial intelligence in audiology: A scoping review of current applications and future directions. *Sensors*, *24*(22), 7126. https://doi.org/10.3390/s24227126

Gaeta, L. (2025). ChatAUD: The utility of generative artificial intelligence and large language models in clinical audiology communication. *The Hearing Journal*, *78*(2), 1–3. https://doi.org/10.1097/01.HJ.0001089324.97514.8c

Genç, N. (2023). Artificial intelligence in physical education and sports: New horizons with ChatGPT. *Akdeniz Spor Bilimleri Dergisi (Mediterranean Journal of Sport Science)*, *6*(3), 546–563. https://doi.org/10.38021/asbid.1291604

İçöz, Ö., & Kocabay, A. P. (2025). ChatGPT as an information source for cochlear implants: A study on accuracy and reproducibility. *European Archives of Oto-Rhino-Laryngology*, *282*(12), 6161–6168. https://doi.org/10.1007/s00405-025-09565-9

Jedrzejczak, W. W., Skarzynski, P. H., Raj-Koziak, D., Sanfins, M. D., Hatzopoulos, S., & Kochanek, K. (2024). ChatGPT for tinnitus information and support: Response accuracy and retest after three and six months. *Brain Sciences*, *14*(5), 465. https://doi.org/10.3390/brainsci14050465

Jedrzejczak, W. W., & Kochanek, K. (2024). Comparison of the audiological knowledge of three chatbots: ChatGPT, Bing Chat, and Bard. *Audiology and Neurotology*, *29*(5), 457–463. https://doi.org/10.1159/000538983

Jedrzejczak, W. W., Szkiełkowska, A., Raj-Koziak, D., Włodarczyk, E., Skarżyński, H., & Kochanek, K. (2026). How easily can AI chatbots spread misinformation in audiology and otolaryngology? *OTO Open*, *10*(1), e70204. https://doi.org/10.1002/ato2.70204

Karaçaylı, C., Tahir, E., & Altuntaş, E. E. (2025). Diagnostic interpretation of pure tone audiograms by multimodal LLMs: A comparative study of ChatGPT-5.0 and Gemini 2.5. *European Archives of Oto-Rhino-Laryngology*. Erken görünüm. https://doi.org/10.1007/s00405-025-09932-6

Kochanek, K., Skarzynski, H., & Jedrzejczak, W. W. (2024). Accuracy and repeatability of ChatGPT based on a set of multiple-choice questions on objective tests of hearing. *Cureus*, *16*(5), e59857. https://doi.org/10.7759/cureus.59857

Krüger, R. J., Krüger, J. J., Hugo, R., & Campbell, N. G. (2001). Relationship patterns between central auditory processing disorders and language disorders, learning disabilities, and sensory integration dysfunction. *Journal of Communication Disorders, Deaf Studies & Hearing Aids*, *1*(1), 1–7. (University of Pretoria publication archive).

Küçük Ceyhan, A., Aslan, C., & Doğan, E. D. (2023). Santral işitsel işlemleme bozukluğu için işitsel becerilerin iyileştirilmesine yönelik terapi yaklaşımları. *Turkish Journal of Audiology and Hearing Research (TJAHR)*, *6*(3), 112–119. https://doi.org/10.34034/tjahr.1270704

Küçükünal, İ. S. (2025). Çocuklarda santral işitsel işlemleme bozukluğuna KBB hekimlerinin yaklaşımı. *KBB-Forum*, *24*(3), 1–8.

Lin, M.-J., Hsieh, L.-C., & Chen, C.-K. (2025). Evaluating ChatGPT's concordance with clinical guidelines of Ménière's disease in Chinese. *Diagnostics*, *15*(16), 2006. https://doi.org/10.3390/diagnostics15162006

Mapholi, A., Snyman, A., Prinsloo, B., Wazara, I., Pottas, L., & le Roux, T. (2024). *Exploring the relationship between reduced sound tolerance, sensory processing disorder, and auditory processing disorder in children: A scoping review* [Yayımlanmamış bitirme tezi / kapsam analizi]. University of Pretoria.

Miller, L. J., Anzalone, M. E., Lane, S. J., Cermak, S. A., & Osten, E. T. (2007). Concept evolution in sensory integration: A proposed nosology for diagnosis. *The American Journal of Occupational Therapy*, *61*(2), 135–140. https://doi.org/10.5014/ajot.61.2.135

Pastucha, M., Ratuszniak, A., Ganca, M., Piłka, E., Drohobycka, I., Skarżyński, H., & Jedrzejczak, W. W. (2025). ChatGPT as a decision-support tool for better self-monitoring of hearing. *American Journal of Otolaryngology*, *46*(2), 104711. https://doi.org/10.1016/j.amjoto.2024.104711

Portelli, D., Loteta, S., D'Angelo, M., Galletti, C., Freni, L., Bruno, R., Ciodaro, F., Alibrandi, A., & Alberti, G. (2025). ChatGPT and Microsoft Copilot for cochlear implant side selection:

A preliminary study. *Audiology Research*, *15*(4), 100. https://doi.org/10.3390/audiolres15040100

Pourhoseingholi, M. A., Killan, C., Rafiee, S., Hoare, D. J., Wray, N., & Bateman, P. (2025). Validity, reliability, and readability of Artificial Intelligence chatbots as public sources of information on hearing loss: A comparative evaluation of ChatGPT, Bing, Gemini, and Perplexity. *International Journal of Audiology*. Erken görünüm. https://doi.org/10.1080/14992027.2025.2569927

Qi, B., Zheng, Y., Wang, Y., & Xu, L. (2025). Comparison of ChatGPT and DeepSeek on a standardized audiologist qualification examination in Chinese: Observational study. *JMIR Formative Research*, *9*, e79534. https://doi.org/10.2196/79534

Ratuszniak, A., Gos, E., Lorens, A., Skarzynski, P. H., Skarzynski, H., & Jedrzejczak, W. W. (2025). Performance of ChatGPT in pediatric audiology as rated by students and experts. *Journal of Clinical Medicine*, *14*(3), 875. https://doi.org/10.3390/jcm14030875

Swanepoel, D. W., & Manchaiah, V. (2024). The transformative potential of AI chatbots in hearing health care. *The Hearing Journal*, *77*(7), 1–4. https://doi.org/10.1097/01.HJ.0001026132.88583.bd

Torun, M. T. (2024). Yapay zeka otoloji ve odyoloji alanlarına ne yenilikler getirdi? *Journal of Medical Sciences*, *5*(4), 149–154.

Türer, F., & Köse, S. (2023). Nörogelişimsel bozukluklar ve duyusal işlemleme. *Turkish Journal of Child and Adolescent Mental Health*, *30*(2), 97–104. https://doi.org/10.4274/tjcamh.galenos.2021.40427

Yiğit, S., Berşe, S., & Dirgar, E. (2023). Yapay zekâ destekli dil işleme teknolojisi olan ChatGPT'nin sağlık hizmetlerinde kullanımı. *Eurasian Journal of Health Technology Assessment (EHTA)*, *7*(1), 57–65.

ISBN NR. : 978-625-8795-33-2

POLİKİSTİK OVER SENDROMU VE D VİTAMİNİ ARASINDAKİ İLİŞKİ

Dr. Diyetisyen Aybüke İMİK

Atatürk Üniversitesi, ATA Tekno-kent, Protek Sağlık Hizmetleri

aybukeimik@gmail.com ORCİD ID: https://orcid.org/0000-0003-4697-812X

ÖZET

Polikistik over sendromu (PKOS), doğurganlık dönemindeki kadınlarda yaygın olarak karşılaşılan hormonal ve endokrin bir bozukluktur. Over fonksiyonlarındaki bozulma ve hormonal düzenlemedeki değişiklikler, bu durumun temel özelliklerini oluşturmakta ve çok çeşitli üreme ve metabolik bozukluklara yol açmaktadır. Sendrom, tek bir bulgu ile tanımlanmak yerine aşırı androjen aktivitesi, düzensiz veya gerçekleşmeyen ovülasyon ve overlerde karakteristik yapısal değişiklikleri içeren geniş bir klinik tabloyu kapsamaktadır. D vitamini, mineral metabolizmasındaki bilinen rolünün yanı sıra immün düzenleme, sinir sistemi fonksiyonları, insülin yanıtı yoluyla metabolik homeostaz ve normal üreme süreçlerinin sürdürülmesinde rol oynayan çok işlevli bir endokrin düzenleyici olarak görev yapmaktadır. PKOS tanısı alan bireylerde dolaşımdaki 25-hidroksivitaminD [25(OH)D] konsantrasyonlarının genellikle düşük olduğu bildirilmektedir. Bu durumun insülin duyarlılığında azalma, menstrüel döngüde düzensizlik ve artmış androjen üretimi ile ilişkili olabileceği belirtilmektedir. Klinik çalışmalar, D vitamini takviyesinin PKOS'lu kadınlarda metabolik bozukluklar ve ovülatuvar fonksiyon üzerinde olumlu etkiler sağlayabileceğini bildirmektedir. Ancak PKOS ile D vitamini düzeyleri arasındaki ilişkiye yönelik bulguların farklılık göstermesi, bu ilişkinin henüz kesinlik kazanmadığını ortaya koymaktadır. Bu derleme, metabolik bozukluklar, üreme sağlığı ve D vitamini takviyesi sonrasında bildirilen sonuçları inceleyerek D vitamini ile PKOS arasındaki ilişkiyi değerlendirmektedir. D vitamininin terapötik yararlarının, optimal dozunun ve tedavi süresinin daha net bir şekilde belirlenebilmesi için daha geniş kapsamlı randomize klinik çalışmalara ve daha uzun takip sürelerine ihtiyaç duyulmaktadır.

Anahtar Kelimeler: polikistik over sendromu, D vitamini, insülin direnci

ISBN NR. : 978-625-8795-33-2

THE RELATIONSHIP BETWEEN POLYCYSTIC OVARY SYNDROME AND VITAMIN D

Ph.D. Dietician Aybüke İMİK

Atatürk University, ATA Techno-City, Protek Health Services

E-posta: aybukeimik@gmail.com ORCİD ID: https://orcid.org/0000-0003-4697-812X

ABSTRACT

Polycystic ovary syndrome (PCOS) is a common hormonal and endocrine disorder affecting women of reproductive age. Deterioration in ovarian functions and changes in hormonal regulation constitute the fundamental characteristics of this condition and lead to a wide range of reproductive and metabolic disorders. The syndrome encompasses a broad clinical picture characterized by excessive androgen activity, irregular or absent ovulation, and characteristic structural changes in the ovaries, rather than being defined by a single finding. Vitamin D serves as a multifunctional endocrine regulator, playing a role in immune regulation, nervous system functions, metabolic homeostasis thru insulin response, and the maintenance of normal reproductive processes, in addition to its known role in mineral metabolism. Circulating 25-hydroxyvitamin D [25(OH)D] concentrations are generally reported to be low in individuals diagnosed with PCOS. This condition may be associated with reduced insulin sensitivity, menstrual irregularities, and increased androgen production. Clinical studies suggest that vitamin D supplementation may have beneficial effects on metabolic disturbances and ovulatory function in women with PCOS. However, variations in findings regarding the relationship between PCOS and vitamin D levels indicate that this association has not yet been conclusively established. This review evaluates the relationship between vitamin D and PCOS by examining reported outcomes related to metabolic disorders, reproductive health, and vitamin D supplementation. To more clearly determine the therapeutic benefits, optimal dosage, and treatment duration of vitamin D, more extensive randomized clinical trials and longer follow-up periods are needed.

Keywords: polycystic ovary syndrome, vitamin D, insulin resistance

1.GİRİŞ

Polikistik over sendromu (PKOS), kadınların üreme döneminde ortaya çıkan endokrin hastalıklardan biridir. Prevelansı tanı kriterlerine bağlı olarak değişebilmekte olup ortalama %6-10 ‘dur. PCOS hiperandrojenizm, ovulasyon bozukluğu ve polikistik over morfolojisi ile karaketerizedir. Hastalık üreme fonksiyonları ile birlikte metabolik sağlığı da etkileyerek obezite, insülin direnci, tip 2 diyabet gelişimini artırabilmektedir (Mohan ve ark 2023).

D vitamini iskelet sistemi ile birlikte bağışıklık, sinir, kardiyovasküler sistemde etkili olup insan sağlığı açısından önemli vitamindir. D vitamininin birçok doku ve organda bulunması ile D vitamini reseptörlerinin over, endometrium ve üreme organlarında bulunması kadın üreme sağlığı açısından önemli fizyolojik işlevlere sahip olduğunu göstermektedir (Zmijewski 2019, Gorelova ve ark 2020). PCOS’lu kadınlarda D vitamini eksikliğinin sağlıklı bireylere göre daha yaygın olduğu bildirilmiş olup düşük serum 25-hidroksivitamin D [25(OH)D] düzeylerinin insülin direnci, hiperandrojenizm, adet düzensizlikleri ile ilişkili olabilmektedir (Menichini, & Facchinetti 2020). Bununla birlikte D vitamini ve PCOS arasındaki ilişki yapılan çalışmalar

ISBN NR. : 978-625-8795-33-2

doğrultusunda çift yönlü ilişki olduğu bildirilmiştir. Bazı bulgular D vitamini takviyesinin metabolik ve üreme sağlığı üzerindeki olumlu etkiler sağlayabileceği bildirilmektedir. Bu derlemenin amacı, polikistik over sendromu ile D vitamini arasındaki ilişkinin değerlendirilmesi, D vitamininin PCOS patofizyolojisindeki olası mekanizmaların incelenmesi, D vitamini takviyesinin metabolik ve üreme sağlığı üzerindeki etkilerinin mevcut bilimsel kanıtlar ile ortaya konulmasıdır.

Polikistik Over Sendromu

Polikistik over sendromu (PCOS), üreme dönemindeki kadınlarda görülen; kronik anovulasyon, hiperandrojenizm, menstrüel düzensizlikler, fertilitede azalma ve polikistik over morfolojisi ile tanımlanan endokrin bozukluktur (Can ve Türker 2023). PCOS kadınlarda yumurtalıkların işleyişini değiştiren durum olup düzensiz adet dönemleri, aşırı androjen üretimi ve polikistik overlerle belirleyici faktörleri içermektedir. Etiyolojisi tam olarak aydınlatılmaması ile birlikte genetik, çevresel, endokrin ve davranışsal faktörler etkili olabilmektedir (Azziz 2018) . PCOS patogenezinde luteinizan hormon (LH), prolaktin ve androjen hormonlarının arttığı, buna karşın seks hormon bağlayıcı globülinin (SHBG) azaldığı bildirilmektedir. Söz konusu hormonal değişimler, obezite, insülin direnci, tip 2 diabetes mellitus, hipertansiyon ve metabolik sendrom gibi metabolik bozukluklarla ilişkilendirilmektedir (Fu ve ark 2023). PCOS tanısının belirlenmesinde NIH(National Institutes of Health) ve Rotterdam kriterleri kullanılmaktadır (DiamantiKandarakis ve Dunaif, 2012). NIH kriterlerinde; kronik anovulasyon, klinik veya biyokimyasal hiperandrojenizm ve diğer nedenlerin dışlanması olup tanı almak için her iki kriterinde varlığı gereklidir. Rotterdam kriterlerinde ise oligo veya anovulasyon, klinik veya biyokimyasal hiperandrojenizm, polikistik overler ve diğer nedenlerin dışlanması (kronik arter hastalığı, cushing sendromu, tümör) olup tanı kriterlerinden ikisi bulunmalıdır. PCOS tanı kriterlerine göre prevelansı değişmekte olup bu kriterlere göre ortalama %6-10 arasında olduğu belirlenmiştir (Saddick 2020). Uzun süreli PCOS obezite, insülin direnci, tip 2 diyabet, kardiyovasküler hastalıklara neden olabileceği bildirilmiştir (Hossain ve ark 2022).

D Vitamini

D vitamini, yağda çözünen vitamin olup, sterol yapıda bir bileşiktir. Temel olarak ergokalsiferol (D2) ve kolekalsiferol (D3) olmak üzere iki farklı formda bulunmaktadır. Başlıca D vitamini kaynakları güneş ışığı, yağlı balıklar, yumurta sarısı, süt gibi besinler oluşturmaktadır. D vitamini beslenme ile D_2 ve D_3 şeklinde alınabilmektedir (Sassi ve ark 2018). Bireylerin D vitamini durumunun değerlendirilmesinde serum 25-hidroksivitamin D [25(OH)D] temel biyokimyasal gösterge olarak kullanılmaktadır. Serum düzeyinin 20 ng/mL'nin altında saptanması D vitamini eksikliği olarak değerlendirilirken, 20–30 ng/mL aralığındaki değerler D vitamini yetersizliği olarak ifade edilmektedir (Morgante ve ark 2022). D vitamini dışarıdan besin formuyla alınır veya ciltte ultraviyole ışınlarına maruz kalındığında 7-dehidrokolesterolden sentezlenir. D vitaminin vücutta etkili olabilmesi için aktif formuna dönüşmesi gerekir. Deride sentezlenen veya besinlerle alınan D vitamini biyolojik olarak aktifleşebilmesinde karaciğerde 25-hidroksilaz enzimi ile 25 hidroksivitamin D'ye daha sonra böbreklerde 1-alfa hidroksilaz enzimi ile 1,25 dihidroksi vitamin D'ye ($1,25(OH)_2$ D)

ISBN NR. : 978-625-8795-33-2

dönüşmektedir. D vitamini kemik ve kalsiyum homeostazının sağlanması ile bağışıklık sistemi, kardiyovasküler sistem solunum sistemi, sinir sistemi gibi birçok organ ve sistemde etkili olup insan sağlığı açısından önemli bir vitamindir (Saponaro ve ark 2020).

PCOS ve D Vitamini Arasındaki İlişki

D vitamini reseptörleri vücutta endometriyum ve yumurtalık gibi çeşitli dokularda bulunmaktadır. Kadınlarda döllenme ve plesanta oluşumunda etkilidir (Fang ve ark 2017, Yang ve ark 2023). Bu durum ise kadınlarda üreme fonksiyonlarında önemli olduğunu göstermektedir D vitamini eksikliğine bağlı olarak insülin direnci, obezite, hiperandrojenizm, üreme fonksiyonlarında bozulma ile PCOS gelişimine zemin hazırlayabilmektedir. PCOS'lu kadınların %67-85'inin serum 25(OH)D düzeyinin düşük olduğu bildirilmiştir (Menichini, D., & Facchinetti, F. 2020). PCOS tanısı konmuş hastaları sağlıklı bireylerle karşılaştıran çalışmalar, PCOS'lu kadınlarda serum D vitamini seviyelerinin daha düşük olduğunu ve bunun preeklampsi ve kısırlıkla ilişkili olabileceğini bildirmiştir (Bindayel 2021) Ayrıca, PCOS'lu kadınlarda D vitamini seviyeleri ile vücut kitle indeksi, serum testosteron ve dehidroepiandrosteron sülfat seviyeleri arasında anlamlı korelasyon olduğu bildirilmiştir (Gokosmanoğlu ve ark 2020). D vitamini seviyeleri ile yüksek testosteron seviyeleri nedeniyle gelişen hirsutizmin şiddeti arasında negatif bir korelasyon bulunmuştur (Mu ve ark 2021). PCOS olan bireylerde D vitamini seviyesi genellikle düşük olup Ghadimi ve ark (2014) yapmış oldukları PCOS hastası olan ve olmayan bireyler arasında D vitamini seviyeleri ölçülmüş olup PCOS olan bireylerde daha düşük D vitamini olduğu saptanmış olup destekleyen çalışmalar mevcuttur (Nestler ve ark 2012, Lin ve ark 2012, Tsakova ve ark 2012, El-Shal ve ark 2013). PCOS sendromu olan kadınlarda bu durumu desteklemeyen çalışmalarda bildirilmiştir (Güdücü ve ark 2014, Sahin ve ark 2014).

PCOS olan bireylerde D vitamini eksikliği ile birlikte obezite prevelansının artışı ile insülin direnci de gözlemlenebilmektedir. D vitamini insülin sentezi ve salgılanması ile insülin reseptör ekspresyonunu artırır buna bağlı olarak pro-enflamatuar sitokinleri baskılar. Üreme açısından ise insülin direnci sonucunda insülin ve androjen üretimini uyararak seks hormonu bağlayıcı globülin azalması ile hiperandrojenizmi artırır (Kiani ve ark 2022). D vitamini tedavisinin PCOS olan bireylerde insülin duyarlılığını artırabileceği bildirilmiştir (Tzotzas ve ark 2010, Selimoğlu ve ark 2010, Belenchia ve ark 2013). Seyyed ve ark (2018) yapmış oldukları çalışmada Pcos olan bireylerde 50.000IU D_3 vitamini haftada bir kez verilmiş olup insülin direncinde iyileşme olduğu ve açlık kan glukozunda azalma olduğu bildirilmiştir. Başka yapılan meta analiz çalışması da bu durumu destekler nitelikte olup < 4000IU D vitamini takviyesinin açlık kan glukozu, HOMA-IR değerini azalttığı insülin direncinde iyileşme olduğu bildirilmiştir (Lagowska ve ark 2018). PCOS'a bağlı olarak takviyenin serum D vitamini artması, glikoz metabolizmasının düzenlenmesi ile adet düzensizliği ve hiperandrojenizm üzerinde de olumlu etki gösterdiği bildirilmiştir (Jawed ve ark 2019,Wehr ve ark 2011, Irani ve ark 2015). Benzer şekilde, PCOS tanısı konmuş infertil kadınlarda yapılan bir çalışma, D vitamini takviyesinin insülin direncini azalttığını ve bunun da embriyo kalitesinin iyileşmesiyle ilişkili olduğunu göstermiştir (Zhao ve ark 2019).

ISBN NR. : 978-625-8795-33-2

2.SONUÇ

Bu derleme polikistik over sendromlu kadınlarda D vitamini düzeyleri ile arasındaki ilişki metabolik ve üreme sağlığı açısından değerlendiriliştir. Güncel bulgular PCOS'lu kadınlarda D vitamini eksikliğinin yaygın olarak gözlemlendiği ve düşük D vitamini düzeylerinin insülin direnci, hiperandrojenizm, adet düzensizliği ile ilişkilendirilebilmektedir. Yeterli düzeyde D vitamini takviyesinin insülin direnci, açlık kan şekeri, üreme fonksiyonu üzerinde olumlu etkiler gösterdiği çalışmalarla bildirilmiştir. Mevcut kanıtlara dayanarak D vitamini takviyesi PCOS yönetiminde destekleyici bir yaklaşım olabilir. Mevcut bulguların doğrulanması, daha uzun izlem süresine sahip ve metodolojik açıdan güçlü randomize kontrollü araştırmalarla mümkün olacaktır.

KAYNAKLAR

Azziz, Ricardo. "Polycystic ovary syndrome." *Obstetrics & Gynecology* 132.2 (2018): 321-336.

Belenchia, Anthony M., et al. "Correcting vitamin D insufficiency improves insulin sensitivity in obese adolescents: a randomized controlled trial." *The American journal of clinical nutrition* 97.4 (2013): 774-781.

Bindayel, Iman Abdullah. "Low vitamin D Level in Saudi women with polycystic ovary syndrome." *Frontiers in Nutrition* 8 (2021): 611351.

Can, Elif Naz, and Perim Fatma Türker. "Polikistik Over Sendromu." *Başkent Üniversitesi Sağlık Bilimleri Fakültesi Dergisi* 8.3 (2023): 245-257.

Diamanti-Kandarakis, Evanthia, and Andrea Dunaif. "Insulin resistance and the polycystic ovary syndrome revisited: an update on mechanisms and implications." *Endocrine reviews* 33.6 (2012): 981-1030.

El-Shal, Amal S., et al. "Genetic variation in the vitamin D receptor gene and vitamin D serum levels in Egyptian women with polycystic ovary syndrome." *Molecular biology reports* 40.11 (2013): 6063-6073.

Fang, Fang, et al. "Effect of vitamin D supplementation on polycystic ovary syndrome: A systematic review and meta-analysis of randomized controlled trials." *Complementary therapies in clinical practice* 26 (2017): 53-60.

Fu, Leyi, et al. "The association between polycystic ovary syndrome and metabolic syndrome in adolescents: a systematic review and meta-analysis." *Reproductive Sciences* 30.1 (2023): 28-40.

Ghadimi, Reza, et al. "Does vitamin D status correlate with clinical and biochemical features of polycystic ovarysyndrome in high school girls?." *Caspian journal of internal medicine* 5.4 (2014): 202.

ISBN NR. : 978-625-8795-33-2

Gokosmanoglu, Feyzi, Attila Onmez, and Hasan Ergenç. "The relationship between Vitamin D deficiency and polycystic ovary syndrome." *African health sciences* 20.4 (2020): 1880-6.

Gorelova, I. V., P. V. Popova, and M. V. Rulev. "Vitamin D and reproductive health." *Problemy Endokrinologii* 66.5 (2020): 96-101.

Güdücü, Nilgün, et al. "25-Hydroxyvitamin D levels are related to hyperinsulinemia in polycystic ovary syndrome." *Gynecological Endocrinology* 30.8 (2014): 557-560.

Hossain, Md Arju, et al. "Bioinformatics and system biology approaches to identify molecular pathogenesis of polycystic ovarian syndrome, type 2 diabetes, obesity, and cardiovascular disease that are linked to the progression of female infertility." *Informatics in Medicine Unlocked* 30 (2022): 100960.

Irani, Mohamad, et al. "Vitamin D supplementation decreases TGF-β1 bioavailability in PCOS: a randomized placebo-controlled trial." *The Journal of Clinical Endocrinology & Metabolism* 100.11 (2015): 4307-4314.

Javed, Zeeshan, et al. "A randomized, controlled trial of vitamin D supplementation on cardiovascular risk factors, hormones, and liver markers in women with polycystic ovary syndrome." *Nutrients* 11.1 (2019): 188.

Kiani, A. K., Donato, K., Dhuli, K., Stuppia, L., & Bertelli, M. Dietary supplements for polycystic ovary syndrome. *Journal of preventive medicine and hygiene*, *63*.2 Suppl 3(2022): E206.

Łagowska, Karolina, Joanna Bajerska, and Małgorzata Jamka. "The role of vitamin D oral supplementation in insulin resistance in women with polycystic ovary syndrome: a systematic review and meta-analysis of randomized controlled trials." *Nutrients* 10.11 (2018): 1637.

Lin, Ming-Wei, et al. "Vitamin D receptor 1a promotor− 1521 G/C and− 1012 A/G polymorphisms in polycystic ovary syndrome." *Taiwanese Journal of Obstetrics and Gynecology* 51.4 (2012): 565-571.

Menichini, Daniela, and Fabio Facchinetti. "Effects of vitamin D supplementation in women with polycystic ovary syndrome: a review." *Gynecological Endocrinology* (2020).

Mohan, Anmol, et al. "Vitamin D and polycystic ovary syndrome (PCOS): a review." *Annals of Medicine and Surgery* 85.7 (2023): 3506-3511.

Morgante, Giuseppe, et al. "PCOS physiopathology and vitamin D deficiency: biological insights and perspectives for treatment." *Journal of clinical medicine* 11.15 (2022): 4509.

Mu, Yang, et al. "Vitamin D and polycystic ovary syndrome: a narrative review." *Reproductive Sciences* 28.8 (2021): 2110-2117.

Nestler, John E., et al. "A pilot study: effects of decreasing serum insulin with diazoxide on vitamin D levels in obese women with polycystic ovary syndrome." *Transactions of the American Clinical and Climatological Association* 123 (2012): 209.

ISBN NR. : 978-625-8795-33-2

Saddick, Salina Y. "Identifying genes associated with the development of human polycystic ovary syndrome." *Saudi Journal of Biological Sciences* 27.5 (2020): 1271-1279.

Saponaro, F., Saba, A., & Zucchi, R. An update on vitamin D metabolism. *International journal of molecular sciences*, *21*.18 (2020): 6573.

Sahin, S., et al. "Intrinsic factors rather than vitamin D deficiency are related to insulin resistance in lean women with polycystic ovary syndrome." *European Review for Medical & Pharmacological Sciences* 18.19 (2014).

Sassi, Francesca, Cristina Tamone, and Patrizia D'Amelio. "Vitamin D: nutrient, hormone, and immunomodulator." *Nutrients* 10.11 (2018): 1656.

Selimoglu, H., Duran, C., Kiyici, S., Ersoy, C. A. N. A. N., Guclu, M., Ozkaya, G., ... & Imamoglu, S. The effect of vitamin D replacement therapy on insulin resistance and androgen levels in women with polycystic ovary syndrome. *Journal of endocrinological investigation*, *33*.4 (2010): 234-238.

Seyyed Abootorabi, M., Ayremlou, P., Behroozi-Lak, T., & Nourisaeidlou, S. The effect of vitamin D supplementation on insulin resistance, visceral fat and adiponectin in vitamin D deficient women with polycystic ovary syndrome: a randomized placebo-controlled trial. *Gynecological Endocrinology*, *34*.6 (2018): 489-494.

Thomson, R. L., Spedding, S., & Buckley, J. D. Vitamin D in the aetiology and management of polycystic ovary syndrome. Clinical endocrinology, 77.3 (2012): 343-350.

Tsakova, A. D., Gateva, A. T., & Kamenov, Z. A. 25 (OH) vitamin D levels in premenopausal women with polycystic ovary syndrome and/or obesity. *Int J Vitam Nutr Res*, *82*.6 (2012): 399-404.

Tzotzas, T., Papadopoulou, F. G., Tziomalos, K., Karras, S., Gastaris, K., Perros, P., & Krassas, G. E. Rising serum 25-hydroxy-vitamin D levels after weight loss in obese women correlate with improvement in insulin resistance. *The Journal of clinical Endocrinology & metabolism*, *95*.9 (2010): 4251-4257.

Wehr, E., Pieber, T. R., & Obermayer-Pietsch, B. Effect of vitamin D3 treatment on glucose metabolism and menstrual frequency in polycystic ovary syndrome women: a pilot study. *Journal of endocrinological investigation*, *34*.10 (2011): 757-763.

Yang, M., Shen, X., Lu, D., Peng, J., Zhou, S., Xu, L., & Zhang, J . Effects of vitamin D supplementation on ovulation and pregnancy in women with polycystic ovary syndrome: a systematic review and meta-analysis. *Frontiers in endocrinology*, *14*, (2023) 1148556.

Zhao, J., Liu, S., Wang, Y., Wang, P., Qu, D., Liu, M., ... & Li, Y . Vitamin D improves in-vitro fertilization outcomes in infertile women with polycystic ovary syndrome and insulin resistance. *Minerva medica*, *110*.3(2019): 199-208.

Zmijewski, M. A. Vitamin D and human health. *International journal of molecular sciences*, *20*.1 (2019): 145.

ISBN NR. : 978-625-8795-33-2

FARKLI ORANLARDA VERİLEN KARABUĞDAYIN MİDE ANTİOKSİDAN SEVİYELERİ VE GEN EKSPRESYONU ÜZERİNDEKİ ETKİSİ

Dr. Diyetisyen Aybüke İMİK[1]

Atatürk Üniversitesi, ATA Tekno-kent, Protek Sağlık Hizmetleri

aybukeimik@gmail.com ORCİD ID: https://orcid.org/0000-0003-4697-812X

Arş. Gör. Ömercan ALAT[2]

Atatürk Üniversitesi, Veteriner Fakültesi, Biyokimya Anabilim Dalı

E-posta: omercanalat@atauni.edu.tr ORCİD ID: https://orcid.org/0009-0000-1781-0323

ÖZET

Bu araştırma, buğday yerine farklı oranlarda karabuğday kullanımının rat mide dokusunda antioksidan parametreler ve gen ekspresyonu üzerindeki etkilerini değerlendirmek amacıyla gerçekleştirildi. Çalışma, 16 adet Sprague Dawley dişi ratın yer aldığı dört gruptan oluşan deneysel bir model olarak tasarlandı [kontrol (K): %36 buğday; deneme 1 (D1): %12 karabuğday + %24 buğday; deneme 2 (D2): %24 karabuğday + %12 buğday; deneme 3 (D3): %36 karabuğday]. Elli günlük besleme sürecinin ardından mide dokusunda antioksidan parametreler [malondialdehit (MDA), glutatyon (GSH), süperoksit dismutaz (SOD) ve katalaz (CAT)] ELISA yöntemiyle; CASP-3, BCL-2, TNF-α ve IL-1β protein ekspresyonları ise Western blot yöntemiyle analiz edildi. MDA düzeyleri değerlendirildiğinde, en yüksek değer kontrol grubunda belirlenmiş olmakla birlikte gruplar arasında istatistiksel açıdan anlamlı bir farklılık bulunmamıştır ($p>0,05$). GSH ve SOD düzeyleri en yüksek D2 grubunda belirlenirken ($p<0,01$), GSH en düşük D3 grubunda, SOD ise en düşük D1 grubunda bulunmuştur. CAT düzeylerinin gruplara göre dağılımı, en yüksek değer D3 grubunda, en düşük değer ise D1 grubunda belirlenmiş ve gruplar arasındaki bu farklılığın istatistiksel açıdan anlamlı olduğu saptanmıştır ($p<0,01$). CASP-3 ekspresyonu en yüksek D2, en düşük kontrol grubunda; BCL-2 ekspresyonu en yüksek D1, en düşük D2 grubunda; TNF-α ekspresyonu en yüksek K, en düşük D2 grubunda; IL-1β ekspresyonu ise en yüksek D3, en düşük D1 grubunda belirlenmiştir ($p<0,01$). Sonuç olarak, farklı oranlarda karabuğday tüketiminin mide dokusunda antioksidan savunma sistemi ile inflamasyon ve apoptozla ilişkili proteinlerin ekspresyonu üzerinde kullanılan orana bağlı farklı etkiler oluşturabileceği düşünülmektedir. Söz konusu etkilerin altında yatan mekanizmaların daha ayrıntılı biçimde ortaya konulabilmesi için daha büyük örneklem gruplarını içeren kapsamlı araştırmaların yürütülmesi gerekmektedir.

Anahtar Kelimeler: karabuğday, antioksidan, gen ekspresyonu

ISBN NR. : 978-625-8795-33-2

THE EFFECT OF BUCKWHEAT GIVEN IN DIFFERENT RATIOS ON STOMACH ANTIOXIDANT LEVELS AND GENE EXPRESSION

Ph.D. Dietician Aybüke İMİK[1]

Atatürk University, ATA Techno-City, Protek Health Services

E-posta: aybukeimik@gmail.com ORCİD ID: https://orcid.org/0000-0003-4697-812X

Res. Asst. Ömercan ALAT[2]

Atatürk University, Faculty of Veterinary Medicine, Department of Biochemistry

E-posta: omercanalat@atauni.edu.tr ORCİD ID: https://orcid.org/0009-0000-1781-0323

ABSTRACT:

The present study aimed to investigate how replacing wheat with buckwheat at varying proportions influences antioxidant parameters and gene expression profiles in the gastric tissue of rats. The study was designed as an experimental model consisting of four groups of 16 female Sprague Dawley rats [control (C): 36% wheat; trial 1 (T1): 12% buckwheat + 24% wheat; trial 2 (T2): 24% buckwheat + 12% wheat; trial 3 (T3): 36% buckwheat]. After a fifty-day feeding period, antioxidant parameters [malondialdehyde (MDA), glutathione (GSH), superoxide dismutase (SOD), and catalase (CAT)] in the stomach tissue were analyzed using the ELISA method; CASP-3, BCL-2, TNF-α, and IL-1β protein expressions were analyzed using the Western blot method. Although the control group exhibited the highest MDA level, no statistically significant difference was observed among the experimental groups ($p>0,05$). While the highest levels of GSH and SOD were found in group D2 ($p<0,01$), the lowest GSH levels were found in group D3, and the lowest SOD levels were found in group D1. CAT activity differed significantly among the experimental groups, reaching its highest level in the D3 group and its lowest level in the D1 group ($p<0,01$). CASP-3 expression was highest in group D2 and lowest in the control group; BCL-2 expression was highest in group D1 and lowest in group D2; TNF-α expression was highest in group K and lowest in group D2; IL-1β expression was highest in group D3 and lowest in group D1 ($p<0,01$). In conclusion, it is thot that the consumption of buckwheat in different proportions may have varying effects on the expression of the antioxidant defense system and proteins related to inflammation and apoptosis in stomach tissue. To better elucidate the mechanisms of these effects, more extensive and comprehensive studies with larger sample sizes are needed.

Keywords: buckwheat, antioxidant, gene expression

1.INTRODUCTİON

Buckwheat is a pseudocereal crop classified under the genus *Fagopyrum* within the Polygonaceae family, with *F. esculentum* Moench and *F. tataricum* being the principal cultivated taxa (Zhu, 2016; Kreft, 2016). Buckwheat is a nutrient-rich food, high in quality protein, dietary fiber, rutin, quercetin, B group vitamins, and minerals such as Na, K, Mg, Ca, Fe, Zn, and Mn (Bonafaccia et al., 2003; Pongrac et al., 2013; Ji et al., 2019; Huda et al., 2021). Additionally, it has a high antioxidant capacity due to flavonoids, phenolic acids, tannins, fagopyrin, and other bioactive components (Kreft, 2016; Zhu, 2016; Huda et al., 2021). The

ISBN NR. : 978-625-8795-33-2

absence of gluten in buckwheat makes it a suitable dietary option for people who need to exclude gluten from their diet, particularly those affected by celiac disease or gluten-related sensitivity (Wanniarachchi et al., 2023).

Oxidative stress develops when cellular antioxidant mechanisms are insufficient to counteract excessive reactive oxygen species, a condition that can disrupt cellular integrity and contribute to the development of various disorders, including gastrointestinal diseases and cancer. The flavonoid and phenolic compounds contained in buckwheat exhibit antioxidant effects by supporting the removal of free radicals (Sofi et al., 2023). Among the most common biomarkers for assessing oxidative stress are glutathione (GSH), superoxide dismutase (SOD), and malondialdehyde (MDA). While GSH plays a role in cellular antioxidant defense, SOD neutralizes superoxide radicals. MDA, on the other hand, reflects oxidative cellular damage by representing the extent of lipid peroxidation (Aslankoç et al., 2019). Nutritional components can regulate inflammation and apoptosis mechanisms by affecting gene expression. In the evaluation of these processes, CASP-3, BCL-2, IL-1β, and TNF-α are important biomarkers (Stauffer et al., 2020). While CASP-3 is one of the executor enzymes of apoptosis, BCL-2 contributes to the preservation of cell viability with its anti-apoptotic effect (Palabiyik, 2025). Expression of the inflammatory mediators IL-1β and TNF-α is enhanced following inflammatory stimulation. (Aggeletopoulou et al., 2024; Preedy et al., 2024).

Despite growing evidence regarding the antioxidant and anti-inflammatory potential of buckwheat, its effects on gastric tissue remain insufficiently characterized. In particular, limited information is available regarding how different levels of dietary buckwheat influence antioxidant defense mechanisms together with transcriptional changes in inflammation- and apoptosis-related genes. Dietary buckwheat was incorporated at varying proportions to assess changes in antioxidant parameters and CASP-3, BCL-2, IL-1β, and TNF-α gene expression in rat gastric tissue.

2.MATERIALS AND METHODS

Ethical authorization for the study was granted on February 26, 2024, by the Atatürk University Local Ethics Committee for Animal Experiments (Decision No. 35). In the study, the stomach tissue of 16 female Sprague Dawley rats, which were euthanized at an average age of 50 days, was collected and analyzed. The control group was given 36% wheat, the Test Group 1 was given 12% buckwheat + 24% wheat, the Test Group 2 was given 24% buckwheat + 12% wheat, Test Group 3 was given 36% buckwheat. In the study, the crude protein ratios in the diets of the groups were adjusted to 24,31; 24,16; 24 and 24 respectively.

2.1.Biochemical Analyzes

2.1.1.Analysis of MDA and GSH Levels in Gastric Tissue

Following disruption of the gastric tissue samples in the presence of liquid nitrogen, the powdered tissue was suspended in 1.15% KCl at a tissue-to-solution ratio of 1:10 (w/v) and subsequently homogenized. Following homogenization, the samples were centrifuged for 15 min at 1,000 × g while maintained at 4 °C. Centrifugation yielded a supernatant in which MDA content was quantified following Placer et al. (1966).MDA content was quantified based on the

ISBN NR. : 978-625-8795-33-2

reaction with thiobarbituric acid, and the absorbance of the reaction product was spectrophotometrically recorded using a wavelength of 532 nm. GSH levels were analyzed after centrifuging the tissue homogenates at 9,000 × g, following the procedure of Sedlak and Lindsay (1968).

2.1.2Analysis of CAT and SOD Enzyme Activities in Gastric Tissue

Stomach tissue samples intended for the assessment of antioxidant enzyme activities were processed using the methodology reported by Dogan T. B. (2025). The resulting supernatant fractions were subsequently used to measure SOD and CAT activities. The assay developed by Sun et al. (1988) was employed to measure SOD activity. This approach relies on the ability of SOD to suppress nitroblue tetrazolium reduction induced by superoxide radicals produced through the xanthine–xanthine oxidase reaction. Catalase activity, on the other hand, was quantified in accordance with Aebi (1984), with the obtained values normalized to the protein content of the tissue samples. Protein concentrations in gastric tissue homogenates were quantified using the Folin–Ciocalteu phenol reagent, following the protocol reported by Lowry et al. (1951)

2.1.3.Analysis of Gene Expression Levels in Stomach Tissue (qRT-PCR)

Rat gastric tissue samples were processed with QIAzol Lysis Reagent (Qiagen, Germany) to obtain RNA. Following RNA isolation, RNA yield and purity were determined by spectrophotometric analysis performed with a NanoDrop spectrophotometer. RNA served as the template for complementary DNA synthesis, which was carried out with the iScript™ cDNA Synthesis Kit (Bio-Rad, USA). Target transcript abundance was quantified in reactions containing QuantiTect SYBR Green PCR Master Mix, with amplification and fluorescence acquisition performed on a Rotor-Gene Q platform (Qiagen, Germany). Three replicate measurements were obtained for each analysis. Gene expression values from all samples were normalized against β-actin. Fold changes in mRNA abundance were derived using the $2^{-}\Delta\Delta Ct$ framework introduced by Livak & Schmittgen (2001).

Table 1. The F and R sequences of the genes

Gen	Base Series (5′-3′)	Length (bp)	Access Number
Bax	F-TTTCATCCAGGATCGAGCAG R-AATCATCCTCTGCAGCTCCA	154	NM_ 017059.2
Bcl-2	F-GACTTTGCAGAGATGTCCAG R-TCAGGTACTCAGTCATCCAC	214	NM_ 016993.2
Caspase-3	F-ACTGGAATGTCAGCTCGCAA R-GCAGTAGTCGCCTCTGAAGA	270	NM_ 012922.2
TNF- α	F: CTCGAGTGACAAGCCCGTAG R: ATCTGCTGGTACCACCAGTT	139	NM_012675.3
IL-1β	F: ATGGCAACTGTCCCTGAACT R: AGTGACACTGCCTTCCTGAA	197	NM_031512.2
ß-Actin	F: CAGCCTTCCTTCTTGGGTATG R: AGCTCAGTAACAGTCCGCCT	360	NM_031144.3

ISBN NR. : 978-625-8795-33-2

Table 2. cDNA synthesis protocol

Priming	5 min at 25 °C
Reverse transcription	20 min at 46 °C
RT inactivation	1 min at 95 °C
Optional step	Hold at 4 °C

Table 3. RT-PCR protocol

Polymerase Activation and DNA Denaturation	Denaturation	Annealing/Extension and Plate Read	Melt Curve Analysis
95 °C, 30 sec	95 °C, 5 sec (40 cycles)	60 °C, 30 sec (40 cycles)	65-95 °C 0,5 °C increments at 2-5 sec/step

For PCR amplification, a 20 µL reaction mixture was prepared for each gene using the specific primer pairs presented in Table 1, together with iTaq Universal SYBR Green Supermix (Bio-Rad), cDNA template, and RNase-free water. The quantities of the individual reaction components were adjusted in accordance with the protocol provided in Table 2. The Rotor-Gene Q platform (Qiagen, Germany) was employed for the qPCR analysis under the thermal cycling conditions detailed in Table 3. The Ct values generated during the analysis were subsequently used to determine relative fold changes in gene expression.

2.2. Statistical Analysis

Numerical findings are expressed as averages with the corresponding standard deviation (SD).Group-level variations were examined through one-way analysis of variance (ANOVA). Duncan's multiple range test was employed for post hoc comparisons whenever the overall analysis reached statistical significance, allowing identification of the groups responsible for the observed variation.

3.FINDINGS AND DISCUSSION

Table 4: Contents of antioxidant and gene expression parameters

PARAMETER	Control	Group 1	Group 2	Group 3	Probabilty
Antioxidant parameters					
MDA	3,239±0,245	3,138±0,136	3,306±0,217	3,211±0,066	0,462
SOD	$4,969±0,132^{b}$	$4,936±0,147^{b}$	$5,293±0,118^{a}$	$4,993±0,246^{b}$	0,005
GSH	$12,595±0,851^{b}$	$12,484±0,336^{b}$	$13,705±0,916^{a}$	$11,824±0,403^{b}$	0,001
CAT	$53,733±4,755^{bc}$	$49,476±4,427^{c}$	$55,851±4,811^{ab}$	$59,853±3,227^{a}$	0,005
Gene expression parameters					
Caspase-3	$1,003±0,093^{c}$	$1,315±0,126^{c}$	$4,424±0,781^{a}$	$2,400±0,312^{b}$	0,000
BCL-2	$1,00±0,006^{b}$	$1,138±0,020^{a}$	$0,510±0,022^{d}$	$0,666±0,004^{c}$	0,000
TNFα	$1,003±0,088^{a}$	$0,778±0,028^{b}$	$0,221±0,031^{d}$	$0,342±0,040^{c}$	0,000

ISBN NR. : 978-625-8795-33-2

IL-1β	1,005±0,078[c]	0,998±0,086[c]	1,313±0,024[b]	1,523±0,171[a]	0,000

3.1. Antioxidant System

Our findings showed marked group-dependent variations in gastric SOD, GSH, and CAT activities ($p<0,01$). In contrast, MDA concentrations remained statistically unchanged ($p>0,05$). Especially, the diet containing 24% buckwheat reaching the highest levels of SOD and GSH suggests that buckwheat may support the antioxidant defense system. The peak CAT activity observed with 36% buckwheat supplementation indicates that antioxidant responses may be influenced by the specific biomarker examined rather than following a uniform dose-dependent pattern. Accordingly, it can be said that the antioxidant effect of buckwheat in gastric tissue creates a parameter-specific response rather than being dose-dependent.

The present results closely resemble those documented in earlier publications. In a systematic review examining the gastrointestinal effects of buckwheat, Valid et al. (2022) concluded that available evidence points to a potential role for buckwheat in promoting digestive health through mechanisms associated with oxidative stress reduction, modulation of inflammatory processes, and protection against carcinogenic activity. Findings obtained mainly from preclinical research indicate a possible contribution of buckwheat to reducing gastrointestinal mucosal inflammation, improving the diversity of intestinal microbiota, and stimulating microbial production of short-chain fatty acids. Furthermore, previous research has demonstrated a reduction in the viability of cancer cells originating from the gastrointestinal tract following exposure to buckwheat-derived extracts. These findings indicate that buckwheat possesses significant bioactive properties that may contribute to reducing oxidative stress and inflammation in the stomach and other gastrointestinal tissues. In a review focusing on the potential detoxifying properties of buckwheat as a functional food, Rajabboyevna and Jomurodovich (2025) highlighted that its diverse phytochemical profile may contribute to protecting against oxidative stress associated with toxin exposure. Compounds including rutin, quercetin, and phenolic acids are widely acknowledged for their ability to counteract oxidative damage, regulating detoxification enzymes like glutathione S-transferase and cytochrome P450, and can also activate cellular protective mechanisms, particularly the SIRT1 pathway.

Hur et al. (2011) reported that buckwheat extract significantly increased the antioxidant capacity by enhancing the bioavailability of phenolic compounds such as rutin and quercetin. Similarly, Pande et al. (2022) demonstrated that despite BPA exposure, the consumption of buckwheat increased SIRT1 levels in gastric tissue, improved catalase, glutathione reductase, and total thiol levels, thereby providing a protective effect against oxidative stress. Kim et al. (2012) demonstrated that buckwheat intake was associated with increased concentrations of glutathione, glutathione peroxidase, and glutathione S-transferase, accompanied by a reduction in indicators of oxidative damage. These studies support the improvements in SOD, GSH, and CAT levels observed in our study. In addition to eliminating reactive free radicals, these constituents promote endogenous antioxidant defense mechanisms through activation of antioxidant enzymes. Indeed, recent reviews published in recent years emphasize that buckwheat not only increases antioxidant capacity but also serves as a functional food that

ISBN NR. : 978-625-8795-33-2

contributes to reducing oxidative stress in the gastrointestinal system. The findings obtained from our study also support this view.

Koç and Coşkun (2025) noted that the lack of gluten in buckwheat broadens its suitability for diets designed for celiac patients and people with sensitivity to gluten-containing foods. In addition to being naturally free of gluten, buckwheat provides considerable nutritional value through its protein and fiber content, balanced amino acid composition, and diverse range of biologically active constituents, while also eliciting a relatively modest glycemic response. These nutritional characteristics suggest that its consumption may offer potential benefits for glycemic control, cardiovascular health, and the maintenance of overall well-being. It is reported that especially the flavonoid components can reduce oxidative stress with their strong antioxidant properties, and thru their prebiotic effects, they can regulate the gut microbiota, thereby supporting gastrointestinal health. Its favorable nutritional profile has encouraged the inclusion of buckwheat in a broad range of products, including baked goods, pasta, fermented beverages, and foods intended to provide physiological benefits beyond basic nutrition. Despite its nutritional advantages, the absence of gluten may adversely influence product texture, making the development of suitable formulations essential

Buckwheat owes much of its antioxidant capacity to a diverse phytochemical profile, with flavonoids such as rutin and quercetin together with phenolic acids making major contributions. These compounds directly neutralize free radicals while simultaneously stimulating endogenous antioxidant enzyme systems. Indeed, recent reviews published in recent years emphasize that buckwheat not only increases antioxidant capacity but also serves as a functional food that contributes to reducing oxidative stress in the gastrointestinal system. The findings obtained from our study also support this view.

3.2. Gene Expression and Inflammation

Our findings revealed statistically significant variations among the experimental groups in the expression of Caspase-3, BCL-2, TNF-α, and IL-1β ($p<0,01$). The elevated expression of Caspase-3, particularly in the 24% and 36% buckwheat groups, suggests that high concentrations of buckwheat may activate cellular apoptotic mechanisms. In contrast, the highest expression of BCL-2 in the 12% buckwheat group and the lowest in the 24% group suggests that mechanisms related to cell survival can be regulated differently depending on the applied buckwheat dose. Additionally, TNF-α expression was greatest in the control group but reached its minimum value in the group receiving 24% buckwheat, suggesting a potential inhibitory effect of buckwheat on inflammatory activity. Meanwhile, variations observed in IL-1β expression may reflect the involvement of distinct regulatory pathways in the inflammatory process.

Current evidence suggests that the biological effects of buckwheat extend beyond its antioxidant activity, with its components also contributing to the modulation of intracellular signaling pathways. Aydın et al. (2026) reported that buckwheat contributes to the maintenance of cellular homeostasis by modulating the PI3K/AKT/mTOR, NF-κB, BCL-2, and Caspase-3 signaling pathways. Similarly, Erbaş et al. (2025) have shown that high levels of buckwheat consumption increase Caspase-3 expression while decreasing the expression of PI3K, JAK2,

ISBN NR. : 978-625-8795-33-2

STAT3, and BCL-2. These findings are consistent with the changes in Caspase-3 and BCL-2 observed in our study.

It is believed that the effects of buckwheat on cellular signaling pathways are based on the flavonoids, phenolic compounds, and other phytochemicals it contains. It has been reported that these compounds can particularly suppress the NF-κB-mediated inflammatory response, regulate the interaction between oxidative stress and inflammation, and modulate the signaling pathways that control apoptosis mechanisms. Therefore, the different expression profiles identified in our study suggest that the biological effects of buckwheat are not dependent on a single molecular mechanism, but rather occur thru a complex network of interactions regulating antioxidant defense, inflammation, and cell survival together.

4.RESULT

Overall, the present results demonstrate that buckwheat enhances antioxidant defenses in gastric tissue while influencing cellular signaling pathways. However, the fact that this effect does not appear in the same direction for all parameters suggests that the biological effect of buckwheat may vary depending on the applied dose, the biomarker studied, and the physiological characteristics of the tissue. Therefore, future molecular and functional studies that more thoroughly elucidate the interactions between buckwheat's antioxidant defense and inflammation and apoptosis mechanisms will contribute to a better understanding of its potential as a functional food.

REFRENCES

Aebi, Hugo. "[13] Catalase in vitro." *Methods in enzymology*. Vol. 105. Academic press, 1984. 121-126.

Aggeletopoulou, I., Kalafateli, M., Tsounis, E. P., & Triantos, C. Exploring the role of IL-1β in inflammatory bowel disease pathogenesis. *Frontiers in medicine*, 11(2024): 1307394.

Aydın, A., Erbaş, E., Kara, A., Özkanlar, S., Uysal, S., & İmik, H. Exploring the Potential Impact of Buckwheat (Fagopyrum esculentum) on PI3K/AKT/mTOR Signaling Pathways in Rat Ovarian Tissue. Bratislava Medical Journal, 127.4(2026): 1500-1511.

Bonafaccia, G., Marocchini, M., & Kreft, I. Composition and technological properties of the flour and bran from common and tartary buckwheat. Food chemistry, 80.1(2003): 9-15.

Dogan, T. B. Eugenol mitigates glyphosate-induced testicular toxicity via modulation of oxidative stress, ER stress, RAGE/NLRP3 and PI3K/AKT signaling pathways in rats. Reproductive Toxicology, (2025): 109038.

Erbaş, E., Uçak, G., Olgun, S., Ektaş Kalaycı, S., İmik, H., & Kara, A. Physiological and molecular effects of buckwheat-enriched diets in male rats with a focus on reproductive tissue. Acta Veterinaria Hungarica, 73.4(2025): 212-221.

Huda, M. N., S. Lu, T. Jahan, M. Ding, R. Jha, K. Zhang, W. Zhang, M. I. Georgiev, S. U. Park, and M. Zhou. Treasure from garden: Bioactive compounds of buckwheat. Food Chemistry 335(2021):127653

ISBN NR. : 978-625-8795-33-2

Hur, S. J., Park, S. J., & Jeong, C. H. Effect of buckwheat extract on the antioxidant activity of lipid in mouse brain and its structural change during in vitro human digestion. Journal of Agricultural and Food Chemistry, 59.19 (2011): 10699-10704.

Ji, X., Han, L., Liu, F., Yin, S., Peng, Q., & Wang, M. A mini-review of isolation, chemical properties and bioactivities of polysaccharides from buckwheat (Fagopyrum Mill). International Journal of Biological Macromolecules, 127(2019): 204–209

Kim, J. Y., Son, B. K., & Lee, S. S. Effects of adlay, buckwheat, and barley on transit time and the antioxidative system in obesity induced rats. Nutrition Research and Practice, 6.3(2012): 208-212.

Koç, S. T., & Coşkun, F. Buckwheat: Nutritional value, health effects and applications in foods. Turkish Journal of Agriculture-Food Science and Technology, 13.6(2025): 1665-1674.

Kreft, M. Buckwheat phenolic metabolites in health and disease. Nutrition Research Reviews, 29.1(2016):30-39.

Livak, K. J. & Schmittgen, T. D. Analysis of relative gene expression data using real-time quantitative PCR and the 2-ΔΔCT method. Methods, 25.4(2001):402-408.

Lowry, O. R. Protein measurement with the Folin phenol reagent. J biol Chem, 193.1(1951): 265-275.

Palabiyik, A. A. The role of Bcl-2 in controlling the transition between autophagy and apoptosis. Molecular Medicine Reports, 32.1(2025):172.

Pande, S., Ranjan, R., Ryazanova, M., Shuvaev, A. N., Salmina, A. B., & Kratasyuk, V. A. Buckwheat-enriched diet alleviates bisphenol A mediated oxidative stress via modulation of sirtuin 1 and antioxidant status in experimental rats. Food chemistry, 373(2022):131507.

Placer, Z. A. Estimation of product of lipid peroxidation (malonyl dialdehyde) in biochemical systems. Analytical biochemistry, 16.2(1966): 359-364.

Pongrac, P., Vogel-Mikuš, K., Jeromel, L., Vavpetič, P., Pelicon, P., Kaulich, B., ... & Kreft, I. Spatially resolved distributions of the mineral elements in the grain of tartary buckwheat (Fagopyrum tataricum). Food Research International, 54.1(2013): 125-131.

Preedy, M. K., White, M. R., & Tergaonkar, V. Cellular heterogeneity in TNF/TNFR1 signalling: live cell imaging of cell fate decisions in single cells. *Cell Death & Disease*, *15*.3(2024): 202.

Rajabboyevna, H. N., & Jomurodovich, I. U. Bıoactıve Compounds of Buckwheat (Fagopyrum Esculentum) in Detoxıfıcatıon Processes: A Comprehensıve Revıew. Food and Environment Safety Journal, 24.3(2025):176-192.

Sedlak, J. & Lindsay, R. H. Estimation of total, protein-bound, and nonprotein sulfhydryl groups in tissue with Ellman's reagent. Analytical biochemistry, 25(1968):192-205.

Sharma, S., Kumar, S., & Singh, R. K. A recent advance on phytochemicals, nutraceutical and pharmacological activities of buckwheat. Combinatorial chemistry & high throughput screening, 27.18(2024):2654-2666.

ISBN NR. : 978-625-8795-33-2

Sofi, S. A., Ahmed, N., Farooq, A., Rafiq, S., Zargar, S. M., Kamran, F., ... & Mousavi Khaneghah, A. Nutritional and bioactive characteristics of buckwheat, and its potential for developing gluten-free products: An updated overview. Food Science & Nutrition, 11.5(2023): 2256-2276.

Stauffer, W. T., Blackwood, E. A., Azizi, K., Kaufman, R. J., & Glembotski, C. C. The ER unfolded protein response effector, ATF6, reduces cardiac fibrosis and decreases activation of cardiac fibroblasts. International journal of molecular sciences, 21.4(2020): 1373.

Sun, Y. I. A simple method for clinical assay of superoxide dismutase. Clinical chemistry, 34.3(1988): 497-500.

Wanniarachchi, P. C., Pavalakumar, D., & Jayasinghe, M. A. Pseudocereals: Nutrition, health benefits, and potential applications in gluten-free food product developments. *Current Nutrition & Food Science, 19*.4(2023): 377-385.

Valido, E., Stoyanov, J., Gorreja, F., Stojic, S., Niehot, C., Kiefte-de Jong, J., ... & Glisic, M. Systematic review of human and animal evidence on the role of buckwheat consumption on gastrointestinal health. Nutrients, 15.1(2022): 1.

Zhu, F. Chemical composition and health effects of Tartary buckwheat. Food Chemistry, 203(2016): 231-245.

.

ISBN NR. : 978-625-8795-33-2

THE CHOLINERGIC ANTI-INFLAMMATORY PATHWAY: VAGAL AFFERENT SIGNALING AND BIOELECTRONIC MEDICINE

Ebru BARDAŞ ÖZKAN
Erzincan Binali Yıldırım University, Faculty of Medicine, Department of Physiology, 24100 Erzincan, TÜRKİYE

Corresponding Author: Ebru BARDAŞ ÖZKAN
E-posta: ebeytut@erzincan.edu.tr
ORCID ID: https://orcid.org/0009-0001-8752-125X

ÖZET

İnflamatuvar refleks, afferent vagal liflerin periferik inflamatuar durumu beyin sapına ilettiği ve makrofaj aktivasyonunu ve pro-inflamatuar sitokinlerin (TNF-α, IL-1β, IL-6) salınımını baskılayan efferent kolinerjik çıktıyı tetiklediği bir nöral-immün devreyi temsil eder. Bu süreç temel olarak α7 nikotinik asetilkolin reseptörü (α7nAChR) aracılığıyla gerçekleşir. İlk tanımlanmasından bu yana, bu yol fizyolojik bir merak konusundan biyoelektronik tıbbın merkezi bir paradigmasına dönüşmüş ve doğrudan sinirsel arayüzleme yoluyla sistemik inflamasyonu modüle etmek için farmakolojik olmayan özgün bir çerçeve sunmuştur. Bu derlemede, kolinerjik anti-inflamatuar yolun anatomik ve moleküler temelleri güncel literatür ışığında sentezlenmekte; özellikle tarihsel olarak efferent vagus sinir stimülasyonu (VNS) çalışmalarının gölgesinde kalmış olan afferent kol incelenmektedir. Kolin asetiltransferaz pozitif ($ChAT^+$) T hücrelerinin, vagus-dalak sinir devresinin ve organa özgü afferent sinyallemenin (hepatik ve intestinal) bölgesel ile sistemik immün yanıtları şekillendirmedeki rolleri detaylandırılmaktadır. Sepsis, inflamatuar bağırsak hastalığı (İBH) ve otoimmün artrit modellerinden elde edilen preklinik kanıtlar, kalp hızı değişkenliğinin (HRV) vagal tonun erişilebilir bir vekil biyobelirteci olarak ele alındığı, implante edilebilir ve transkutanöz kulak VNS (taVNS) cihazlarından elde edilen translasyonel verilerle birlikte değerlendirilmektedir. Ayrıca vagal efferentler ile hedef bağışıklık organları arasındaki anatomik boşluklar ve makrofaj aktivasyon durumlarının redoks duyarlılığı göz önüne alınarak bu yolun oksidatif stres biyolojisiyle entegrasyonu ele alınmaktadır.

Anahtar Kelimeler: kolinerjik anti-inflamatuar yol, vagal afferent sinyalleme, α7 nikotinik asetilkolin reseptörü, biyoelektronik tıp, inflamatuvar refleks.

ABSTRACT

The inflammatory reflex sort of acts like a neural-immune loop where the afferent vagal fibers carry the peripheral inflammatory status upstream to the brainstem, and then from there it kind of triggers an efferent cholinergic signal which, in a fairly direct sense, can calm the macrophage activation and reduce the pro-inflammatory cytokine outpouring through the α7 nicotinic acetylcholine receptor (α7nAChR). Ever since researchers first described it, this pathway hasn't only remained a physiological curiosity; it has basically become a central blueprint for bioelectronic medicine, giving a route that is not purely pharmacological for tuning whole-body inflammation using direct neural interfacing. To this end, a synthesis of anatomical and molecular evidence will be presented that focuses on the afferent vagus instead of the

ISBN NR. : 978-625-8795-33-2

efferent vagus, which has received considerable attention thus far. In particular, we will concentrate on the role of choline acetyltransferase-positive ($ChAT^+$) T cells, vagus-splenic nerve interactions and organ-specific vagus signalling. We consider emerging evidence that regional immune responses in the liver and intestine can be quite different from the rest of the body, as well as evidence on the importance of laryngeal afferents, vagus fibers that innervate multiple organs, experimental models of sepsis, inflammatory bowel disease and autoimmune arthritis, and models of disease that both translate to clinical trial designs for implantable and transcutaneous auricular VNS devices. Furthermore, since not all research groups have access to the same neural readouts, heart rate variability is considered a simple and accessible surrogate readout of vagal tone.

Key words: cholinergic anti-inflammatory, vagal afferent signalling, α7 nicotinic acetylcholine receptor, bioelectronic medicine, ,nflammatory reflex.

INTRODUCTION

The inflammatory reflex sort of acts like a neural-immune loop where the afferent vagal fibers carry the peripheral inflammatory status up to the brainstem and then from there it kind of triggers an efferent cholinergic signal which, in a fairly direct sense, can calm the macrophage activation and reduce the pro-inflammatory cytokine outpouring through the α7 nicotinic acetylcholine receptor (α7nAChR). Ever since it was first described, this is not just a physiological curiosity; it has basically become a central blueprint for bioelectronic medicine, giving a route that is not purely pharmacological for tuning whole-body inflammation using direct neural interfacing.

1.1 The Inflammatory Reflex: A Conceptual Framework

The thing sitting at the centre of this neuroimmune interface is kind of the inflammatory reflex; it was first put forward by Kevin J. Tracey, like a hard-wired, real-time circuit that works a bit like the reflex for heart rate or blood pressure (Tracey, 2002). It starts out peripherally, meaning out in tissues, where the pathogen-associated molecular patterns and damage-associated molecular patterns, PAMPs and DAMPs, as people usually say, and the proinflammatory cytokines they trigger in these local tissues, like TNF-α and IL-1β, are picked up by sensory (afferent) fibers travelling in the vagus nerve. So the early work by Niijima and later work by Watkins and Maier and others showed that systemically administered IL-1β elicited vagal afferent activation and when vagotomy or depleting vagal afferents was performed, it was found that these manipulations attenuated all the central nervous system and behavioral effects of peripheral cytokines, including fever, hyperalgesia and sickness behavior (Niijima, 1996; Ek et al., 1998).

These afferent signals are then relayed to the nucleus tractus solitarius NTS in the brainstem, where the main hub, the primary relay thing for visceral sensory and immune-related interoceptive information is located (Andresen and Yang, 1990; Berthoud and Neuhuber, 2000). From the NTS and the surrounding dorsal vagal complex, the processing of afferent signals is then relayed to the dorsal motor nucleus of the vagus (DMNX), from where the efferent parasympathetic influence arises. During the activation of these efferent pathways, the anti-inflammatory arm of the reflex is engaged. Acetylcholine is released from vagal efferent

ISBN NR. : 978-625-8795-33-2

terminals. In the spleen, acetylcholine release is executed by a unique, specialised subset of T cells expressing choline acetyltransferase ($ChAT^+$) (i.e., they are $ChAT^+$ T cells). With these cells, the idea is that they kind of shuttle the message across the synapse region between the splenic sympathetic nerve and the immune compartment.

Acetylcholine then binds to the α7 nicotinic acetylcholine receptor (α7nAChR) on tissue macrophages and many other natural immune cells (Rosas-Ballina et al., 2011). Genetic and pharmacological evidence have pretty much pinned the α7nAChR down to be essential and mostly not replaceable by other pathways in this context. Finally, agonism of the α7nAChR can suppress NF-κB driven transcription as well as the secretion of the pro-inflammatory cytokines TNF-α, IL-1β and IL-6, but not of the anti-inflammatory cytokine IL-10 (Wang et al., 2003; Borovikova et al., 2000).

1.2 From Efferent-Centered Physiology to Afferent Signal Specificity

For the first three decades of the inflammatory-reflex literature, the dominant bias was pretty strongly toward the efferent, cholinergic, anti-inflammatory arm, driven in large part by the therapeutic charm of vagus nerve stimulation (VNS) as a way to suppress the release of systemic cytokines in experimental endotoxaemia and sepsis (Borovikova et al., 2000; Pavlov et al., 2003). In that context, the afferent side was handled mostly as a kind of trigger, where its physiological richness was kind of treated as secondary to the efferent output it kicks off. More recently, however, it has been demonstrated that vagal sensory neurones in the nodose ganglion do not have stereotypic signatures for inflammatory input, but rather differentially map pro- and anti-inflammatory cytokines and can be pharmacologically and molecularly differentiated (and project to distinct subregions of the NTS) (Zanos et al., 2018; Huerta et al., 2025). The afferent vagus is now seen as an active, signal-aware sensory machine, rather than simply a passive pipe in the nervous system. This encoded pattern is likely to offer further resolution of specificity in the immune reflex, even for the specific states that are recruited in chronic low-grade inflammatory states when the signaling tinput buterent to the nodose ganglion is likely to be dysregulated (Steinberg et al., 2016; Bonaz et al., 2021). In support of this, in vivo calcium imaging demonstrated that single nodose gaal.,on neurones are able to distinguish TNF-α, IL-1β, and IL-10, and this response was lost in a murine model of colitis. So, the afferent code, per se, not merely the efferent aftermath, can be one locus for disease-related dysfunction (Huerta et al., 2025).

1.3 The Birth of Bioelectronic Medicine

The convergence of a well-defined neural circuit, a druggable and genetically tractable receptor target (α7nAChR), and an easily accessible peripheral nerve (the cervical vagus) sort of created the physiological rationale to begin a whole new therapeutic model of direct electrical or biophysical neuromodulation, rather than whole-body pharmacological manipulation, for which the term 'bioelectronic medicine' or, historically, 'electroceuticals' was coined in a widely cited 2013 white paper that laid out a multidisciplinary research agenda that left little doubt as to the intent of electrical modulation of the signaling properties of neural circuits to treat diseases (Famm et al., 2013). Since then, both intrusive and non-intrusive VNS studies targeting the cholinergic anti-inflammatory pathway have progressed beyond proof-of-concept

ISBN NR. : 978-625-8795-33-2

endotoxaemia models to formal clinical trials in prolonged inflammatory and autoimmune diseases, such as rheumatoid arthritis. Over time this whole track of work has led to regulatory approval and a licensed implantable vagus nerve stimulation device for that particular indication (Pavlov and Tracey 2022). So, this trajectory from a specific physiology observation to a licensed, non-pharmacological therapy sets up the historical arc of the present submission before Section 5 turns to a less-explored corner of the intersection of this circuitry and the immunological redox crosstalk.

2. ANATOMICAL AND MOLECULAR FOUNDATIONS

2.1 Afferent Vagal Pathway and Brainstem Integration

The vagus nerve (cranial nerve X) is a mixed nerve, and its fibre makeup is asymmetric in a really clear way. Roughly 80% of its fibres are sensory (afferent), and only about 20% are motor (efferent) (Berthoud and Neuhuber, 2000; Prescott and Liberles, 2022). This setup matters functionally too; it sort of frames the vagus as more of a pathway for interoceptive notifications coming from the viscera into the brain, not just a simple motor cable. Vagal afferent terminations ramify through the liver, the gastrointestinal tract, the lungs and the heart; there are receptors there that can spot changes in cytokine levels, plus other immune-signals. This can involve receptors tuned to IL-1β and TNF-α (Goehler et al., 1998; Ek et al., 1998). The primary sensory neurones, cell bodies tend to sit mostly in the nodose ganglion, and there is also a smaller population in the jugular ganglion, which is developmentally different in some important way (Kupari et al., 2019). From there, the central projections that come out of the nodose ganglion go to the nucleus tractus solitarius (NTS). The NTS isn't just a "wait here and pass it along" kind of station. Instead, it acts as the main integration hub in the brainstem for visceral sensory plus immune-tinged interoceptive information. Then, from the NTS, these second-order pathways start to veer off toward spots like the hypothalamus, amygdala, and the dorsal motor nucleus of the vagus (DMNX) along with other targets (Berthoud and Neuhuber, 2000; Ricardo and Koh, 1978).

When the signals project toward the paraventricular nucleus of the hypothalamus, this route connects vagal afferent input to the recruitment of the hypothalamic-pituitary-adrenal (HPA) axis. That process helps drive corticotropin-releasing hormone and, later, glucocorticoid release, but the overall pace is slower and more "humorally" mediated compared to the rapid neural reflex (Sternberg, 2006). Meanwhile, projections to the amygdala and other limbic bits are often proposed to support the emotional and behaviour patterns tied to peripheral inflammation, like sickness behaviour (Dantzer and Kelley, 2007). Also, the NTS has reciprocal connections back to the DMNX, which kind of closes the reflex circuitry. So the story is that brainstem integration, not just peripheral cytokine concentration, helps determine the efferent anti-inflammatory output.

2.2 The Vagus-Spleen Circuit and ChAT^{+} T Cells

One of the more obscure aspects of the efferent cholinergic anti-inflammatory pathway has been that vagus nerve itself does not innervate spleen (Bellinger et al. 1989; Nance and Sanders 2007). This mystery was partly explained by the late discovery that postganglionic sympathetic noradrenergic neurones in the coeliac-superior mesenteric ganglion complex do

ISBN NR. : 978-625-8795-33-2

have inputs from vagal preganglionic efferents arising from the DMNX, creating a sort of two-neurone conduit (Bellinger et al. 1989). Thus it appears that it is really the splenic nerve rather than the vagus itself that innervates the spleen (Rosas-Ballina et al., 2008). You can do a splenic nerve cut or a chemical sympathectomy, and then VNS will no longer be able to inhibit splenic TNF-α production. This essentially makes the splenic nerve an obligatory relay, not some leftover or redundant side-route (Rosas-Ballina et al., 2008).

Then norepinephrine released from a splenic nerve terminal hits the β_2-adrenergic receptor, a facilitator of the production of a form of locally synthesized ACh. Inside the spleen, $CD4^+$ T cells have been shown to express the acetylcholine synthesizing enzyme choline acetyltransferase ($ChAT^+$) and to release ACh after adrenergic stimulation. These are described as the functional "last synapse" of the reflex, preceding the binding of ACh to the α7nAChR-expressing splenic macrophages (Rosas-Ballina et al., 2011; Vida et al., 2011). Other experimental data, such as that showing that vagus nerve stimulation of inflammation could be blocked either by denervating the spleen, or by using mice with no functional T cells (e.g. athymic nude mice), supports that the lymphocyte relay was required in the older model (Vida et al., 2011).

That said, for rigour's sake, the cellular bottleneck can be contested in different ways. Simon et al. (2023) argued that in conscious, non-lymphopenic transgenic setups, splenic-nerve-derived norepinephrine may act directly on β_2-adrenergic receptors on the splenic myeloid (macrophage) cells rather than relaying through T lymphocytes (Simon et al., 2023). And a follow-up study that used systematic in situ hybridisation plus qPCR mapping was more precise, and showed that neither Chat (choline acetyltransferase) nor Chrna7 (the gene for α7nAChR) transcripts, nor ChAT-reporter-labeled cells or axons, could be found in the mouse spleen even after LPS challenge, and that β2-adrenergic receptor expression was high. These authors therefore suggested that the functional α7nAChR site for this reflex is extrasplenic, e.g. on autonomic or sensory neurones, rather than on the splenic immune cells themselves (Merchant et al., 2025).

Table 1: Bioelectronic Medicine Vagus Nerve Stimulation (VNS) Devices, Stimulation Parameters, and Clinical Translational Data

Device Type and Name	Clinical Indication	Stimulation Parameters	Target Organ / Receptor	Clinical Phase and Key Findings / Biomarkers	References
Implantable VNS (iVNS) (e.g., SetPoint Medical Microstimulator)	**Rheumatoid Arthritis (RA)**	• Frequency: 10 Hz • Current: 0.25 - 1.5 mA • Pulse Width: 200 µs • Dose: 1-4 times/day (1-	Celiac Ganglion Splenic Nerve Tissue Macrophages (α7nAChR)	Phase II / Approval Stage: Significant reduction in DAS28-CRP scores; 20-30% suppression of plasma TNF-	Koopman et al., 2016; Genovese et al., 2020

ISBN NR. : 978-625-8795-33-2

Device Type and Name	Clinical Indication	Stimulation Parameters	Target Organ / Receptor	Clinical Phase and Key Findings / Biomarkers	References
		4 min)		α, IL-6, and IL-1β levels.	
Implantable VNS (iVNS) (e.g., Cyberonics / LivaNova)	**Crohn's Disease / IBD**	• Frequency: 10 Hz • Current: 1.25 - 2.5 mA • Pulse Width: 500 µs • Dose: 30 sec on / 5 min off (Continuous)	Enteric Neurons Lamina Propria Macrophages	**Pilot / Phase II:** Clinical remission in 60-70% of patients and endoscopic/mucosal healing; significant reduction in serum CRP and faecal calprotectin levels.	Bonaz et al., 2016; D'Haens et al., 2023
Transcutaneous Auricular VNS (taVNS) (e.g., NEMOS / tVNS Technologies)	**Inflammatory Bowel Diseases (IBD) & Fibromyalgia**	• Frequency: 20-30 Hz • Current: 0.5 - 2.0 mA (below pain threshold) • Pulse Width: 200-300 µs • Dose: 1-2 hours/day	Cymba Conchae Vagal Afferent (Nodose/ NTS) Efferent Reflex	**Phase I / II:** Reduction in systemic inflammatory parameters, increase in heart rate variability (HF-HRV) and vagal tone, and clinical improvement in pain and fatigue scores.	Kaniusas et al., 2019; Bonaz et al., 2021
Non-Invasive Cervical VNS (nVNS) (e.g., gammaCore)	**Sepsis / Acute Systemic Inflammation (Preclinical & Emergency)**	• Frequency: 25 Hz • Burst stimulation: 5 kHz • Current: 24V / 60 mA max • Dose: 2 min stimulation	Cervical Vagus Trunk NTS / DMNX Systemic Immune Modulatio	**Preclinical / Phase II:** Suppression of cytokine storms in LPS-induced endotoxaemia and sepsis models.	

3. ORGAN-SPECIFIC AFFERENT SIGNALING: HEPATIC AND INTESTINAL AXES

Beyond the systemic (spleen-mediated) effects of the cholinergic anti-inflammatory

ISBN NR. : 978-625-8795-33-2

pathway, the organ-specific sensory functions of the vagal afferent system are critical for understanding the regional dynamics of neuro-immune communication. These organ-specific afferent axes demonstrate that the inflammatory reflex is not merely a "fire alarm" but rather an active regulator of tissue homeostasis.

3.1 Hepatic Afferent Signaling: The Metabolic-Immune Interface

So basically the liver is the first organ that has to deal with gut-derived PAMPs like LPS, plus DAMPs and also metabolic products (fatty acids and glucose) coming in through the portal venous system. And in that same region, vagal afferent terminals seem to have this sort of unusual sensitivity, like they react to those ligands at concentrations that are much higher than what you typically see in systemic circulation (Niijima, 1996; Berthoud and Neuhuber, 2000).

Signal Mechanism: Hepatic vagal afferents can respond to IL-1β, TNF-α, and prostaglandin E2, which are released by portal endothelial cells and Kupffer cells. The effect happens through TLR4 and cytokine receptors present on the afferent nerve endings (Ek et al., 1998; Hosoi et al., 2005). When they get hit with this, action potentials get generated in the cell bodies of the nodose ganglion, and then those signals are carried onwards to the NTS.

Physiological Consequences: Hepatic afferent stimulation is tied to how food intake gets regulated, especially around glucose and lipid balance (Schwartz, 2000; Imai and Katagiri, 2022). During these inflammatory states, this signalling then starts talking to the brainstem and hypothalamus, and there is this one region that really stands out, the arcuate nucleus. From there, it ends up steering acute-phase protein production in the liver, such as CRP and serum amyloid A, though it also helps to mould whole-body energy metabolism, for example, anorexia, and insulin resistance (Dantzer and Kelley, 2007; Romanovsky et al., 2005). Overall it acts like an early warning setup, so the liver kinda shifts its metabolic supplies toward immune work when infection shows up.

Clinical Significance: In obesity, and even in non-alcoholic fatty liver disease (NAFLD), for example, hepatic vagal afferent sensitivity appears to be weakened (Raybould, 2011). And that weakening is thought to play a role in systemic inflammation and insulin resistance (Waise et al., 2018). So it follows that the hepatic afferent axis could end up being a kind of bioelectronic target for metabolic inflammation, or at least a reasonable candidate.

3.2 Intestinal Afferent Signaling: The Microbiota Interface and Barrier Integrity

The gastrointestinal tract is one of those zones that are really heavily innervated by vagal afferent fibres, and they sort of ramble, or wind up, across a few layers of the intestinal wall—like the mucosa, lamina propria, and also the muscle layer. They basically stay alert for what's going on inside the lumen, microbial byproducts and even more local inflammatory cues, all day long, every day.

Luminal sensing: In real life, intestinal vagal afferents can kind of "get the gist" of nutrients and microbial metabolites (like, short-chain fatty acids) without actually touching them directly, more like by noticing neurotransmitters and gut hormones. Stuff such as serotonin (5-HT), cholecystokinin (CCK), and GLP-1 is released by enteroendocrine cells, for

ISBN NR. : 978-625-8795-33-2

example, L-cells and I-cells, which sit inside the intestinal epithelium (Furness et al., 2013; Kaelberer et al., 2018). And also, once the intestinal epithelial barrier starts acting a bit leaky, PAMPs like LPS, or bacterial DNA, can engage TLRs, mostly TLR4 and TLR9, right by the afferent endings (Hosoi et al., 2005).

Microbiota-derived modulation: The gut microbiota can nudge vagal efferent signalling back and forth, like steering it toward restraint or pushing it toward amplification, pretty much either way, depending on the context. For instance, probiotic strains such as Lactobacillus and Bifidobacterium can adjust responses, inhibitory versus stimulatory, and this may feed into anxiety-like behaviour and visceral sensitivity through the gut-brain loop (Bravo et al., 2011; Bercik et al., 2011). A bunch of these effects are often hooked up to serotonin receptors, specifically 5-HT_3, or to Toll-like receptors that sit right on those afferent endings, so it's really not just one clean hallway pathway. It's more like a messy set of overlapping relays, with small switches clicking in different places.

Barrier integrity and protective reflex: Barrier integrity, along with a protective reflex, in the middle of intestinal inflammation, like you'd see in colitis models, shows a pattern where vagal afferent signalling goes up and then sets off an efferent anti-inflammatory pathway. That pathway essentially runs through the NTS and the DMNX. The goal is to keep the barrier firm and to curb bacterial translocation, mostly by increasing tight junction constituents, for example, zonula occludens-1 (ZO-1) and occludin, which end up positioned within the intestinal epithelium (Krzyzaniak et al., 2011; Matteoli et al., 2014). Taken as one whole system, this circuit feels like a quite persuasive way to help mend a bruised mucosal barrier in inflammatory bowel diseases (IBD).

4. BIOELECTRONIC MEDICINE AND TRANSLATIONAL APPLICATIONS

Bioelectronic medicine is a therapeutic platform that is slowly but surely getting more mature; it tries to get around pharmacokinetic and side-effect problems we usually see with drugs by aiming at electrical cues that are already in the body, mainly in peripheral nerves (Famm et al., 2013). The cholinergic anti-inflammatory pathway is often framed as the strongest sort of "proof of concept", at least for how this whole idea could work in practice (Pavlov and Tracey, 2022).

4.1 Implantable Vagus Nerve Stimulation (iVNS)

iVNS, sent via electrodes that are surgically attached to the cervical vagus nerve, has shown pretty encouraging clinical outcomes in studies. It tends to come up especially in scenarios like drug-resistant rheumatoid arthritis and some inflammatory bowel conditions.

Rheumatoid Arthritis: In randomised controlled trials, patients with RA who received iVNS demonstrated a notable 20–30% drop in plasma TNF-α and IL-6. At the same time, clinical indicators such as DAS28-CRP (Disease Activity Score) improved more clearly in the iVNS group vs placebo (Koopman et al., 2014; Genovese et al., 2023). Taken together, these papers suggest iVNS is relatively safe and quite well tolerated, and that the biological effect tracks back to α7nAChR-mediated cytokine downregulation.

ISBN NR. : 978-625-8795-33-2

Crohn's Disease: Early pilot work implies IVNS may help push Crohn's disease toward clinical remission and may also back mucosal repair (Bonaz et al., 2017; Manrai et al., 2024). The working interpretation is that stimulation helps re-establish the intestinal epithelial barrier and simultaneously tones down local inflammation; in other words, it is not just symptomatic.

Component	Anatomical / Cellular Structure	Agent / Receptor	Physiological Function
Afferent Limb	Nodose Ganglion, NTS	Cytokine receptors, TLR4	Detection of peripheral inflammation and transmission to CNS
Central Integration	NTS, DMNX, Paraventricular Nucleus	Glutamate, GABA	Processing of reflex response and adjustment of efferent output
Efferent Limb	DMNX, Vagus Nerve, Celiac Ganglion	Acetylcholine, Norepinephrine	Splenic nerve stimulation and visceral organ regulation
Immune Relay	$ChAT^{+}$ $CD4^{+}$ T Cells	β_2-Adrenergic Receptor	Acetylcholine synthesis and release in response to norepinephrine stimulation
Target Cell	Tissue Macrophages, Monocytes	α7nAChR	NF-κB inhibition, STAT3 activation, cytokine suppression

Limitations: Even so, iVNS isn't a "plug-and-play" option; patient selection needs to be careful since there is an invasive surgical step involved, plus there can be adverse effects such as hoarseness, cough and bradycardia, so clinicians have to weigh risk benefits closely.

Table 2: Key Structural and Molecular Elements of the Cholinergic Anti-Inflammatory Pathway

4.2 Non-Invasive Transcutaneous Auricular VNS (taVNS)

To get around the invasive part and the side effect burden usually seen with cervical VNS, taVNS devices have been made; they focus on the auricular branch of the vagus nerve. This happens in the cymba conchae area on the outer ear. Even though this route typically needs a lower stimulus intensity than iVNS, it still can trigger α7nAChR-mediated anti-inflammatory responses (Kaniusas et al., 2019; Baker et al., 2023).

Clinical Applications: taVNS has been reported as rather encouraging in inflammatory bowel disorders, including ulcerative colitis and Crohn's, plus depression, migraine, and ongoing pain conditions like fibromyalgia (Bonaz et al., 2021; Farmer et al., 2021). Because it is non-invasive and can be used at home, it likely helps patient adherence the most in a practical sense.

Mechanism and Efficacy: With taVNS, afferent fibres of the auricular branch get stimulated, and then they send signals toward the NTS, which in turn engages the efferent anti-inflammatory reflex in a way that resembles cervical iVNS. That said, it is not fully settled if the mechanism is 100% the same as in cervical VNS, or if the best stimulation settings (for

ISBN NR. : 978-625-8795-33-2

example, frequency and pulse width) are identical, or whether they should be tuned separately.

4.3 Heart Rate Variability (HRV) and Vagal Tone Biomarkers

When the goal is to estimate autonomic nervous system balance without invasive steps, heart rate variability, or HRV, it is one of the most dependable approaches for capturing vagal tone (Damoun et al., 2024).

HRV as a Vagal Indicator: The high-frequency band in HRV (HF-HRV, 0.15–0.40 Hz) reflects respiratory sinus arrhythmia and is generally accepted as a valid readout of parasympathetic, meaning vagal, activity. When HF-HRV is low, it usually points toward reduced vagal tone, like a quieter “brake” system.

Correlation with Inflammation: Some clinical work has kind of shown that lower HF-HRV values go along with an inverse pattern toward higher systemic inflammation markers, like CRP, IL-6 and TNF-α (Aeschbacher et al., 2017; Williams et al., 2019). So the idea is that reduced vagal output may be part of what pushes inflammation along, the kind that doesn’t get properly regulated, or at least not in a timely way.

Role in Treatment Monitoring: HRV can function as a kind of surrogate marker for dosing bioelectronic interventions. This includes, for instance, personalising stimulation intensity and duration. In closed-loop setups, if HRV data are available in real time, the system could update stimulation parameters automatically, allowing therapy that shifts with the patient (Ottaviani et al., 2022). In other words, it could aim for the “sweet spot” of vagal tone per individual (Zanos et al., 2018).

5. UN RESOLVED MECHANISMS AND OXIDATIVE STRESS INTERACTION

5.1 Anatomical and neuro-immune synaptic gaps

The vagal efferent output to peripheral immune cells directly is the key principle behind the cholinergic anti-inflammatory pathway but remains a major unanswered question. It is currently thought that vagal neurones indirectly access macrophages by what has been termed "$ChAT^+$ T cell relays" in the spleen and elsewhere, including the gastrointestinal tract and lung. There has yet to be convincing evidence that these neuro-immune synapses actually exist and are functional.

Neuro-Immune Synapses: Cell-cell contacts are increasingly reported between the enteric nervous system and vagal terminals within the wall of the intestine and between macrophages at the intestinal lamina propria (Veiga-Fernandes and Mucida, 2016; Godinho-Silva et al., 2019). However, whether these contacts provide sufficient local concentrations of ACh to engage α7nAChR signalling remains uncertain.

Acetylcholinesterase (AChE) Barrier: Acetylcholine (ACh) is hydrolysed within milliseconds in the synaptic cleft by acetylcholinesterase (AChE) (Soreq and Seidman, 2001). Thus, ACh released from the vagal terminal has to act at short range to avoid being rapidly hydrolysed before binding to the vagus innervating α7nAChRs on parenchymal macrophages. A question, however, arises as to how these mediators (norepinephrine → ACh) can bypass this

ISBN NR. : 978-625-8795-33-2

enzymatic barrier and reach the target cells in organs without vagal innervation (e.g., spleen). The studies by Simon et al. (2023) and Merchant et al. (2025), described in Section 2.2 above, raise serious questions not only about the mechanism by which this synapse is formed in the spleen (the T-cell relay concept and targeting myeloid cells directly) but also about whether the functional locus of α7nAChR may be extrasplenic (e.g., on sympathetic neurones or sensory neurones). Further work will be needed in trying to define how this synapse might be formed outside the spleen (e.g., mesenteric lymph nodes or intestinal mucosa) (Wang et al., 2026).

5.2 Oxidative Stress and Redox Sensitivity: Integration of the α7nAChR-Nrf2 Axis

Inflammation and oxidative stress are two fundamental, interconnected pathophysiological processes in chronic diseases. Recently it was discovered that α7nAChR, as a common component for both processes, plays a role of inflammation suppressor and a strong redox regulator of the stress response in the cell (Piovesana et al., 2021).

M1/M2 Polarization and Redox: Much like polarization of immune cells can be modulated by ROS production, the polarization of macrophages towards pro-inflammatory M1 or anti-inflammatory M2 functional phenotypes can be modulated by redox: M1 polarization is associated with an increased mitochondrial concentration of ROS and decreased GSH concentration, whereas M2 polarization is associated with an increased concentration of antioxidants and decreased concentration of ROS (Mills et al., 2016; Tan et al., 2016). Oxidative stress within chronic inflammation changes this balance towards M1 and supports a continuing inflammatory response.

Redox regulatory role of α7nAChR: Cholinergic activation through α7nAChR actually kicks off two core routes for antioxidative, cytoprotective messaging: (i) Janus kinase 2 / Signal transducer and activator of transcription (JAK2/STAT3) and (ii) phosphoinositide 3-kinase, PI3K/Akt pathways, which then promote the activation plus nuclear movement of Nuclear Factor Erythroid 2-Related Factor 2 (Nrf2) (Yu et al., 2019). After the Nrf2 enters the nucleus and binds to the gene promoter's ARE, it regulates the transcription of other ARE-driven and antioxidant genes, such as the phase II antioxidants heme oxygenase 1 (HO-1), superoxide dismutase (SOD), catalase, and glutathione peroxidase (Farré-Alins et al., 2020).

Mitochondrial protection: Stimulation of α7nAChR signaling has also been reported to induce mitochondrial biogenesis, regulate mitochondrial function, inhibit mitochondrial reactive oxygen species production, regulate oxidative phosphorylation and energy metabolism in cells and stabilize the mitochondrial inner membrane potential (Skok, 2022; Gamage et al., 2020). Altogether, this is linked with a sort of “resilience” against oxidative injury, including inflammatory damage, in both cells and tissues.

Pathophysiological Relevance: This interface may offer targets for bioelectronic medicine to inhibit the production of pro-inflammatory cytokines and repair tissue damage through restoring redox balance as an explanation for the reduced efficiency of α7nAChR signalling in chronic inflammation in conditions with redox imbalance and treatment variability. Future studies may need to consider how this redox sensitivity is reflected in stimulation parameters at different disease stages.

6. Conclusion and Future Perspectives

ISBN NR. : 978-625-8795-33-2

The cholinergic anti-inflammatory pathway is a new and exciting interdisciplinary field of research, from neurophysiology and immunology to molecular biology and biomedical engineering. However, the cellular and molecular mechanisms underlying the afferent and efferent (including the anatomical localisation of α7nAChR and the origin of ACh) must be elucidated before bioelectronic medicine can be personalised and the relevant electrodes can be rationally selected.

Closed-loop bioelectronic systems to read in real time and automatically stimulate peripheral nerves, HRV, cytokines (including TNF), and tissue impedance are likely to become standard clinical practice when the questions around biomarker selection discussed in Section 5 are solved. Additionally, the redox signalling hypothesis of vagal signalling presented in Section 4.3 as merely a plausible analogy is likely to become at some point the new mechanism of treating diseases of inflammation (including sepsis, IBD, RA, SLE, and the neurodegenerative diseases) when considered as a possible mechanism rather than merely a plausible analogy.

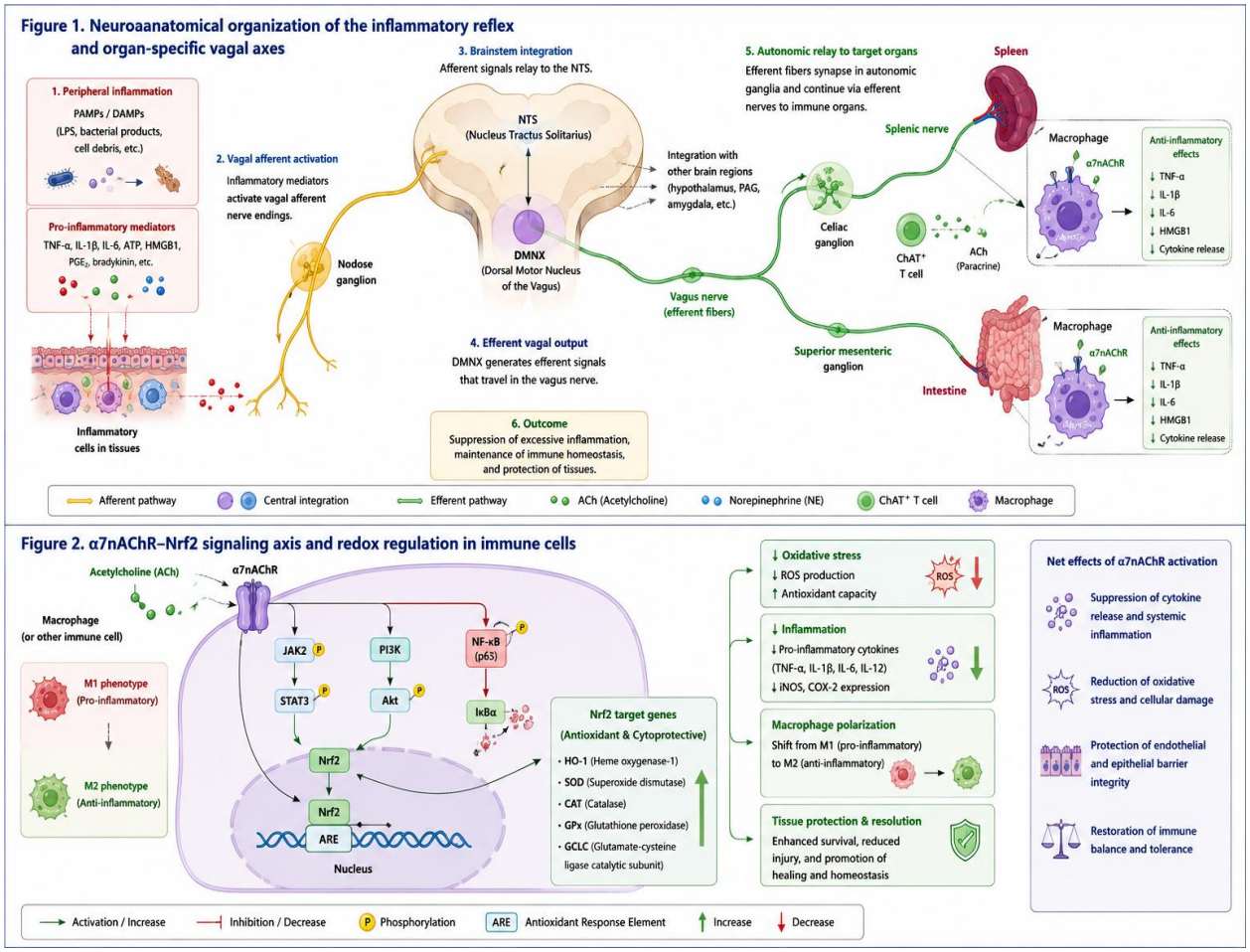

Figure 1. Neuroanatomical organisation of the inflammatory reflex.

Peripheral inflammatory mediators activate vagal afferents within the nucleus tractus solitarius (NTS) from the nodose ganglion. Brainstem processing of this signal leads to efferent vagus nerve activity from the dorsal motor nucleus of the vagus (DMNX) through the coeliac ganglion and splenic nerve to influence immune activity in the

ISBN NR. : 978-625-8795-33-2

spleen and gut. $ChAT^+$ T cells and α7nAChR-expressing macrophages are among the important effector cells of the pathway.

Figure 2: α7nAChR-mediated anti-inflammatory and redox signaling in macrophages.

Acetylcholine binding to the α7nAChR activates the JAK2/STAT3 and PI3K/Akt signaling pathways, inhibits the NF-κB signaling pathway, induces the nuclear translocation of Nrf2, and activates the expressions of the oxidative stress-associated genes HO-1, SOD, catalase, and GPx. α7nAChR activation also has the ability to inhibit oxidative stress, induce M2 macrophage polarisation, promote the resolution of inflammation, and protect tissues.

REFERENCES

1. Aeschbacher, S., Schoen, T., Dörig, L., Kreuzmann, R., Neuhauser, C., Schmidt-Trucksäss, A., .. Conen, D. Heart rate, heart rate variability and inflammatory biomarkers among young and healthy adults. Annals of Medicine, 49(1), 32-41, 2017.
2. Andresen, M. C., Yang, M. Y. Non-NMDA receptors mediate sensory afferent synaptic transmission in medial nucleus tractus solitarius. American Journal of Physiology-Heart and Circulatory Physiology, 259(4), H1307-H1311, 1990.
3. Baker, M. C., Kavanagh, S., Cohen, S., Matsumoto, A. K., Dikranian, A., Tesser, J., ... Genovese, M. C. A randomized, double-blind, sham-controlled, clinical trial of auricular vagus nerve stimulation for the treatment of active rheumatoid arthritis. Arthritis & Rheumatology, 75(12), 2107-2115, 2023.
4. Bellinger, D. L., Felten, S. Y., Lorton, D., Felten, D. L. Origin of noradrenergic innervation of the spleen in rats. Brain, Behavior, and İmmunity, 3(4), 291-311, 1989.
5. Bercik, P., Denou, E., Collins, J., Jackson, W., Lu, J., Jury, J., ... Collins, S. M. The intestinal microbiota affect central levels of brain-derived neurotropic factor and behavior in mice. Gastroenterology, 141(2), 599-609, 2011.
6. Berthoud, H. R., Neuhuber, W. L. Functional and chemical anatomy of the afferent vagal system. Autonomic Neuroscience, 85(1-3), 1-17, 2000.
7. Bonaz, B., Sinniger, V., Pellissier, S. Vagus nerve stimulation: a new promising therapeutic tool in inflammatory bowel disease. Journal of Internal Medicine, 282(1), 46-63, 2017.
8. Bonaz, B., Sinniger, V., Pellissier, S. Therapeutic potential of vagus nerve stimulation for inflammatory bowel diseases. Frontiers in Neuroscience, 15, 650971, 2021.
9. Bonaz, B., Sinniger, V., Hoffmann, D., Clarençon, D., Mathieu, N., Dantzer, C., ... Pellissier, S. Chronic vagus nerve stimulation in Crohn's disease: a 6-month follow-up pilot study. Neurogastroenterology & Motility, 28(6), 948-953, 2016.
10. Borovikova, L. V., Ivanova, S., Zhang, M., Botchkina, G. I., Watkins, L. R., Wang, H., ... & Tracey, K. J. Vagus nerve stimulation attenuates the systemic inflammatory response to endotoxin. Nature, 405(6785), 458-463, 2000.
11. Bravo, J. A., Forsythe, P., Chew, M. V., Escaravage, E., Savignac, H. M., Dinan, T. G., ... Cryan, J. F. Ingestion of Lactobacillus strain regulates emotional behavior and central GABA receptor expression in a mouse via the vagus nerve. Proceedings of the National Academy of Sciences, 108(38), 16050-16055, 2011.
12. D'Haens, G., Eberhardson, M., Cabrijan, Z., Danese, S., van den Berg, R., Löwenberg, M., ... Levine, Y. A. Neuroimmune modulation through vagus nerve stimulation reduces inflammatory activity in Crohn's disease patients: a prospective open-label study. Journal of Crohn's and Colitis, 17(12), 1897-1909, 2023.
13. Damoun, N., Amekran, Y., Taiek, N., El Hangouche, A. J. Heart rate variability measurement and influencing factors: Towards the standardization of methodology. Global Cardiology Science & Practice, 2024(4), e202435, 2024.
14. Dantzer, R., Kelley, K. W. Twenty years of research on cytokine-induced sickness behavior. Brain, Behavior, and Immunity, 21(2), 153-160, 2007.
15. Egea, J., Buendia, I., Parada, E., Navarro, E., León, R., Lopez, M. G. Anti-inflammatory role of microglial alpha7 nAChRs and its role in neuroprotection. Biochemical Pharmacology, 97(4), 463-

472, 2015.
16. Ek, M., Kurosawa, M., Lundeberg, T., Ericsson, A. Activation of vagal afferents after intravenous injection of interleukin-1β: role of endogenous prostaglandins. Journal of Neuroscience, 18(22), 9471-9479, 1998.
17. Famm, K., Litt, B., Tracey, K. J., Boyden, E. S., Slaoui, M. A jump-start for electroceuticals. Nature, 496(7444), 159-161, 2013.
18. Farmer, A. D., Strzelczyk, A., Finisguerra, A., Gourine, A. V., Gharabaghi, A., Hasan, A., ... Koenig, J. International consensus based review and recommendations for minimum reporting standards in research on transcutaneous vagus nerve stimulation (version 2020). Frontiers in Human Neuroscience, 14, 568051, 2021.
19. Farré-Alins, V., Narros-Fernández, P., Palomino-Antolín, A., Decouty-Pérez, C., Lopez-Rodriguez, A. B., Parada, E., ... Egea, J. Melatonin reduces NLRP3 inflammasome activation by increasing α7 nAChR-mediated autophagic flux. Antioxidants, 9(12), 1299, 2020.
20. Furness, J. B., Rivera, L. R., Cho, H. J., Bravo, D. M., Callaghan, B. The gut as a sensory organ. Nature reviews Gastroenterology & Hepatology, 10(12), 729-740, 2013.
21. Gamage, R., Wagnon, I., Rossetti, I., Childs, R., Niedermayer, G., Chesworth, R., Gyengesi, E. Cholinergic modulation of glial function during aging and chronic neuroinflammation. Frontiers in Cellular Neuroscience, 14, 577912, 2020.
22. Genovese, M. C., Gaylis, N. B., Sikes, D., Kivitz, A., Lewis Horowitz, D., Peterfy, C., Glass, E. V., Levine, Y. A., Chernoff, D. Safety and efficacy of neurostimulation with a miniaturised vagus nerve stimulation device in patients with multidrug-refractory rheumatoid arthritis: a two-stage multicentre, randomised pilot study. The Lancet Rheumatology, 2(9), e527-e538, 2020.
23. Gerber, M., Mughrabi, I., Kurata-Sato, I., Paliwoda, E., Vu, T. A., Diamond, B., Zanos, S. Continuous vs. intermittent chronic vagus nerve stimulation: effects on T-cell dependent antibody response, heart rate variability and body weight in immunized mice. Bioelectronic Medicine, 12(1), 17, 2026.
24. Godinho-Silva, C., Cardoso, F., Veiga-Fernandes, H. Neuro–immune cell units: a new paradigm in physiology. Annual Review of Immunology, 37(1), 19-46, 2019.
25. Goehler, L. E., Gaykema, R. P., Hammack, S. E., Maier, S. F., Watkins, L. R. Interleukin-1 induces c-Fos immunoreactivity in primary afferent neurons of the vagus nerve. Brain Research, 804(2), 306-310, 1998.
26. Haensel, A., Mills, P. J., Nelesen, R. A., Ziegler, M. G., Dimsdale, J. E. The relationship between heart rate variability and inflammatory markers in cardiovascular diseases. Psychoneuroendocrinology, 33(10), 1305-1312, 2008.
27. Hosoi, T., Okuma, Y., Matsuda, T., Nomura, Y. Novel pathway for LPS-induced afferent vagus nerve activation: possible role of nodose ganglion. Autonomic Neuroscience, 120(1-2), 104-107, 2005.
28. Huerta, T. S., Chen, A. C., Chaudhry, S., Tynan, A., Morgan, T., Park, K., ... Chang, E. H. Neural representation of cytokines by vagal sensory neurons. Nature Communications, 16(1), 3840, 2025.
29. Imai, J., Katagiri, H. Regulation of systemic metabolism by the autonomic nervous system consisting of afferent and efferent innervation. International Immunology, 34(2), 67-79, 2022.
30. Kaelberer, M. M., Buchanan, K. L., Klein, M. E., Barth, B. B., Montoya, M. M., Shen, X., Bohórquez, D. V. A gut-brain neural circuit for nutrient sensory transduction. Science, 361(6408), eaat5236, 2018.
31. Kaniusas, E., Kampusch, S., Tittgemeyer, M., Panetsos, F., Gines, R. F., Papa, M., ... Széles, J. C. Current directions in the auricular vagus nerve stimulation I–a physiological perspective. Frontiers in Neuroscience, 13, 464811, 2019.
32. Koopman, F. A., Chavan, S. S., Miljko, S., Grazio, S., Sokolovic, S., Schuurman, P. R., ... Tak, P. P. Vagus nerve stimulation inhibits cytokine production and attenuates disease severity in rheumatoid arthritis. Proceedings of the National Academy of Sciences, 113(29), 8284-8289, 2016.
33. Krzyzaniak, M., Peterson, C., Loomis, W., Hageny, A. M., Wolf, P., Reys, L., ... Coimbra, R. Postinjury vagal nerve stimulation protects against intestinal epithelial barrier breakdown. Journal of Trauma and Acute Care Surgery, 70(5), 1168-1176, 2011.

34. Kupari, J., Häring, M., Agirre, E., Castelo-Branco, G., Ernfors, P. An atlas of vagal sensory neurons and their molecular specialization. Cell Reports, 27(8), 2508-2523, 2019.
35. Manrai, M., Jha, A. A., Dawra, S., Pachisia, A. V. Biologics, Small Molecules and More in Inflammatory Bowel Disease: The Present and the Future. Future Pharmacology, 4(1), 2024.
36. Matteoli, G., Gomez-Pinilla, P. J., Nemethova, A., Di Giovangiulio, M., Cailotto, C., van Bree, S. H., ... Boeckxstaens, G. E. A distinct vagal anti-inflammatory pathway modulates intestinal muscularis resident macrophages independent of the spleen. Gut, 63(6), 938-948, 2014.
37. Merchant, W., Wyler, S., Chen, B., Gautron, L. The molecular components of the anti-inflammatory cholinergic pathway are extrasplenic. PloS One, 20(9), e0331707, 2025.
38. Mills, E. L., Kelly, B., Logan, A., Costa, A. S., Varma, M., Bryant, C. E., ... O'Neill, L. A. Succinate dehydrogenase supports metabolic repurposing of mitochondria to drive inflammatory macrophages. Cell, 167(2), 457-470, 2016.
39. Nance, D. M., Sanders, V. M. Autonomic innervation and regulation of the immune system (1987–2007). Brain, Behavior, and Immunity, 21(6), 736-745, 2007.
40. Niijima, A. The afferent discharges from sensors for interleukin 1β in the hepatoportal system in the anesthetized rat. Journal of the Autonomic Nervous System, 61(3), 287-291, 1996.
41. Ottaviani, M. M., Vallone, F., Micera, S., Recchia, F. A. Closed-loop vagus nerve stimulation for the treatment of cardiovascular diseases: state of the art and future directions. Frontiers in Cardiovascular Medicine, 9, 866957, 2022.
42. Parada, E., Egea, J., Buendia, I., Negredo, P., Cunha, A. C., Cardoso, S., Soares, M. P., Lopez, M. G. The microglial alpha7-acetylcholine nicotinic receptor is a key element in promoting neuroprotection by inducing heme oxygenase-1 via nuclear factor erythroid-2-related factor 2. Antioxidants & Redox Signaling, 19(11), 1135-1148, 2013.
43. Pavlov, V. A., Wang, H., Czura, C. J., Friedman, S. G., Tracey, K. J. The cholinergic anti-inflammatory pathway: a missing link in neuroimmunomodulation. Molecular Medicine, 9(5), 125-134, 2003.
44. Pavlov, V. A., Tracey, K. J. Bioelectronic medicine: preclinical insights and clinical advances. Neuron, 110(21), 3627-3644, 2022.
45. Pikov, V. Vagus nerve stimulation and sacral nerve stimulation for inflammatory bowel disease: a systematic review. Journal of Translational Gastroenterology, 1(2), 94, 2023.
46. Piovesana, R., Salazar Intriago, M. S., Dini, L., Tata, A. M. Cholinergic modulation of neuroinflammation: focus on α7 nicotinic receptor. International Journal of Molecular Sciences, 22(9), 4912, 2021.
47. Prescott, S. L., Liberles, S. D. Internal senses of the vagus nerve. Neuron, 110(4), 579-599, 2022.
48. Raybould, H. E. Diet-induced obesity leads to the development of leptin resistance in vagal afferent neurons 2. American Journal of Physiological Endocrinologic Metabolism, 26, 1-30, 2011.
49. Ricardo, J. A., Koh, E. T. Anatomical evidence of direct projections from the nucleus of the solitary tract to the hypothalamus, amygdala, and other forebrain structures in the rat. Brain Research, 153(1), 1-26, 1978.
50. Romanovsky, A. A., Almeida, M. C., Aronoff, D. M., Ivanov, A. I., Konsman, J. P., Steiner, A. A., Turek, V. F. Fever and hypothermia in systemic inflammation: recent discoveries and revisions. Fronties in Bioscience, 10(1-3), 2193-2216, 2005.
51. Rosas-Ballina, M., Ochani, M., Parrish, W. R., Ochani, K., Harris, Y. T., Huston, J. M., ... Tracey, K. J. Splenic nerve is required for cholinergic antiinflammatory pathway control of TNF in endotoxemia. Proceedings of the National Academy of Sciences, 105(31), 11008-11013, 2008.
52. Rosas-Ballina, M., Olofsson, P. S., Ochani, M., Valdés-Ferrer, S. I., Levine, Y. A., Reardon, C., ... Tracey, K. J. Acetylcholine-synthesizing T cells relay neural signals in a vagus nerve circuit. Science, 334(6052), 98-101, 2011.
53. Schwartz, G. J. The role of gastrointestinal vagal afferents in the control of food intake: current prospects. Nutrition, 16(10), 866-873, 2000.
54. Simon, T., Kirk, J., Dolezalova, N., Guyot, M., Panzolini, C., Bondue, A., ... Blancou, P. The cholinergic anti-inflammatory pathway inhibits inflammation without lymphocyte relay. Frontiers in Neuroscience, 17, 1125492, 2023.

ISBN NR. : 978-625-8795-33-2

55. Skok, M. Mitochondrial nicotinic acetylcholine receptors: Mechanisms of functioning and biological significance. The International Journal of Biochemistry & Cell Biology, 143, 106138, 2022.
56. Soreq, H., Seidman, S. Acetylcholinesterase—new roles for an old actor. Nature Reviews Neuroscience, 2(4), 294-302, 2001.
57. Steinberg, B. E., Silverman, H. A., Robbiati, S., Gunasekaran, M. K., Tsaava, T., Battinelli, E., ... Huerta, P. T. Cytokine-specific neurograms in the sensory vagus nerve. Bioelectronic Medicine, 3(1), 7-17, 2016.
58. Sternberg, E. M. Neural regulation of innate immunity: a coordinated nonspecific host response to pathogens. Nature Reviews Immunology, 6(4), 318-328, 2006.
59. Tan, H. Y., Wang, N., Li, S., Hong, M., Wang, X., Feng, Y. The reactive oxygen species in macrophage polarization: reflecting its dual role in progression and treatment of human diseases. Oxidative Medicine and Cellular Longevity, 2016(1), 2795090, 2016.
60. Task Force of the European Society of Cardiology and the North American Society of Pacing and Electrophysiology. Heart rate variability: standards of measurement, physiological interpretation, and clinical use. European Hearty of Journal, 17(3), 354-381, 1996.
61. Tracey, K. J. The inflammatory reflex. Nature, 420(6917), 853-859, 2002.
62. Veiga-Fernandes, H., Mucida, D. Neuro-immune interactions at barrier surfaces. Cell, 165(4), 801-811, 2016.
63. Vida, G., Peña, G., Kanashiro, A., del Rocio Thompson-Bonilla, M., Palange, D., Deitch, E. A., Ulloa, L. β2-Adrenoreceptors of regulatory lymphocytes are essential for vagal neuromodulation of the innate immune system. The FASEB Journal, 25(12), 4476, 2011.
64. Waise, T. Z., Dranse, H. J., Lam, T. K. The metabolic role of vagal afferent innervation. Nature reviews Gastroenterology & Hepatology, 15(10), 625-636, 2018.
65. Wang, X., Mei, W., Wang, Z., Ma, M., Wang, J., Ji, J., Xing, X. Neuro-immune interactions in gastrointestinal oncology: Mechanisms, challenges, and therapeutic potential. The Innovation, 7(5), 2026.
66. Wang, H., Yu, M., Ochani, M., Amella, C. A., Tanovic, M., Susarla, S., ... Tracey, K. J. Nicotinic acetylcholine receptor α7 subunit is an essential regulator of inflammation. Nature, 421(6921), 384-388, 2003.
67. Williams, D. P., Koenig, J., Carnevali, L., Sgoifo, A., Jarczok, M. N., Sternberg, E. M., & Thayer, J. F. Heart rate variability and inflammation: a meta-analysis of human studies. Brain, Behavior, and Immunity, 80, 219-226, 2019.
68. Yu, T., Liu, D., Gao, M., Yang, P., Zhang, M., Song, F., ... Liu, Y. Dexmedetomidine prevents septic myocardial dysfunction in rats via activation of α7nAChR and PI3K/Akt-mediated autophagy. Biomedicine & Pharmacotherapy, 120, 109231, 2019.
69. Zanos, T. P., Silverman, H. A., Levy, T., Tsaava, T., Battinelli, E., Lorraine, P. W., …Bouton, C. E. Identification of cytokine-specific sensory neural signals by decoding murine vagus nerve activity. Proceedings of the National Academy of Sciences, 115(21), E4843-E4852, 2018.

ISBN NR. : 978-625-8795-33-2

YARIK DAMAK VE DUDAK HASTALARINDA AMELİYAT ETME YAŞININ TEDAVİNİN BAŞARISINA ETKİSİ

Dr.Saffet Ulutaş

Dr.Saffet Ulutaş muayenehanesi

saffetulutas@gmail.com - ORCID ID:0000-0002-8214-4002

ÖZET

Yarık dudak ve damak, çocukluk çağının en sık görülen doğumsal kraniyofasiyal anomalileri arasında yer almakta olup estetik, fonksiyonel ve psikososyal açıdan uzun dönemli tedavi gerektiren kompleks bir klinik tablodur. Cerrahi onarımın zamanlaması, yüz gelişimi, konuşma fonksiyonu, beslenme, işitme ve yaşam kalitesi üzerinde belirleyici rol oynayan önemli bir faktördür. Bununla birlikte, ideal cerrahi yaş konusunda farklı merkezler arasında tam bir görüş birliği bulunmamaktadır. Erken dönemde gerçekleştirilen cerrahinin çocuğun beslenmesini kolaylaştırdığı, ebeveyn-çocuk bağlanmasını güçlendirdiği ve sosyal uyumu desteklediği bildirilirken, çok erken cerrahi girişimlerin maksillofasiyal büyüme üzerine olası olumsuz etkileri de tartışılmaktadır. Buna karşılık cerrahinin gecikmesi, konuşma gelişiminde bozulma, kompansatuvar artikülasyon alışkanlıklarının yerleşmesi, tekrarlayan üst solunum yolu enfeksiyonları ve psikososyal problemlerin ortaya çıkmasına neden olabilmektedir. Son yıllarda multidisipliner yaklaşımın yaygınlaşmasıyla birlikte yalnızca kronolojik yaşın değil, hastanın genel sağlık durumu, yarığın morfolojik özellikleri, beslenme yeterliliği, kilo artışı ve eşlik eden sendromların da cerrahi zamanlamada dikkate alınması gerektiği vurgulanmaktadır. Güncel literatür, uygun hasta seçimi ve deneyimli ekipler tarafından gerçekleştirilen zamanında cerrahi müdahalenin fistül gelişimi, konuşma sonuçları, estetik görünüm ve revizyon cerrahisi gereksinimi üzerinde olumlu etkiler oluşturduğunu göstermektedir. Bu nedenle tedavisinde cerrahi zamanlamasının tek başına belirli bir yaş sınırına indirgenmemesi, hasta özelliklerine göre bireyselleştirilmiş, kanıta dayalı ve multidisipliner bir yaklaşımın benimsenmesi tedavi başarısını artırabilecek en önemli stratejilerden biri olarak değerlendirilmektedir.

Anahtar Kelimeler : Yarık damak ve dudak, cerrahi zamanlama, tedavi başarısı, post op komplikasyon

ISBN NR. : 978-625-8795-33-2

HİPOTİROİDİNİN MANDİBULA ÜZERİNE ETKİSİ: BİR FRAKTAL ANALİZ ÇALIŞMASI

Arş. Gör., Elif ÇEÇEN EROL
Hatay Mustafa Kemal Üniversitesi/ Diş Hekimliği Fakültesi
E-posta: dis.elif.cecen@gmail.com - ORCID ID: 0009-0003-1624-3963
Arş. Gör., Merve KÜÇÜK KURTGÖZ
Hatay Mustafa Kemal Üniversitesi/ Diş Hekimliği Fakültesi
E-posta: mervekucuk911@gmail.com - ORCID ID: 0009-0003-1624-3963
Doç. Dr., Ceren AKTUNA BELGİN
Hatay Mustafa Kemal Üniversitesi/ Diş Hekimliği Fakültesi
E-posta: dtcaktuna@gmail.com- ORCID ID: 0000-0001-7780-3395

ÖZET

Amaç: Hipotiroidizmin kemik metabolizması üzerine olan olumsuz etkileri literatürde bilinmekle birlikte, bu etkinin mandibular trabeküler kemik yapısına yansıması henüz yeterince araştırılmamıştır. Bu çalışmada hipotiroidi hastalarında mandibular kemik mikro-mimarisinin panoramik radyografiler üzerinden fraktal analiz yöntemiyle incelenmesi amaçlanmıştır.

Yöntem: Çalışmaya hipotiroidi tanısı almış 40 hasta ile 40 sağlıklı kontrol bireyden oluşan toplam 80 kişi dahil edildi. Gruplar cinsiyet açısından eşleştirilmiş olup her birinde 20 kadın, 20 erkek yer almaktadır. Panoramik radyograflar üzerinde ImageJ yazılımı aracılığıyla kondil, angulus ve mental foramen bölgelerinde fraktal boyut değerleri hesaplanmıştır. Dağılım özelliklerine göre Angulus bölgesi için Welch düzeltmeli bağımsız örneklem t-testi, Kondil ve Mental Foramen bölgeleri için Mann-Whitney U testi uygulanmıştır.

Bulgular: Hipotiroidi grubunda üç bölgenin tamamında fraktal boyut değerleri sağlıklı kontrollerden anlamlı düzeyde düşük bulunmuştur. Kondil bölgesinde sağlıklı grupta ortalama 1,189, hipotiroidi grubunda 0,977 olarak ölçülmüştür ($p<0,001$). Angulus bölgesinde iki grup arasındaki ortalama fark 0,209 olup bu fark istatistiksel olarak anlamlıdır ($p<0,001$). Mental foramen bölgesinde ise sağlıklı grupta ortalama 1,278, hipotiroidi grubunda 0,958 değeri elde edilmiş; bu bölge en yüksek azalma oranını (%25,1) göstermiştir ($p<0,001$). Bu farkın klinik açıdan da anlamlı olduğu görülmüştür.

Sonuç: Hipotiroidizmin mandibular trabeküler kemik yapısını üç anatomik bölgede de tutarlı biçimde bozduğu görülmektedir. Fraktal analiz bu değişiklikleri noninvaziv olarak saptayabilmekte olup sistemik hastalıkların kemik üzerindeki etkilerinin erken dönemde değerlendirilmesinde klinik kullanım potansiyeli taşıyan bir yöntem olarak değerlendirilebilir.

Anahtar Kelimeler: Hipotiroidi, fraktal analiz, mandibula, trabeküler kemik, panoramik radyografi

ISBN NR. : 978-625-8795-33-2

KAN DOKUSUNDA ALFA-NAFTİL ASETAT ESTERAZ (ANAE) DEMONSTRASYONU

Dr. Öğr. Üyesi Ayhan AKGÜN

ORCID ID: 0000-0001-6585-8655

e-mail :ayhanakgun7676@gmail.com

Öz

Alfa-naftil asetat esteraz (ANAE), non-spesifik esterazlar grubuna ait bir enzim olup özellikle T lenfositlerin tanımlanmasında kullanılan önemli bir histokimyasal belirteçtir. Sitoplazmada granüler boyanma paterni ile karakterize olan bu enzim, lenfosit alt popülasyonlarının ayırt edilmesinde uzun yıllar boyunca güvenilir bir yöntem olarak kullanılmıştır. Bu çalışmasının amacı, kan dokusunda ANAE demonstrasyonunun biyokimyasal temellerini, histokimyasal uygulama süreçlerini, tanısal değerini ve modern analiz yöntemleri ile ilişkisini kapsamlı şekilde incelemektir.

ANAE boyaması, lenfosit alt popülasyonlarının ayrımında klasik bir yöntem olarak uzun yıllar kullanılmış olup, özellikle T hücrelerinin sitokimyasal olarak belirlenmesinde önemli katkılar sağlamıştır. Bununla birlikte, akım sitometrisi, immünohistokimya ve moleküler biyoloji tekniklerinin gelişmesiyle birlikte hücresel tanımlama yöntemleri daha spesifik ve duyarlı hale gelmiş, bu durum ANAE demonstrasyonunun kullanım sıklığında azalmaya yol açmıştır.

Buna rağmen, ANAE demonstrasyonu düşük maliyetli olması, hızlı uygulanabilirliği ve özel ekipman gerektirmemesi gibi avantajları nedeniyle önemini korumaktadır. Ayrıca, hücresel morfolojinin korunarak değerlendirme yapılabilmesi, bu yöntemi histokimyasal analizler arasında ayrıcalıklı bir konuma getirmektedir. Günümüzde ANAE demonstrasyonu, tek başına bir tanı aracı olmaktan ziyade, modern tekniklerle birlikte kullanılan tamamlayıcı bir yöntem olarak değerlendirilmektedir.

Bu çalışma, ANAE demonstrasyonunun avantajlarını ve sınırlılıklarını ortaya koyarak, özellikle dijital patoloji ve yapay zeka destekli analiz sistemleri ile entegrasyon potansiyelini tartışmayı amaçlamaktadır. Bu bağlamda, klasik histokimyasal yöntemlerin modern tanı yaklaşımları ile birlikte kullanılması, hematolojik hastalıkların değerlendirilmesinde daha kapsamlı ve güvenilir sonuçların elde edilmesine katkı sağlayabilir.

ISBN NR. : 978-625-8795-33-2

Anahtar Kelimeler: ANAE, Esteraz, Histokimya, Kan Dokusu, T Lenfosit.

DEMONSTRATION OF ALPHA NAPHTHYL ACETATE ESTERASE (ANAE) IN BLOOD TISSUE

Abstract

Alpha-naphthyl acetate esterase (ANAE) is an enzyme belonging to the group of non-specific esterases and is an important histochemical marker used especially in the identification of T lymphocytes. Characterized by a granular staining pattern in the cytoplasm, this enzyme has been used for many years as a reliable method for differentiating lymphocyte subpopulations. The aim of this study is to comprehensively examine the biochemical basis of ANAE demonstration in blood tissue, histochemical application processes, diagnostic value, and its relationship with modern analytical methods.

ANAE staining has been used for many years as a classic method in the differentiation of lymphocyte subpopulations, and has made significant contributions, especially in the cytochemical determination of T cells. However, with the development of flow cytometry, immunohistochemistry, and molecular biology techniques, cellular identification methods have become more specific and sensitive, which has led to a decrease in the frequency of use of ANAE demonstration. Nevertheless, ANAE demonstration retains its importance due to its advantages such as low cost, rapid applicability, and lack of need for special equipment. Furthermore, the ability to evaluate cellular morphology while preserving it gives this method a privileged position among histochemical analyses. Today, ANAE demonstration is considered not a standalone diagnostic tool, but rather a complementary method used in conjunction with modern techniques.

This study aims to highlight the advantages and limitations of ANAE demonstration, particularly discussing its potential for integration with digital pathology and artificial intelligence-supported analysis systems. In this context, the combined use of classical histochemical methods with modern diagnostic approaches can contribute to obtaining more comprehensive and reliable results in the evaluation of hematological diseases.

Keywords: ANAE, Blood Tissue, Histochemistry, T Lymphocyte, Esterase.

ISBN NR. : 978-625-8795-33-2

1. Giriş

Kan dokusu, bağ dokusunun özelleşmiş bir formu olup dolaşım sistemi içerisinde hücresel ve humoral bileşenleri ile immün yanıtın temel yapı taşlarını oluşturmaktadır (Mescher, 2021; Ross & Pawlina, 2020). Eritrositler, lökositler ve trombositler gibi şekilli elemanların yanı sıra plazma, bu dokunun fonksiyonel bütünlüğünü sağlayan temel bileşenlerdir. Özellikle lökositler, immün sistemin efektör hücreleri olarak görev yapmakta ve organizmanın enfeksiyonlara karşı savunmasında kritik rol oynamaktadır (Abbas ve ark., 2021; Murphy, 2012). Lenfositler ise bağışıklık sisteminin temel hücreleri olup başlıca T ve B lenfositler şeklinde sınıflandırılmaktadır (Janeway ve ark., 2017). Bu hücrelerin doğru şekilde tanımlanması, hematolojik hastalıkların tanı, prognoz ve tedavi planlamasında belirleyici bir faktördür (Prasannan ve ark. 2020; Kumar ve ark., 2020).

Hücresel düzeyde farklılaşmanın ortaya konulmasında histokimyasal yöntemler uzun yıllardır güvenilir araçlar olarak kullanılmaktadır. Bu yöntemler, hücre içi enzim aktivitelerini ve biyokimyasal özellikleri ortaya koyarak hücre tiplerinin ayırt edilmesini sağlamaktadır (Bancroft & Gamble, 2019; Kiernan, 2015). Histokimyasal analizler, özellikle hücresel morfolojinin korunarak fonksiyonel değerlendirme yapılabilmesine olanak tanıması açısından önemli avantajlar sunmaktadır (Carson & Hladik, 2009). Bu kapsamda kullanılan yöntemlerden biri olan alfa-naftil asetat esteraz (ANAE) demonstrasyonu, özellikle T lenfositlerin belirlenmesinde yaygın olarak tercih edilen klasik bir tekniktir (Yam ve ark., 1971; Knowles, 2001).

Modern tıpta akım sitometrisi, immünohistokimya ve moleküler biyoloji tekniklerinin yaygınlaşması ile birlikte hücresel analizler daha hassas ve çok parametreli hale gelmiştir (Abbas ve ark., 2021; McPherson & Pincus, 2017). Bununla birlikte, klasik histokimyasal yöntemler, düşük maliyetli olmaları, teknik olarak kolay uygulanabilirlik sağlamaları ve ileri düzey ekipman gerektirmemeleri nedeniyle hâlâ belirli klinik ve araştırma ortamlarında tercih edilmektedir (Bancroft & Gamble, 2019; Kiernan, 2015; Suvarna ve ark., 2018). Özellikle sınırlı kaynaklara sahip laboratuvarlarda, ANAE demonstrasyonu gibi yöntemler, lenfosit alt gruplarının ayrımında pratik ve erişilebilir bir alternatif olarak önemini sürdürmektedir (Knowles, 2001).

2. ANAE'nin Biyokimyasal ve Histolojik Temeli

ANAE, ester bağlarını hidrolize eden non-spesifik esterazlar grubuna ait bir enzim olup, özellikle hematopoietik hücrelerin sitokimyasal karakterizasyonunda önemli bir biyobelirteç

ISBN NR. : 978-625-8795-33-2

olarak kabul edilmektedir (Johnson, 1972; Kiernan, 2015). Bu enzim, alfa-naftil asetat substratını hidrolize ederek alfa-naftol oluşumuna yol açar. Ortaya çıkan alfa-naftol, diazonyum tuzları ile reaksiyona girerek çözünmeyen renkli bir azo boya kompleksi oluşturur. Bu reaksiyon ürünü, hücre sitoplazmasında birikerek mikroskop altında enzim aktivitesinin lokalizasyonunu belirgin hale getirir (Bancroft & Gamble, 2019; Carson & Hladik, 2009). Bu nedenle ANAE demonstrasyonu, hem morfolojik hem de fonksiyonel değerlendirme sağlayan bir histokimyasal teknik olarak öne çıkmaktadır.

Histolojik açıdan değerlendirildiğinde, ANAE aktivitesi hücre tipine özgü belirgin farklılıklar göstermektedir. T lenfositlerde genellikle sitoplazmada sınırlı sayıda, keskin sınırlı ve granüler boyanma odakları izlenirken, bu durum enzimin lizozomal dağılımını yansıtmaktadır (Knowles, 2001; Kumar ve ark., 2020). Buna karşılık, B lenfositlerde ANAE aktivitesi çoğunlukla negatif olup, bazı durumlarda zayıf ve diffüz bir boyanma paterni görülebilmektedir (Janeway ve ark., 2017). Monositler ise geniş sitoplazmaları boyunca yaygın ve yoğun pozitiflik sergileyerek diğer lenfosit alt gruplarından kolaylıkla ayırt edilebilmektedir (McPherson & Pincus, 2017; Prasannan ve ark. 2020).

Bu hücreler arası boyanma farklılıkları, ANAE'nin hücresel diferansiyasyon ve immün fonksiyonlarla ilişkili olduğunu düşündürmektedir. Özellikle T lenfositlerde gözlenen granüler boyanma paterni, bu hücrelerin lizozomal aktivitesi ve antijen işleme süreçleri ile bağlantılıdır (Abbas ve ark., 2021; Murphy, 2012). ANAE'nin lizozomal kökenli olması, hücre içi sindirim mekanizmaları ve immün yanıt sırasında gerçekleşen antijen sunumu süreçlerinde rol oynayabileceğini göstermektedir (Mescher, 2021). Bu bağlamda, ANAE aktivitesi yalnızca bir tanımlayıcı belirteç olmanın ötesinde, hücresel fonksiyonel durum hakkında da önemli bilgiler sunmaktadır.

3. ANAE Demonstrasyon Yöntemi

ANAE demonstrasyonu, belirli aşamalardan oluşan klasik bir histokimyasal teknik olup hematolojik hücrelerin sitokimyasal özelliklerinin ortaya konulmasında yaygın olarak kullanılmaktadır (Bancroft & Gamble, 2019; Suvarna ve ark., 2018). İlk aşamada periferik kandan ince yaymalar hazırlanmakta ve preparatların hücresel morfolojiyi koruyacak şekilde uygun koşullarda fikse edilmesi gerekmektedir. Fiksasyon işlemi, enzim aktivitesinin korunması açısından kritik bir basamak olup, genellikle formalin, glutaraldehit veya asetona dayalı fiksatifler tercih edilmektedir (Kiernan, 2015; Carson & Hladik, 2009). Uygun olmayan

ISBN NR. : 978-625-8795-33-2

fiksasyon, enzim aktivitesinin kaybına ya da artefakt oluşumuna neden olabileceğinden, bu aşama yöntemin güvenilirliği açısından belirleyicidir (Bancroft & Gamble, 2019).

İkinci aşamada, preparatlar alfa-naftil asetat içeren substrat çözeltisi ile belirli süre ve sıcaklık koşullarında inkübe edilmektedir. Bu aşamada ANAE enzimi substratı hidrolize ederek alfa-naftol oluşumuna yol açar. Oluşan bu ara ürün, diazonyum tuzları ile reaksiyona girerek çözünmeyen renkli bir azo boya kompleksi meydana getirir (Johnson, 1972; Kiernan, 2015). İnkübasyon süresi, pH ve sıcaklık gibi faktörler reaksiyonun etkinliğini doğrudan etkileyen önemli parametrelerdir ve standardizasyon gerektirir (Suvarna ve ark., 2018).

Boyama işlemi tamamlandıktan sonra preparatlar ışık mikroskobu altında değerlendirilir. Pozitif hücreler sitoplazmalarında genellikle kırmızımsı-kahverengi granüler boyanma gösterirken, negatif hücrelerde boyanma gözlenmez ya da minimal düzeydedir (Carson & Hladik, 2009; Knowles, 2001). Değerlendirme sürecinde yalnızca boyanma varlığı değil, aynı zamanda boyanmanın yoğunluğu, dağılımı ve hücre içindeki lokalizasyonu da dikkate alınmalıdır (Kumar ve ark., 2020).

Bu yöntemin önemli bir sınırlılığı, değerlendirme sürecinin büyük ölçüde gözlemci deneyimine bağlı olmasıdır. Boyanma paternlerinin yorumlanması subjektif farklılıklara yol açabilir ve bu durum sonuçların tekrarlanabilirliğini etkileyebilir (McPherson & Pincus, 2017). Bu nedenle, standart protokollerin uygulanması ve mümkün olduğunda dijital görüntü analiz sistemleri ile desteklenmesi önerilmektedir (Litjens ve ark., 2017).

4. Klinik ve Tanısal Önemi

ANAE demonstrasyonu, hematolojik hastalıkların tanısında uzun yıllar boyunca önemli bir rol oynamış ve özellikle sitokimyasal sınıflandırma yöntemlerinin temel bileşenlerinden biri olarak kabul edilmiştir (Yam ve ark., 1971; Knowles, 2001). Bu yöntem, özellikle T lenfositlerin belirlenmesinde gösterdiği yüksek duyarlılık sayesinde lenfoproliferatif hastalıkların ayırıcı tanısında değerli bir araç olmuştur (Prasannan ve ark. 2020; McPherson & Pincus, 2017). ANAE pozitifliği, T hücre kökenli hücrelerde sitoplazmik granüler boyanma şeklinde ortaya çıkar ve bu özellik, hücre alt tiplerinin morfolojik olarak ayırt edilmesine katkı sağlar (Kumar ve ark., 2020; Abbas ve ark., 2021).

Özellikle T hücreli lösemilerde ve bazı T hücreli lenfomalarda ANAE pozitifliğinin belirgin olması, bu yöntemin tanısal değerini artırmaktadır (Kumar ve ark., 2020). Buna karşılık, B hücreli malignitelerde genellikle ANAE aktivitesi saptanmaz veya çok zayıf düzeyde görülür; bu durum, hücre kökeninin belirlenmesinde önemli bir ayırt edici kriter olarak

ISBN NR. : 978-625-8795-33-2

kullanılmaktadır (Knowles, 2001; Janeway ve ark., 2017). Bununla birlikte, monositlerin de ANAE pozitiflik gösterebilmesi, bazı durumlarda yorumlamada dikkatli olunmasını gerektirmektedir (McPherson & Pincus, 2017).

ANAE demonstrasyonu yalnızca malign hastalıkların sınıflandırılmasında değil, aynı zamanda immün sistem fonksiyonlarının değerlendirilmesinde de kullanılmaktadır. Özellikle immün yetmezlik hastalıklarında lenfosit alt popülasyonlarının dağılımındaki değişikliklerin belirlenmesi, hastalığın patofizyolojisinin anlaşılmasına katkı sağlamaktadır (Abbas ve ark., 2021; Murphy, 2012). Ayrıca, kemoterapi veya immünmodülatör tedaviler sonrası lenfosit yanıtlarının izlenmesinde de yardımcı bir yöntem olarak değerlendirilmektedir (Prasannan ve ark. 2020).

Her ne kadar günümüzde akım sitometrisi ve immünohistokimya gibi daha spesifik ve duyarlı yöntemler yaygın olarak kullanılsa da, ANAE demonstrasyonu düşük maliyetli olması ve hızlı sonuç vermesi nedeniyle özellikle sınırlı teknik altyapıya sahip laboratuvarlarda hâlâ önemli bir alternatif olarak kabul edilmektedir (Bancroft & Gamble, 2019; Kiernan, 2015). Bu nedenle, ANAE boyaması modern tanı yöntemleriyle birlikte kullanıldığında, hematolojik hastalıkların değerlendirilmesinde tamamlayıcı bir rol oynamaya devam etmektedir.

5. Avantajlar ve Sınırlılıklar

ANAE demonstrasyonunun en önemli avantajlarından biri düşük maliyetli olması ve teknik açıdan kolay uygulanabilir bir yöntem olarak öne çıkmasıdır (Bancroft & Gamble, 2019; Suvarna ve ark., 2018). Özel ve pahalı ekipman gerektirmemesi, bu yöntemin özellikle gelişmekte olan ülkelerdeki laboratuvarlarda yaygın olarak kullanılabilmesine olanak sağlamaktadır. Ayrıca, kısa sürede sonuç verebilmesi, klinik uygulamalarda hızlı ön değerlendirme yapılmasına katkı sunmaktadır (Kiernan, 2015). Bunun yanı sıra, hücresel morfolojinin korunarak değerlendirme yapılabilmesi, histokimyasal analizlerin en önemli avantajlarından biridir. Bu özellik, hücre tiplerinin yalnızca biyokimyasal değil aynı zamanda morfolojik kriterlere göre de değerlendirilmesine imkân tanımaktadır (Carson & Hladik, 2009; Ross & Pawlina, 2020).

ANAE demonstrasyonu, özellikle temel laboratuvar koşullarında lenfosit alt popülasyonlarının ayırt edilmesinde pratik ve erişilebilir bir yöntem sunmaktadır. Bu durum, ileri teknoloji gerektiren akım sitometrisi veya immünohistokimyasal yöntemlerin bulunmadığı ortamlarda önemli bir avantaj sağlamaktadır (McPherson & Pincus, 2017; Abbas ve ark., 2021). Ayrıca, preparatların arşivlenebilmesi ve gerektiğinde yeniden değerlendirilebilmesi de

ISBN NR. : 978-625-8795-33-2

yöntemin kullanım kolaylığını artıran faktörler arasında yer almaktadır (Bancroft & Gamble, 2019). Bununla birlikte, ANAE demonstrasyonunun bazı önemli sınırlılıkları da bulunmaktadır. Öncelikle yöntemin spesifitesinin sınırlı olması, bazı hücre tiplerinde yanlış pozitif veya yanlış negatif sonuçlara yol açabilmektedir (Kiernan, 2015; Kumar ve ark., 2020). Özellikle monositlerin de ANAE pozitiflik gösterebilmesi, lenfosit alt tiplerinin ayırt edilmesinde karışıklığa neden olabilmektedir (Knowles, 2001). Ayrıca, boyanma yoğunluğu ve paterni çevresel faktörlerden, kullanılan reaktiflerden ve inkübasyon koşullarından etkilenebilmektedir (Suvarna ve ark., 2018).

Bir diğer önemli sınırlılık ise değerlendirme sürecinin büyük ölçüde gözlemciye bağımlı olmasıdır. Boyanma paternlerinin yorumlanması subjektif farklılıklar gösterebilir ve bu durum sonuçların tekrarlanabilirliğini azaltabilir (Kumar ve ark., 2020; McPherson & Pincus, 2017). Bu nedenle, standart protokollerin uygulanması ve mümkün olduğunda dijital görüntü analiz sistemleri ile desteklenmesi önerilmektedir (Litjens ve ark., 2017). Sonuç olarak, ANAE demonstrasyonu avantajları ve sınırlılıkları birlikte değerlendirildiğinde, özellikle tamamlayıcı bir yöntem olarak kullanıldığında klinik açıdan değerli bilgiler sunmaya devam etmektedir.

6. Modern Yöntemlerle Karşılaştırma

Günümüzde akım sitometrisi, immünohistokimya ve moleküler biyoloji temelli teknikler, hücre yüzey belirteçlerinin yüksek doğruluk ve duyarlılıkla belirlenmesini sağlayarak hematolojik tanı süreçlerinde önemli bir yer edinmiştir (Abbas ve ark., 2021; McPherson & Pincus, 2017). Akım sitometrisi, aynı anda çok sayıda parametrenin analiz edilebilmesine olanak tanıyarak hücre popülasyonlarının detaylı bir şekilde sınıflandırılmasını mümkün kılmaktadır (Brown & Wittwer, 2000). İmmünohistokimyasal yöntemler ise spesifik antijen-antikor etkileşimlerine dayanarak hücrelerin fenotipik özelliklerinin doku bütünlüğü içerisinde değerlendirilmesini sağlar (Taylor & Levenson, 2006). Bunun yanı sıra, moleküler teknikler, gen ekspresyonu ve mutasyon analizleri yoluyla hastalıkların patogenezine ilişkin daha derin bilgiler sunmaktadır (Kumar ve ark., 2020).

Bu ileri yöntemler, yüksek spesifite ve duyarlılık sunmaları nedeniyle modern tanı algoritmalarında altın standart olarak kabul edilmektedir. Ancak, bu tekniklerin uygulanabilmesi için ileri düzey cihaz altyapısı, deneyimli personel ve yüksek maliyet gereksinimi söz konusudur (McPherson & Pincus, 2017; Abbas ve ark., 2021). Bu durum, özellikle kaynakları sınırlı olan laboratuvarlarda bu yöntemlerin rutin kullanımını zorlaştırmaktadır.

ISBN NR. : 978-625-8795-33-2

Buna karşın, ANAE demonstrasyonu hızlı, ekonomik ve teknik olarak daha az karmaşık bir yöntem olması nedeniyle önemini korumaktadır (Bancroft & Gamble, 2019; Kiernan, 2015). Özel cihaz gerektirmemesi ve kısa sürede sonuç verebilmesi, bu yöntemi özellikle temel laboratuvar koşullarında uygulanabilir kılmaktadır. Ayrıca, hücresel morfolojinin korunarak değerlendirilmesi, histokimyasal yöntemlerin önemli bir avantajı olarak öne çıkmaktadır (Carson & Hladik, 2009).

Modern yaklaşımlarda, ANAE demonstrasyonunun tek başına kullanımı yerine, diğer ileri tekniklerle birlikte tamamlayıcı bir yöntem olarak değerlendirilmesi önerilmektedir (Knowles, 2001; Prasannan ve ark. 2020). Bu kombinasyon yaklaşımı, hem maliyet etkinliği sağlamakta hem de tanısal doğruluğun artırılmasına katkıda bulunmaktadır. Özellikle ön tarama veya ilk değerlendirme aşamalarında ANAE boyaması, daha ileri analizlerin yönlendirilmesine yardımcı olabilir. Bu nedenle, ANAE demonstrasyonu, modern tanı algoritmaları içerisinde destekleyici bir rol oynamaya devam etmektedir.

7. Güncel Araştırmalar ve Gelecek Perspektifi

Son yıllarda dijital patoloji ve yapay zeka (YZ) uygulamalarındaki hızlı gelişmeler, histolojik ve sitokimyasal analizlerin daha objektif, tekrarlanabilir ve yüksek doğrulukla yapılabilmesine olanak sağlamıştır (Litjens ve ark., 2017; Bera ve ark., 2019). Geleneksel mikroskobik değerlendirme yöntemlerinde gözlemciye bağlı değişkenlik önemli bir sınırlılık oluştururken, dijital görüntüleme sistemleri ve bilgisayar destekli analizler bu sorunun büyük ölçüde aşılmasına katkıda bulunmaktadır (Madabhushi & Lee, 2016). Bu bağlamda, ANAE boyaması gibi klasik histokimyasal tekniklerin dijital patoloji ile entegre edilmesi, hücre sınıflandırmasının daha standart ve kantitatif bir şekilde yapılmasını mümkün kılmaktadır (Litjens ve ark., 2017).

Yüksek çözünürlüklü tarayıcılar ile elde edilen dijital preparatlar, görüntü işleme algoritmaları aracılığıyla analiz edilmekte ve boyanma yoğunluğu, dağılımı ve paternleri sayısal veriler halinde değerlendirilebilmektedir (Komura & Ishikawa, 2018). Bu sayede, ANAE pozitif hücrelerin oranı ve boyanma özellikleri daha hassas bir şekilde belirlenebilmekte ve insan gözünün algılayamayacağı ince farklılıklar ortaya konulabilmektedir (Bera ve ark., 2019).

Derin öğrenme algoritmaları, özellikle konvolüsyonel sinir ağları (CNN) kullanılarak histolojik görüntülerin otomatik analizinde önemli başarılar göstermiştir (Esteva ve ark., 2019; Campanella ve ark., 2019). Bu algoritmalar, boyanma paternlerini tanıyarak hücre tiplerini

ISBN NR. : 978-625-8795-33-2

sınıflandırabilmekte ve gözlemciye bağlı hataları önemli ölçüde azaltmaktadır (Madabhushi & Lee, 2016). Ayrıca, bu sistemler büyük veri setleri ile eğitildiklerinde, tanısal doğruluğu artıran güçlü karar destek araçları haline gelmektedir.

Bu gelişmeler, ANAE demonstrasyonunun modern tanı sistemleri ile entegrasyonunu mümkün kılmakta ve klasik yöntemlerin yeniden değerlendirilmesine zemin hazırlamaktadır. Özellikle düşük maliyetli histokimyasal yöntemlerin yapay zeka destekli analizlerle birleştirilmesi, hem ekonomik hem de yüksek doğruluklu tanı yaklaşımlarının geliştirilmesine katkı sağlayabilir (Komura & Ishikawa, 2018). Gelecekte, ANAE gibi klasik boyama tekniklerinin dijital patoloji platformları ile entegre edilmesi, hematolojik tanı süreçlerinde daha standart ve güvenilir sonuçlar elde edilmesini mümkün kılacaktır.

8. Sonuç

ANAE demonstrasyonu, klasik bir histokimyasal yöntem olmasına rağmen kan dokusunda hücresel analiz açısından günümüzde de önemini korumaktadır (Yam ve ark., 1971; Bancroft & Gamble, 2019). Özellikle T lenfositlerin sitokimyasal olarak tanımlanmasında sağladığı katkılar, bu yöntemin hematolojik değerlendirmelerde uzun yıllar boyunca güvenilir bir araç olarak kullanılmasına olanak tanımıştır (Knowles, 2001; Prasannan ve ark. 2020). Her ne kadar günümüzde akım sitometrisi, immünohistokimya ve moleküler teknikler daha yüksek duyarlılık ve spesifite sunarak tanı süreçlerinde ön plana çıkmış olsa da, ANAE demonstrasyonu hâlen belirli klinik ve araştırma ortamlarında tamamlayıcı bir yöntem olarak değerlendirilmektedir (Abbas ve ark., 2021; McPherson & Pincus, 2017).

Modern tekniklerle birlikte kullanılması, ANAE'nin tanısal değerini artıran önemli bir yaklaşımdır. Özellikle ön tarama veya destekleyici analiz yöntemi olarak kullanıldığında, hücresel farklılaşmanın hızlı bir şekilde değerlendirilmesine katkı sağlayabilmektedir (Kumar ve ark., 2020). Ayrıca, hücresel morfolojinin korunması sayesinde histolojik bağlam içerisinde değerlendirme yapılabilmesi, bu yöntemin diğer tekniklere kıyasla önemli avantajlarından biri olarak öne çıkmaktadır (Carson & Hladik, 2009). Bu nedenle, ANAE demonstrasyonu tek başına bir tanı aracı olmaktan ziyade, çok parametreli tanı yaklaşımlarının bir parçası olarak ele alınmalıdır (Knowles, 2001).

Gelecekte dijital patoloji ve yapay zeka uygulamalarının gelişmesi ile birlikte, ANAE demonstrasyonunun yeniden önem kazanması beklenmektedir. Özellikle dijital görüntü analiz sistemleri ve derin öğrenme algoritmaları, boyanma paternlerinin daha objektif ve kantitatif bir şekilde değerlendirilmesine olanak sağlayarak yöntemin güvenilirliğini artırabilir (Litjens ve

ISBN NR. : 978-625-8795-33-2

ark., 2017; Bera ve ark., 2019). Bu entegrasyon, klasik histokimyasal tekniklerin modern tanı sistemleri ile uyumlu hale getirilmesini sağlayarak, maliyet etkin ve yüksek doğruluklu tanı yaklaşımlarının geliştirilmesine katkıda bulunabilir (Komura & Ishikawa, 2018).

Sonuç olarak, ANAE demonstrasyonu geçmişten günümüze uzanan klinik değeri ile, modern teknolojilerle desteklendiğinde yeniden önem kazanabilecek potansiyele sahip bir yöntemdir. Bu bağlamda, klasik ve modern tekniklerin entegrasyonu, hematolojik hastalıkların tanı ve değerlendirilmesinde daha kapsamlı ve güvenilir sonuçların elde edilmesini sağlayacaktır.

KAYNAKÇA

1. Abbas, A. K., Lichtman, A. H., & Pillai, S. (2021). *Cellular and molecular immunology* (10th ed.). Elsevier.
2. Bancroft, J. D., Suvarna, S. K., & Layton, C. (2019). *Bancroft's theory and practice of histological techniques* (8th ed.). Elsevier.
3. Brown, M., & Wittwer, C. (2000). Flow cytometry: Principles and clinical applications. *Clinical Chemistry*, *46*(8), 1221–1229.
4. Campanella, G., Hanna, M. G., Geneslaw, L., Miraflor, A., Silva, V. W. K., Busam, K. J., Brogi, E., Reuter, V. E., Klimstra, D. S., & Fuchs, T. J. (2019). Clinical-grade computational pathology using weakly supervised deep learning on whole slide images. *Nature Medicine, 25*(8), 1301–1309. https://doi.org/10.1038/s41591-019-0508-1
5. Carson, F. L., & Hladik, C. (2009). *Histotechnology: A self-instructional text* (3rd ed.). American Society for Clinical Pathology Press.
6. Esteva, A., Kuprel, B., Novoa, R. A., Ko, J., Swetter, S. M., Blau, H. M., & Thrun, S. (2017). Dermatologist-level classification of skin cancer with deep neural networks. *Nature, 542*(7639), 115–118.
7. Prasannan, N., Ademokun, C. O., & Radia, D. H. (2020). Haematology. Medicine for MRCP, 271.
8. Janeway, C. A., Murphy, K., Travers, P., & Walport, M. (2017). *Janeway's immunobiology* (9th ed.). Garland Science.
9. Kiernan, J. A. (2015). *Histological and histochemical methods: Theory and practice* (5th ed.). Scion Publishing Ltd.

ISBN NR. : 978-625-8795-33-2

10. Knowles, D. M. (Ed.). (2001). *Neoplastic hematopathology* (2nd ed.). Lippincott Williams & Wilkins.
11. Komura, D., & Ishikawa, S. (2018). Machine learning methods for histopathological image analysis. *Computational and Structural Biotechnology Journal, 16*, 34–42.
12. Kumar, V., Abbas, A. K., & Aster, J. C. (2020). *Robbins and Cotran pathologic basis of disease* (10th ed.). Elsevier.
13. Litjens, G., Kooi, T., Bejnordi, B. E., Setio, A. A. A., Ciompi, F., Ghafoorian, M., van der Laak, J. A. W. M., van Ginneken, B., & Sánchez, C. I. (2017). A survey on deep learning in medical image analysis. *Medical Image Analysis, 42*, 60–88.
14. Madabhushi, A., & Lee, G. (2016). Image analysis and machine learning in digital pathology: Challenges and opportunities. *Medical Image Analysis, 33*, 170–175. https://doi.org/10.1016/j.media.2016.06.037
15. McPherson, R. A., & Pincus, M. R. (Eds.). (2017). *Henry's clinical diagnosis and management by laboratory methods* (23rd ed.). Elsevier.
16. Mescher, A. L. (2021). *Junqueira's basic histology: Text and atlas* (16th ed.). McGraw-Hill Education.
17. Murphy, K., & Weaver, C. (2022). *Janeway's immunobiology* (10th ed.). W. W. Norton & Company.
18. Johnson, F. (1972). Histochemistry Theoretical And Applied. Volume 2. By Ag Everson Pearse. Edinburgh and London: Churchill Livingstone. Pp. 757.
19. Ross, M. H., & Pawlina, W. (2020). *Histology: A text and atlas* (8th ed.). Wolters Kluwer.
20. Suvarna, S. K., Layton, C., & Bancroft, J. D. (2018). *Bancroft's theory and practice of histological techniques* (8th ed.). Elsevier.
21. Taylor, C. R., & Levenson, R. M. (2006). Quantification of immunohistochemistry—Issues concerning methods, utility and semiquantitative assessment II. *Applied Immunohistochemistry & Molecular Morphology, 14*(1), 1–10.
22. Yam, L. T., Li, C. Y., & Crosby, W. H. (1971). Cytochemical identification of monocytes and granulocytes. *American Journal of Clinical Pathology, 55*(3), 283–290. https://doi.org/10.1093/ajcp/55.3.283

ISBN NR. : 978-625-8795-33-2

UV KATKILARLA GÜÇLENDİRİLMİŞ, BOYA GEREKTİRMEYEN ABS/PMMA TEMELLİ POLİMER LEVHALARIN OTOMOTİV DIŞ TRİM UYGULAMALARI İÇİN GELİŞTİRİLMESİ

Talha AYDIN

Farform Otomotiv A.Ş. Ar-Ge Merkezi,

E-posta: talha.aydin@farform.com.tr- ORCID ID: 0009-0003-1278-9600

Didem Elif SOYDAN

Farform Otomotiv A.Ş. Ar-Ge Merkezi,

E-posta: didem.yasa@farform.com.tr - ORCID ID: 0009-0008-8894-9275

ÖZET

Bu çalışmada, otomotiv dış trim uygulamalarında kullanılmak üzere boya gerektirmeyen, kendinden renkli, UV dayanımı yüksek ve geri dönüştürülebilir ABS/PMMA temelli çok katmanlı polimer levha geliştirilmiştir. Çalışma, önceki projelerde 1200 saat seviyesine kadar doğrulanan UV dayanım performansının 1500 saat ve üzerine çıkarılması, uzun süreli dış ortam koşullarında renk farkı ve parlaklık kaybının minimize edilmesi ve ithal benchmark ürünlere alternatif yerli bir malzeme çözümü oluşturulması amacıyla yürütülmüştür. Proje kapsamında öncelikle benchmark plakaların katman yapısı, yüzey karakteri ve malzeme bileşimi detaylı olarak incelenmiştir. FTIR, DSC, TGA, SEM ve temas açısı analizlerinden elde edilen veriler doğrultusunda ABS/PMMA esaslı çok katmanlı yapı kurgusu doğrulanmış; UV dayanımını artırmaya yönelik reçete geliştirme çalışmaları başlatılmıştır. Bu kapsamda UV stabilizatörleri, optik katkılar, masterbatch sistemleri ve katman bazlı katkı oranları değiştirilerek farklı deneme reçeteleri oluşturulmuştur. Hazırlanan plakalar ko-ekstrüzyon hattında üretilmiş ve termoform prosesine uygunluk, yüzey kalitesi, katman bütünlüğü, renk stabilitesi ve parlaklık davranışı açısından karşılaştırmalı olarak değerlendirilmiştir.

Geliştirilen numuneler ISO 4892-2 standardına göre Xenon Arc hızlandırılmış yaşlandırma testlerine tabi tutulmuştur. Test sonuçlarında hedeflenen 1500 saat UV dayanımı sağlanmış; uzun süreli UV maruziyeti sonrasında renk stabilitesi ve yüzey parlaklığı korunmuştur. Reçete 3, yüksek UV performansı ve teknik kararlılığı ile öne çıkarken; Reçete 6, maliyet-performans dengesi açısından uygulanabilir bir alternatif olarak değerlendirilmiştir.

Elde edilen sonuçlar, geliştirilen ABS/PMMA temelli çok katmanlı levhaların otomotiv dış trim parçalarında boya prosesine ihtiyaç duymadan kullanılabilecek teknik yeterliliğe sahip olduğunu göstermektedir. Bu yönüyle çalışma; VOC emisyonlarının, su ve enerji tüketiminin azaltılması, yerli üretim kabiliyetinin güçlendirilmesi, ithalat bağımlılığının düşürülmesi ve seri üretime uyarlanabilir sürdürülebilir dış trim malzemelerinin geliştirilmesi açısından güçlü bir Ar-Ge çıktısı sunmaktadır.

Anahtar Kelimeler: ABS/PMMA, dış trim, UV dayanımı, ko-ekstrüzyon.

ISBN NR. : 978-625-8795-33-2

DEVELOPMENT OF UV-ADDITIVE-REINFORCED, PAINT-FREE ABS/PMMA-BASED POLYMER SHEETS FOR AUTOMOTIVE EXTERIOR TRIM APPLICATIONS

Talha AYDIN

Farform Otomotiv A.Ş. R&D Center

E-mail: talha.aydin@farform.com.tr - ORCID ID: 0009-0003-1278-9600

Didem Elif SOYDAN

Farform Otomotiv A.Ş. R&D Center

E-mail: didem.yasa@farform.com.tr - ORCID ID: 0009-0008-8894-9275

ABSTRACT

In this study, a multilayer ABS/PMMA-based polymer sheet with high UV resistance, self-colored structure, recyclability, and no need for painting was developed for use in automotive exterior trim applications. The study was carried out to increase the UV resistance performance, which had been validated up to 1200 hours in previous projects, to 1500 hours and above, to minimize color difference and gloss loss under long-term outdoor conditions, and to develop a domestic material solution as an alternative to imported benchmark products.

Within the scope of the project, the layer structure, surface characteristics, and material composition of benchmark sheets were first examined in detail. Based on the data obtained from FTIR, DSC, TGA, SEM, and contact angle analyses, the ABS/PMMA-based multilayer structure was verified, and formulation development studies were initiated to improve UV resistance. In this context, different trial formulations were prepared by varying UV stabilizers, optical additives, masterbatch systems, and layer-based additive ratios. The prepared sheets were produced on a co-extrusion line and comparatively evaluated in terms of thermoforming suitability, surface quality, layer integrity, color stability, and gloss behavior.

The developed samples were subjected to Xenon Arc accelerated weathering tests in accordance with ISO 4892-2. The test results showed that the targeted 1500-hour UV resistance was achieved, while color stability and surface gloss were maintained after long-term UV exposure. Recipe 3 stood out with its high UV performance and technical stability, whereas Recipe 6 was evaluated as an applicable alternative in terms of cost-performance balance.

The results indicate that the developed ABS/PMMA-based multilayer sheets have the technical capability to be used in automotive exterior trim parts without the need for a painting process. In this respect, the study presents a strong R&D output by contributing to the reduction of VOC emissions, water and energy consumption, the strengthening of domestic production capability, the reduction of import dependency, and the development of sustainable exterior trim materials adaptable to mass production.

Keywords: ABS/PMMA, exterior trim, UV resistance, co-extrusion.

ISBN NR. : 978-625-8795-33-2

EXPERIMENTAL EVALUATION OF HEAT TRANSFER ENHANCEMENT IN A PLATE HEAT EXCHANGER USING MAGNETIC NANOFLUID

Ataollah KHANLARI
Department of Mechanical Engineering, Faculty of Engineering, Tarsus University, Mersin, Türkiye
E-posta Adresi: atahanlar@tarsus.edu.tr - ORCID ID: 0000-0001-9691-9799

ABSTRACT

A wide range of thermal enhancement techniques has been developed to increase the heat transfer performance of heat exchangers. One of the most effective approaches to enhance the thermal performance of heat exchangers is the use of nanofluids, which are prepared by dispersing nanoparticles into a conventional base fluid. In the present study, $ZnFe_2O_4$ nanoparticles were dispersed in water to prepare a $ZnFe_2O_4$/water magnetic nanofluid. Accordingly, $ZnFe_2O_4$ nanoparticles were dispersed in water at a weight concentration of 1% (wt./wt.) to prepare the magnetic nanofluid. The main aim of this study is to evaluate the thermal performance of a plate-type heat exchanger with 12 plates using the prepared $ZnFe_2O_4$/water magnetic nanofluid and to investigate its effect on heat transfer enhancement. The thermal performance of the plate heat exchanger was evaluated at different outlet temperature setpoints and Reynolds numbers. The experimentally obtained results revealed that employing the $ZnFe_2O_4$/water nanofluid in the plate heat exchanger enhanced the heat transfer coefficient by an average of 9.6% compared with water. Overall, the findings confirm that the prepared $ZnFe_2O_4$/water magnetic nanofluid is a promising working fluid for enhancing heat transfer in plate heat exchangers. The outcomes of this study may serve as a useful reference for future research on magnetic nanofluid-based heat transfer enhancement.

Keywords: Plate heat exchanger; Magnetic nanofluid; $ZnFe_2O_4$/water; Thermal performance

ISBN NR. : 978-625-8795-33-2

EXPERİMENTAL İNVESTİGATİON OF THE EFFECT OF DİFFERENT MESH CONFİGURATİONS ON THE ADHESİON STRENGTH BETWEEN GEOPOLYMER CONCRETE AND REBAR

Doç. Dr. Barış BAYRAK

İnşaat Mühendisliği Bölümü, Kafkas Üniversitesi

bbayrak@kafkas.edu.tr - 0000-0002-7438-1227

ABSTRACT

Bond between reinforcing steel and geopolymer concrete is one of the governing parameters affecting the structural performance and serviceability of reinforced geopolymer concrete members. Various strengthening and confining approaches have been put forward to improve the bond performance. However, whether the bonds mechanism is different with the wrapping materials of various mesh is not yet well cleared. Hence, this research experimentally examines the influence of glass mesh, steel mesh and carbon mesh on bond behavior between ribbed reinforcing bars and geopolymer concrete. Cylindrical geopolymer concrete specimens with a 10 mm diameter ribbed reinforcing bar at specimen center underwent a sequence of pull-out tests. A total of four specimen groups were prepared, including an unwrapped reference specimen and wrapped glass mesh, steel mesh, and carbon mesh specimens. Bond strength-slip relationships, maximum bond strength (τmax), slip corresponding to the maximum bond stress (smax), ultimate slip (su) and energy dissipation capacity (E) were evaluated. The results indicated that the maximum bond strength of the reference specimen was 12.13 MPa, whereas using glass mesh reduced the performance by about 37.5%, steel by 48.1% and carbon mesh final resulted in a reduction of approximately 61.5%. The bond strength at peak is less than the control specimen, but with that deformation capacity of glass mesh specimens obtained were between 19.67 mm to 40.01 mm (ultimate slip). In addition, the glass mesh design had the greatest energy absorption ability (76.15 N/mm), which is around 34% higher than that of reference specimen. On the other hand, steel and carbon mesh had relatively brittle post-peak bond behavior with less energy absorption. Overall, the results demonstrate that while mesh wrapping does not increase peak bond strength, glass mesh provides a significant improvement in post-peak slag response, ductility and energy dissipation capacity and appear to be a viable confinement alternative for reinforced geopolymer concrete where deformation capacity and failure performance are a primary consideration.

Keywords: Bond strength, pull-out, geopolymer

1. INTRODUCTION

Geopolymer concrete is a type of concrete based on an alternative binder system obtained by reacting fly ash, blast furnace slag, metakaolin, silica fume, red mud, rice husk ash, and similar SiO_2–Al_2O_3-rich industrial or natural aluminosilicate sources with alkali activators instead of Portland cement. In this system, sodium hydroxide, sodium silicate, or different alkali/reactive activators dissolve the silica and alumina in the raw material, enabling the formation of a three-

ISBN NR. : 978-625-8795-33-2

dimensional inorganic polymeric network structure. The resulting N-A-S-H, C-S-H, or C-(A)-S-H type gel structures are the basic binder phases that determine the mechanical strength and matrix density of the concrete. In this respect, geopolymer concrete, unlike classical hydration-based cement concrete, has a polymerization/alkali activation-based binder mechanism (Zhao et al. (2024); Kishore et al. (2025); Onutai et al. (2026)). One of the most important advantages of geopolymer concrete is that it offers a more sustainable building material thanks to the utilization of industrial waste as binders or aggregates. The use of waste such as fly ash, slag, red mud, and electric arc furnace slag reduces the consumption of natural resources and prevents waste from being sent to landfills. In addition, geopolymer concrete can exhibit performance advantages such as high compressive strength, low shrinkage, low creep, good acid resistance, high temperature resistance, and improved impermeability to chloride attack. Especially when appropriate raw materials, activator ratios, and curing conditions are provided, a dense microstructure is formed; this positively affects the strength and durability properties (Manzoor et al. (2024); Shahedan et al. (2024); Kishore et al. (2025)). Another advantage of geopolymer systems is that their performance can be improved with additives. For example, additives such as carbon nanotubes, graphene oxide, fibers, nano-silica, or CaO can increase matrix density, limit crack development, and improve mechanical/durability properties. However, the effectiveness of these improvements is directly related to the homogeneous distribution of additives, their compatibility with alkaline environments, and their use at optimum dosages (Zhao et al. (2024); Kishore et al. (2025)).

Studies (Qin et al. (2026); Zhang et al. (2026); Li et al. (2026); Guo et al. (2026)) show that geopolymer concrete has significant potential not only as an alternative to traditional concrete but also for specialized engineering applications. Repair and strengthening applications in marine structures are one such area. The low permeability, resistance to chloride ions, and dense microstructure of fly ash-based geopolymer concrete provide significant advantages in reducing corrosion-induced deterioration in reinforced concrete marine structures. Therefore, it is considered a suitable repair/strengthening material for piers, port structures, bridge abutments, offshore platforms, and coastal infrastructure. Geopolymer concrete also has the potential to be used in structures that may be exposed to high temperatures or fire. The uploaded review states that, thanks to its three-dimensional inorganic network structure, geopolymer concrete exhibits more stable behavior at high temperatures compared to OPC concrete and can maintain its strength to a certain extent up to the 1000–1200 °C range. Therefore, it stands out as an important alternative for tunnels, industrial structures, high-fire-risk infrastructure, and structural elements exposed to high temperatures (Manzoor et al. (2024)). In addition, geopolymer -based materials have a wide range of applications, including injection/grout applications, permeable concrete pavements, sustainable road and pavement systems, corrosion-resistant coatings, recycled aggregate concretes, precast structural elements, and special functional building materials. For example, red mud-fly ash-based geopolymer grout materials are developed for low-carbon soil improvement and subsurface engineering applications; while EAF slag and fly ash-based permeable geopolymer concretes are developed for sustainable drainage and permeable pavement systems (Onutai et al. (2026)).

ISBN NR. : 978-625-8795-33-2

The primary reason for the environmental superiority of geopolymer concrete is the significant elimination of the energy-intensive clinkerization and calcination processes involved in Portland cement production. Cement production is estimated to be responsible for approximately 6–8% of global CO_2 emissions; in contrast, geopolymer concrete achieves significant emission reductions by using low-carbon footprint industrial by-products as binders instead of cement. Some studies have reported that geopolymer systems can reduce greenhouse gas emissions by approximately 44–64%, and in some cases by 55–75%, compared to OPC concrete (Shahedan et al. (2024); Ye et al. (2026)).

The safe and efficient behavior of reinforced concrete structures depends on the adequate establishment of the bond mechanism between the concrete and the reinforcement. This bond ensures the continuity of load transfer, enabling deformation compliance in reinforced concrete elements and guaranteeing a uniform stress distribution across the cross-section. Insufficient bond capacity leads to stress redistribution in reinforced concrete elements, which can result in excessive displacements under service loads and a significant reduction in load-carrying capacity (Zhao et al. (2013); Dalalbashi et al. (2019)). The bond strength between concrete and reinforcement consists of three main components: surface bond, mechanical interlock, and friction. Especially when using ribbed reinforcement, the greatest contribution to bond strength comes from mechanical interlock. Therefore, in modern reinforced concrete design, accurate modeling of bond behavior is considered a critical parameter for determining structural performance at both service loads and ultimate load levels (Zhao et al. (2013); Das et al. (2023)).

Bond behavior is not solely dependent on material properties; it is also affected by numerous parameters such as concrete strength, cover thickness, reinforcement diameter, anchor length, stirrup presence, and environmental factors. Significant reductions in the bond capacity between concrete and reinforcement occur, particularly under high temperatures, and even after short-term fire exposure, losses of up to approximately 50% in bond strength can be observed. The primary reason for this is thermal cracking and material degradation caused by high temperatures (Soares et al. (2020); Hutaibat et al. (2024)). Similarly, it has been noted that the bond performance of early-age concrete changes significantly after fire, and parameters such as anchor length, concrete strength, and stirrup presence now play a decisive role in bond capacity. In particular, it is stated that increasing the reinforcement diameter under high temperature conditions reduces bond strength, while increasing the cover thickness has a limiting effect on bond loss (Xue et al. (2008); Lu et al. (2019)). Bond behavior changes significantly not only under static loads but also under repeated and cyclic loading conditions. Under repeated loading, the widening of longitudinal cracks along the reinforcement leads to an increase in bond shear and earlier bond failure. Therefore, considering the type of loading is of great importance in evaluating bond behavior (Li and Lam (2018); Lindorf et al. (2019)). With the increasing interest in sustainable building materials in recent years, the bond performance of combinations of recycled aggregate concrete (RAC) and fiber-reinforced polymer (FRP) reinforcement has become a subject of research. Studies show that the bond behavior between recycled aggregate concrete and FRP reinforcement can vary depending on the microstructure of the aggregate, and that the reinforcement surface geometry plays a

ISBN NR. : 978-625-8795-33-2

decisive role in the bond mechanism. Furthermore, it has been reported that the bond mechanism changes at high strain rates and that the bond strength differs depending on the dynamic loading conditions (Li et al. (2021)).

2. EXPERIMENTAL PROGRAM

2.1. Materials, mix proportions and specimen preparation

In this study, geopolymer concrete mixtures containing ground granulated blast furnace slag (GBFS) and waste marble powder (WMP) have been prepared. GBFS was chosen due to its high calcium and silica composition as alkaline activation products of the geopolymerization reactions and these will produce a dense framework gelatinous binder gels. A waste-derived supplementary material (WMP) was used with the aim of exploit sustainability in matrix compaction and aiming to be within the circular economy. The chemical and physical compositions of GBFS and WMP are given in Table 1. The GBFS is composed of 41.2% CaO and 35.1% SiO_2, while the WMP contained a very high content of CaO (55.6%). The specific gravities of both GBFS and WMP were 2.88 and 2.76 respectively.

Table 1. Physical and chemical properties of GBFS and WMP (% by weigth)

	CaO	SiO_2	Al_2O_3	Fe_2O_3	MgO	Na_2O	K_2O	SO_3	LOI	Spec. gravity
GBFS	41,2	35,1	8,8	1,2	11,3	0,4	0,7	0,3	0,8	2,88
WMP	55,6	0,8	0,7	<0,1	<0,1	0,5	0,1	<0,1	41,7	2,76

The geopolymer was prepared using sodium hydroxide (NaOH) and sodium silicate (Na_2SiO_3) as alkali activators. It was selected in order to guarantee enough dissolution of aluminosilicate phases and enhance the geopolymerization process. The compositions of the mixtures used in this study are represented in Table 2. The geopolymer concrete mix was clearly 800 kg/m³ of GBFS + 529 kg/m³ WMP + 80 kg/m³ of water, and 168 kg/m³ NaOH + 432 kg/m³ of Na_2SiO_3.

Table 2. Mixture design (kg/m^3)

GBFS	WMP	Water	NaOH	Na_2SiO_3
800	529	80	168	432

Specimens for bond amounts were created in cylindrical molds. Bond were created at the center of specimens by centrally embedding ribbed reinforcing steel bars. In bond tests, 10 mm diameter ribbed reinforcement was used for all samples. Figure 1 illustrates the reinforcement stress-strain behavior used in the analysis. Four different specimen groups were created with the aim of exploring how an alternative wrapping material impacted bond performance. Table 3 summarizes the particulars of the specimens. The reference specimens (Ref) were produced without a wrapping material. The S-GM series used wrapping with glass mesh as the circumferential diameter, where 5d was selected (or 5 times of a rebar diameter). Carbon mesh wrapping of diameter 5d was employed in the S-CM series, and steel mesh wrapping of diameter 5d was used in the S-SM series. With a bond length of 5d, the specimens were heat cured at 75 °C for 120 min.

ISBN NR. : 978-625-8795-33-2

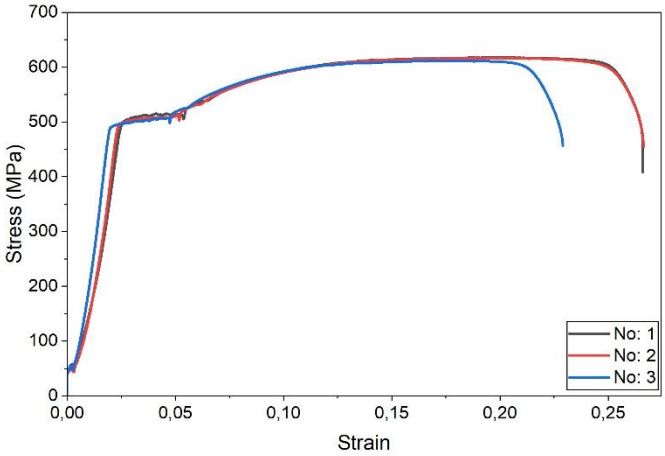

Figure 1. Stress–strain curves of rebar

Table 3. Specimen details

Sample ID	Bond length	Wrapping material	Curing conditions
Ref	5d	-	75 ^{o}C for 120 min
S-GM	5d	Glass	75 ^{o}C for 120 min
S-SM	5d	Steel	75 ^{o}C for 120 min
S-CM	5d	Carbon	75 ^{o}C for 120 min

In case of specimen preparation, all the dry materials were foremost maintained together to retain uniform distribution in the mixture. Then, the alkaline activators and water were introduced to the dry mixture and mixed until a homogenous consistency was obtained. All specimens were conducted and were compacted to reduce the air voids between aggregates during casting, which were kept in molds for 24 h. After demolding all specimens underwent heat curing at a temperature of 75°C for 120 min prior testing. This curing regime was opted to fasten geopolymerization reactions and enhance the mechanical behavior of geopolymer concrete at early ages. All samples were tested on day 7.

2.2. Test procedure

The bond between geopolymer concrete and reinforcing steel was tested using the pull-out test method. The test methodology was reported in literature and based on the procedures presented by researchers. Specimens were prepared and tested in a monotonic tensile load using a computer controlled universal testing machine. The concrete sample was cast in a rigid steel loading frame, and the extending rebar was held in place by the upper jaws of the testing machine during the tests. Pull-out test was conducted by applying axial tensile load to the reinforcement and could be used to investigate bond characteristics between rebar and geopolymer concrete matrix.

Test setups accumulated load loss and slip were measured in the vertical direction using a loading rate control experiment at a constant 0.2 mm/min, which would keep bond-slip behavior stable during testing. The applied load and associated slip values were recorded during testing until the occurrence of bond failure. Maximum bond stress was calculated according to following Equation (1):

ISBN NR. : 978-625-8795-33-2

$$\tau = \frac{F}{\pi d L} \quad (1)$$

where τ is the bond stress (MPa), F is the applied pull-out force (N), d is the diameter of the reinforcing bar (mm), and L is the bond length (mm).

Post-testing inspection of the failure modes of all tested specimens was performed to study how different wrapping materials influenced crack propagation, and bond failure characteristics. Bond stress-slip relationships were determined to assess the bond performance of the geopolymer concrete specimens based on wrapping conditions. The experimental setup is shown in Figure 2.

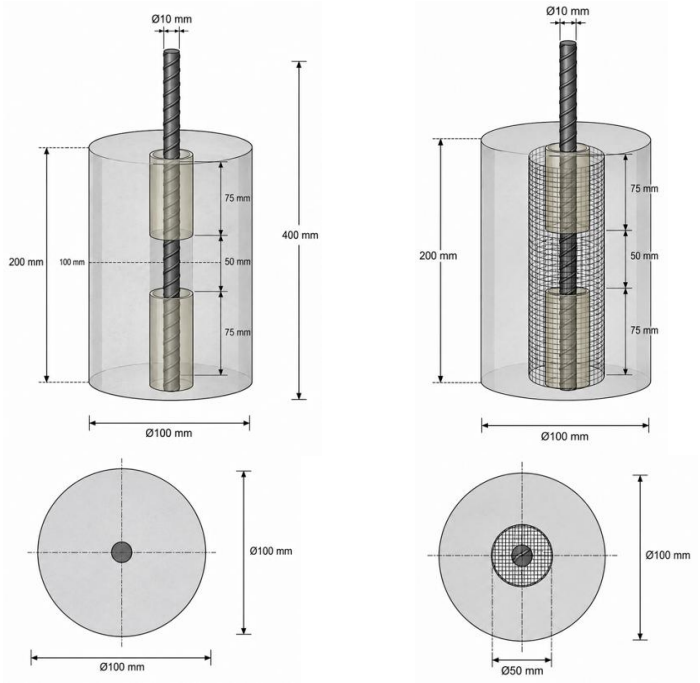

Figure 2. Experimental setup

3. RESULTS AND DISCUSSION

The bond strength-displacement graphs of the samples are presented in Figures 3 and 4. Figure 2 shows that different mesh types significantly alter the concrete-reinforcement bond behavior, not only in terms of maximum bond stress but also in terms of ductility and energy dissipation capacity. The highest bond strength as seen in the reference specimens was 12.13 MPa The curve exhibits a relatively sharp rise until the attaining maximum load, after which there is almost immediate reduction in bond stress. Although the bond capacity is high so this a sign of brittle bond fracture. While the maximum bond strength is very low in specimens using glass mesh, this curve has a much longer tail. The adhesion does not completely vanish after the maximum strength, but compensates by bearing very high loads (over 30 MPa) reaching nearly 40 mm of slip. This means that the glass mesh restricts crack propagation, incrementally losing its adhesion too. Steel mesh test specimens attain a peak early as with the glass mesh. However, the load-carrying capacity decreases more rapidly after the peak. Since the tail region of the curve is shorter, ductility and energy dissipation capacity remain limited. Samples using carbon mesh exhibit the lowest maximum bond strength. The curve initially reaches a peak quickly

ISBN NR. : 978-625-8795-33-2

and then shows a continuously decreasing behavior. This result indicates that carbon mesh cannot improve the bond mechanism under these experimental conditions.

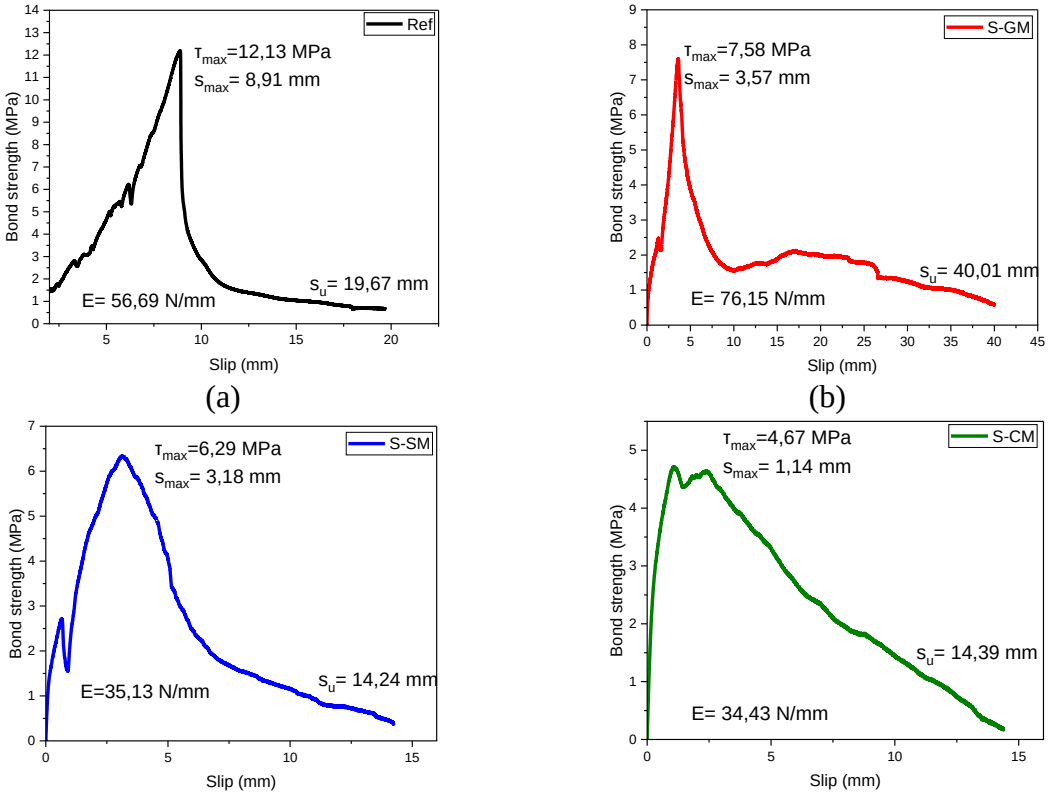

Figure 3. Bond strength-slip curves of (a) Ref (b) S-GM (c) S-SM (d) S-CM

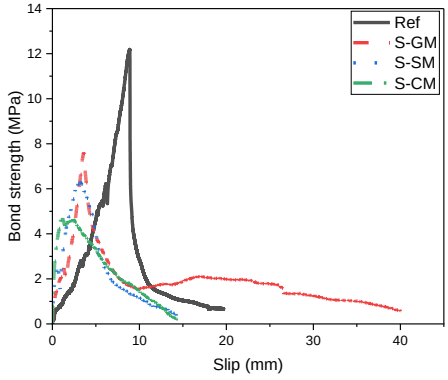

Figure 4. Bond strength -slip curves of all specimens

The summary of the results is shown in Table 4. T_{max} represents the maximum bond strength, s_{max} represents the slip corresponding to the maximum bond strength, and s_u represents the slip at the moment of failure. Furthermore, the energy dissipation capacity (E) was calculated from the area under the bond strength-slip graph. Table 4 shows that the highest maximum bonding stress (τ_{max}) value of 12.13 MPa was obtained in the reference (Ref) specimen. The τ_{max} values for specimens using glass mesh (S-GM), steel mesh (S-SM), and carbon mesh (S-CM) were determined as 7.58, 6.29, and 4.67 MPa, respectively. Compared to the reference specimen, there was a decrease in maximum bonding stress of approximately 37.5%, 48.1%, and 61.5%, respectively. These results indicate that the mesh materials used, instead of strengthening the

ISBN NR. : 978-625-8795-33-2

direct mechanical bonding mechanism between the concrete and the ribbed reinforcement, limit it to a certain extent. The lowest τ_{max} value obtained in specimens using carbon mesh, in particular, may be due to the higher rigidity of carbon mesh, which prevents the load from being distributed more homogeneously at the concrete-reinforcement interface and leads to earlier local stress concentrations. In contrast, glass mesh specimens provided a higher maximum bonding strength compared to other mesh types, thus preserving the bonding capacity more effectively. Significant differences were also observed in terms of the shear amount (s_{max}) corresponding to the maximum bond stress. While the maximum bond stress occurred at a shear value of 8.91 mm in the reference specimen, these values were determined as 3.57, 3.18, and 1.14 mm in the S-GM, S-SM, and S-CM specimens, respectively. Accordingly, it is seen that the maximum bond stress is reached at much lower shear levels in all specimens using mesh. In particular, in the specimen using carbon mesh, maximum bond occurred at only 1.14 mm shear, which is approximately 87% lower than the reference specimen. This indicates that the bond mechanism is mobilized faster in the initial stages in specimens surrounded by mesh, but the maximum capacity is reached earlier. In other words, the use of mesh reduced the deformation level at which maximum bond occurs, but this also caused a significant decrease in the maximum bond capacity.

Table 4. Summary of results

Sample ID	τ_{max} (MPa)	s_{max} (mm)	s_u (mm)	E (N/mm)
Ref	12,13	8,91	19,67	56,69
S-GM	7,58	3,57	40,01	76,15
S-SM	6,29	3,18	14,24	35,13
S-CM	4,67	1,14	14,39	34,43

The shear amount at fracture is an important parameter in evaluating the bond ductility of the specimens. According to the results in Table 4, the highest water loss value was obtained in the S-GM sample using glass mesh, with a value of 40.01 mm. This value corresponds to approximately twice that of the reference sample (19.67 mm) and represents an increase of approximately 103%. In contrast, the fracture slips in the S-SM and S-CM samples were determined as 14.24 mm and 14.39 mm, respectively, and were lower than the reference sample. Despite the reduced maximum bond strength in glass mesh-reinforced samples, the fact that load-carrying capacity is sustained over high slip levels indicates controlled propagation of cracks and gradual (as opposed to sudden) loss of bond. In contrast, in the samples using steel and carbon mesh, the loss of bond occurred at lower deformation levels, which indicates a more brittle bond behavior. The energy dissipation capacity (E) was obtained by calculating the area under the bond stress-slip curve and represents the total energy that the samples can absorb during the bond behavior. When the results were examined, the highest energy dissipation capacity was determined in the S-GM sample with 76.15 N/mm². This value is approximately 34.3% higher than the reference sample. Although the maximum bond stress in samples using glass mesh was lower than in the reference sample, the fact that the bond stress could be maintained for a long time after the maximum load and that the load transfer continued up to high shear levels significantly increased the area under the curve. In contrast, the energy

ISBN NR. : 978-625-8795-33-2

dissipation capacities in S-SM and S-CM samples were calculated as 35.13 and 34.43 N/mm², respectively, and decreased by approximately 38% and 39% compared to the reference sample. This indicates that bond is lost more quickly after the maximum load in samples using steel and carbon mesh, and that the energy dissipation capacity of the system remains limited. In conclusion, although glass mesh did not increase the maximum bond strength, it made the bond behavior more ductile, extended the load-carrying time, and provided the highest energy dissipation capacity.

4. CONCLUSION

This study experimentally investigated the bond behavior between geopolymer concrete and ribbed reinforcing steel wrapped with different mesh materials, namely glass mesh, steel mesh, and carbon mesh. Pull-out tests were performed to evaluate the effects of these wrapping materials on the bond stress-slip response, maximum bond strength, slip characteristics, and energy dissipation capacity. Based on the experimental findings, the following conclusions can be drawn:

- The reference specimen exhibited the highest maximum bond strength (τ_{max} = 12.13 MPa), whereas the incorporation of mesh materials reduced the maximum bond capacity. Compared with the reference specimen, the bond strength decreased by approximately 37.5%, 48.1%, and 61.5% for glass, steel, and carbon mesh specimens, respectively.
- Glass mesh significantly improved the post-peak bond behavior despite its lower maximum bond strength. The ultimate slip increased from 19.67 mm for the reference specimen to 40.01 mm for the glass mesh specimen, indicating a substantially more ductile bond failure mechanism with a gradual loss of bond capacity.
- Among all wrapping materials, the glass mesh provided the highest energy dissipation capacity (76.15 N/mm), representing an increase of approximately 34% compared with the reference specimen. In contrast, steel and carbon mesh reduced the energy absorption capacity due to their relatively brittle post-peak bond behavior.
- Overall, the results indicate that the selection of wrapping material strongly influences the bond mechanism between geopolymer concrete and reinforcing steel. Although none of the investigated mesh materials enhanced the maximum bond strength, glass mesh effectively improved the ductility, deformation capacity, and energy dissipation characteristics of the bond interface, demonstrating its potential as a confinement material for applications where post-peak performance is more critical than peak bond capacity.

REFERENCES

Dalalbashi, A., Ghiassi, B., & Oliveira, D. V. Textile-to-mortar bond behaviour in lime-based textile reinforced mortars. Construction and Building Materials, 227, 116682, 2019. https://doi.org/10.1016/j.conbuildmat.2019.116682

Das, A., Bošnjak, J., & Sharma, A. Post-fire bond behaviour of reinforcement in concrete considering different bonded lengths and position of rebars, Engineering Structures, 296, 116908, 2023. https://doi.org/10.1016/j.engstruct.2023.116908

Guo, S., Wang, H., Duan, Z., Zhang, H., Qian, H., & Ye, H. Effect of different reactive activators on the setting time and compressive strength of geopolymer in high-temperature environment, Construction and Building Materials, 518, 145750, 2026. https://doi.org/10.1016/j.conbuildmat.2026.145750

Hutaibat, M., Ghiassi, B., & Tizani, W. Bond behaviour of prestressed basalt textile reinforced concrete, Construction and Building Materials, 438, 137309, 2024. https://doi.org/10.1016/j.conbuildmat.2024.137309

Kishore, K., Sheikh, M. N., & Hadi, M. N. Functionalization of carbon nanotubes for enhanced dispersion and improved properties of geopolymer concrete: A review, Journal of Building Engineering, 111, 113096, 2025. https://doi.org/10.1016/j.jobe.2025.113096

Li, B., & Lam, E. S. S. Influence of interfacial characteristics on the shear bond behaviour between concrete and ferrocement, Construction and Building Materials, 176, 462-469, 2018. https://doi.org/10.1016/j.conbuildmat.2018.05.084

Li, L., Mai, G., He, S., Xiong, Z., Wei, W., Luo, H., & Liu, F. Experimental study on bond behaviour between recycled aggregate concrete and basalt fibre-reinforced polymer bars under different strain rates, Construction and Building Materials, 290, 123218, 2021. https://doi.org/10.1016/j.conbuildmat.2021.123218

Li, B., Ma, Q. Q., Li, Z. C., Han, Z. X., Zhang, C., Zhou, Y. W., & Liu, L. Y. Long-term performance and protective mechanism of graphene oxide-geopolymer anticorrosive coatings: Molecular dynamics simulation and exposure experiment, Case Studies in Construction Materials, e06045, 2026. https://doi.org/10.1016/j.cscm.2026.e06045

Lindorf, A., Lemnitzer, L., & Curbach, M. Experimental investigations on bond behaviour of reinforced concrete under transverse tension and repeated loading, Engineering Structures, 31(7), 1469-1476, 2009. https://doi.org/10.1016/j.engstruct.2009.02.025

Lu, L., Yuan, G., Shu, Q., Huang, Z., Zhong, C., & Xu, B. Bond behaviour between early age concrete and steel bar subjected to cyclic loading after fire, Fire Safety Journal, 105, 129-143, 2019. https://doi.org/10.1016/j.firesaf.2019.02.012

Manzoor, T., Bhat, J. A., & Shah, A. H. Performance of geopolymer concrete at elevated temperature− A critical review, Construction and Building Materials, 420, 135578 , 2024. https://doi.org/10.1016/j.conbuildmat.2024.135578

Onutai, S., Maliyam, W., Zhou, Y., & Nawaukkaratharnant, N. Development of eco-friendly permeable geopolymer concrete derived from electric arc furnace slag and fly ash, Construction and Building Materials, 523, 146218, 2026. https://doi.org/10.1016/j.conbuildmat.2026.146218

Qin, Z., Cheng, Y., Song, Z., & Zhang, Z. Optimization and mechanism analysis of mix proportion for CaO-modified red mud-fly ash geopolymer, Construction and Building Materials, 522, 146191, 2026. https://doi.org/10.1016/j.conbuildmat.2026.146191

Shahedan, N. F., Hadibarata, T., Abdullah, M. M. A. B., Jusoh, M. N. H., Abd Rahim, S. Z., Isia, I., ... & Juwono, F. H. Potential of fly ash geopolymer concrete as repairing and retrofitting

solutions for marine infrastructure: A review, Case Studies in Construction Materials, 20, e03214, 2024. https://doi.org/10.1016/j.cscm.2024.e03214

Soares, S., Freitas, N., Pereira, E., Nepomuceno, E., Pereira, E., & Sena-Cruz, J. Assessment of GFRP bond behaviour for the design of sustainable reinforced seawater concrete structures, Construction and Building Materials, 231, 117277, 2020. https://doi.org/10.1016/j.conbuildmat.2019.117277

Ye, P., Lin, Z., Chen, Y., He, Q., & Chen, Z. Research on bond-slip behavior of steel-reinforced geopolymer recycled concrete, Structures, 87, 111648, 2026. https://doi.org/10.1016/j.istruc.2026.111648

Xue, W., Zeng, L., & Tan, Y. Experimental studies on bond behaviour of high strength CFRP plates, Composites Part B: Engineering, 39(4), 592-603, 2008. https://doi.org/10.1016/j.compositesb.2007.09.002

Zhang, Y., Chen, Q., Song, M., Zheng, Y., & Wu, Z. Performance optimization of red mud-based geopolymer modified grouting materials via response surface methodology, Case Studies in Construction Materials, e06019, 2026. https://doi.org/10.1016/j.cscm.2026.e06019

Zhao, Y., Lin, H., Wu, K., & Jin, W. Bond behaviour of normal/recycled concrete and corroded steel bars, Construction and building materials, 48, 348-359, 2013. https://doi.org/10.1016/j.conbuildmat.2013.06.091

Zhao, C., Li, Z., Peng, S., Liu, J., Wu, Q., & Xu, X. State-of-the-art review of geopolymer concrete carbonation: From impact analysis to model establishment, Case Studies in Construction Materials, 20, e03124, 2024. https://doi.org/10.1016/j.cscm.2024.e03124

ISBN NR. : 978-625-8795-33-2

INTERFACE STATE DENSITY, SERIES RESISTANCE AND RELAXATION TIME ANALYSIS OF AL/CUPC/N-GAAS MIS SCHOTTKY DIODES

Assist. Prof. Dr. ZEYNEP KİŞNİŞCİ

Selçuk University, Faculty of Science, Department of Physics, Konya, Türkiye

znalcacigil@selcuk.edu.tr-0000-0001-7500-3247

ABSTRACT

In this work, an Al/CuPc/n-GaAs metal–interlayer–semiconductor (MIS) Schottky diode was fabricated and electrically characterized using frequency-dependent capacitance (C–f) and conductance (G–f) measurements over a broad frequency range. The influence of frequency on the electrical response of the device was systematically investigated to reveal the effects of the CuPc interfacial layer on the interface properties. The series resistance (Rs) was determined using the Nicollian–Goetzberger method, demonstrating a pronounced frequency dependence with relatively high values at low frequencies and a gradual decrease toward higher frequencies.

To evaluate the interface-state characteristics, the parallel conductance technique was employed by calculating the Gp/ω–f characteristics. A well-defined conductance peak was observed, indicating the interaction between interface traps and the alternating electric field. The interface-state density (Nss) and carrier relaxation time (τ) were extracted from the peak conductance and its corresponding peak frequency. The calculated values were found to be **1.01×10^{14} eV^{-1} cm^{-2}** for the interface-state density and **2.81×10^{-7} s** for the relaxation time, suggesting the presence of a considerable density of interface traps and relatively fast carrier exchange processes at the CuPc/GaAs interface.

The obtained results demonstrate that frequency-dependent admittance spectroscopy combined with the Nicollian–Goetzberger approach provides an effective and reliable method for evaluating the series resistance, interface-state density, and carrier relaxation dynamics of CuPc-based MIS Schottky structures. These findings contribute to a better understanding of charge transport and interface phenomena in organic/inorganic hybrid semiconductor devices and may support the optimization of high-performance electronic and optoelectronic applications.

Keywords: CuPc, C-f, G-f, interface state density, relaxation time

1. INTRODUCTION

Metal–semiconductor (MS) and metal–insulator–semiconductor (MIS) Schottky barrier diodes have attracted considerable attention owing to their simple fabrication, low power consumption, rapid switching capability, and compatibility with modern electronic and optoelectronic technologies [1]. These devices are widely employed in microwave electronics, high-speed integrated circuits, photodetectors, solar cells, sensors, and communication systems because of

ISBN NR. : 978-625-8795-33-2

their excellent rectifying characteristics and fast carrier transport [2]. The electrical performance of Schottky diodes is primarily governed by the metal–semiconductor interface, where the presence of native oxides, lattice imperfections, dangling bonds, and interface defects significantly influences the barrier height, ideality factor, leakage current, and overall device reliability [3]. Consequently, considerable effort has been devoted to improving interface quality through the incorporation of thin insulating or organic interfacial layers.

Among various semiconductor materials, gallium arsenide (GaAs) occupies a unique position due to its direct bandgap, high electron mobility, high saturation velocity, and excellent high-frequency response [4]. Compared with silicon, GaAs exhibits superior transport properties, making it particularly attractive for microwave devices, radio-frequency electronics, photonic components, laser diodes, and high-speed integrated circuits. However, the electrical performance of GaAs-based Schottky devices is frequently limited by the relatively high density of interface states originating from native surface oxides and surface imperfections. These interface states act as charge trapping centers, resulting in frequency dispersion, increased recombination, instability of the Schottky barrier, and degradation of carrier transport. Therefore, reducing interface-state density remains one of the major challenges in improving the electrical performance of GaAs-based MIS structures.

One of the most effective approaches to suppress interface-related defects is the introduction of an organic semiconductor interlayer between the metal contact and the semiconductor surface [5]. Organic materials provide several advantages, including solution-processability, low-temperature fabrication, mechanical flexibility, tunable electronic properties, and effective surface passivation [6]. Among them, copper phthalocyanine (CuPc) has become one of the most extensively investigated organic semiconductors owing to its excellent thermal and chemical stability, high environmental durability, strong π-conjugated molecular structure, and relatively high charge transport capability [7]. Owing to these properties, CuPc has found widespread applications in organic light-emitting diodes, photovoltaic devices, thin-film transistors, gas sensors, photodetectors, and hybrid electronic structures [7]. In MIS Schottky diodes, CuPc can simultaneously modify the metal work function, reduce interface defect density, and facilitate carrier transport across the interface, thereby improving device performance.

Although numerous investigations have reported the current–voltage (I–V) characteristics and rectification behavior of CuPc-based Schottky diodes, studies focusing on their frequency-dependent admittance characteristics remain relatively limited. Electrical parameters extracted solely from current–voltage measurements cannot fully describe the dynamic interaction between interface states and alternating electric fields. Frequency-dependent capacitance and conductance measurements provide substantially richer information concerning polarization mechanisms, dielectric relaxation, carrier trapping–detrapping processes, interface-state response, and charge transport dynamics. Consequently, admittance spectroscopy has become one of the most powerful and reliable techniques for investigating interface-related electrical phenomena in MIS structures.

The measured capacitance and conductance of practical MIS devices are considerably affected by the presence of series resistance (Rs), particularly at medium and high frequencies. The

ISBN NR. : 978-625-8795-33-2

influence of Rs distorts the intrinsic admittance response, leading to significant errors in the determination of interface parameters if not properly corrected. Therefore, elimination of the series resistance contribution is essential before evaluating the interface characteristics. Among various correction techniques, the Nicollian–Goetzberger method is one of the most widely accepted approaches because it enables reliable extraction of the intrinsic capacitance and conductance from the experimentally measured admittance data [1]. Following this correction, the parallel conductance technique (Gp/ω method) can be employed to evaluate the interface-state density (Nss) and carrier relaxation time (τ), both of which provide valuable insight into the charge exchange kinetics between interface traps and the semiconductor. The characteristic conductance peak observed in the Gp/ω–f spectrum reflects the relaxation behavior of interface states and allows quantitative determination of their density and response time.

Despite the increasing interest in organic/inorganic hybrid Schottky structures, comprehensive investigations combining series resistance correction with interface-state and relaxation-time analyses over a broad frequency range remain scarce for Al/CuPc/n-GaAs MIS Schottky diodes. Most previous studies have focused primarily on conventional current–voltage characterization or basic capacitance analysis, whereas detailed admittance investigations capable of revealing the intrinsic interface dynamics have received comparatively less attention. This lack of comprehensive frequency-dependent analysis constitutes an important gap in the literature.

In the present study, an Al/CuPc/n-GaAs MIS Schottky diode was fabricated and electrically characterized using capacitance–frequency (C–f) and conductance–frequency (G–f) measurements over a wide frequency range. The series resistance was extracted using the Nicollian–Goetzberger method, and the corrected admittance data were subsequently employed to obtain the Gp/ω–f characteristics. The interface-state density and carrier relaxation time were determined from the maximum conductance peak, providing quantitative information regarding the interface quality and charge relaxation dynamics. The obtained results demonstrate the capability of frequency-dependent admittance spectroscopy to evaluate the intrinsic electrical properties of CuPc/GaAs interfaces and provide valuable insight into the optimization of high-performance organic/inorganic hybrid MIS Schottky devices.

2. EXPERIMENTAL PROCEDURE

In this study, a commercially available n-type GaAs crystal with a (100) orientation and an approximate thickness of 500 μm was employed. The GaAs crystals were cleaned using the RCA cleaning procedure. After the cleaning process, a 1500 Å thick In layer with a purity of 99.99% was deposited onto the unpolished side of the n-GaAs crystal by thermal evaporation. During the deposition process, the vacuum pressure was maintained at approximately 5×10^{-5} Torr. To obtain a low-resistance ohmic contact, the sample was subjected to vacuum annealing at 500 °C for about 3 min. Subsequently, the polished surface of the ohmic-contacted sample was coated with the organic material CuPc using the drop-casting method. Finally, 99.99% pure Al was thermally evaporated onto the CuPc-coated surface through a mask under a vacuum pressure of 5×10^{-5} Torr, forming the Schottky contacts. As a result, rectifying contacts with a

ISBN NR. : 978-625-8795-33-2

diameter of 2 mm and a thickness of 1500 Å were fabricated. The fabrication process and electrical measurement configuration of the Al/CuPc/n-GaAs Schottky diode was illustrated in Fig. 1. The capacitance-frequency (C-f) and conductance-frequency (G-f) characteristics of the diode were measured at room temperature under dark conditions using an HP 4192A LF impedance analyzer. The measurements were performed over a frequency range of 100 Hz to 10 MHz.

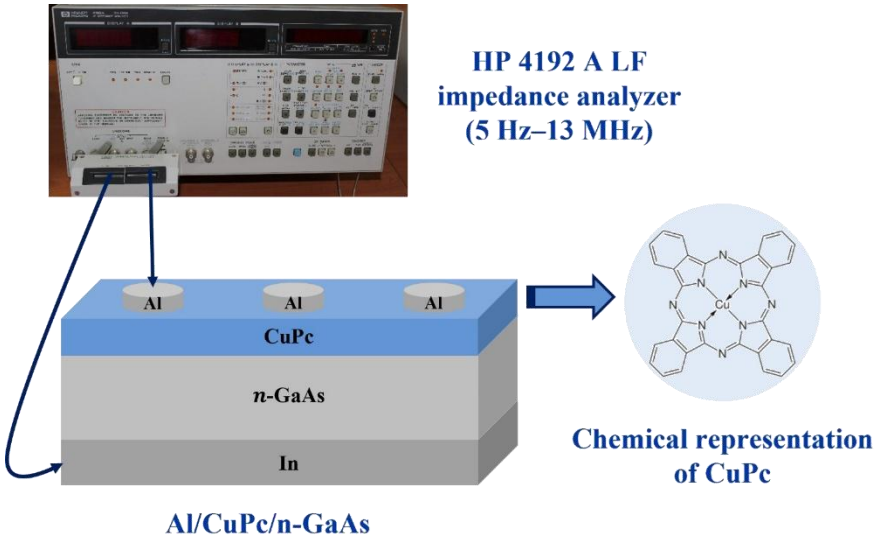

Figure 1. Schematic diagram of prepared diode with the measurement system

3. RESULTS AND DISCUSSION

3.1. Frequency-Dependent Capacitance and Conductance Characteristics

The frequency-dependent capacitance (C–f) and conductance (G–f) characteristics of the fabricated Al/CuPc/n-GaAs MIS Schottky diode measured over the frequency range of 100 Hz–10 MHz are presented in Fig. 2(a) and Fig. 2(b), respectively. These measurements provide valuable information regarding the electrical response of the CuPc interfacial layer and the interface states under alternating electric fields.

ISBN NR. : 978-625-8795-33-2

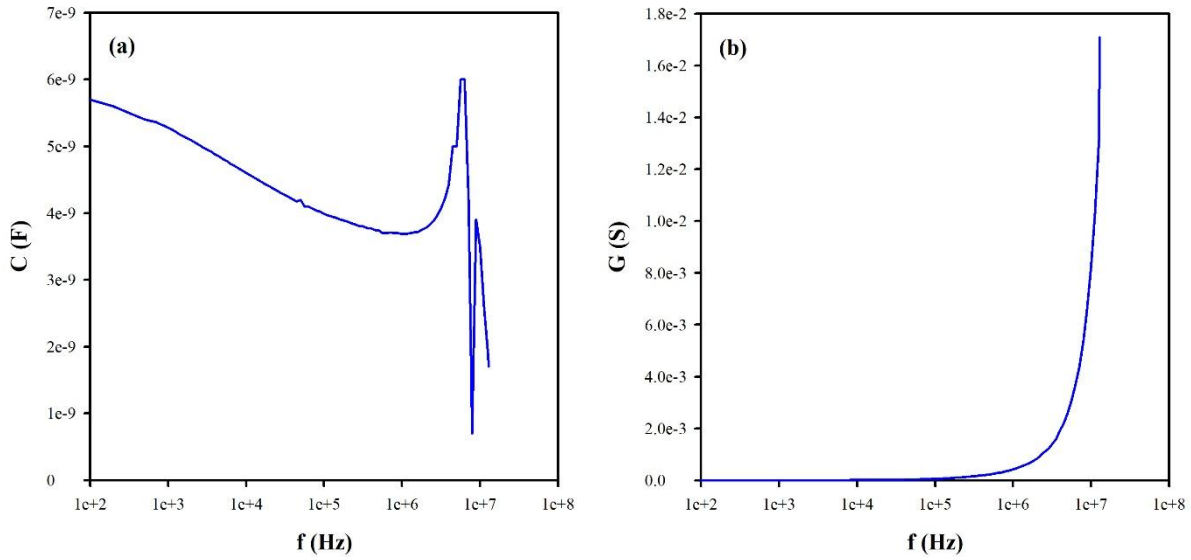

Figure 2. Frequency-dependent electrical characteristics of the Al/CuPc/n-GaAs MIS Schottky diode: (a) capacitance versus frequency (C–f) and (b) conductance versus frequency (G–f)

As seen in Fig. 2(a), the capacitance decreases continuously with increasing frequency up to approximately 10^6 Hz. This behaviour originates from the gradual inability of interface states to follow the applied AC signal. At low frequencies, interface traps exchange charge efficiently with the semiconductor and contribute to the measured capacitance. However, as the frequency increases, the response of these traps becomes progressively slower, causing a reduction in capacitance [8].

A slight increase followed by a sudden decrease is observed in the very high-frequency region. Such behaviour is generally associated with parasitic capacitances, resonance effects, cable inductance, or instrumental limitations rather than intrinsic interface phenomena.

The conductance spectrum shown in Fig. 2(b) exhibits the opposite tendency. The conductance increases monotonically with frequency because the alternating electric field facilitates carrier transport and charge exchange through the interface states. At sufficiently high frequencies, displacement current and series resistance contributions become increasingly dominant.

These observations clearly demonstrate that the electrical behaviour of the Al/CuPc/n-GaAs MIS Schottky diode is strongly governed by frequency-dependent polarization and interface-state relaxation mechanisms.

3.2. Series Resistance Analysis

The frequency dependence of the series resistance was determined using the Nicollian–Goetzberger method. The series resistance was calculated using [1]

ISBN NR. : 978-625-8795-33-2

$$R_s = \frac{G_m}{G_m^2 + (\omega C_m)^2} \quad (1)$$

where

- G_m is the measured conductance,
- C_m is the measured capacitance,
- ω=2πf.

The calculated Rs values are presented in Fig. 3.

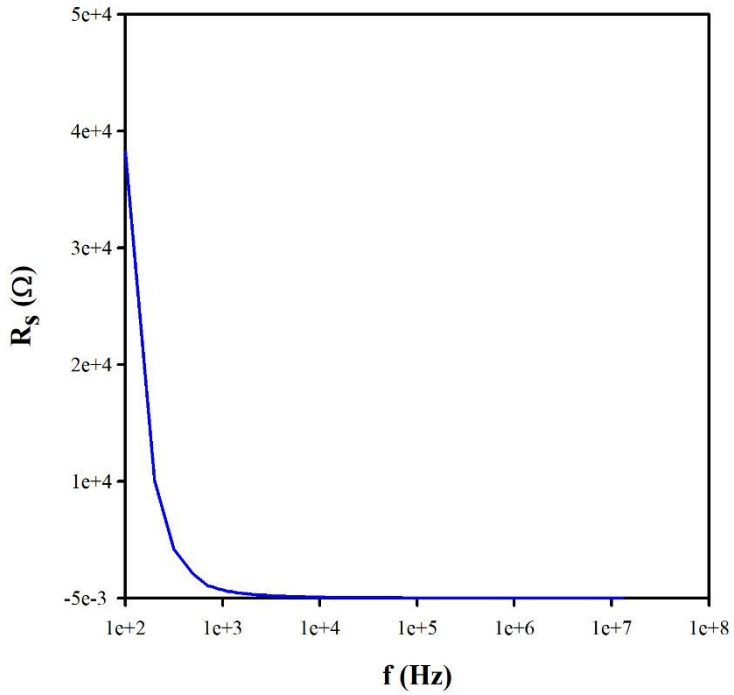

Figure 3. Variation of the series resistance (Rs) with frequency calculated using the Nicollian–Goetzberger method

Figure 3 shows that the series resistance exhibits relatively high values at low frequencies and decreases rapidly with increasing frequency before approaching an almost constant value at higher frequencies.

ISBN NR. : 978-625-8795-33-2

The high Rs values at low frequencies are mainly attributed to interface-state charging, carrier accumulation, and polarization occurring within the CuPc interfacial layer. Since interface traps can efficiently exchange charge at low frequencies, they contribute significantly to the measured impedance.

As the measurement frequency increases, these interface states gradually lose their ability to follow the AC signal. Consequently, the impedance associated with interface charging decreases, resulting in a lower extracted series resistance. The obtained behaviour agrees well with previous reports for MIS Schottky structures and confirms that correction of Rs is necessary before evaluating the intrinsic interface parameters [9].

3.3. Parallel Conductance Analysis

After eliminating the effect of series resistance, the corrected conductance was converted into parallel conductance using [10]

$$\frac{G_{it}}{\omega} = \frac{\omega C_{ox}^2 G_m}{G_m^2 + \omega^2 (C_{ox} - C_m)^2} \tag{2}$$

where

- C_{ox} denotes the oxide/interfacial capacitance,
- C_m and G_m are the measured capacitance and conductance.

The calculated G_p/ω spectrum is presented in Fig. 4.

ISBN NR. : 978-625-8795-33-2

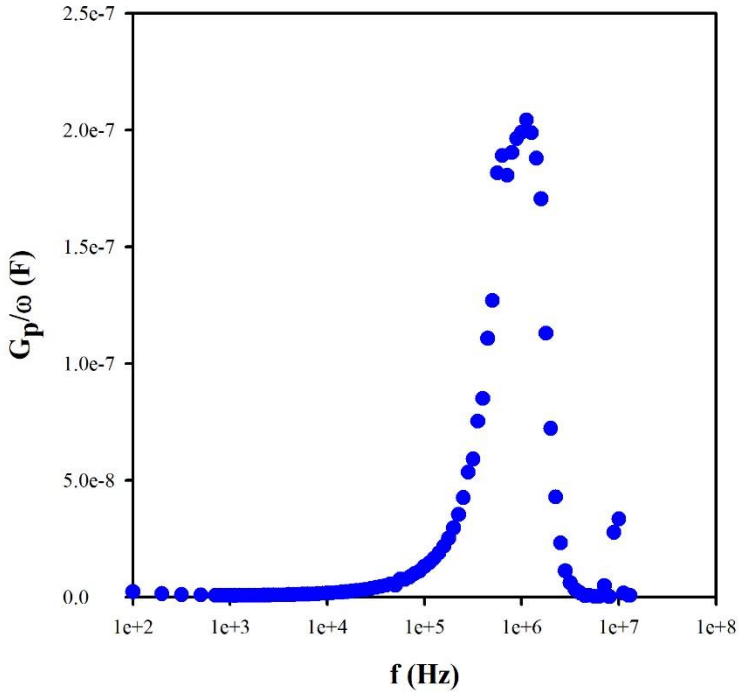

Figure 4. Frequency dependence of the normalized parallel conductance (Gp/ω) of the Al/CuPc/n-GaAs MIS Schottky diode

A pronounced conductance peak is clearly observed around

$$f_{max} = 1.12\text{x}10^{6}\ \text{Hz}$$

The appearance of this peak is characteristic of interface-state relaxation processes.

At low frequencies, interface traps respond completely to the alternating electric field and therefore contribute significantly to the measured conductance.

Near the characteristic relaxation frequency, the charge exchange rate between interface states and the semiconductor reaches its maximum, resulting in the observed conductance peak.

At frequencies higher than the peak frequency, interface traps are no longer able to follow the AC excitation, causing a rapid decrease in Gp/ω.

The presence of a single dominant conductance peak indicates that one principal relaxation process governs the electrical behaviour of the CuPc/GaAs interface within the investigated frequency range.

3.4. Interface-State Density and Relaxation Time

The interface-state density and carrier relaxation time were determined from the maximum value of the parallel conductance spectrum using the Nicollian–Goetzberger equations [1, 11]

ISBN NR. : 978-625-8795-33-2

$$N_{ss} = \frac{(G_p/\omega)_{max}}{0.402qA} \quad (3)$$

And

$$\tau = \frac{1.98}{2\pi f_{max}} \quad (4)$$

where

- q is the electronic charge,
- A is the contact area,
- f_{max} is the peak frequency.

The parameters obtained from the Gp/ω spectrum are summarized in Table 1.

Table 1. Interface parameters extracted from the Gp/ω analysis

Parameter	Value
C_{ox}	3.69x10^{-9} F
f_{max}	1.12x10^{6} Hz
$(G_p/\omega)_{max}$	2.04x10^{-7} F
N_{ss}	1.01x10^{14} eV^{-1} cm^{-2}
τ	2.81x10^{-7} s

As listed in Table 1, the extracted interface-state density is approximately 1.01x10^{14} eV^{-1} cm^{-2}, indicating a considerable density of electrically active interface traps at the CuPc/GaAs interface. These traps are most likely associated with dangling bonds, native oxide layers, structural imperfections, and localized defect states within the organic interlayer.

The calculated relaxation time of 2.81x10^{-7} s indicates a relatively fast carrier exchange process between the interface traps and the semiconductor. Such a short relaxation time suggests that the dominant interface states can efficiently respond to alternating electric fields up to frequencies on the order of 10^6 Hz.

The combination of a relatively high interface-state density and a sub-microsecond relaxation time indicates that charge trapping and detrapping processes play a dominant role in determining the electrical characteristics of the Al/CuPc/n-GaAs MIS Schottky diode.

Overall, the combined analyses of the C–f, G–f, Rs–f, and Gp/ω–f characteristics demonstrate that frequency-dependent admittance spectroscopy, together with the Nicollian–Goetzberger

ISBN NR. : 978-625-8795-33-2

correction procedure, provides a reliable approach for investigating the intrinsic interface properties of CuPc-based MIS Schottky diodes. The extracted values of N_{ss} and τ confirm that the electrical response of the fabricated device is predominantly controlled by interface-state relaxation processes.

4. CONCLUSION

The frequency-dependent electrical behavior of the fabricated Al/CuPc/n-GaAs MIS Schottky diode was systematically investigated using admittance spectroscopy. The obtained C–f and G–f characteristics revealed that the electrical response of the device is strongly influenced by interface-related polarization and charge trapping processes. The frequency-dependent variation of the series resistance further demonstrated that correcting the measured admittance is essential for obtaining reliable interface parameters.

After applying the Nicollian–Goetzberger correction, a distinct peak was observed in the G_p/ω spectrum, confirming the existence of a dominant interface-state relaxation process. The extracted interface-state density (N_{ss}=1.01x10^{14} eV^{-1} cm^{-2} and relaxation time (τ=2.81x10^{-7} s) indicate that electrically active interface traps play a significant role in the charge transport dynamics of the CuPc/GaAs interface.

In conclusion, this study demonstrates that the combined use of frequency-dependent admittance spectroscopy, series resistance correction, and parallel conductance analysis provides a reliable and effective approach for accurately characterizing interface states and carrier relaxation phenomena in organic/inorganic MIS Schottky structures. The proposed methodology can also be extended to similar hybrid semiconductor devices for the optimization of their electrical performance and the development of high-frequency electronic and optoelectronic applications.

REFERENCES

1. Nicollian, E.H., Brews, J.R., MOS (Metal Oxide Semiconductor) Physics and Technology, John Wiley & Sons/New York, 1982.

2. Akın, Ü., Yüksel, Ö. F., Taşcı, E., Tuğluoğlu, N. Fabrication of a New Hybrid Coronene/n-Si Structure by Using Spin Coating Technique and its Photoresponse and Admittance Spectroscopy Studies. Silicon, 12, 1399–1407, 2020.

3. Shehata, M.M., Abdelhady, K., Temperature and Frequency Dependence of Dielectric Relaxation and AC Electrical Conductivity in p-Si/CuPc Hybrid Photodiode, Applied Physics A, 124, 591, 2018.

4. Zhang, Y., Wang, Q., Review of Research Progress on Two-Dimensional Metamaterials Prepared on GaAs Substrates, Academic Journal of Materials & Chemistry, 5, 134–142, 2024.

ISBN NR. : 978-625-8795-33-2

5. Tuğluoğlu, N., Çalışkan, F., Yüksel, Ö.F., Analysis of Inhomogeneous Barrier and Capacitance Parameters for Al/Rubrene/n-GaAs (100) Schottky Diodes, Synthetic Metals, 199, 270–275, 2015.

6. Reddy, P.R.S., Janardhanam, V., Shim, K.-H., Lee, S.-N., Kumar, A.A., Reddy, V.R., Choi, C.J., Temperature Dependent Schottky Barrier Characteristics of Al/n-Type Si Schottky Barrier Diode with Au–Cu Phthalocyanine Interlayer, Thin Solid Films, 713, 138343, 2020.

7. Opitz, A., Bronner, M., Brütting, W., Himmerlich, M., Schaefer, J.A., Krischok, S., Electronic Properties of Organic Semiconductor Blends: Ambipolar Mixtures of Phthalocyanine and Fullerene, Applied Physics Letters, 90, 212112, 2007.

8. Nicollian, E.H., Goetzberger, A., The Si–SiO_2 Interface—Electrical Properties as Determined by the Metal–Insulator–Silicon Conductance Technique, Bell System Technical Journal, 46, 1055–1133, 1967.

9. Şahin, B., Çetin, H., Ayyildiz, E., The Effect of Series Resistance on Capacitance–Voltage Characteristics of Schottky Barrier Diodes, Solid-State Electronics, 135, 8, 490–495, 2005.

10. Schroder, D.K., *Semiconductor Material and Device Characterization*, John Wiley & Sons/New York, 2006.

11. Nicollian, E.H., Goetzberger, A., The Si–SiO_2 Interface—Electrical Properties as Determined by the Metal–Insulator–Silicon Conductance Technique, Bell System Technical Journal, 46, 1055–1133, 1967.

ISBN NR. : 978-625-8795-33-2

IEEE 33 BARALI RADYAL DAĞITIM ŞEBEKESİNDE DAĞITIK ÜRETİM SİSTEMLERİNİN MISOCP VE GUROBİ ÇÖZÜCÜSÜ KULLANILARAK OPTİMUM TAHSİSİ

Ahmet Hamdi Gülcü

Sivas Cumhuriyet Üniversitesi,

20249233003@cumhuriyet.edu.tr-0009-0007-1636-2865

Dr. Öğr. Üyesi Mikail Pürlü

Sivas Cumhuriyet Üniversitesi,

mikailpurlu@cumhuriyet.edu.tr-0000-0002-1194-3931

ÖZET

Artan enerji talebi ile birlikte dağıtık üretim sistemlerinin (DÜS) elektrik dağıtım şebekelerine optimal entegrasyonu, güç sistemleri planlamasının en kritik aşamalarından biri haline gelmiştir. Bu ünitelerin şebekeye rastgele bağlanması, güç kayıplarını artırmakta ve gerilim profilini bozmaktadır. Bu çalışmada, IEEE 33 baralı radyal dağıtım şebekesinde üç adet DÜS'ün eş zamanlı konum ve boyutlandırma problemi ele alınmıştır. Literatürde sıklıkla başvurulan meta-sezgisel yöntemler, stokastik doğaları gereği her çalıştırmada farklı sonuçlar üreterek tekrarlanabilirlik sorunu oluşturmakta ve yerel optimuma takılma riski barındırmaktadır. Bu durum şebeke operatörlerinin karar alma süreçlerinde belirsizliklere neden olmaktadır. Bu kısıtları aşmak amacıyla, problem deterministik bir Karma Tam Sayılı İkinci Dereceden Konik Programlama (Mixed Integer Second-Order Cone Programming-MISOCP) formülasyonu ile modellenmiştir. Güç akışı denklemlerinin konveks bir yapıya dönüştürüldüğü bu model, endüstri standardı olan yüksek performanslı Gurobi Optimizasyon çözücüsü kullanılarak tasarlanmıştır. Gurobi; sınırla ve dallan algoritması ile iç nokta yöntemlerini harmanlayan hibrit mimarisi sayesinde, yüksek karmaşıklığa sahip bu problemi dakikalar mertebesinde hiçbir ince ayar gerektirmeksizin hatasız olarak çözümlemektedir. Optimizasyon modelinde temel amaç fonksiyonu olarak toplam güç kayıplarının minimizasyonu hedeflenirken, şebekenin güç kalitesini değerlendirmek için Gerilim Devinim İndeksi (GDI) analizlere entegre edilmiştir. Geliştirilen model, IEEE 33 baralı radyal dağıtım şebekesi üzerinde uygulanmıştır. Elde edilen analiz sonuçları, Gurobi çözücüsü ile belirlenen 3 adet DÜS'ün optimum entegrasyonu sayesinde aktif güç kayıplarında belirgin bir azalma sağlandığını ve gerilim profilinin nominal aralıkta kaldığını kanıtlamaktadır. Sonuç olarak, önerilen MISOCP tabanlı yaklaşım; şebeke operatörleri için yüksek güvenilirliğe sahip, hızlı çalışan ve her çalıştırmada aynı kesin sonucu üreten tekrarlanabilir bir planlama aracı sunmaktadır.

ISBN NR. : 978-625-8795-33-2

Anahtar Kelimeler: Dağıtık Üretim, MISOCP, Gurobi, Gerilim Devinim İndeksi, IEEE 33 Bara.

GİRİŞ

Günümüzde artan enerji talebi ve mevcut dağıtım şebekelerinin sınırlarına ulaşması, elektrik şebekelerinde güç kayıplarının artmasına ve gerilim profilinin bozulmasına yol açmaktadır. Bu sorunların aşılmasında, dağıtık üretim sistemlerinin (DÜS) şebekeye optimum konum ve boyutta entegre edilmesi en etkili çözümlerden biri olarak öne çıkmaktadır [1]. Literatürde, DÜS birimlerinin şebekeye entegrasyonu problemi genellikle çok kısıtlı ve doğrusal olmayan karmaşık bir optimizasyon problemi olarak ele alınmaktadır [2], [3]. Bu problemin çözümü için literatürdeki çalışmaların büyük çoğunluğu meta-sezgisel optimizasyon algoritmalarına odaklanmıştır. Örneğin, literatürdeki çalışmalarda, Krill Sürüsü Algoritması (KSA) [1], Karınca Aslanı Algoritması (KAA) [2], Kaotik Sinüs Kosinüs Algoritması (KSKA) [4], Parçacık Sürüsü Optimizasyonu (PSO) [5] gibi çeşitli meta-sezgisel yöntemler kullanılarak şebekedeki güç kayıplarının minimize edilmesi hedeflenmiştir. Örneğin, KSKA kullanılarak 3 adet DÜS yerleşimi ile güç kayıplarının azaltıldığı çalışmalar mevcuttur [4]. Bunun yanı sıra, çok amaçlı Balina Optimizasyon Algoritması (BOA) tercih edilerek şebekenin gerilim profilinin iyileştirildiği ve bu sürecin tekno-ekonomik analizlerle desteklendiği yaklaşımlar da öne çıkmaktadır [6].

Ancak, dağıtık üretim birimlerinin optimizasyonunda sıklıkla tercih edilen meta-sezgisel algoritmalar, esneklik ve hızlı çözüm uzayı tarama avantajlarına rağmen, olasılıksal ve stokastik doğaları gereği temel bazı yapısal kısıtlar barındırmaktadır. Bu yöntemler, problemin karmaşıklığı arttıkça erken yakınsama eğilimi göstermekte ve çözüm sürecinde yerel optimum noktalarına takılabilmektedir [7].

Doğadan ilham alan algoritmaların başlangıç değerlerine olan yüksek bağımlılığı ve kararsız hareketleri, bu yöntemlerin çözüm kalitesini şüpheli hale getirmektedir [8]. Nitekim güncel çalışmalarda, sezgisel yöntemlerin hiçbir zaman kesin bir global optimumu garanti edemediği ve elde edilen yerel bir çözümün aynı zamanda global bir çözüm olup olmadığını kanıtlayacak matematiksel bir kriterin bulunmadığı açıkça vurgulanmaktadır [1], [9], [10].

Bu algoritmaların en kritik dezavantajlarından biri de tekrarlanabilirlik ve tutarsızlık sorunudur. Sezgisel optimizasyon süreçleri; iterasyon sayısı, popülasyon büyüklüğü ve varyasyon katsayıları gibi tamamen rastgele atanan parametrelere sıkı sıkıya bağlıdır [11], [12]. Bu durum, algoritmaların her çalıştırıldığında birbirinden farklı sonuçlar üretmesine ve sıfırdan farklı standart sapmalar vermesine yol açmaktadır [13]. Dolayısıyla, bu algoritmaların tekrarlanabilir kapasitelerini ispatlamak adına literatürde sürekli olarak istatistiksel analizlere ihtiyaç duyulduğu, ancak bu testlerin dahi deterministik olmayan yapıdan kaynaklanan belirsizlikleri ortadan kaldıramadığı ifade edilmektedir [14].

Sezgisel algoritmaların barındırdığı bu belirsizlikler ve kesin olmayan sonuçlar, özellikle elektrik dağıtım şebekelerini yöneten ve gün öncesi operasyonel planlamalar gibi kritik kararlar alan sistem operatörleri açısından ciddi zorluklar oluşturmaktadır. Şebeke operatörlerinin mevcut kısıtlar altında güvenilir, ekonomik ve uygulanabilir kararlar alabilmesi için algoritmaların yüksek dayanıklılık ve güvenilirlik sunması şarttır [15], [16]. Ancak meta-

ISBN NR. : 978-625-8795-33-2

sezgisel yöntemlerin zayıf matematiksel temelleri ve garanti edilemeyen çözüm kaliteleri, sistem entegrasyonu ve planlama süreçlerinde operasyonel riskler barındırmaktadır. Bu nedenle son dönem araştırmaları; sağlam ve katı matematiksel temellere dayanan, analizi ve yorumlanması daha kolay olan ve her koşturulduğunda global optimumu teorik olarak garanti ederek şebeke operatörleri için daha yüksek güvenilirlik sunan MISOCP gibi deterministik analitik yöntemlerin meta-sezgisellere tercih edilmesi gerektiğini güçlü bir şekilde savunmaktadır [17], [18], [19].

Son yıllarda güç akışı denklemlerinin konveks hale getirilmesiyle oluşturulan MISOCP modelleri literatürde dikkat çekmektedir. Bu yaklaşımın, ticari çözücüler kullanılarak problemin global optimum çözümünü matematiksel olarak garanti ettiği gösterilmiştir [20], [21]. Üstelik, deterministik konveks modellerin işlem yükü açısından meta-sezgisel yöntemlerden daha verimli olduğu ve saniyeler mertebesinde kesin sonuçlar ürettiği vurgulanmaktadır [22].

Sistem performansının tam olarak değerlendirilebilmesi için güç kayıplarının yanı sıra gerilim profilinin iyileştirilmesi de hayati önem taşımaktadır. Şebekedeki güç kalitesini maksimize etmek için 3 adet DÜS yerleşiminin doygunluk noktası olduğu ve en ideal kayıp azaltımını sağladığı tespit edilmiştir [23]. Ayrıca, gerilim profilindeki iyileşmeyi ölçmek amacıyla GDI metriği sıklıkla kullanılmaktadır [5]. Ancak literatürde, 3 adet DÜS'ün eş zamanlı yerleşimini GDI analizini de kapsayacak şekilde ele alan ve bunu global optimum garantisi veren MISOCP yöntemiyle çözen çalışmalar oldukça sınırlıdır.

Belirtilen bu eksiklikler doğrultusunda, bu çalışmada radyal dağıtım şebekelerinde 3 adet DÜS'ün optimum konum ve boyutlandırılması problemi ele alınmıştır. Çalışmanın temel amacı, aktif ve reaktif güç kayıplarını en aza indirirken GDI değerlerini iyileştirmek ve meta-sezgisel yöntemlerin belirsizliğinden uzaklaşarak MISOCP formülasyonu ile global optimum çözümü elde etmektir. Önerilen matematiksel model, IEEE 33 baralı radyal dağıtım şebekesi üzerinde uygulanmış ve analiz sonuçları değerlendirilmiştir.

PROBLEMİN MATEMATİKSEL FORMÜLASYONU

Radyal dağıtım şebekelerinde güç kaybının minimizasyonu ve optimum DÜS yerleşimi, karmaşık ve doğrusal olmayan bir optimizasyon problemidir [3]. Bu çalışmada, problemin çözümünde yüksek hassasiyet ve küresel optimum garantisi sunan MISOCP yaklaşımı benimsenmiştir. Problem, 96 saatlik zaman adımını içeren her mevsimden 24 saatlik günlük yük profili dikkate alınarak modellenmiştir.

Geliştirilen matematiksel modelde amaç fonksiyonu, analiz edilen zaman periyodu boyunca şebekedeki toplam güç kayıplarının minimize edilmesi olarak kurgulanmıştır. Bu hedefe ulaşılırken şebekenin güvenilirliğini sağlamak amacıyla; aktif ve reaktif güç dengesi denklemleri, bara gerilim sınırları, hatların termal akım taşıma kapasiteleri ve DÜS birimlerinin üretim limitleri gibi işletme kısıtları modele dahil edilmiştir. Ek olarak, gerçekleştirilen optimizasyonun sistemin güç kalitesine olan etkisini bütüncül bir şekilde değerlendirebilmek için literatürde yaygın olarak kullanılan GDI analizlere entegre edilmiştir.

ISBN NR. : 978-625-8795-33-2

Amaç Fonksiyonu

Çalışmanın temel amacı, yıllık bazda şebekedeki toplam güç kaybının minimize edilmesidir. Amaç fonksiyonu Denklem (1) ve (2)'de tanımlanmıştır:

$$P_{loss} = \sum_{j=1}^{i} I_j^2 r_j \tag{1}$$

$$Q_{loss} = \sum_{j=1}^{i} I_j^2 x_j \tag{2}$$

Denklemde yer alan parametrelerden P_{loss} ve Q_{loss} sırasıyla sistemdeki aktif ve reaktif güç kayıplarını temsil ederken; I_j akımı, r_j ve x_j ise ilgili iletkenin direnç ve reaktans değerlerini, i ise sistemdeki toplam bara sayısını ifade etmektedir.

Güç Akışı Denklemleri ve Konik Gevşetme

Sistemdeki güç akışı, radyal şebekeler için literatürde yaygın olarak kullanılan güç akış denklemleri ile ifade edilmiştir. Her bir i barası için aktif güç, reaktif güç ve gerilim düşümü denklemleri şu şekildedir [24]:

$$\sum_{\forall ki \in \Omega_l} P_{ki} - \sum_{\forall ij \in \Omega_l} \left(P_{ij} + R_{ij} I_{ij}^2\right) + P_i^s = P_i^d; \quad \forall i \in \Omega_b \tag{3}$$

$$\sum_{\forall ki \in \Omega_l} Q_{ki} - \sum_{\forall ij \in \Omega_l} \left(Q_{ij} + X_{ij} I_{ij}^2\right) + Q_i^s = Q_i^d; \quad \forall i \in \Omega_b \tag{4}$$

$$V_i^2 - 2\left(R_{ij} P_{ij} + X_{ij} Q_{ij}\right) - \left(R_{ij}^2 + X_{ij}^2\right) I_{ij}^2 - V_j^2 = 0; \quad \forall ij \in \Omega_l \tag{5}$$

$$I_{ij}^2 = \frac{P_{ij}^2 + Q_{ij}^2}{V_i^2} \tag{6}$$

Burada k üst bara, j alt bara, i üzerinde çalışılan bara olmak üzere P_{ki} ve Q_{ki} k barasından çıkıp, üzerinde çalışılan i barasına giriş yapan aktif ve reaktif güç miktarını, P_{ij} ve Q_{ij} üzerinde çalışılan i barasından çıkarak, j barasına doğru akan aktif ve reaktif güç miktarını, P_{si}, Q_{si} i barasındaki aktif ve reaktif güç üretimini, P_{id}, Q_{id} i barasındaki aktif ve reaktif güç talebini, I_{ij} koldan akan akımın karesini ifade etmektedir.

Denklem (6)'deki ifadenin konveks olmaması ve problemin deterministik çözücülerle çözülebilmesi amacıyla konveks İkinci Dereceden Konik Programlama (SOCP) formatına dönüştürmek için değişken dönüşümü ve eşitsizlik gevşetmesi uygulanarak denklem (7) oluşturulmuştur [25], [26].

ISBN NR. : 978-625-8795-33-2

$$P_{ij}^2 + Q_{ij}^2 \leq V_i \cdot I_{ij} \quad \forall ij \in \Omega_l \tag{7}$$

Sistem Kısıtları ve DÜS Yerleşimi

Gerilim Kısıtları

Model, sistemin kararlılığı ve şebekenin güvenli işletimi için her baradaki gerilim büyüklüğü belirlenen alt ve üst sınırlar arasında kalmalıdır.

$$V_{min} \leq V_i \leq V_{max} \quad \forall i \in N \tag{8}$$

Bu çalışmada, V_{min}=0,95 pu ve V_{max}=1,05 pu olarak alınmıştır.

Her *i* barasındaki gerilim, şebeke standartları tarafından belirlenen alt ve üst limitler arasında kalmalıdır. MISOCP modellerinde bu değişken gerilimin karesi olarak alındığı için formülasyon şöyledir [28]:

$$V_{min}^2 \leq u_i \leq V_{max}^2 \quad \forall i \in N \tag{9}$$

DÜS gücü kısıtları

Şebekeye entegre edilecek DÜS'lerin fiziksel ve operasyonel kısıtları gereği, güç üretimleri belirli alt ve üst sınırlar dahilinde gerçekleşmek zorundadır.

Bu kapsamda, aktif ve reaktif güç üretim kapasitelerini tanımlayan limit denklemleri aşağıda verilmiştir [29].

$$P_{\text{DÜS},i}^{\min} \leq P_{\text{DÜS},i} \leq P_{\text{DÜS},i}^{\max} \tag{10}$$

$$Q_{\text{DÜS},i}^{\min} \leq Q_{\text{DÜS},i} \leq Q_{\text{DÜS},i}^{\max} \tag{11}$$

İlgili eşitsizliklerde yer alan $P_{\text{DÜS},i}$ ve $Q_{\text{DÜS},i}$ değişkenleri, i. baraya entegre edilen DÜS biriminin sırasıyla aktif ve reaktif güç üretimlerini belirtmektedir. Öte yandan $P_{\text{DÜS},i}^{\min}$ ile $P_{\text{DÜS},i}^{\max}$ parametreleri bu birimin şebekeye sağlayabileceği aktif gücün fiziksel alt ve üst sınırlarını; $Q_{\text{DÜS},i}^{\min}$ ile $Q_{\text{DÜS},i}^{\max}$ parametreleri ise reaktif güç üretim kapasitesinin teknik limitlerini tanımlamaktadır.

Termal kısıtlar

Hatlardan geçen akım iletkenin maksimum taşıma kapasitesini aşmamalıdır [30].

$$I_{DÜS}^i < I_{Limit}^i \tag{12}$$

DÜS Kapasiteleri ve İkili Karar Değişkenleri

Optimizasyon algoritmasının DÜS ünitelerinin baralardaki "varlık/yokluk" durumunu algılayabilmesi için ikili karar değişkenleri kullanılır [31].

ISBN NR. : 978-625-8795-33-2

$$0 \leq P_{DÜS}^{k} \leq P_{DÜS}^{max} \cdot \sigma_k \tag{13}$$

Burada $\sigma_k \in \{0,1\}$, k numaralı baraya bir DÜS yerleştirilip yerleştirilmediğini ifade eden ikili değişkendir.

DÜS'lerin sisteme yerleştirilip yerleştirilmeyeceğine karar veren $x_k = 1$ veya $x_k = 0$ ikili değişkenleri ile aktif/reaktif güç sınırları belirlenir [20], [32]

$$x_k \cdot P_{DÜS,min}^{k} \leq P_{DÜS}^{k} \leq x_k \cdot P_{DÜS,max}^{k} \tag{14}$$

$$x_k \cdot Q_{DÜS,min}^{k} \leq Q_{DÜS}^{k} \leq x_k \cdot Q_{DÜS,max}^{k} \tag{15}$$

Gerilim Devinim İndeksi (GDI)

Çalışmada elde edilen çözümün şebeke gerilim kalitesine etkisini ölçmek için Denklem (16)'da tanımlanan karesel GDI performansı hesaplanmıştır [27].

$$GDI_{karesel} = \sum_{t=1}^{T} \sum_{i=1}^{N} \left(V_{ref} - V_{i,t}\right)^2 \tag{16}$$

İlgili denklemde yer alan *GDI* gerilim devinim indeksini ifade ederken; *T* hesaplamaya dahil edilen toplam zaman periyodunu (saat); *N* ise sistemdeki toplam bara sayısını göstermektedir. Ayrıca V_{ref} dağıtım şebekesinin nominal işletme gerilimini (pu, kV) ve V_{it} ise i. baranın t zaman adımındaki anlık gerilim değerini (pu, kV) temsil etmektedir.

ÖNERİLEN METOT

Bu çalışmada, dağıtım şebekelerinde çoklu DÜS yerleşimi ve boyutlandırması problemi, meta-sezgisel yöntemlerin doğasında bulunan yerel optimuma takılma ve tekrarlanabilirlik sorunlarını ortadan kaldırmak amacıyla, kesin bir matematiksel yöntem olan MISOCP denklemleri Python ortamında kodlanmış ve endüstri standardı olan Gurobi çözücüsü entegrasyonu kullanılarak çözülmüştür.

MISOCP ve Konvekslik Avantajı

Dağıtım şebekelerinde güç akışı denklemleri, aktif ve reaktif güç dengelerini ve gerilim düşümlerini ifade eden yapıları gereği doğrusal ve konveks olmayan oldukça karmaşık bir matematiksel forma sahiptir [15]. Geleneksel meta-sezgisel algoritmalar (PSO, WOA, vb.) böylesine karmaşık bir çözüm uzayında rastgele ve olasılıksal arama stratejileri izledikleri için ciddi teknik kısıtlamalar barındırırlar [3]. Rastgele başlatma ve parametre ayarlarına yüksek oranda bağımlı olmaları sebebiyle, meta-sezgisel yöntemlerin kesin çözüme ulaşma garantisi yoktur ve sıklıkla yerel minimum noktalarında takılı kalma riski taşırlar [4], [7], [12]

Önerilen MISOCP modelinde ise, güç akışı denklemlerindeki konveks olmayan terimler, SOCP (Second Order Cone Programming) gevşetmesi ile konveks forma dönüştürülmüştür [17], [26], [33]. Bu dönüşüm sürecinde, akım ve gerilim karesi çarpımlarını barındıran doğrusal olmayan eşitlikler hiperbolik bir eşdeğerlik kullanılarak yeniden yazılır. Katı eşitlik kısıtlarının uygun

ISBN NR. : 978-625-8795-33-2

bir küçük eşittir eşitsizliğine dönüştürüldüğü bu konik gevşetme işlemi, doğrusal olmayan güç akışı ifadelerini konveks bir ikinci mertebeden koni kısıtına evirir [3], [34].

Bu dönüşüm sayesinde, problemin çözüm uzayı dışbükey bir yapıya kavuşturulmuş ve aranan çözümün global optimum olduğu matematiksel olarak kanıtlanabilir hale gelmiştir [3], [15], [17], [35].

Gurobi Çözücü ve Hesaplama Verimliliği

Geliştirilen matematiksel model, Python ortamında kodlanarak yüksek performans gerektiren konik optimizasyon problemlerinin çözümünde sahip olduğu güçlü matematiksel temeller ve hesaplama verimliliği ile literatürde endüstri standardı olarak kabul edilen Gurobi çözücüsü ile çözülmüştür [35]. Gurobi'nin algoritmik mimarisindeki temel üstünlük, kesikli optimizasyon problemlerinde kullanılan sınırla ve dallan algoritması ile konveks sürekli optimizasyon problemlerinin çözümünde son derece etkin olan iç nokta yöntemlerini hibrit bir yapıda başarılı bir şekilde kombine etmesidir [34].

Bu entegre algoritma mimarisi, konik kısıtlı güç akışı problemlerinin polinom zamanda çözülebilmesini ve sistemin global optimuma kesin olarak ulaşmasını matematiksel düzeyde güvence altına almaktadır [36] [37].Meta-sezgisel yöntemlerin performansının başlangıç parametrelerine (popülasyon boyutu, mutasyon oranı vb.) aşırı duyarlı olduğu literatürde sıkça vurgulanırken [8], [10], MISOCP ve Gurobi kombinasyonu herhangi bir "ince ayar" gerektirmeksizin her çalıştırmada aynı kesin sonucu garanti etmektedir [3].

Geliştirilen bu model, 3 adet DÜS'ün şebekeye yerleşimi gibi yüksek kombinasyonel karmaşıklığa sahip bir optimizasyon senaryosunu, geleneksel MINLP (Karma Tam Sayılı Doğrusal Olmayan Programlama) çözücülerinin aksine, hızlı ve hatasız bir şekilde sonuçlandırmaktadır [3], [17]. Bu deterministik yaklaşım, şebeke operatörleri için hem planlama aşamasında yüksek güvenilirlik sağlamakta hem de karmaşık operasyonel süreçlerde hızlı ve kesin karar alma imkânı sunmaktadır [12], [15].

UYGULANAN SENARYOLAR VE ANALİZ SONUÇLARI

Bu çalışmada, önerilen MISOCP tabanlı yöntemin performansını ve doğruluğunu test etmek amacıyla nominal gerilimi 12,66 kV olan Görsel 1'de sunulan IEEE 33 baralı radyal dağıtım şebekesi kullanılmıştır.

ISBN NR. : 978-625-8795-33-2

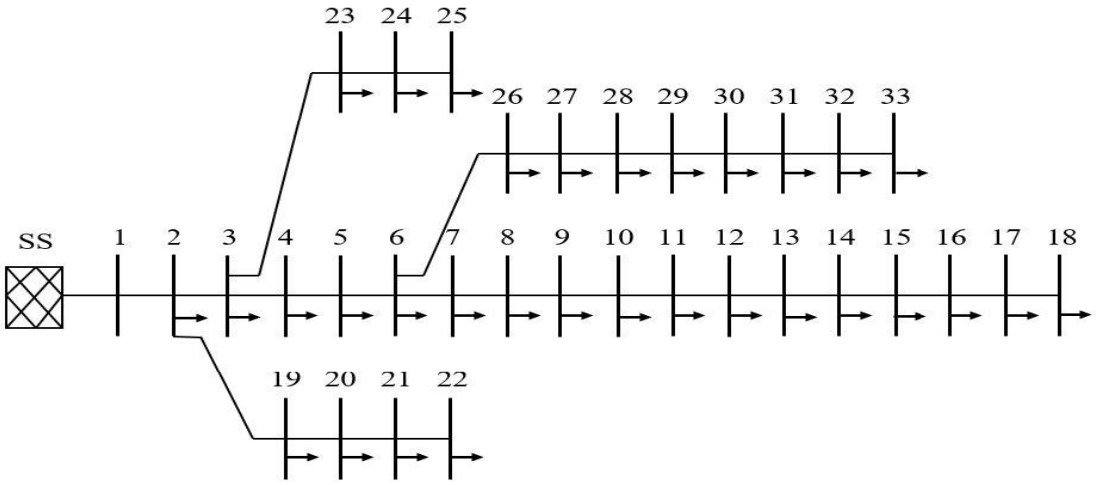

Görsel 1. IEEE 33-baralı radyal dağıtım sistemi tek hat şeması [38]

Geliştirilen model, sisteme entegre edilecek DÜS sayısı baz alınarak dört farklı konfigürasyon altında test edilmiştir. Bu kapsamda; herhangi bir DÜS bağlantısının olmadığı (K=0) durum temel durum olarak alınmış, sisteme sırasıyla bir (K=1), iki (K=2) ve üç (K=3) adet DÜS entegrasyonu yapılarak elde edilen veriler kapsamlı bir şekilde analiz edilmiştir.

Analiz edilen senaryolara, her bir mevsimi temsil eden 24 saatlik günlük yük profillerinin birleştirilmesiyle oluşturulan 96 saatlik zaman adımı dahil edilmiş olup, kullanılan bu mevsimsel yük profili Şekil 2'de sunulmaktadır. Yaz mevsimi, en yüksek yük talebinin olduğu mevsimken kış aylarında talep biraz daha düşmektedir. Bahar geçiş dönemlerinde ise güç tüketiminin yıl içerisindeki minimum seviyelerde ve birbirine oldukça yakın değerlerde olduğu gözlemlenmektedir.

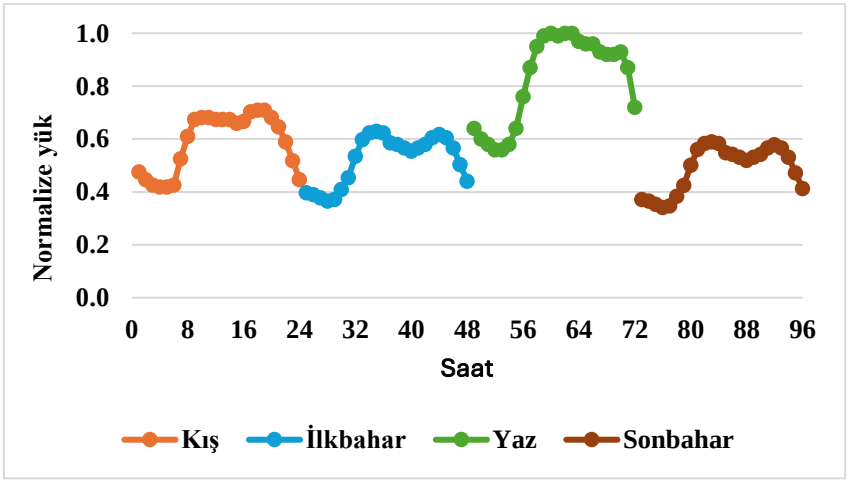

Görsel 2. Mevsimsel yük profili

Optimizasyon sonuçları toplu olarak Çizelge 1 ve Çizelge 2'de sunulmuştur. Çizelge 1, her bir senaryo için şebekeye entegre edilen DÜS'lerin yapılan optimizasyonla optimum olarak hangi baraya konumlandıklarını, aktif reaktif kapasite boyutlarını ve sistemdeki aktif ve reaktif güç kaybı azalmalarını detaylandırmaktadır. Çizelge 2'de ise şebekenin güç kalitesindeki iyileşmeyi yansıtacak şekilde GDI değerlerini, gün içi minimum maksimum gerilim seviyelerini ve bu sınırların gerçekleştiği kritik baraları göstermektedir.

ISBN NR. : 978-625-8795-33-2

Çizelge 1. Farklı DÜS Sayılarına Göre Toplam Güç Kaybı Sonuçları

Senaryo	Seçilen DÜS Baraları	Puant Zaman Aktif Güç Kaybı (kW)	Puant Zaman Reaktif Güç Kaybı (kVAr)	DÜS Aktif Güç Üretimi (kW)	DÜS Reaktif Güç Üretimi (kVAr)
K=0	-	198,023	132,006	-	-
K=1	30	98,036	66,631	900	435,890
K=2	13-30	60,388	40,429	13. Bara 492,97 30. Bara 791,09	13. Bara 238,76 30. Bara 383,14
K=3	14-25-30	64,144	42,693	14. Bara 399,84 25. Bara 240,02 30. Bara 659,42	14. Bara 193,65 25. Bara 116,25 30. Bara 319,37

Çizelge 2. Farklı DÜS Sayılarına Göre VDI ve Toplam Güç Kaybı Oranı

Senaryo	Puant Zaman Aktif Güç Kaybı Azalması Oranı	Puant Zaman Reaktif Güç Kayıp Azalması Oranı	Yıllık GDI Değeri	Gün İçi Minimum V (p.u.)	Gün İçi Minimum Bara	Gün İçi Maksimum V (p.u.)	Gün İçi Maksimu Bara
K=0	-	-	4,237	0,9141	18	1.0000	1
K=1	50,49%	49,52%	1,369	0,9320	18	1.0126	30
K=2	69,50%	69,37%	0,412	0,9618	18	1.0179	13
K=3	67,61%	67,66%	0,531	0,9570	18	1.0125	14

Temel Durum (K=0): Bu aşamada, IEEE-33 baralı radyal dağıtım şebekesi üzerinde gerçekleştirilen yük akışı analizleri ile şebekenin mevcut durumu detaylıca ortaya konulmuştur. Yapılan simülasyonlar neticesinde, sistemin en yoğun yüklenme yaşadığı puant saatinde toplam aktif güç kaybı 198,023 kW, toplam reaktif güç kaybı ise 132,006 kVAr olarak saptanmıştır. Şebekenin gerilim profili incelendiğinde ise, sistemin en zayıf halkası olan 18. barada minimum gerilim değerinin 0,9141 p.u. seviyesine kadar gerilediği ve şebekenin genel gerilim kalitesizliğini gösteren yıllık GDI değeri ise 4,237 olduğu tespit edilmiştir. Bu temel veriler, ilerleyen bölümlerdeki DÜS yerleşimi sonrası elde edilecek iyileşme oranlarının kıyaslanması için referans teşkil etmektedir. Görsel 3'de IEEE 33 baralı radyal dağıtım şebekesinin DÜS entegrasyonu yapılmayan temel durumu için puant yük için gerilim profili sunulmaktadır.

ISBN NR. : 978-625-8795-33-2

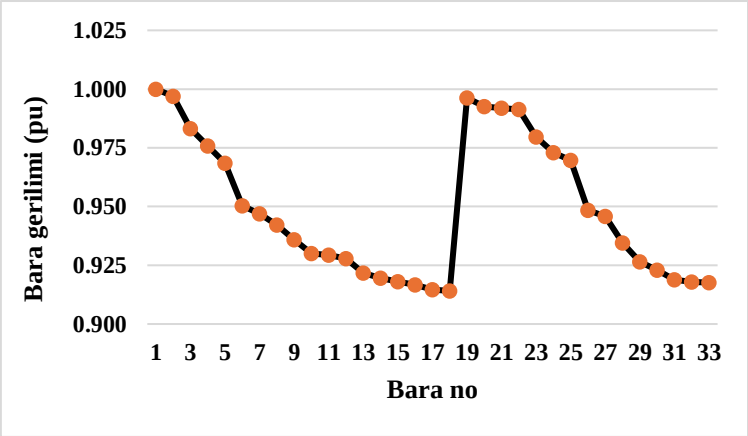

Görsel 3. IEEE 33 baralı radyal dağıtım şebekesinin puant yük için gerilim profili

Tekli DÜS Yerleşimi (K=1): Sisteme tek bir DÜS ünitesinin kurulmasına izin verildiğinde, model optimum konum olarak 30 numaralı barayı seçmiş ve buraya 900 kW aktif güç kapasitesi atamıştır. Bu entegrasyon sonucunda puant zaman aktif güç kaybında %50,49, reaktif güç kaybında ise %49,52 oranında iyileşme sağlanmıştır. Minimum bara gerilimi 0.9320 p.u. seviyesine yükselirken, yıllık GDI değeri 1,369'a gerilemiştir.

İkili DÜS Yerleşimi (K=2): DÜS sayısı 2'ye çıkarıldığında, model eş zamanlı olarak 13 ve 30 numaralı baraları en uygun konumlar olarak belirlemiştir. Bu senaryoda puant zaman aktif güç kaybı %69,50, reaktif güç kaybı ise %69,37 oranında azalmıştır. Şebeke gerilim profili ciddi bir rahatlama yaşamış; minimum gerilim değeri 0.9618 p.u. seviyesine çıkarak güvenli bölgeye taşınmış ve yıllık GDI değeri 0,412 ile en optimum gerilim dengesini yakalamıştır.

Üçlü DÜS Yerleşimi (K=3): Şebekeye 3 adet DÜS yerleştirildiğinde model; 14, 25 ve 30 numaralı baraları seçmiştir. Bu konfigürasyonda puant zaman aktif güç kaybı 64,144 kW, reaktif güç kaybı ise 42,693 kVAr olarak gerçekleşmiştir. Kayıpların azaltılmasında K=2 senaryosuna göre daha yüksek bir performans beklense de K=3 senaryosu aktif kayıp azaltma oranında %67,61 ile K=2'nin (%69,50) bir miktar gerisinde kalmıştır bu durum DÜS sayısı ile toplam aktif ve reaktif güç kaybı arasında her zaman doğrusal ve güçlü bir korelasyon olmadığını göstermektedir.

İlk iki DÜS, şebekedeki en kritik yük merkezlerini ve en yüksek empedanslı hatlardaki kayıpları büyük ölçüde telafi etmekte ve K=2 senaryosundan K=3 senaryosuna geçildiğinde 3. DÜS'ün şebeke kayıplarını azaltmadaki etkisi önemsiz kalabilmektedir [39]. Hatta şebekeye optimum üretim kapasitesinin ötesinde daha fazla DÜS eklenmesi, aktif güç kayıplarının iyileşmek yerine artmasına bile neden olabilmektedir. Yanlış konumlandırılmış veya gereğinden yüksek kapasiteli DÜS'ler, şebekede ters güç akışı oluşturarak hat kayıplarını artırmaktadır [10].

Üç adet DÜS ünitesinin şebekeye entegrasyonu neticesinde oluşan aktif güç kayıpları Görsel 4'de sunulmaktadır.

ISBN NR. : 978-625-8795-33-2

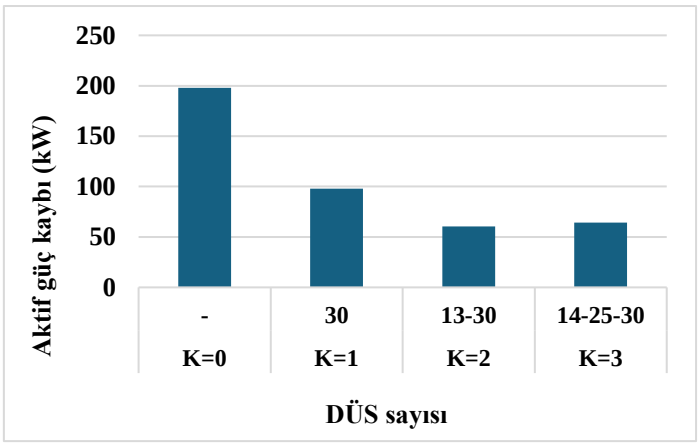

Görsel 4. Üç adet DÜS entegrasyonu sonrasındaki aktif güç kayıp durumu

Üç adet DÜS ünitesinin şebekeye entegrasyonu neticesinde oluşan aktif güç kayıp azalma oranları Görsel 5'de sunulmaktadır.

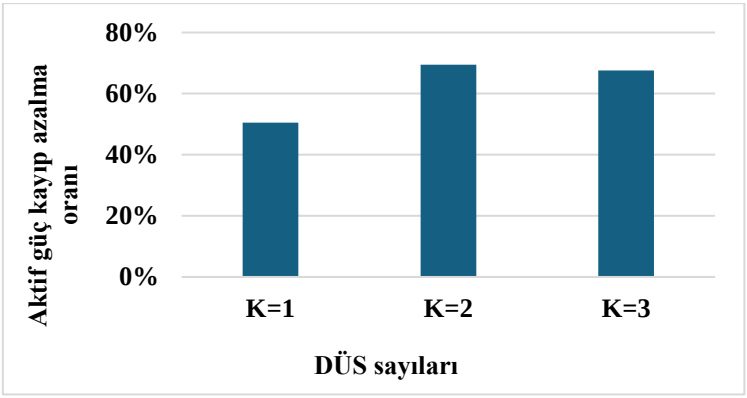

Görsel 5. Üç adet DÜS entegrasyonu sonrasındaki aktif güç kayıp azalma oranı

Analiz sonuçları genel olarak değerlendirildiğinde, DÜS sayısının optimum artırılmasıyla gerilim profilinin nominal değerlere yaklaştığı ve sistem kararlılığının güçlendiği Görsel 6'da görülmektedir.

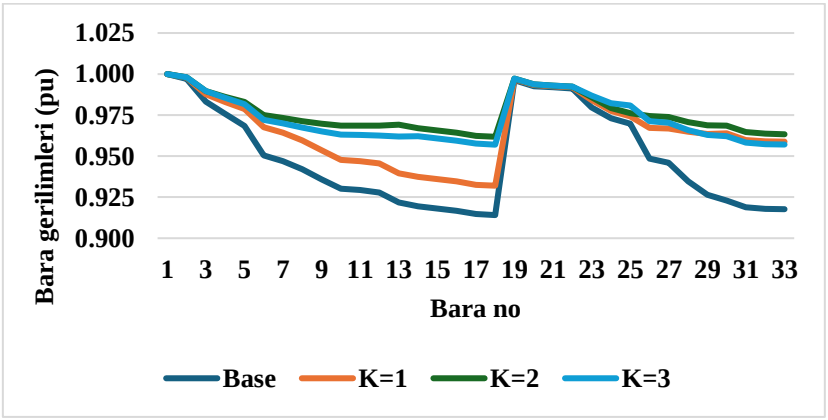

Görsel 6. Üç adet DÜS gerilim profil kıyaslaması

Gerilim Devinim İndeksi (GDI) verileri, DÜS entegrasyonunun şebeke gerilim kalitesini iyileştirmede etkili bir yöntem olduğunu Görsel 7'de görülmektedir. Özellikle K=2 senaryosu

ISBN NR. : 978-625-8795-33-2

hem kayıp azaltma oranları hem de gerilim dengesi açısından modelin sağladığı en verimli sonuçları sunmuştur.

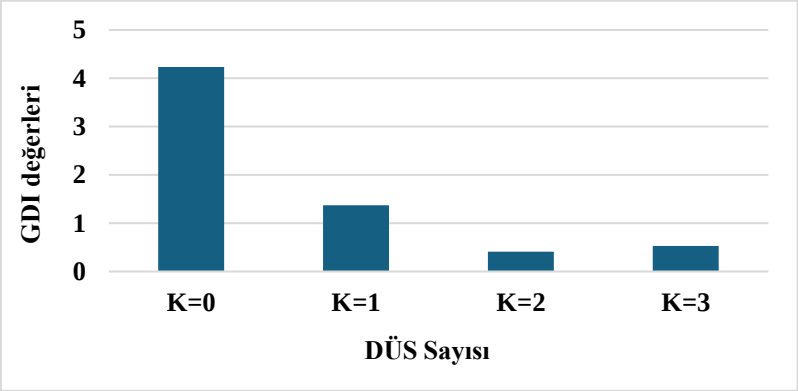

Görsel 7. GDI değişimi

SONUÇLAR VE DEĞERLENDİRME

Bu çalışmada, radyal dağıtım şebekelerinde çoklu DÜS'lerin optimal konumlandırılması ve boyutlandırılması problemi Karma Tam Sayılı İkinci Dereceden Konik Programlama (MISOCP) yöntemi kullanılarak deterministik bir yaklaşımla çözülmüştür. Çalışma kapsamında, günlük yük profili dikkate alınarak 96 zaman adımlı toplam aktif ve reaktif güç kaybı analizi yapılmış ve model Gurobi çözücüsü ile koşturulmuştur. Geliştirilen matematiksel model, IEEE 33 baralı radyal dağıtım şebekesinde üzerinde DÜS'lerin şebekeye entegrasyon seviyesine göre (K=0,1,2,3) dört farklı senaryo altında test edilmiştir.

Elde edilen optimizasyon sonuçlarından varılan temel çıkarımlar şu şekildedir:

- Şebekede herhangi bir DÜS ünitesinin bulunmadığı referans durumda (K=0) puant zaman aktif güç kaybı 198,023 kW olarak gerçekleşmiş ve 18. barada minimum gerilim 0.9141 p.u. değerine kadar düşmüştür.
- Sisteme 3 adet DÜS ünitesinin eş zamanlı olarak entegre edildiği nihai senaryoda (K=3), model optimum bağlantı noktaları olarak 14, 25 ve 30 numaralı baraları seçmiştir.
- DÜS entegrasyonu ile şebekenin güç kalitesini ve gerilim kararlılığını temsil eden yıllık GDI değeri, baz senaryodaki 4,237 seviyesinden en optimum senaryo olan K=2'de 0,412 seviyesine kadar geriletilerek gerilim profilinde beklenilen iyileşme sağlanmıştır.
- Kayıp azaltma performansları incelendiğinde, K=2 senaryosu aktif güç kayıplarında %69,50, reaktif güç kayıplarında ise %69,37 oranında iyileşme ile en üstün performansı sergilemiştir. K=3 Senaryosunda ise aktif güç kayıp azaltma oranı %67,61 seviyesinde kalmıştır.

Sonuçlar bütün olarak değerlendirildiğinde, şebekeye entegre edilen DÜS sayısı arttıkça gerilim profilinin nominal işletme sınırları içerisinde başarıyla düzleştirildiği kanıtlanmıştır. Ancak, DÜS sayısının artışı kayıp azaltma oranlarında her zaman doğrusal bir iyileşme getirmemektedir. Özellikle iki adet ve üç adet DÜS senaryoları arasındaki kıyaslama, sistemin belirli bir DÜS kapasitesinden sonra doygunluğa ulaştığını ve üçüncü bir DÜS'ün konum-boyut optimizasyonunun, hat empedans yapısı ve sistemdeki akım akış yönleri nedeniyle şebeke

kayıplarını K=2 seviyesinde tutamadığını göstermektedir. Bu durum, dağıtım şebekesi planlamasında optimum DÜS sayısının şebeke topolojisine bağlı olarak titizlikle belirlenmesi gerektiğini ve daha fazla DÜS'ün her zaman daha az kayıp anlamına gelmediğini kanıtlamaktadır.

Literatürde sıkça kullanılan meta-sezgisel yöntemlerin aksine, önerilen MISOCP ve Gurobi tabanlı yaklaşım; herhangi bir parametre ince ayarına ihtiyaç duymadan ve her çalıştırmada aynı kesin sonucu vererek global optimumu matematiksel olarak garanti etmiştir. Bu doğrultuda geliştirilen model, modern ve akıllı dağıtım şebekelerinin planlama, işletme ve entegrasyon süreçlerinde şebeke operatörleri için son derece güvenilir, hızlı ve tekrarlanabilir bir karar destek mekanizması sunmaktadır.

KAYNAKÇA

[1] S. Sultana ve P. K. Roy, "Krill herd algorithm for optimal location of distributed generator in radial distribution system", *Appl. Soft Comput.*, c. 40, ss. 391-404, Mar. 2016, doi: 10.1016/j.asoc.2015.11.036.

[2] E. S. Ali, S. M. Abd Elazim, ve A. Y. Abdelaziz, "Ant Lion Optimization Algorithm for optimal location and sizing of renewable distributed generations", *Renew. Energy*, c. 101, ss. 1311-1324, Şub. 2017, doi: 10.1016/j.renene.2016.09.023.

[3] W. Gil-González, A. Garces, O. D. Montoya, ve J. C. Hernández, "A Mixed-Integer Convex Model for the Optimal Placement and Sizing of Distributed Generators in Power Distribution Networks", *Appl. Sci.*, c. 11, sy. 2, s. 627, Oca. 2021, doi: 10.3390/app11020627.

[4] A. Selim, S. Kamel, ve F. Jurado, "Efficient optimization technique for multiple DG allocation in distribution networks", *Appl. Soft Comput.*, c. 86, s. 105938, Oca. 2020, doi: 10.1016/j.asoc.2019.105938.

[5] M. Purlu ve B. E. Turkay, "Optimal Allocation of Renewable Distributed Generations Using Heuristic Methods to Minimize Annual Energy Losses and Voltage Deviation Index", *IEEE Access*, c. 10, ss. 21455-21474, 2022, doi: 10.1109/ACCESS.2022.3153042.

[6] H. P. C, K. Subbaramaiah, ve P. Sujatha, "Optimal DG unit placement in distribution networks by multi-objective whale optimization algorithm & its techno-economic analysis", *Electr. Power Syst. Res.*, c. 214, s. 108869, Oca. 2023, doi: 10.1016/j.epsr.2022.108869.

[7] R. Sirjani ve A. Rezaee Jordehi, "Optimal placement and sizing of distribution static compensator (D-STATCOM) in electric distribution networks: A review", *Renew. Sustain. Energy Rev.*, c. 77, ss. 688-694, Eyl. 2017, doi: 10.1016/j.rser.2017.04.035.

[8] M. Pesaran H.A, P. D. Huy, ve V. K. Ramachandaramurthy, "A review of the optimal allocation of distributed generation: Objectives, constraints, methods, and algorithms", *Renew. Sustain. Energy Rev.*, c. 75, ss. 293-312, Ağu. 2017, doi: 10.1016/j.rser.2016.10.071.

[9] R. Sanjay, T. Jayabarathi, T. Raghunathan, V. Ramesh, ve N. Mithulananthan, "Optimal Allocation of Distributed Generation Using Hybrid Grey Wolf Optimizer", *IEEE Access*, c. 5, ss. 14807-14818, 2017, doi: 10.1109/ACCESS.2017.2726586.

[10] B. K. Malika *vd.*, "A critical review of distribution system planning: Optimal placement and sizing of distributed generation and energy storage devices in microgrids", *Energy Strategy Rev.*, c. 62, s. 101947, Kas. 2025, doi: 10.1016/j.esr.2025.101947.

[11] R. A. Ufa, Y. Y. Malkova, A. L. Gusev, N. Y. Ruban, ve A. S. Vasilev, "Algorithm for optimal pairing of res and hydrogen energy storage systems", *Int. J. Hydrog. Energy*, c. 46, sy. 68, ss. 33659-33669, Eki. 2021, doi: 10.1016/j.ijhydene.2021.07.094.

[12] R. A. Ufa, Y. Y. Malkova, V. E. Rudnik, M. V. Andreev, ve V. A. Borisov, "A review on distributed generation impacts on electric power system", *Int. J. Hydrog. Energy*, c. 47, sy. 47, ss. 20347-20361, Haz. 2022, doi: 10.1016/j.ijhydene.2022.04.142.

[13] W. Gil-González, A. Molina-Cabrera, O. D. Montoya, ve L. F. Grisales-Noreña, "An MI-SDP Model for Optimal Location and Sizing of Distributed Generators in DC Grids That Guarantees the Global Optimum", *Appl. Sci.*, c. 10, sy. 21, s. 7681, Eki. 2020, doi: 10.3390/app10217681.

[14] O. D. Montoya, W. Gil-González, ve C. Orozco-Henao, "Vortex search and Chu-Beasley genetic algorithms for optimal location and sizing of distributed generators in distribution networks: A novel hybrid approach", *Eng. Sci. Technol. Int. J.*, c. 23, sy. 6, ss. 1351-1363, Ara. 2020, doi: 10.1016/j.jestch.2020.08.002.

[15] L. Fu, W. Wang, Z. Y. Dong, ve Y. Li, "Optimal Reconfiguration for Active Distribution Networks Incorporating a Phase Demand Balancing Model", *IEEE Trans. Power Syst.*, c. 39, sy. 5, ss. 6183-6195, Eyl. 2024, doi: 10.1109/TPWRS.2024.3355127.

[16] A. M. Shaheen, A. M. Elsayed, A. R. Ginidi, R. A. El-Sehiemy, ve E. Elattar, "A heap-based algorithm with deeper exploitative feature for optimal allocations of distributed generations with feeder reconfiguration in power distribution networks", *Knowl.-Based Syst.*, c. 241, s. 108269, Nis. 2022, doi: 10.1016/j.knosys.2022.108269.

[17] R. Cometa *vd.*, "Employing MISOCP Relaxations to Solve Distribution Optimal Network Reconfiguration", içinde *2025 IEEE Power & Energy Society General Meeting (PESGM)*, Austin, TX, USA: IEEE, Tem. 2025, ss. 1-5. doi: 10.1109/PESGM52009.2025.11224978.

[18] A. M. Fathabad, J. Cheng, K. Pan, ve F. Qiu, "Data-Driven Planning for Renewable Distributed Generation Integration", *IEEE Trans. Power Syst.*, c. 35, sy. 6, ss. 4357-4368, Kas. 2020, doi: 10.1109/TPWRS.2020.3001235.

[19] J. E. Suarez Patiño, L. A. Gallego Pareja, ve O. Gómez Carmona, "Optimal placement, sizing and operation of D-STATCOMs in power distribution systems using a Mixed-Integer Linear Programming model", *Results Eng.*, c. 26, s. 104749, Haz. 2025, doi: 10.1016/j.rineng.2025.104749.

[20] F. Molina-Martin, O. D. Montoya, L. F. Grisales-Noreña, ve J. C. Hernández, "A Mixed-Integer Conic Formulation for Optimal Placement and Dimensioning of DGs in DC Distribution Networks", *Electronics*, c. 10, sy. 2, s. 176, Oca. 2021, doi: 10.3390/electronics10020176.

[21] O. D. Montoya, A. Molina-Cabrera, ve W. Gil-González, "A mixed-integer convex approximation for optimal load redistribution in bipolar DC networks with multiple constant power terminals", *Results Eng.*, c. 16, s. 100689, Ara. 2022, doi: 10.1016/j.rineng.2022.100689.

[22] N.-V. Pham, T.-S. Vo, T.-H. Nguyen, D.-P. Vu, ve School of Electrical and Electronic Engineering, Hanoi University of Science and Technology, Hanoi, Vietnam, "Multi-objective optimization using MISOCP model for service restoration in electrical distribution grids in the presence of distributed generation and voltage-dependent loads", *AIMS Energy*, c. 13, sy. 5, ss. 1012-1051, 2025, doi: 10.3934/energy.2025038.

[23] I. A. Quadri, S. Bhowmick, ve D. Joshi, "A comprehensive technique for optimal allocation of distributed energy resources in radial distribution systems", *Appl. Energy*, c. 211, ss. 1245-1260, Şub. 2018, doi: 10.1016/j.apenergy.2017.11.108.

[24] L. A. Gallego, J. M. Lopez-Lezama, ve O. G. Carmona, "A Mixed-Integer Linear Programming Model for Simultaneous Optimal Reconfiguration and Optimal Placement of Capacitor Banks in Distribution Networks", *IEEE Access*, c. 10, ss. 52655-52673, 2022, doi: 10.1109/ACCESS.2022.3175189.

[25] D. Wan, M. Zhao, Z. Yi, F. Jiang, Q. Guo, ve Q. Zhou, "Mixed-integer second-order cone programming method for active distribution network", *Front. Energy Res.*, c. 11, s. 1259445, Ağu. 2023, doi: 10.3389/fenrg.2023.1259445.

[26] L. H. Macedo, J. F. Franco, M. J. Rider, ve R. Romero, "Optimal Operation of Distribution Networks Considering Energy Storage Devices", *IEEE Trans. Smart Grid*, c. 6, sy. 6, ss. 2825-2836, Kas. 2015, doi: 10.1109/TSG.2015.2419134.

[27] M. Pürlü, "NİSAN 2022 DAĞITIK ÜRETİM SİSTEMLERİNİN AKILLI ŞEBEKELER ÜZERİNE ETKİLERİNİN İNCELENMESİ", 2022.

[28] A. Valencia-Díaz, R. A. Hincapié, ve R. A. Gallego, "Optimal Placement and Sizing of Distributed Generation in Electrical DC Distribution Networks Using a Stochastic Mixed-Integer LP Model", *Arab. J. Sci. Eng.*, c. 50, sy. 8, ss. 5835-5851, Nis. 2025, doi: 10.1007/s13369-024-09655-6.

[29] M. H. Ali, S. Kamel, M. H. Hassan, M. Tostado-Véliz, ve H. M. Zawbaa, "An improved wild horse optimization algorithm for reliability based optimal DG planning of radial distribution networks", *Energy Rep.*, c. 8, ss. 582-604, Kas. 2022, doi: 10.1016/j.egyr.2021.12.023.

[30] M. M. Aman, G. B. Jasmon, A. H. A. Bakar, ve H. Mokhlis, "A new approach for optimum simultaneous multi-DG distributed generation Units placement and sizing based on maximization of system loadability using HPSO (hybrid particle swarm

optimization) algorithm", *Energy*, c. 66, ss. 202-215, Mar. 2014, doi: 10.1016/j.energy.2013.12.037.

[31] S. Kaur, G. B. Kumbhar, ve J. Sharma, "Performance of Mixed Integer Non-linear Programming and Improved Harmony Search for optimal placement of DG units", içinde *2014 IEEE PES General Meeting | Conference & Exposition*, National Harbor, MD, USA: IEEE, Tem. 2014, ss. 1-5. doi: 10.1109/PESGM.2014.6939165.

[32] B. R. Pereira, G. R. M. Martins Da Costa, J. Contreras, ve J. R. S. Mantovani, "Optimal Distributed Generation and Reactive Power Allocation in Electrical Distribution Systems", *IEEE Trans. Sustain. Energy*, c. 7, sy. 3, ss. 975-984, Tem. 2016, doi: 10.1109/TSTE.2015.2512819.

[33] S. H. Low, "Convex Relaxation of Optimal Power Flow—Part I: Formulations and Equivalence".

[34] W. Gil-González, O. D. Montoya, L. F. Grisales-Noreña, C. L. Trujillo, ve D. A. Giral-Ramírez, "A mixed-integer second-order cone model for optimal siting and sizing of dynamic reactive power compensators in distribution grids", *Results Eng.*, c. 15, s. 100475, Eyl. 2022, doi: 10.1016/j.rineng.2022.100475.

[35] T. Altun, "Optimal allocation of distributed generation on DC Networks", *Eng. Sci. Technol. Int. J.*, c. 57, s. 101817, Eyl. 2024, doi: 10.1016/j.jestch.2024.101817.

[36] F. Alizadeh ve D. Goldfarb, "Second-Order Cone Programming",

[37] W. Gil-González, A. Garces, Oscar Danilo Montoya, ve J. C. Hernández, "Exact mixed-integer convex model for the optimal selection and sizing of distributed generators in AC distribution network".

[38] S. N. Gopiya Naik, D. K. Khatod, ve M. P. Sharma, "Analytical approach for optimal siting and sizing of distributed generation in radial distribution networks", *IET Gener. Transm. Distrib.*, c. 9, sy. 3, ss. 209-220, Şub. 2015, doi: 10.1049/iet-gtd.2014.0603.

[39] I. Oladeji, R. Zamora, ve T. T. Lie, "Security constrained optimal placement of renewable energy sources distributed generation for modern grid operations", *Sustain. Energy Grids Netw.*, c. 32, s. 100897, Ara. 2022, doi: 10.1016/j.segan.2022.100897.

ISBN NR. : 978-625-8795-33-2

EFFECT OF ISATIS FLORIBUNDA EXTRACT CONCENTRATION ON THE STRUCTURAL, MORPHOLOGICAL, AND OPTICAL CHARACTERISTICS OF NANOSTRUCTURED ZnO THIN FILMS PREPARED BY SILAR

Assist. Prof. Dr., ÜMMÜHAN AKIN

Selçuk University, Faculty of Science, Department of Physics, Konya, Türkiye

uakin@selcuk.edu.tr - ORCID: 0000-0001-7754-9681

ABSTRACT

Zinc oxide (ZnO) is a versatile semiconductor material with diverse technological applications, from sensors and optoelectronic devices to photocatalysis and biomedical applications, owing to its wide band gap (3.3 eV), high optical transmittance, high electron mobility, excellent transparency, and chemical stability. These outstanding properties make ZnO a highly promising material for emerging and advanced technological applications. In particular, nanostructured ZnO has gained significant research attention over recent years because of its tunable physical properties. In this study, the effect of incorporating Isatis floribunda extract at different concentrations on the structural, morphological, and optical features of nanostructured ZnO films was investigated. With this aim, nanostructured ZnO films with and without extract were successfully synthesized on glass substrates via the successive ionic layer adsorption and reaction (SILAR) technique. The obtained films were examined in terms of their structural and morphological features using the X-ray diffraction and the scanning electron microscopy, respectively, while their optical features were analyzed with the ultraviolet-visible-near spectrophotometer. The analysis results indicated that Isatis floribunda plays a significant role in the formation of nanostructured ZnO films and in the modulation of their physical properties.

Keywords: ZnO, Isatis floribunda, Thin film, Extract, SILAR

1. INTRODUCTION

In recent years, semiconductor materials based on group II-VI metal oxides, such as titanium dioxide (TiO_2), cadmium oxide (CdO), copper oxide (CuO), zinc oxide (ZnO) and magnesium oxide (MgO) have attracted considerable attention due to their exceptional optical, electrical, antibacterial, and photocatalytic properties. Among these metal oxide semiconductor materials, ZnO stands out as a versatile n-type semiconductor due to its impressive physical, chemical, and biological properties, its harmless and low-cost, and its technological and environmental applications [1-3]. ZnO is also an enormous transition metal oxide with an exciton binding energy of 60 meV [3] and a direct optical band gap of 3.3 eV [4]. ZnO naturally crystallizes in a hexagonal wurtzite structure with lattice parameters of a = 3.25 Å and c = 5.12 Å [5].

Especially nowadays, the nanostructured ZnO particles are extensively used in many application areas including dye-sensitized solar cells, light-emitting diodes, photocatalysts, biosensors, and pharmaceutical industry [3, 6]. The high-quality ZnO nanoparticles are obtained by many production methods including sputtering, sol-gel, chemical vapor deposition, spray pyrolysis, molecular beam epitaxy, hydrothermal, and successive ionic layer adsorption

ISBN NR. : 978-625-8795-33-2

and reaction [7-10]. Among these methods, particularly in thin film preparation, the successive ionic layer adsorption and reaction (SILAR) method is a highly preferred method due to its simplicity, flexibility, and quite cost-effective, as it does not require a complex vacuum system [3, 5].

In recent years, with the increasing interest in environmentally friendly and sustainable approaches in the synthesis of nanostructured metal oxides, green synthesis methods using plant extracts have become an important research area. Plant extracts contain biologically active compounds, which can influence the crystal growth processes, thereby enabling the modulation of the structural, morphological, and optical features of the resulting thin films. Compared with chemical additives, these natural extracts offer advantages, such as low toxicity, biodegradability, easy availability, and cost-effectiveness, while also minimizing the environmental impact of the synthesis process. The literature contains numerous reports on the green synthesis of a wide range of nanostructured metal oxides using plant-derived extracts [3, 11]. Among these studies, Pakzad et al. [11] performed the biosynthesis of CuO and Ni@Fe_3O_4 nanoparticles with *Euphorbia maculata* extract acting as a photocatalyst. The structural properties of biosynthesized metal nanoparticles were investigated, and their photocatalytic processes in MB, CR, and RhB organic pollutants were studied. In a separate study, Şahin et al. [3] investigated the effect of *Thymus syriacus* plant extract on the antibacterial activities and physical properties of ZnO nanoparticles. Their study demonstrated that the plant extract used is a promising option against plant bacterial diseases.

In the presented study, an extract obtained from the *Isatis floribunda* plant, found in the local flora, was used as an additive in the synthesis of nanostructured ZnO thin films produced by the SILAR method. *Isatis floribunda* is an endemic woad species native to Türkiye [12-14]. In recent years, owing to its rich phytochemical composition, it has attracted increasing interest in the fields of materials science and biomedicine. Studies have shown that *Isatis floribunda* extracts possess antioxidant and antimicrobial properties and demonstrate inhibitory effects against Alzheimer's disease-related enzymes [12, 13]. The roots and flowers of this yellow-flowering plant have been found to contain high concentrations of phenolic compounds, flavonoids, and other biologically active secondary metabolites [12, 13, 15]. In particular, root extracts have been reported to possess strong antimicrobial and antioxidant properties and to contain various bioactive compounds, with chlorogenic acid being one of the major constituents. This rich phytochemical profile highlights the potential of *Isatis floribunda* extract as a natural additive for the green synthesis of nanostructured metal oxides. Therefore, investigating the effects of different plant extracts and their concentrations on the properties of ZnO thin films is of considerable importance for enhancing material performance. Due to its rich phytochemical content, *Isatis floribunda* influences the formation and growth of ZnO nanostructures. These phytochemicals can act as natural complexing, stabilizing, and growth-modifying agents during the deposition process, thereby affecting the crystallization behavior and the resulting physicochemical properties of the thin films. Therefore, the nanostructured ZnO films, both with and without extract, were synthesized on glass substrates using the SILAR technique, and the effect of different concentrations of *Isatis floribunda* extract on the structural, morphological, and optical features of nanostructured ZnO films was investigated. The findings are expected to provide valuable insights into the influence of *Isatis floribunda* extract concentration on the behavior of ZnO thin films and to promote the use of sustainable, plant extract-assisted synthesis routes for optoelectronic and sensor applications.

2. EXPERIMENTAL PROCEDURE

2.1. Preparation of *Isatis floribunda* Extract

ISBN NR. : 978-625-8795-33-2

Isatis floribunda, used in the preparation of ZnO nanostructures, is an endemic herbaceous and medicinal plant species that grows in Türkiye [12-14]. It was collected from its natural habitat in Konya province, located in the Central Anatolia Region of Türkiye (*Isatis floribunda* EŞ 834). The *Isatis floribunda* dried leaves intended for extraction were first washed with distilled water and then ground using a plant mill. Afterward, the powdered plant leaves were steeped in boiled water for 15 minutes and left to cool to room temperature. Finally, the extract was prepared by carefully filtering it through filter paper (Figure 1).

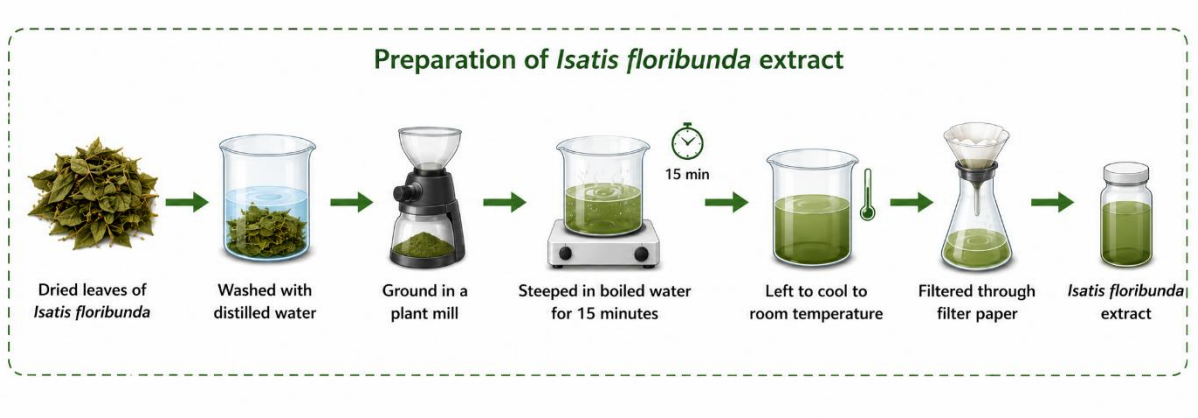

Figure 1. Schematic illustration of the preparation of *Isatis floribunda* extract

2.2. Preparation and Characterization of Nanostructured ZnO Films With and Without *Isatis floribunda* Extract

In study, nanostructured ZnO thin films were prepared via SILAR method onto glass substrates with multiple cycles. At first, Zn^{2+} ion solution of 100 ml 0.1 M was prepared by using zinc acetate dihydrate salt ($C_4H_{10}O_6Zn$). The solution was stirred on a heated magnetic stirrer until a clear and homogeneous solution was obtained. Afterward, ammonium hydroxide (NH_4OH) was introduced to adjust the solution pH, followed by heating the mixture to 90°C. Initially, the substrate was immersed in the Zn^{2+} solution for 15 seconds, followed by immersion in pure water maintained at 90°C for another 15 seconds to eliminate weakly bound ions. After completing rinsing step, the substrate was dried in air for 15 seconds. To investigate the concentration effect of *Isatis floribunda* on nanostructured ZnO films, *Isatis floribunda* extract was added to the Zn ion solution at concentrations of 10%, 15%, and 20%. Nanostructured ZnO thin films incorporating *Isatis floribunda* extract were subsequently prepared using the SILAR method described above. Figure 2 illustrates the SILAR cycle employed in the preparation of all ZnO films. The obtained films were examined in terms of their structural and morphological features by using the X-ray diffraction (XRD; Bruker D8 Advance; CuKα; $\lambda = 0.1518$ nm) and the scanning electron microscopy (SEM; ZEISS EVO LS10), respectively, while their optical features were analyzed with the ultraviolet-visible-near spectrophotometer (Jasco V-670).

ISBN NR. : 978-625-8795-33-2

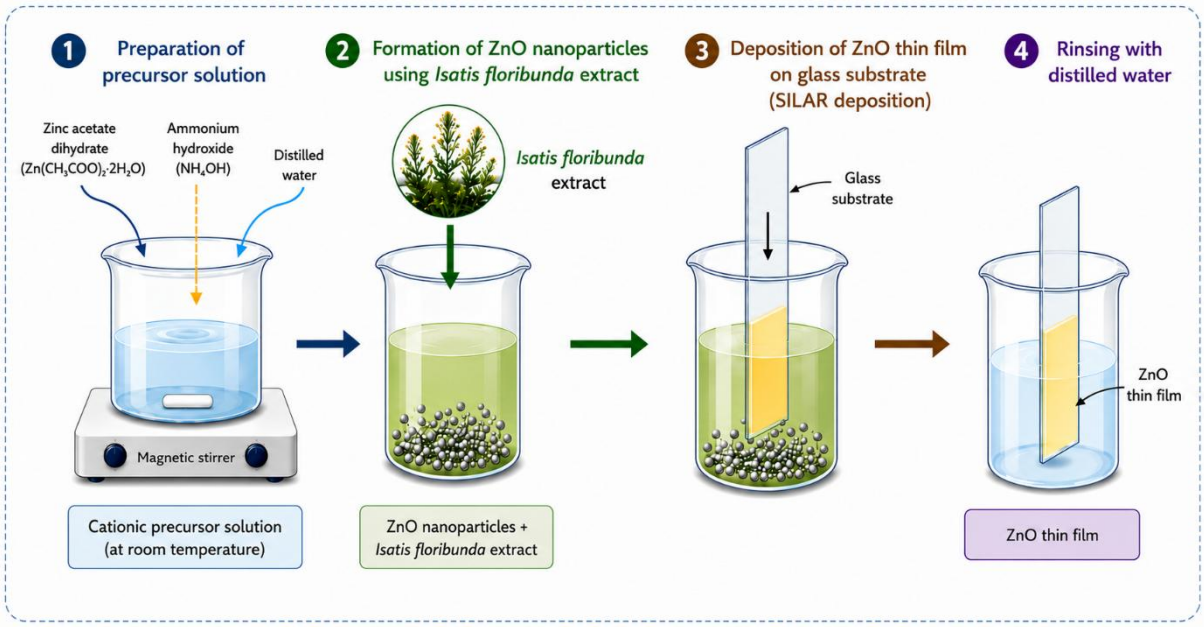

Figure 2. SILAR procedure for the preparation of ZnO thin films using *Isatis floribunda* extract

3. RESULT AND DISCUSSIONS

3.1. Structural Properties of Nanostructured ZnO Films

The crystal structural of ZnO films prepared with and without different amounts of *Isatis floribunda* was examined by XRD analyses. Figure 3 shows the XRD patterns of all ZnO films grown on glass substrates. As seen from the patterns, all ZnO films have three dominant peaks primarily in the (100), (002) and (101) crystal planes, and in addition to these three main peaks in XRD pattern, there are four diffraction lines of (102), (110), (103) and (112) planes. The measured XRD patterns showed similar behavior to the XRD patterns of ZnO nanoparticles containing *Thymus syriacus* plant extract presented by Şahin et al [3]. As can be seen from Figure 3, the plane densities of films change with the incorporation of *Isatis floribunda* extract. Also, the crystalline size of ZnO samples also varies with the extract concentrations (Table 1). The addition of *Isatis floribunda* extract to the solution may cause changes in the crystal size of ZnO films, as it affects the growth and nucleation processes by changing the surface tension of the growth solution.

Table 1. Crystallite Size of ZnO Samples at Different *Isatis floribunda* Concentrations

***Isatis Floribunda* Concentration (%)**	**Crystallite Size (nm)**
0	23.87
10	24.74
15	26.39
20	23.17

ISBN NR. : 978-625-8795-33-2

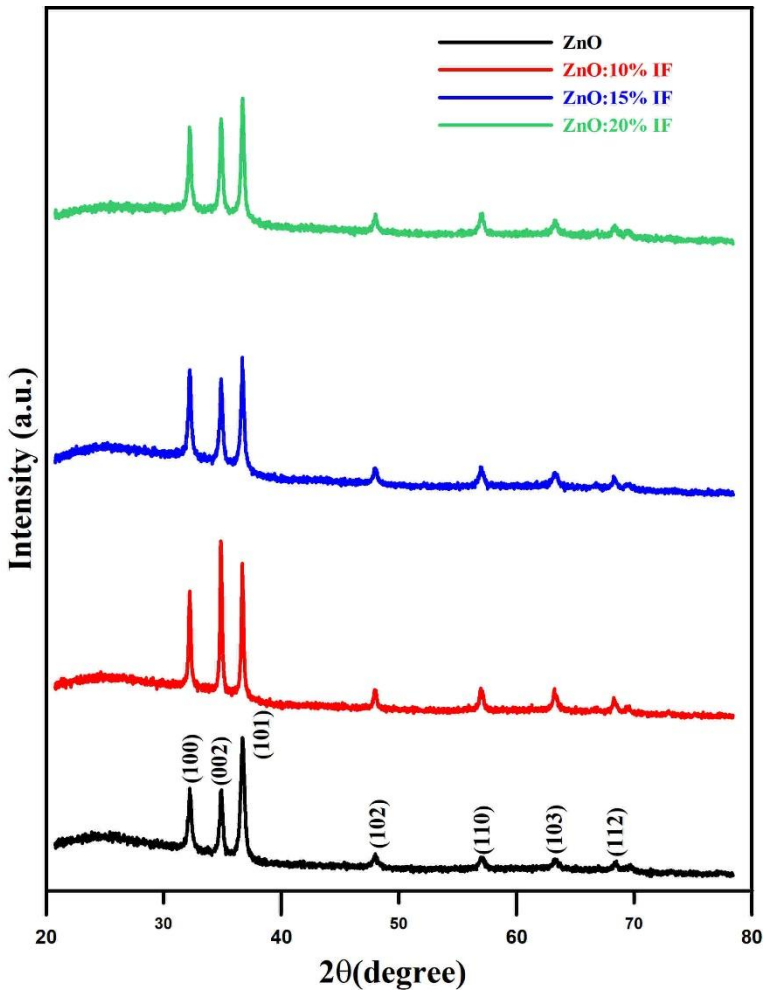

Figure 3. XRD patterns of nanostructured ZnO films prepared by varying *Isatis floribunda* extract concentrations

3.2. Surface Morphology of Nanostructured ZnO Films

The morphological characteristics of films prepared with *Isatis floribunda* extract (0%, 10%, 15%, and 20.0%, respectively) were examined using SEM. It is seen that all films produced from the SEM photographs in Figure 4 have a homogeneous and dense surface structure. The surface structure of ZnO film changes drastically by adding different percentages of *Isatis floribunda* to the reaction solution. The presence of *Isatis floribunda* can change the crystallinity quality of films. This change observed in the images may be the electrostatically reaction between Zn^{2+} and *Isatis floribunda* during the synthesis process. Also, after the nucleation, *Isatis floribunda* may affect particle growth and morphology [3, 5, 10].

ISBN NR. : 978-625-8795-33-2

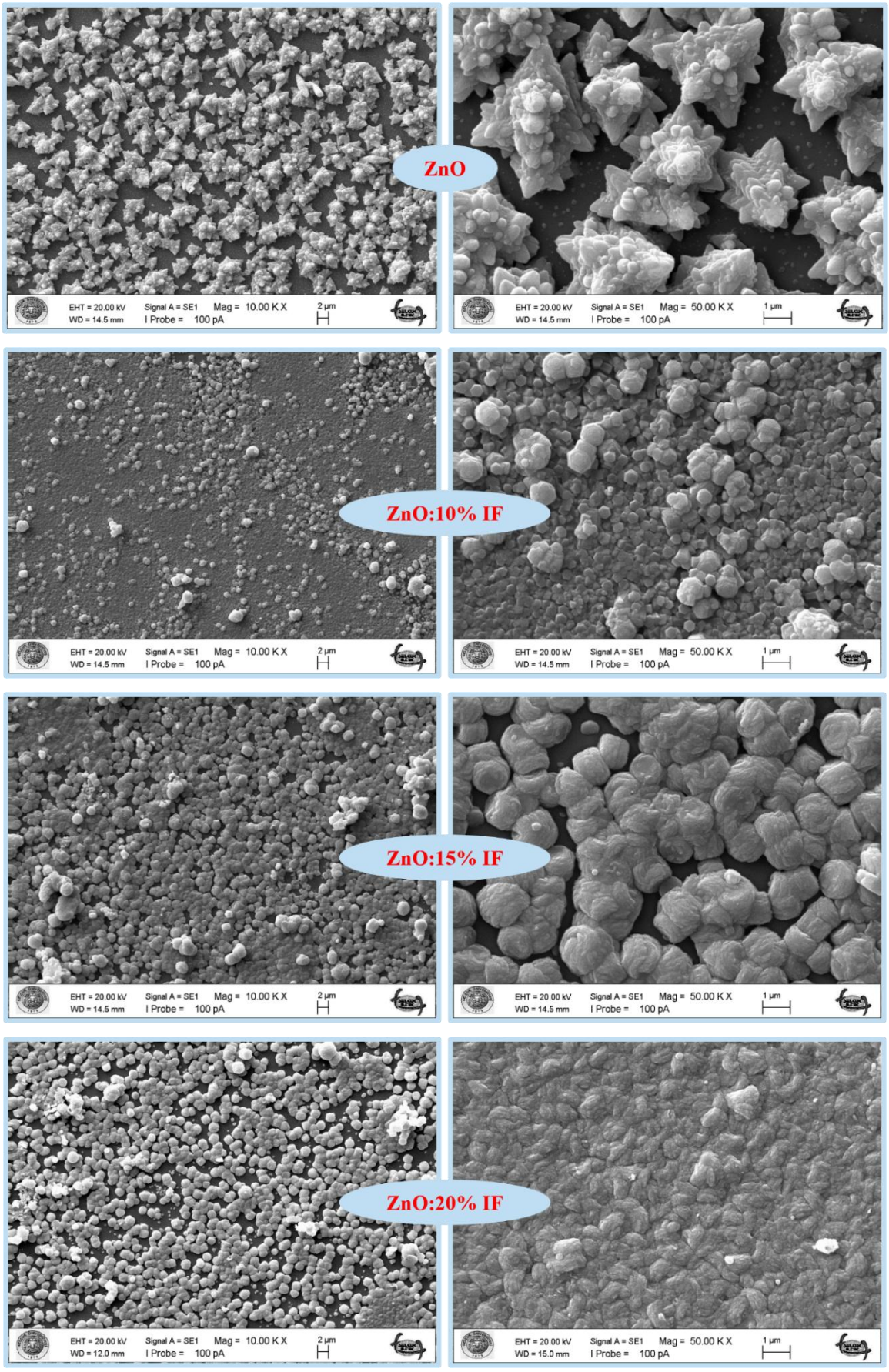

ISBN NR. : 978-625-8795-33-2

Figure 4. SEM images of nanostructured ZnO thin films prepared by varying *Isatis floribunda* extract concentrations

3.3. Optical Properties of Nanostructured ZnO Films

The absorbance and transmittance curves of ZnO films prepared depending on their extract concentration in the wavelength region of 400-2000 nm are presented in Figure 5 and 6, respectively. The graphs demonstrate that increasing the extract concentration resulted in a decrease in the absorbance values of the films, accompanied by a corresponding increase in their transmittance values. The spectrum change observed in films depending on the increased extract concentration can be attributed to changes in the thickness of produced films [3, 10].

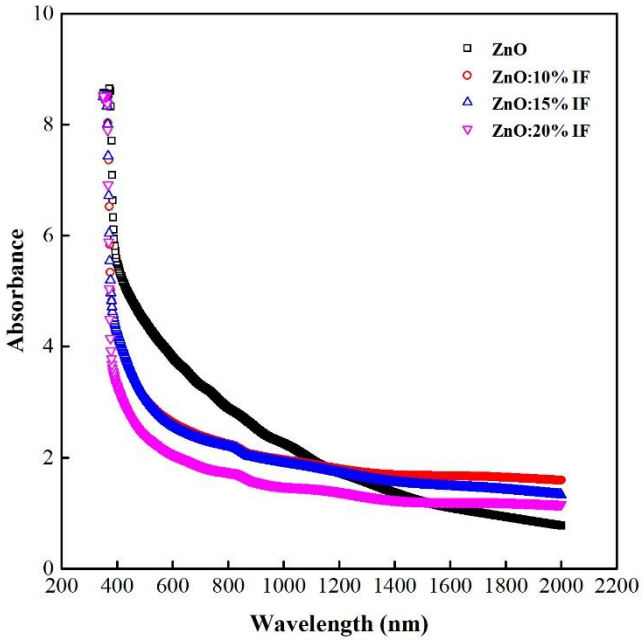

Figure 5. The absorbance spectra of nanostructured ZnO films prepared by varying *Isatis floribunda* extract concentrations

ISBN NR. : 978-625-8795-33-2

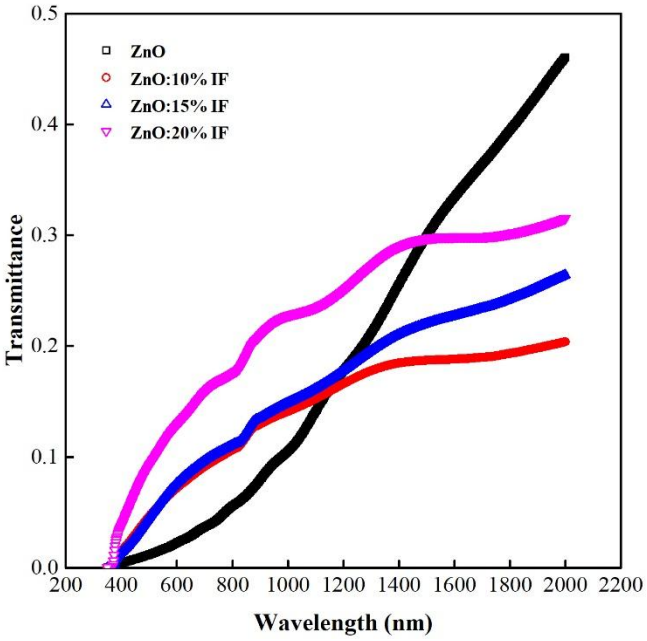

Figure 6. The transmittance spectra of nanostructured ZnO films prepared by varying *Isatis floribunda* extract concentrations

4. CONCLUSION

The present study successfully achieved the fabrication of nanostructured ZnO films via the SILAR method using solutions with different concentrations of *Isatis floribunda* extract. XRD, SEM, and UV-Vis/NIR spectroscopy were employed to characterize the structural, morphological, and optical features of ZnO films, respectively. The XRD patterns demonstrated that changes in the extract concentration had a pronounced effect on the crystallization quality of the ZnO films. In addition, the SEM results revealed that the incorporation of *Isatis floribunda* extract contributed to the improvement of the morphological properties of the ZnO films. These findings indicate that *Isatis floribunda* extract has a considerable influence on the morphology of ZnO films. Furthermore, the UV-Vis analysis revealed that the addition of *Isatis floribunda* extract altered the optical spectra of ZnO films. Overall, the obtained results demonstrate that nanostructured ZnO films incorporating *Isatis floribunda* extract exhibit promising potential for optoelectronic and sensor applications.

Acknowledgement

I am deeply grateful to Assoc. Prof. Dr. Emrah ŞİRİN and Asst. Prof. Dr. Erdoğan GÜNEŞ from Selçuk University for their valuable support in the procurement, identification, and extraction processes of *Isatis floribunda* plant used in this study.

REFERENCES

1. Hanna, B., Manuraj, M., Surendran, K. P., Narayanan Unni K. N. Opto Electronic Properties of Solution Processed Zinc Oxide Thin Films: Role of Solvents and Doping, Journal of Materials Science: Materials in Electronics, 31, 13570-13577, 2020. https://doi.org/10.1007/s10854-020-03913-7

2. Ahammed, K. R., Ashaduzzaman, M., Paul, S. C., Nath, M. R., Bhowmik, S., Saha, O., Rahaman, M. M., Bhowmik, S., Aka, T. D. Microwave Assisted Synthesis of Zinc

Oxide (ZnO) Nanoparticles in A Noble Approach: Utilization for Antibacterial and Photocatalytic Activity, SN Applied Sciences, 2, 955, 2020. https://doi.org/10.1007/s42452-020-2762-8

3. Şahin, B., Aydin, R., Soylu, S., Türkmen, M., Kara, M., Akkaya, A., Çetin, H., Ayyıldız, E. The Effect of *Thymus syriacus* Plant Extract on The Main Physical and Antibacterial Activities of ZnO Nanoparticles Synthesized by SILAR Method, Inorganic Chemistry Communications, 135, 109088, 2022. https://doi.org/10.1016/j.inoche.2021.109088

4. Zhenguo, J., Kun, L., Chengxing, Y., Ruixin, F., Zhizhen, Y. Structural, Optical and Electrical Properties of ZnO Thin Films Prepared by Reactive Deposition, Journal of Crystal Growth, 253, 246-251, 2003. doi:10.1016/S0022-0248(03)01005-4

5. Taşdemir, A., Akman, N., Akkaya, A., Aydın, R., Şahin, B. Green and Cost-Effective Synthesis of Zinc Oxide Thin Films by L-Ascorbic Acid (AA) and Their Potential for Electronics and Antibacterial Applications, Ceramics International, 48, 10164-10173, 2022. https://doi.org/10.1016/j.ceramint.2021.12.228

6. Zhang, Q., Dandeneau, C. S., Zhou, X., Cao, G. ZnO Nanostructures for Dye-Sensitized Solar Cells, Advanced Materials, 21, 4087-4108, 2009. DOI: 10.1002/adma.200803827

7. Dahnoun, M., Attaf, A., Saidi, H., Yahia, A., Khelif, C. Structural, Optical and Electrical Properties of Zinc Oxide Thin Films Deposited by Sol-Gel Spin Coating Technique, Optik, 134, 53-59, 2017. http://dx.doi.org/10.1016/j.ijleo.2017.01.014

8. Muchuweni, E., Sathiaraj, T.S., Nyakotyo, H. Effect of Gallium Doping on The Structural, Optical and Electrical Properties of Zinc Oxide Thin Films Prepared by Spray Pyrolysis, Ceramics International, 42, 10066-10070, 2016. http://dx.doi.org/10.1016/j.ceramint.2016.03.110

9. Toma, F. T. Z., Rahman, M. S., Maria, K. H. A Review of Recent Advances in ZnO Nanostructured Thin Films by Various Deposition Techniques, Discover Materials, 5, 60, 2025. https://doi.org/10.1007/s43939-025-00201-1

10. Taşdemir, A., Aydin, R., Akkaya, A., Akman, N., Altınay, Y., Çetin, H., Şahin, B., Uzun, A., Ayyıldız, E. A Green Approach for The Preparation of Nanostructured Zinc Oxide: Characterization and Promising Antibacterial Behaviour, Ceramics International, 47, 19362-19373, 2021. https://doi.org/10.1016/j.ceramint.2021.03.273

11. Pakzad, K., Alinezhad, H., Nasrollahzadeh, M. Green Synthesis of Ni@Fe_3O_4 and CuO Nanoparticles Using *Euphorbia Maculata* Extract as Photocatalysts for The Degradation of Organic Pollutants Under UV-Irradiation, Ceramics International, 45, 17173-17182, 2019. https://doi.org/10.1016/j.ceramint.2019.05.272

12. Karakoca, K., Asan Ozusaglam, M., Cakmak, Y. S., Karaman Erkul, S. Antioxidative, Antimicrobial and Cytotoxic Properties of *Isatis floribunda* Boiss. ex Bornm. Extracts, EXCLI Journal, 12, 150-167, 2013. DOI:10.17877/DE290R-10660

13. Güzel, E., Yücel, Y. Y., Alkan, M., Polatoğlu, K. Essential Oil Composition of *Isatis floribunda* Boiss. ex. Bornm. and Acetylcholinesterase Inhibitory Activity of Its Extract, Acta Pharmaceutica Sciencia, 62, 581-592, 2024. DOI: 10.23893/1307-2080.APS6237

14. https://turkiyebitkileri.com/foto%C4%9Fraf-galerisi/brassicaceae-turpgiller/isatis-civitotu/isatis-floribunda.html (Accessed: 21.07.2026)

ISBN NR. : 978-625-8795-33-2

15. Albayrak, İ., Cessur, A., Demirci, T., Tuğlu, Ü., Göktürk Baydar, N. Enhancement of Indigotin and Indirubin Production in Root Cultures of *Isatis* Species by H_2O_2: Biochemical and Molecular Responses, Scientific Reports, 15, 33637, 2025. https://doi.org/10.1038/s41598-025-10242-4

ISBN NR. : 978-625-8795-33-2

A MULTI-SPECIES CHEMOTAXIS SYSTEM WITH MULTIPLE CHEMICALS AND LOGISTIC GROWTH

Doç. Dr. Halil İbrahim KURT
Karadeniz Teknik Üniversitesi
hkurt@ktu.edu.tr - 0000-0002-9549-6445

Doç. Dr. Tuncay KÖROGLU
Karadeniz Teknik Üniversitesi
tkor@ktu.edu.tr - 0000-0002-1341-1074

ABSTRACT

This study considers a multi-species, multi-chemical chemotaxis model with regular sensitivity and general logistic-type interactions, given by

$$\begin{cases} u_t = \Delta u - \chi_1 \nabla \cdot (u \nabla w) - \lambda_1 \nabla \cdot (u \nabla z) + \mathrm{f}_1(u,v), & x \in \Omega, t > 0, \\ v_t = \Delta u - \chi_2 \nabla \cdot (v \nabla w) - \lambda_2 \nabla \cdot (v \nabla z) + \mathrm{f}_2(u,v), & x \in \Omega, t > 0 \\ 0 = \Delta w - w + \alpha_1 u + \beta_1 v, & x \in \Omega, t > 0 \\ 0 = \Delta z - z + \alpha_2 u + \beta_2 v, & x \in \Omega, t > 0, \end{cases}$$

Here, unknown functions u, v denote the densities of two species, while w, z represent the concentrations of chemical substances concentrations of chemical substances. The parameters $\chi_{1,2}$ and $\lambda_{1,2}$ are chemotactic sensitivities (positive for attraction and negative for repulsion). The functions $\mathrm{f}_{1,2}(u,v)$ describe growth and interaction effects, typically of Lotka–Volterra type. The constants $\alpha_{1,2}$ and $\beta_{1,2}$ represent production rates of the chemicals.

Chemotaxis refers to the directed movement of cells or organisms in response to chemical gradients. It plays a crucial role in many biological processes, including population dynamics, tumor growth, immune response, and embryonic development. Mathematically, key challenges in chemotaxis systems include the study of local and global existence, boundedness, finite-time blow-up, and asymptotic behavior of solutions such as persistence, stability, coexistence, and extinction. Over the past decades, these topics have been extensively studied, leading to significant advances in understanding the global dynamics of such systems.

In this paper, we introduce the above system and discuss its mathematical properties. In particular, we aim to present a framework for analyzing global existence, boundedness, and mass persistence of solutions under suitable assumptions on the nonlinear terms.

Key words: Chemotaxis, multi-species, multi-chemical, regular sensitivity, logistic growth.

ISBN NR. : 978-625-8795-33-2

1. INTRODUCTION

Chemotaxis models, pioneered by Keller and Segel in their seminal works, provide a fundamental mathematical framework for describing the directed movement of cellular organisms in response to chemical gradients. Over the past decades, these models have proven essential in clarifying the mechanisms underlying various complex biological phenomena, including immune system responses, embryonic development, cell population dynamics, tumor invasion, and even gravitational collapse in astrophysics. While classical Keller–Segel models focus on a single species responding to a single chemical signal, realistic biological environments often involve multiple competing or cooperating species that secrete and react to multiple distinct chemoattractants or chemorepellents. To capture these complex interactions, this study examines a multi-species, multi-chemical chemotaxis system derived from fundamental conservation laws and quasi-steady-state assumptions. The primary objective is to analyze the system's core dynamical properties such as global boundedness, pattern formation, and long-time asymptotic behavior from both biological and mathematical perspectives. See the research papers for more details.

1.1. MODEL FORMULATION AND PHYSICAL INTERPRETATION

We consider a two-species, two-chemical cross-diffusive chemotaxis system defined over a bounded domain $\Omega \subset \mathbb{R}^n$ $(n \geq 1)$ with a smooth boundary $\partial\Omega$. The spatiotemporal densities of the two biological species are denoted by $u(x,t)$ and $v(x,t)$, while $w(x,t)$ and $z(x,t)$ represent the concentrations of two chemical substances, respectively:

$$\begin{cases} u_t = \Delta u - \chi_1 \nabla \cdot (u \nabla w) - \lambda_1 \nabla \cdot (u \nabla z) + f_1(u,v), & x \in \Omega,\ t > 0, \\ v_t = \Delta v - \chi_2 \nabla \cdot (v \nabla w) - \lambda_2 \nabla \cdot (v \nabla z) + f_2(u,v), & x \in \Omega,\ t > 0, \\ 0 = \Delta w - w + \alpha_1 u + \beta_1 v, & x \in \Omega,\ t > 0, \\ 0 = \Delta z - z + \alpha_2 u + \beta_2 v, & x \in \Omega,\ t > 0, \end{cases} \tag{1.1}$$

supplemented with homogeneous Neumann boundary conditions

$$\frac{\partial u}{\partial \nu} = \frac{\partial v}{\partial \nu} = \frac{\partial w}{\partial \nu} = \frac{\partial z}{\partial \nu} = 0, \quad x \in \partial\Omega,\ t > 0, \tag{1.2}$$

and initial conditions $u(x,0) = u_0(x) \geq 0$ and $v(x,0) = v_0(x) \geq 0$. Here, ν denotes the outward unit normal vector on $\partial\Omega$.

The derivation of system (1.1) rests on mass conservation principles and constitutive flux relations. The temporal evolution of the population densities u and v is governed by the divergence of their respective total fluxes. These fluxes consist of two components: unbiased random motion described by Fickian diffusion $(\Delta u, \Delta v)$ and directed migration along the spatial gradients of the chemical signals (w and z). The sensitivity parameters χ_i and λ_i $(i = 1,2)$ govern the direction and strength of chemotaxis: positive values $(\chi_i, \lambda_i > 0)$ correspond to chemoattraction (movement toward higher chemical concentrations), whereas negative values denote chemorepulsion (movement away from chemical concentrations). The non-local reaction kinetics $f_1(u,v)$ and $f_2(u,v)$ describe local growth, intra-species self-limitation, and

ISBN NR. : 978-625-8795-33-2

inter-species interactions, typically modeled via Lotka–Volterra competitive terms such as $f_1(u,v) = r_1 u(1 - a_1 u - a_2 v)$.

In contrast to the parabolic PDEs for cellular densities, the chemical concentrations w and z are governed by elliptic equations. This formulation originates from a quasi-steady-state approximation. Because molecular chemical diffusion occurs on a significantly faster time scale than cellular movement and proliferation ($D_{\text{chem}} \gg D_{\text{cell}}$), the temporal derivatives w_t and z_t can be formally set to zero without loss of physical accuracy. The biological species u and v linearly produce chemical signals w and z at rates $\alpha_i, \beta_i \geq 0$ ($i = 1,2$), which undergo natural linear degradation at normalized unit rates.

2. BIOLOGICAL AND MATHEMATICAL PROPERTIES

2.1. BIOLOGICAL IMPLICATIONS

From a biological standpoint, system (1.1) models complex multi-signal navigation and spatial organization within cellular communities. Organisms frequently navigate environments containing conflicting signal cues—such as moving toward nutrient sources (w) while simultaneously avoiding toxic metabolic waste or alarm pheromones (z). The competition between dispersal mechanisms (random diffusion and chemorepulsion) and aggregation mechanisms (chemoattraction) triggers spontaneous spatial pattern formation, traveling waves, or phase separation. Furthermore, the inclusion of logistic reaction kinetics $f_i(u,v)$ prevents unrealistic population growth, determining whether competing populations coexist within a shared ecological niche or undergo competitive exclusion despite chemotactic pressures.

2.2. MATHEMATICAL FEATURES

Mathematically, system (1.1) is a strongly coupled, non-local system of parabolic-elliptic partial differential equations characterized by nonlinear cross-diffusion terms. The primary mathematical features of the system include:

- **Positivity Preservation:** For any non-negative initial data $u_0, v_0 \in C^0(\overline{\Omega})$, maximum principle arguments ensure that classical solutions remain non-negative for all $t > 0$, maintaining biological consistency.

- **Mass Conservation Structure:** In the absence of reaction kinetics ($f_1 = f_2 \equiv 0$), integration over Ω alongside Neumann boundary conditions (1.2) yields total mass conservation:

$$\int_\Omega u\,(x,t)\,dx = \int_\Omega u_0\,(x)\,dx \quad \text{and} \quad \int_\Omega v\,(x,t)\,dx = \int_\Omega v_0\,(x)\,dx, \quad \forall t > 0. \tag{2.1}$$

- **Nonlinear Cross-Coupling:** The elliptic operator maps biological densities (u,v) directly to chemical gradients $(\nabla w, \nabla z)$. Consequently, terms like $\nabla \cdot (u \nabla w)$ generate quadratic-like non-local nonlinearities that heavily influence the analytical regularity of solutions.

ISBN NR. : 978-625-8795-33-2

3. DYNAMICAL PROPERTIES AND CENTRAL RESEARCH QUESTIONS

The mathematical dynamics of system (1.1) are governed by a delicate balance between aggregation driven by chemoattraction and stabilization induced by diffusion and quadratic logistic dampening. The central analytical problems concerning this system encompass:

1. **Global Boundedness vs. Finite-Time Blow-up:** Whether solutions remain bounded for all time or develop singularities, particularly in higher dimensions. In multi-dimensional domains ($n \geq 2$), strong chemoattraction ($\chi_i, \lambda_i \gg 1$) can cause mathematical blow-up in finite time ($\| u(\cdot,t) \|_{L^\infty} \to \infty$ as $t \to T^*$), representing localized biological aggregation. A major question is establishing explicit parameter thresholds for (χ_i, λ_i, r_i) under which quadratic logistic dampening ($f_i \leq r_i u - \mu_i u^2$) completely prevents blow-up, guaranteeing global-in-time classical bounded solutions.

2. **Pattern Formation and Turing Instability:** Chemotactic interactions may destabilize homogeneous states, leading to spatially heterogeneous solutions. Whether solutions converge to steady states and under what conditions such equilibria are stable. By linearizing the system around a spatially homogeneous equilibrium point (u^*, v^*, w^*, z^*), cross-diffusive terms can destabilize the homogeneous state through a chemotaxis-driven Turing mechanism. This leads to spatial heterogeneity, such as persistent spots, stripes, or labyrinthine patterns.

3. **Long-time behavior:** Analysis of convergence to equilibria, coexistence of species, or extinction scenarios. Another core objective is determining the long-time behavior ($t \to \infty$) of classical solutions. This includes analyzing asymptotic convergence toward non-constant steady states or spatial equilibria, as well as establishing conditions for pointwise persistence, species coexistence, or competitive extinction.

These aspects make the system a rich framework for studying the interplay between biological mechanisms and nonlinear PDE dynamics.

REFERENCES

1. E. F. Keller and L. A. Segel, Initiation of slime mold aggregation viewed as an instability, *Journal of Theoretical Biology*, **26** (1970), 399-415.

2. E. F. Keller and L. A. Segel, A model for chemotaxis, *Journal of Theoretical Biology*, **30** (1971), 225-234.

3. N. Bellomo, A. Bellouquid, Y. Tao, and M. Winkler, Toward a mathematical theory of Keller–Segel models of pattern formation in biological tissues. *Mathematical Methods in the Applied Sciences*, **25** (2015), 1663–1763.

4. K. Fujie, M. Winkler, and T. Yokota, Boundedness of solutions to parabolic-elliptic Keller-Segel systems with signal dependent sensitivity, *Mathematical Methods in the Applied Sciences*, **38(6)** (2015), 1212-1224.

ISBN NR. : 978-625-8795-33-2

5. T. Hillen, and K. Painter, A user's guide to PDE models for chemotaxis. *Journal of Theoretical Biology*, **58** (2009), 183–217.

6. D. Horstmann, From 1970 until present: the Keller–Segel model in chemotaxis. *Jahresber DMV*, **106** (2004), 51–69.

7. M. Isenbach, Chemotaxis, Imperial College Press, London, 2004.

8. Y. Ke , J. Li , and Y. Wang, Analysis of reaction-diffusion models with the taxis mechanism, Springer, Singapore, 2022.

9. H. I. Kurt and L. Bao, Analytical and numerical results for solutions in a mixed-type two-species chemotaxis-competition system: I. Global existence, *Nonlinear Analysis: Real World Applications*, **93,** (2027), 104677.

10. H. I, Kurt, L. Bao, Analytical and numerical results for solutions in a mixed-type two-species chemotaxis-competition system: II. Boundedness and persistence, *Journal of Computational and Applied Mathematics*, **488** (2026), 117822.

11. H. I. Kurt, Boundedness in a chemotaxis system with weak singular sensitivity and logistic kinetics in any dimensional setting, *Journal of Differential Equations*, **416(2)**, (2025), 1429-1461.

12. H. I. Kurt, Improvement of criteria for global boundedness in a minimal parabolic-elliptic chemotaxis system with singular sensitivity, *Applied Mathematics Letters*, **167** (2025), 109570.

13. H. I. Kurt, Large-time dynamics of solutions in a logistic chemotaxis system with weak singular sensitivity: Uniform boundedness, pointwise persistence, and stability, *Discrete and Continuous Dynamical Systems*, **52** (2026), 255-292.

14. H. I. Kurt and W. Shen, Finite-time blow-up prevention by logistic source in chemotaxis models with singular sensitivity in any dimensional setting, *SIAM Journal on Mathematical Analysis*, **53(1)** (2021), 973–1003.

15. H. I. Kurt and W. Shen, Chemotaxis models with singular sensitivity and logistic source: Boundedness, persistence, absorbing set, and entire solutions, *Nonlinear Analysis: Real World Applications*, **69** (2023), 103762-27.

16. H.I. Kurt, W. Shen, and S. Xue, Stability, bifurcation and spikes of stationary solutions in a chemotaxis system with singular sensitivity and logistic source, *Mathematical Models and Methods in Applied Sciences*, **34(09)**, (2024), 1649-1700.

17. H. I. Kurt and W. Shen, Two-species chemotaxis-competition system with singular sensitivity: Global existence, boundedness, and persistence, *Journal of Differential Equations* **355** (2023), 248-295.

18. M. Le, and H. I. Kurt, Persistence of positive classical solutions in a logistic chemotaxis system with weak singular sensitivity, *Discrete and Continuous Dynamical Systems - Series B*, **33** (2026), 188-199.

ISBN NR. : 978-625-8795-33-2

19. M. Winkler, Aggregation vs. global diffusive behavior in the higher-dimensional Keller-Segel model, *Journal of Differential Equations*,**248** (2010), 2889-2905.

20. M. Winkler, Blow-up in a higher-dimensional chemotaxis system despite logistic growth restriction, *Journal of Mathematical Analysis and Applications*, **384** (2011), 261-272.

ISBN NR. : 978-625-8795-33-2

LOCAL EXISTENCE OF A MULTI-SPECIES CHEMOTAXIS SYSTEM WITH MULTIPLE CHEMICALS AND LOGISTIC GROWTH

Doç. Dr. Halil İbrahim KURT
Karadeniz Teknik Üniversitesi
hkurt@ktu.edu.tr - 0000-0002-9549-6445

Doç. Dr. Tuncay KÖROGLU
Karadeniz Teknik Üniversitesi
tkor@ktu.edu.tr - 0000-0002-1341-1074

ABSTRACT

This paper investigates a multi-species, multi-chemical chemotaxis system incorporating both cross-diffusion and nonlinear interaction effects over a bounded domain. The study focuses on the local existence, uniqueness, and regularity of positive classical solutions. Utilizing the Banach fixed-point theorem and parabolic regularity theory, it is established that the system possesses a unique classical solution on a maximal existence interval. Furthermore, nonnegativity of the solutions is verified through the maximum principle.

Keywords: Chemotaxis, Cross-diffusion, Local existence, Regularity, Multi-species system, Parabolic-elliptic PDEs.

1. INTRODUCTION

Chemotaxis models, originally introduced by Keller and Segel, provide a fundamental framework for describing the directed motion of biological organisms in response to chemical gradients. These models have been widely used to explain various phenomena such as cell aggregation, immune response, tumor growth, and pattern formation. Classical Keller–Segel systems typically involve a single species interacting with a single chemical signal. However, many real-world biological systems consist of multiple interacting species responding to multiple chemical cues. Motivated by this, we study a multi-species, multi-chemical chemotaxis system incorporating both cross-diffusion and nonlinear interaction effects. The main goal is to investigate qualitative properties such as boundedness, stability, and long-time behavior of solutions.

In this paper, we consider a two-species, two-chemical cross-diffusive chemotaxis system defined over a bounded domain $\Omega \subset \mathbb{R}^n$ $(n \geq 1)$ with a smooth boundary $\partial\Omega$

$$\begin{cases} u_t = \Delta u - \chi_1 \nabla \cdot (u \nabla w) - \lambda_1 \nabla \cdot (u \nabla z) + f_1(u,v), & x \in \Omega,\ t > 0, \\ v_t = \Delta v - \chi_2 \nabla \cdot (v \nabla w) - \lambda_2 \nabla \cdot (v \nabla z) + f_2(u,v), & x \in \Omega,\ t > 0, \\ 0 = \Delta w - w + v, & x \in \Omega,\ t > 0, \\ 0 = \Delta z - z + u, & x \in \Omega,\ t > 0, \end{cases} \tag{1.1}$$

ISBN NR. : 978-625-8795-33-2

where the logistic growth functions are

$$\begin{cases} f_1(u,v) = u(a_1 - b_1 u - c_1 v), \\ f_2(u,v) = u(a_2 - b_2 u - c_2 v), \end{cases} \tag{1.2}$$

with $a_i, b_i, c_i > 0$ for $i = 1,2$ are positive numbers. Moreover, system (1.1) supplemented with homogeneous Neumann boundary conditions

$$\frac{\partial u}{\partial \nu} = \frac{\partial v}{\partial \nu} = \frac{\partial w}{\partial \nu} = \frac{\partial z}{\partial \nu} = 0, \quad x \in \partial\Omega,\ t > 0, \tag{1.3}$$

where ν denotes the outward unit normal vector on $\partial\Omega$. Here, initial functions satisfy the following conditions

$$\begin{cases} u(\cdot\,,0) = u_0(\cdot) \ \text{ with } \ u_0 \geq 0 \ \text{ and } \ u_0 \in C^0(\bar{\Omega}), \\ v(\cdot\,,0) = v_0(\cdot) \ \text{ with } \ v_0 \geq 0 \ \text{ and } \ v_0 \in C^0(\bar{\Omega}). \end{cases} \tag{1.4}$$

The aim of this paper is to investigate whether system (1.1) has a local solution or not for given initial data satisfying (1.3). The main result of this paper reads as follows.

Theorem 1. *For all given $u_0, v_0 \in C^0(\bar{\Omega})$ satisfying (1.4), there exists $T_{\max}(u_0, v_0) \in (0, \infty]$ such that system (1.1) possesses a unique positive classical solution, which is denoted by $(u(\cdot, t; u_0, v_0),\ v(\cdot, t; u_0, v_0),\ w(\cdot, t; u_0, v_0),\ z(\cdot, t; u_0, v_0))$, on the maximal existing interval $\big(0, T_{\max}(u_0, v_0)\big)$ with initial condition $(u(\cdot\,,0; u_0, v_0),\ v(\cdot\,,0; u_0, v_0)) = (u_0, v_0)$. Moreover, if $T_{\max}(u_0, v_0) < \infty$, then*

$$\limsup_{t \nearrow T_{\max}(u_0, v_0)} \big(\| u(\cdot, t) \|_{L^\infty(\Omega)} + \| v(\cdot, t) \|_{L^\infty(\Omega)} + \| z(\cdot, t) \|_{L^\infty(\Omega)} + \| w(\cdot, t) \|_{L^\infty(\Omega)} \big) = \infty. \tag{1.5}$$

The proof relies on the fixed-point argument of Banach in parabolic regularity theory. For further details, we refer the reader to and.

1.1. EXISTENCE OF MILD SOLUTION

In this step, we prove the existence of a unique mild solution $(u(x, t; u_0, v_0),\ v(x, t; u_0, v_0))$ of (1.1) with $u(x, 0; u_0, v_0) = u_0(x)$ and $v(x, 0; u_0, v_0) = v_0(x)$ on a maximal interval $\big(0, T_{\max}(u_0, v_0)\big)$, that is,

$$\begin{aligned} u(\cdot, t; u_0, v_0) = \ & e^{-t\Delta} u_0(\cdot) - \chi_1 \int_0^t e^{-t\Delta} \nabla \cdot \big(u(\cdot, \tau) \nabla w(\cdot, \tau) \big) d\tau \\ & - \lambda_1 \int_0^t e^{-t\Delta} \nabla \cdot \big(u(\cdot, \tau) \nabla z(\cdot, \tau) \big) d\tau \\ & + \int_0^t e^{-t\Delta} u(\cdot, \tau) \big(a_1 - b_1 u(\cdot, \tau) - c_1 v(\cdot, \tau) \big) d\tau, \end{aligned}$$

and

ISBN NR. : 978-625-8795-33-2

$$\begin{aligned} v(\cdot,t;u_0,v_0) = \quad & e^{-t\Delta}v_0(\cdot) - \chi_2\int_0^t e^{-t\Delta}\nabla\cdot\big(v(\cdot,\tau)\nabla w(\cdot,\tau)\big)d\tau \\ & -\lambda_2\int_0^t e^{-t\Delta}\nabla\cdot\big(v(\cdot,\tau)\nabla z(\cdot,\tau)\big)d\tau \\ & +\int_0^t e^{-t\Delta}\,v(\cdot,\tau)\big(a_2 - b_2(\cdot,\tau) - c_2u(\cdot,\tau)\big)d\tau, \end{aligned}$$

for $t \in [0, T_{\max}(u_0, v_0))$, where $w(\cdot,\tau,u_0,v_0)$ solves $(1.1)_3$ and $z(\cdot,\tau,u_0,v_0)$ solves $(1.1)_4$ for $\tau \in [0, T_{\max}(u_0, v_0))$. To do so, first, let $R > \| u_0(x) \|_{L^\infty(\bar{\Omega})} + \| v_0(x) \|_{L^\infty(\bar{\Omega})}$. For given $T > 0$, define the Banach space $\mathcal{X}_T := (C^0(\bar{\Omega}\times[0,T]))^2$ equipped with the norm

$$\| (u,v) \|_{\mathcal{X}_T} = \max_{0\le t\le T} \| u(x,t) \|_{L^\infty(\bar{\Omega})} + \max_{0\le t\le T} \| v(x,t) \|_{L^\infty(\bar{\Omega})}.$$

Set the closed subset

$$\mathcal{S}(T) = \big\{(u,v) \in \mathcal{X}_T : \| (u,v) \|_{\mathcal{X}_T} \le R \quad \text{for all } t \in [0,T]\big\},$$

and define the map

$$\mathcal{M}(u,v)(\cdot,t) \quad := \begin{pmatrix} e^{-t\Delta}u_0 + \int_0^t e^{-t\Delta}\,[-\chi_1\nabla\cdot(u\nabla w) - \lambda_1\nabla\cdot(u\nabla z) + a_1u - b_1u^2 - c_1uv]d\tau \\ \\ e^{-t\Delta}v_0 + \int_0^t e^{-t\Delta}\,[-\chi_2\nabla\cdot(v\nabla w) - \lambda_2\nabla\cdot(v\nabla z) + a_2v - b_2v^2 - c_2uv]d\tau \end{pmatrix}$$

It is not difficult to prove that $\mathcal{M}$ maps $\mathcal{S}(T)$ into itself and becomes a contraction on $\mathcal{S}(T)$ for sufficiently small $0 < T \ll 1$. To do so, $\mathcal{M}$ maps $\mathcal{S}$ is a contraction for $0 < T \ll 1$. To this end, for given $u, \tilde{u} \in \mathcal{S}$, we have

$$\begin{aligned} & \| (\mathcal{M}(u)(t,\cdot) - (\mathcal{M}(\tilde{u})(t,\cdot) \|_{C^0(\bar{\Omega})} \\ & \le \chi_1 C\int_s^t \| (I-\Delta)^\beta e^{-\Delta(t-\tau)}\nabla\cdot(u(\tau,\cdot)\nabla w(\tau,\cdot) - \tilde{u}(\tau,\cdot)\nabla w(\tau,\cdot)) \|_{L^p(\Omega)}\,d\tau \\ & \quad +\lambda_1 C\int_s^t \| (I-\Delta)^\beta e^{-\Delta(t-\tau)}\nabla\cdot(u(\tau,\cdot)\nabla z(\tau,\cdot) - \tilde{u}(\tau,\cdot)\nabla z(\tau,\cdot)) \|_{L^p(\Omega)}\,d\tau \\ & \quad +C\int_s^t \| (I-\Delta)^\beta e^{-A(t-\tau)}\big(u(\tau,\cdot) - \tilde{u}(\tau,\cdot)\big)[a_1 + b_1\big(u(\tau,\cdot) + \tilde{u}(\tau,\cdot)\big)] \|_{L^p(\Omega)}\,d\tau \\ & \le \chi_1 C_1\int_s^t (t-\tau)^{-\beta-\frac{1}{2}-\epsilon} \| u(\tau) - \tilde{u}(\tau) \|_{C^0(\Omega)}\cdot(\| u(\tau) \|_{C^0(\Omega)} + \| \tilde{u}(\tau) \|_{C^0(\Omega)})d\tau \\ & \quad +\lambda_1 C_2\int_s^t (t-\tau)^{-\beta} \| u(\tau) - \tilde{u}(\tau) \|_{C^0(\Omega)} \Big(a_1 + b_1\big(\| u(\tau) \|_{C^0(\Omega)} + \| \tilde{u}(\tau) \|_{C^0(\Omega)}\big)\Big)\,d\tau \\ & \le T_1^{\frac{1}{2}-\beta-\epsilon}(\chi_1C_1(R+R^2) + \lambda_1C_2|\Omega|^{1/p}(a_1 + 2b_1R)) \| u - \tilde{u} \|_{\mathcal{X}} \end{aligned}$$

for all $t \in [s, s+T_1]$. It then follows that $\mathcal{M}(\quad)$ is a uniform contraction on $\mathcal{S}(T_1)$ for any $T_1 > 0$ satisfying

ISBN NR. : 978-625-8795-33-2

$$T_1 < \left[\chi_1 C_1(R+R^2) + \lambda_1 C_2 |\Omega|^{1/p}(a_1 + 2b_1 R)\right]^{\frac{-1}{\frac{1}{2}-\beta-\epsilon}}.$$

Similarly we can find

$$\| (\mathcal{M}(u)(t,\cdot) - (\mathcal{M}(\tilde{u})(t,\cdot) \|_{C^0(\bar{\Omega})} \leq T_2^{\frac{1}{2}-\beta-\epsilon}(\chi_2 C_3(R+R^2) + \lambda_2 C_4 |\Omega|^{1/p}(a_2 + 2b_2 R)) \| u - \tilde{u} \|_{\chi}$$

for all $t \in [s, s+T_2]$. It then follows that $\mathcal{M}$ is a uniform contraction on $\mathcal{S}(T_2)$ for any $T_2 > 0$ satisfying

$$T_2 < \left[\chi_2 C_3(R+R^2) + \lambda_2 C_4 |\Omega|^{1/p}(a_2 + 2b_2 R)\right]^{\frac{-1}{\frac{1}{2}-\beta-\epsilon}}.$$

Letting $T := \min\{T_1, T_2\}$ yields that $\mathcal{M}$ is a contraction for $0 < T \ll 1$. Therefore, by the Banach fixed point theorem, $\mathcal{M}$ admits a unique fixed point $u \in \mathcal{S}(T)$. Then, defining $\big(u(\cdot,t;u_0,v_0), v(\cdot,t;u_0,v_0)\big) := \big(u(t)(\cdot), v(t)(\cdot)\big)$, we obtain a mild solution of (1.1) on $[0,T]$ with $u(\cdot,0;u_0,v_0) = u_0(\cdot)$ and $v(\cdot,0;u_0,v_0) = v_0(\cdot)$. Finally, by a standard continuation argument, this mild solution can be extended to a maximal interval $[0, T_{\max}(u_0,v_0))$. Moreover, if $T_{\max}(u_0,v_0) < \infty$, then the blow-up alternative (1.5) holds.

1.2. REGULARITY

In this step, we prove that

$$(u(\cdot,t), v(\cdot,t), w(\cdot,t), z(\cdot,t)) := (u(\cdot,t;u_0,v_0), v(\cdot,t;u_0,v_0), w(\cdot,t;u_0,v_0), z(\cdot,t;u_0,v_0))$$

is a classical solution of (1.1), where $\big(u(\cdot,t;u_0,v_0), v(\cdot,t;u_0,v_0)\big)$ is the mild solution of (1.1) obtained in Subsection 1 and $w(\cdot,t;u_0,v_0) = (I-\Delta)^{-1}v(\cdot,t)$ and $z(\cdot,t;u_0,v_0) = (I-\Delta)^{-1}u(\cdot,t)$. Fix $0 < s_1 < T < T_{\max}(u_0,v_0)$ and consider the problem

$$\begin{cases} \tilde{u}_t(x,t) = (\Delta - I)\tilde{u}(x,t) + F_1(x,t), & x \in \Omega, \quad t \in (s_1,T) \\ \tilde{v}_t(x,t) = (\Delta - I)\tilde{v}(x,t) + F_2(x,t), & x \in \Omega, \quad t \in (s_1,T) \\ \tilde{u}(x,t_1) = u(x,t_1), & x \in \Omega, \\ \tilde{v}(x,t_1) = v(x,t_1), & x \in \Omega, \\ \frac{d\tilde{u}}{d\nu} = \frac{d\tilde{v}}{d\nu} = 0, & x \in \partial\Omega, \end{cases} \tag{1.6}$$

where

$$\begin{aligned} F_1(x,t) \quad &= -\chi_1 \nabla \cdot (u(x,t)\nabla((I-\Delta)^{-1}v(\cdot,t))) - \lambda_1 \nabla \cdot (u(x,t)\nabla\big((I-\Delta)^{-1}u(\cdot,t)\big)) \\ &\quad + u(x,t)[a_1 - b_1 u(x,t) - c_1 v(x,t)], \end{aligned}$$

and

$$\begin{aligned} F_2(x,t) \quad &= -\chi_2 \nabla \cdot (v(x,t)\nabla((I-\Delta)^{-1}v(\cdot,t))) - \lambda_1 \nabla \cdot (v(x,t)\nabla\big((I-\Delta)^{-1}u(\cdot,t)\big)) \\ &\quad + u(x,t)[a_2 - b_2 u(x,t) - c_2 v(x,t)], \end{aligned}$$

ISBN NR. : 978-625-8795-33-2

It is not difficult to see that $F_i(t,x)$ for $i = 1,2$ are Hölder continuous in $t \in \left(0, T_{\max}(u_0, v_0)\right)$ with some exponent $\theta \in (0,1)$. Then by [3, Theorem 15.1, Corollary 15.3], system (1.6) has a unique classical solution $\tilde{u}, \tilde{v} \in C^{2,1}\left((s_1, T) \times \Omega\right) \cap C^0([s_1, T) \times \Omega)$ and

$$\tilde{u}(\cdot, t) = e^{-t\Delta} u(\cdot, s_1) - \chi_1 \int_{s_1}^{t} e^{-t\Delta} F_1(\cdot, \tau) d\tau$$

and

$$\tilde{v}(\cdot, t) = e^{-t\Delta} v(\cdot, s_1) - \chi_2 \int_{s_1}^{t} e^{-t\Delta} F_2(\cdot, \tau) d\tau$$

Thus $\tilde{u}(x,t) = u(x,t)$ and $\tilde{v}(x,t) = v(x,t)$ for $t \in [s_1, T)$ and $u, v \in C^{2,1}\left((s_1, T) \times \Omega\right) \cap C^0([s_1, T) \times \Omega)$. Letting $s_1 \to 0$ and $T \to T_{\max}(u_0, v_0)$, we have

$$u, v \in C^{2,1}\left((0, T_{\max}) \times \Omega\right) \cap C^0([0, T_{\max}) \times \Omega).$$

1.3. NONNEGATIVITY

In this step, we establish the nonnegativity of classical solutions. Since $\left(u(\cdot, t; u_0, v_0), v(\cdot, t; u_0, v_0)\right)$ is classical solution of (1.1), by maximum principle for parabolic equations, we have that (u, v) is nonnegative. Moreover, since (u, v) is nonnegative, maximum principle for elliptic equations yields that (w, z) is nonnegative.

1.4. UNIQUENESS

In this step, we prove the uniqueness of the solutions of (1.1). Assume that (u, v, w, z) and $(\bar{u}, \bar{v}, \bar{w}, \bar{z})$ are the solutions of (1.1) on the interval $(0, T)$ with $0 < T < T_{\max}(u_0, v_0)$. First, set

$$u^* = u - \bar{u}, \quad v^* = v - \bar{v}, \quad w^* = w - \bar{w}, \quad \text{and} \quad z^* = z - \bar{z},$$

then, (u^*, w^*) satisfies the following system:

$$\begin{cases} u_t^* = \Delta u^* - \chi_1 \nabla(u \nabla w - \bar{u} \nabla \bar{w}) - \lambda_1 \nabla(u \nabla z - \bar{u} \nabla \bar{z}) + u^*[a_1 - b_1(u + \bar{u}) - c_1 u^* v], & x \in \Omega, \\ v_t^* = \Delta v^* - \chi_2 \nabla(v \nabla w - \bar{v} \nabla \bar{w}) - \lambda_2 \nabla(v \nabla z - \bar{v} \nabla \bar{z}) + v^*[a_2 - b_2(v + \bar{v}) - c_2 v^* u], & x \in \Omega, \\ 0 = \Delta w^* + w^* - v^*, & x \in \Omega, \\ 0 = \Delta z^* + z^* - u^*, & x \in \Omega, \\ u^*(x, 0) = 0, & x \in \Omega, \\ v^*(x, 0) = 0, & x \in \Omega. \end{cases}$$

Multiplying the first, second, third, and fourth equations of the above system by u^*, v^*, w^*, and z^*, respectively, and integrating over Ω, along with straightforward simplifications, and using the boundedness of

$$u,\ \bar{u},\ v,\ \bar{v},\ w,\ \bar{w},\ z,\ \bar{z},\ \nabla w,\ \nabla \bar{w},\ \nabla z,\ \nabla \bar{z}$$

in $L^\infty(\Omega)$ on $(0, T)$ to obtain that

ISBN NR. : 978-625-8795-33-2

$$\frac{d}{dt}\left(\int_{\Omega} u^{*2} + \int_{\Omega} v^{*2}\right) \leq C(T^*)\left(\int_{\Omega} u^{*2} + \int_{\Omega} v^{*2}\right),$$

for any fixed $T^* \in (0, T)$. This shows that $u^* = 0$, $v^* = 0$, $w^* = 0$, and $z^* = 0$, which implies the uniqueness of solutions to system (1.1).

2. PROOF OF THE MAIN RESULT

Proof of Theorem1: In lights of the results obtained in subsections (1.1)-(1.4), we can conclude that $(u(\cdot, t; u_0, v_0),\ v(\cdot, t; u_0, v_0),\ w(\cdot, t; u_0, v_0),\ z(\cdot, t; u_0, v_0))$ is a unique positive classical solution of system (1.1) on $\left(0, T_{\max}(u_0, v_0)\right)$ with $u(\cdot\ ,0; u_0, v_0) = u_0(x)$ and $v(\cdot\ ,0; u_0, v_0) = v_0(x)$.

3. REFERENCES

1. E. F. Keller and L. A. Segel, Initiation of slime mold aggregation viewed as an instability, *Journal of Theoretical Biology*, **26** (1970), 399-415.

2. E. F. Keller and L. A. Segel, A model for chemotaxis, *Journal of Theoretical Biology*, **30** (1971), 225-234.

3. H. Amann, Existence and regularity for semilinear parabolic evolution equations, *Ann. Scuola Norm. Sup. Pisa Cl. Sci.* **11** (1984), no. 4, 593-676.

4. K. Fujie, M. Winkler, and T. Yokota, Boundedness of solutions to parabolic-elliptic Keller-Segel systems with signal dependent sensitivity, *Mathematical Methods in the Applied Sciences*, **38(6)** (2015), 1212-1224.

5. M. Isenbach, Chemotaxis, Imperial College Press, London, 2004.

6. T. B. Issa and W. Shen, Dynamics in chemotaxis models of parabolic-elliptic type on bounded domain with time and space dependent logistic sources, *SIAM J. Appl. Dyn. Syst.* **16** (2017), no. 2, 926-973.

7. Y. Ke , J. Li , and Y. Wang, Analysis of reaction-diffusion models with the taxis mechanism, Springer, Singapore, 2022.

8. H. I. Kurt and L. Bao, Analytical and numerical results for solutions in a mixed-type two-species chemotaxis-competition system: I. Global existence, *Nonlinear Analysis: Real World Applications*, **93,** (2027), 104677.

9. H. I, Kurt, L. Bao, Analytical and numerical results for solutions in a mixed-type two-species chemotaxis-competition system: II. Boundedness and persistence, *Journal of Computational and Applied Mathematics*, **488** (2026), 117822.

10. H. I. Kurt, Boundedness in a chemotaxis system with weak singular sensitivity and logistic kinetics in any dimensional setting, *Journal of Differential Equations*, **416(2)**, (2025), 1429-1461.

ISBN NR. : 978-625-8795-33-2

11. H. I. Kurt, Improvement of criteria for global boundedness in a minimal parabolic-elliptic chemotaxis system with singular sensitivity, *Applied Mathematics Letters*, **167** (2025), 109570.

12. H. I. Kurt, Large-time dynamics of solutions in a logistic chemotaxis system with weak singular sensitivity: Uniform boundedness, pointwise persistence, and stability, *Discrete and Continuous Dynamical Systems*, **52** (2026), 255-292.

13. H. I. Kurt and W. Shen, Finite-time blow-up prevention by logistic source in chemotaxis models with singular sensitivity in any dimensional setting, *SIAM Journal on Mathematical Analysis*, **53(1)** (2021), 973–1003.

14. H. I. Kurt and W. Shen, Chemotaxis models with singular sensitivity and logistic source: Boundedness, persistence, absorbing set, and entire solutions, *Nonlinear Analysis: Real World Applications*, **69** (2023), 103762-27.

15. H.I. Kurt, W. Shen, and S. Xue, Stability, bifurcation and spikes of stationary solutions in a chemotaxis system with singular sensitivity and logistic source, *Mathematical Models and Methods in Applied Sciences*, **34(09)**, (2024), 1649-1700.

16. H. I. Kurt and W. Shen, Two-species chemotaxis-competition system with singular sensitivity: Global existence, boundedness, and persistence, *Journal of Differential Equations* **355** (2023), 248-295.

17. M. Le, and H. I. Kurt, Persistence of positive classical solutions in a logistic chemotaxis system with weak singular sensitivity, *Discrete and Continuous Dynamical Systems - Series B*, **33** (2026), 188-199.

ISBN NR. : 978-625-8795-33-2

A MODİFİED EQUATIONS APPROACH TO PHASE AND AMPLITUDE ERROR ANALYSIS IN EXPLICIT TWO STEP METHODS

Mehmet Ali KARADAĞLI[1]
Master's Student, Department of Mathematics, Institute of Graduate Education,
Batman University, Batman, Türkiye
malikara86@gmail.com

Asst. Prof. Ahmet GÜZEL
Department of Accounting and Tax Applications, Vocational School of Social Sciences,
Batman University, Batman, Türkiye
ahmet.guzel@batman.edu.tr - 0000-0002-6514-9805

Abstract

Classical local truncation error metrics establish formal convergence but often fail to predict the long-term qualitative dynamics—such as artificial damping or phase shifting—inherent to numerical integrators. To address this limitation, this work leverages backward error analysis to rigorously characterize the phase (dispersion) and amplitude (dissipation) errors of explicit linear two-step methods. By applying these schemes to the standard harmonic test problem, $u'(t) = i\,\omega\,u(t)$, we construct the corresponding continuous modified differential equations. Through systematic Taylor series expansions and the algebraic elimination of higher-order time derivatives, we isolate the fundamental spectral errors. Our formulation explicitly demonstrates that even-order derivative terms in the modified equations map directly to numerical dissipation, whereas odd-order terms govern phase dispersion. To illustrate the predictive power of this framework, we contrast the Adams-Bashforth (AB2) and Leapfrog (explicit midpoint) schemes. The analysis reveals that AB2 suffers from unphysical amplitude growth and a phase lead, rendering it inherently unstable for purely oscillatory dynamics. In contrast, the Leapfrog method preserves amplitude exactly—exhibiting zero numerical dissipation—while introducing a characteristic phase lag. Ultimately, this methodology provides a robust diagnostic tool for evaluating and selecting multi-step integrators in domains such as wave propagation, orbital mechanics, and structural dynamics, where spectral fidelity over long integration times is paramount.

Keywords : Phase Error, Amplitude Error, Modified Equations

ISBN NR. : 978-625-8795-33-2

RİSK-AWARE REVERSE LOGİSTİCS NETWORK DESİGN FOR END-OF-LİFE PHOTOVOLTAİC PANELS İN CONFLİCT-AFFECTED REGİONS: A CASE STUDY OF IDLİB, SYRİA

Assistant Professor, Jamil Hallak
Hasan Kalyoncu University, Department of Industrial Engineering, Gaziantep, 27010, Türkiye,
jamil.hallak@hku.edu.tr - 0000-0001-5975-4075

Abstract

Expansion of rooftop photovoltaic systems and small-scale solar applications in Syria has created an emerging end-of-life management challenge, especially in conflict-affected regions where formal waste systems, technical inspection capacity, and recycling infrastructure remain limited. This study proposes a one-period reverse logistics network design model for end-of-life photovoltaic panels in Idlib, northwest Syria. The proposed network consists of source zones, collection centers, testing and refurbishment centers, recycling/pre-processing centers, and safe-disposal sites. Unlike conventional PV waste models that route panels directly to recycling, this study explicitly includes a testing and grading stage to distinguish between panels suitable for direct reuse, panels requiring refurbishment, and panels that must be recycled.

A mixed-integer linear programming formulation is developed to determine facility-opening decisions and material-flow allocations across the network. The model considers four planning objectives: minimizing total net cost, minimizing carbon emissions, minimizing operational risk, and minimizing environmental risk. These objectives are integrated using a non-preemptive weighted goal programming approach. Operational risk reflects accessibility, road reliability, security conditions, and continuity of operations, while environmental risk reflects proximity to population centers, camps, water resources, agricultural land, and sensitive disposal areas. Because official PV waste data are limited, the Idlib case is structured using scenario-based estimates for end-of-life panel quantities, panel weights, collection rates, facility capacities, and processing ratios.

The proposed framework provides a practical decision-support tool for planning circular PV waste systems in data-scarce and unstable environments. It also highlights the importance of integrating reuse, refurbishment, recycling, and safe disposal within one coordinated reverse logistics network.

Keywords : photovoltaic panels, reverse logistics, end-of-life management, goal programming, facility location, recycling, conflict-affected regions, Syria, Idlib.

ISBN NR. : 978-625-8795-33-2

YER ALTI MEKANLARINDA PEYZAJLA BÜTÜNLEŞİK TASARIM STRATEJİLERİ: KARŞILAŞTIMALI ÖRNEKLER ÜZERİNDEN BİR DEĞERLENDİRME

Esra SÖNMEZ

Ege Üniversitesi/Peyzaj Mimarlığı,

esrasonmezz2000@gmail.com - 0009-0009-9064-366X

Prof. Dr. Emine MALKOÇ TRUE

Ege Üniversitesi/Peyzaj Mimarlığı,

emine.malkoc@ege.edu.tr - 0000-0003-1235-1978

ÖZET

Hızlı kentleşme, artan nüfus yoğunluğu ve yüzey alanlarının giderek sınırlanması, yer altı mekânlarının ulaşım, kültür ve kamusal kullanım gibi farklı işlevlerle daha yaygın kullanılmasını beraberinde getirmiştir. Bununla birlikte doğal ışık yetersizliği, yön bulma güçlüğü, kapalılık hissi ve doğal çevreyle kurulan ilişkinin zayıflaması, kullanıcı deneyimini olumsuz etkileyen temel tasarım sorunları arasında yer almaktadır. Bu çalışma, yer altı mekânlarında uygulanan peyzajla bütünleşik tasarım stratejilerinin mekânsal okunabilirlik, kullanıcı deneyimi ve psikolojik konfor üzerindeki etkilerini değerlendirmeyi ve bu doğrultuda gelecekteki tasarım süreçlerine katkı sağlayacak bütüncül bir yaklaşım ortaya koymayı amaçlamaktadır.

Araştırma, nitel araştırma yöntemine dayalı olup literatür taraması ile birlikte Derinkuyu Yer Altı Şehri, Sancaklar Camii, Manisa Kurtuluş Müzesi, Lowline Projesi, Survival Condo Apartmanları, RÉSO Yer Altı Kent Sistemi örneklerinin karşılaştırmalı olarak incelenmesine dayanmaktadır. Seçilen örnekler; doğal ışık kullanımı, topografya ile bütünleşme, iç avlu sistemleri, bitkisel tasarım ve yönlendirme, kamusal dolaşım sürekliliği ve kullanıcı odaklı mekânsal çözümler açısından değerlendirilmiştir.

Araştırma bulguları, peyzajla bütünleşik tasarım stratejilerinin mekânsal okunabilirliği güçlendirdiğini, kullanıcı yönlenmesini kolaylaştırdığını, kapalılık algısını azaltarak psikolojik konforu desteklediğini ve kullanıcı deneyimini iyileştirdiğini göstermektedir.

Karşılaştırmalı analizler sonucunda doğal ışığın etkin kullanımı, topoğrafya ile bütünleşme, bitkisel tasarım sistemlerinin farklı örneklerde ortak başarı ölçütleri olarak öne çıktığı belirlenmiştir.

Sonuç olarak, peyzajın yer altı mekânlarında yalnızca estetik bir unsur olmadığı; mekânsal organizasyonu, kullanıcı deneyimini ve sürdürülebilirliği yönlendiren temel bir tasarım bileşeni olduğu ortaya konulmuştur. Bu doğrultuda çalışma, yer altı mekânlarının planlama ve tasarım süreçlerinde kullanılabilecek peyzaj odaklı bütünleşik tasarım stratejilerine ilişkin kavramsal bir değerlendirme ve uygulamaya yönelik bir çerçeve sunmaktadır.

ISBN NR. : 978-625-8795-33-2

Anahtar Kelimeler: Yer altı mekânları, peyzajla bütünleşik tasarımı, mekânsal okunabilirlik, kullanıcı deneyimi, tasarım stratejileri.

1. GİRİŞ

İnsanoğlunun yeraltı mekanları ile kurduğu ilişki, tarihin ilk dönemlerinden itibaren barınma, savunma, ibadet ve iklimsel koruma gibi temel yaşamsal ihtiyaçlara dayanmaktadır. Kapadokya'daki Derinkuyu gibi derin yeraltı kentlerinden kaya oyma yapılara ve katakomplara kadar uzanan bu tarihsel süreç, endüstri devrimiyle birlikte büyük bir işlevsel kırılma yaşamıştır (Carmody & Sterling, 1993). Modern dönemde yeraltı mekanları, madencilik faaliyetlerinin ötesine geçerek metro hatları, alt geçitler, sığınaklar ve teknik altyapı ağları gibi yoğun kentsel donatılara dönüşmüştür (Bobylev, 2009). Günümüzde ise kontrolsüz nüfus artışı, hızlı kentleşme, yüzeydeki nitelikli arazi kıtlığı ve küresel iklim krizi gibi çevresel faktörler; yeraltı mimarisini sadece teknik bir altyapı çözümü olmaktan çıkarıp, kentsel yaşam alanlarının sürdürülebilir ve efektif bir şekilde genişletilmesinde kritik bir planlama alternatifi haline getirmiştir (Durmisevic, 1999; Admiraal & Cornaro, 2018).

Bununla birlikte, yeraltı yapılarının kendine has morfolojik ve fiziksel koşulları, insan-mekan ilişkisi üzerinde derin psikolojik ve algısal bariyerler inşa etmektedir. Doğal ışık yetersizliği, temiz hava sirkülasyonunun sınırlı yapısı, dış dünya ile görsel/işitsel bağın tamamen kopması ve kapatılmışlık (klostrofobik) hissi; kullanıcıların mekansal algısını olumsuz yönde etkilemekte ve mekandaki psikolojik konfor düzeylerini minimuma indirmektedir (Evans et al., 1996; Soh et al., 2016). Bu durum, çağdaş yeraltı mekanlarında sadece strüktürel, statik ve mühendislik çözümlerinin yeterli olamayacağını; kullanıcı deneyimini, mekansal aidiyeti ve konforu iyileştirecek mimari ve peyzaj tabanlı tasarım stratejilerinin bütüncül bir yaklaşımla ele alınması gerektiğini açıkça göstermektedir (Kim et al., 2021).

Yeraltı mekanlarında peyzajla bütünleşik tasarım stratejileri, bu alanların yarattığı kasvetli, monoton ve izole edici etkiyi kırmak adına en güçlü tasarım enstrümanlarından biridir. Canlı bitki materyalinin, su ögelerinin, doğal ışık simülasyonlarının ve biyofilik tasarım kriterlerinin yeraltı mimarisine entegre edilmesi, mekanın peyzajla olan bağını yeniden kurarken duyusal çeşitliliği de maksimuma çıkarmaktadır (Kellert et al., 2008; Ryan et al., 2014). Biyofilik tasarım prensipleri doğrultusunda şekillendirilen peyzaj entegrasyonu, insanların doğaya olan evrimsel ve içgüdüsel bağlılığını (*biophilia*) tetikleyerek yeraltı ortamlarındaki stresi azaltmakta, yön bulma (*wayfinding*) becerilerini geliştirmekte ve mekanın estetik-işlevsel değerini kökten değiştirmektedir (Browning et al., 2014; Yin et al., 2020).

Bu gerekçeler doğrultusunda kurgulanan bu çalışma, *"Yeraltı Mekanlarında Peyzajla Bütünleşik Tasarım Stratejileri: Karşılaştırmalı Örnekler Üzerinden Bir Değerlendirme"* başlığı altında yürütülmüştür. Araştırmanın kapsamını; yeraltı yaşam, çalışma ve sirkülasyon alanlarında peyzaj ögelerinin kullanım tipolojileri, bu ögelerin insan-mekan ilişkisindeki rasyonel rolü, mekansal algı, kullanıcı deneyimi ve psikolojik konfor parametreleri üzerindeki doğrudan etkilerinin incelenmesi oluşturmaktadır. Bu bağlamda, dünyadan ve Türkiye'den seçilen başarılı yeraltı mimarisi ve peyzaj entegrasyonu örnekleri karşılaştırmalı bir

ISBN NR. : 978-625-8795-33-2

metodolojiyle analiz edilerek, gelecekte tasarlanacak yeraltı mekanları için sürdürülebilir, insan odaklı ve doğa ile bütünleşik tasarım kriterlerinin alt yapısının oluşturulması amaçlanmaktadır.

2. KAVRAMSAL ÇERÇEVE VE YER ALTI MEKANLARINA YÖNELİK KARŞILAŞTIRMALI ÖRNEK ANALİZLERİ

2.1. Yer Altı Mekânlarının Morfolojisi ve Kullanıcı Psikolojisi Üzerindeki Etkileri

Yer altı mekânı, üst sınırları doğal topografya veya yapay yüzey katmanlarıyla sınırlandırılmış, düşey doğrultuda yeryüzünün altında konumlanan yapısal hacimleri ifade etmektedir. Bu mekânların morfolojik yapısı; penceresizlik, doğal ışık yetersizliği, sınırlı hava sirkülasyonu ve dış dünya ile görsel/işitsel temasın tamamen kesilmesi gibi majör fiziksel sınırlılıklarla karakterize edilmektedir (Evans et al., 1996; Soh et al., 2016) (Görsel 1)

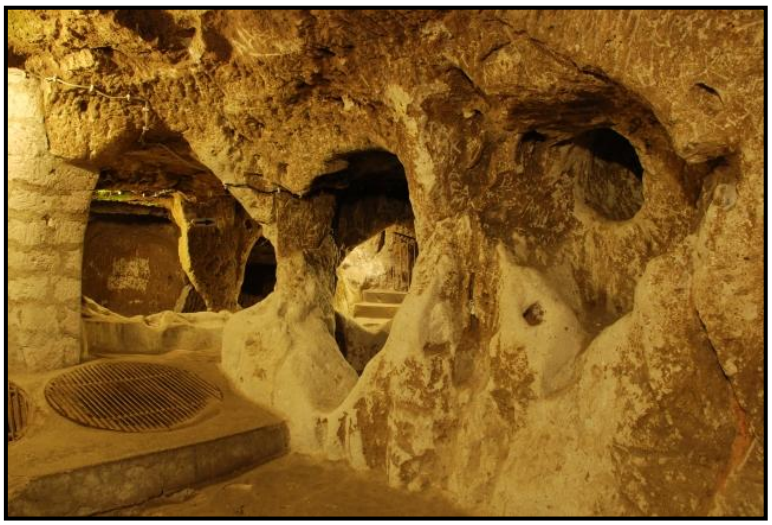

Görsel 1. Yer Altı Mekan Morfolojisi

Söz konusu morfolojik sınırlar, insan-mekân etkileşiminde derin algısal bariyerlerin oluşmasına zemin hazırlar. Doğal ışıktan yoksun yer altı ortamları, insan biyolojisindeki sirkadiyen ritmi (biyolojik saat) bozarak uyku düzensizliklerine ve kronik yorgunluğa neden olurken; kapalılık hissi, bireylerde klostrofobik reaksiyonları ve anksiyete seviyelerini tetiklemektedir (Soh et al., 2016). Ayrıca, gökyüzü, ufuk çizgisi ve referans kentsel nirengi noktalarının (landlines) bulunmayışı, kullanıcıların oryantasyon kaybı (yön bulma zorluğu) yaşamasına ve mekân içinde güvensizlik hissetmesine yol açmaktadır (Yin et al., 2020). Bu psikolojik bariyerler, yer altı yapılarında sadece mühendislik odaklı çözümlerin ötesine geçilerek, insan odaklı iç mekân konfor parametrelerinin tasarlanmasını zorunlu kılmaktadır (Kim et al., 2021).

2.2. Yer Altı Mekânlarının Tarihsel Gelişimi

İnsanoğlunun yer altı mekânlarıyla kurduğu ilişki, tarihin ilk dönemlerinden itibaren sığınma, barınma, savunma, ibadet ve iklimsel korunma gibi temel yaşamsal ihtiyaçlara dayanmaktadır. Doğal mağaraların kullanımından Kapadokya'daki Derinkuyu gibi karmaşık ve derin yer altı şehirlerine, kaya oyma yapılara ve katakomplara uzanan bu ilk tarihsel evrede yer altı, öncelikli olarak tehlikelerden korunma, gizlenme ve kutsal ritüelleri gerçekleştirme (tapınma) işlevi görmüştür. Ancak bu tarihsel süreç, Endüstri Devrimi ve sanayileşme ile birlikte büyük bir

ISBN NR. : 978-625-8795-33-2

işlevsel kırılma yaşamıştır (Carmody & Sterling, 1993). Sanayi çağında madencilik ve depolama faaliyetleriyle sınırlı kalan yer altı kullanımı, 20. yüzyıldan itibaren metro hatları, alt geçitler, sığınaklar ve teknik altyapı ağları gibi yoğun kentsel donatılara dönüşmüştür (Bobylev, 2009). Günümüzde ise kontrolsüz nüfus artışı, hızlı kentleşme, dikey ve yatay büyümenin sınırlarına ulaşarak yetersiz kalması, yüzeydeki nitelikli arazi kıtlığı ve küresel iklim krizi gibi etkenler; insanlığı yeniden yer altına dönmeye zorlamıştır (Görsel 2).

Görsel 2. Geçmişten Günümüze Yer Altı Mekanlarının İşlevsel Evrimi ve Kamusal Alana Dönüşüm Süreci

Bu süreçte yer altı mimarisi, sadece teknik bir altyapı çözümü olmaktan çıkarak kentsel yaşam alanlarının sürdürülebilir ve efektif bir şekilde genişletilmesinde kritik bir konut, kamusal alan ve ulaşım alternatifi haline gelmiştir (Durmisevic, 1999; Admiraal & Cornaro, 2018).

2.3. Yeraltı Mekânlarında Peyzaj ve Biyofilik Tasarım Entegrasyonu

Yeraltı mimarisinin yarattığı izole edici, klostrofobik ve monoton etkiyi hafifletmede peyzaj mimarlığı ve biyofilik tasarım parametreleri en etkili enstrümanlar olarak kabul edilmektedir (Kellert et al., 2008). Biyofilik tasarım, insanların doğaya olan evrimsel ve genetik bağlılığını yapılı çevre içerisinde canlandırmayı amaçlar (Browning et al., 2014). Canlı bitki materyalinin iç mekâna entegrasyonu, bitkilerin fizyolojik özellikleri sayesinde hava kalitesini artırırken, görsel olarak da monotonluğu kırmakta ve duyusal çeşitliliği en üst seviyeye çıkarmaktadır (Ryan et al., 2014). Su ögelerinin kullanımı, akustik konfor sağlama ve yeraltındaki boğucu sessizliği veya mekanik gürültüyü maskeleme işlevi görür. Doğal ışık simülasyonları ve ileri teknoloji gün ışığı yönlendirme sistemleri ise, kullanıcıların sirkadiyen ritimlerini destekleyerek psikolojik konfor hissini maksimuma ulaştırır (Kim et al., 2021). Bu peyzaj tabanlı stratejiler, yeraltı mekânlarını sadece bir geçiş alanı olmaktan çıkarıp, sosyal etkileşimin, duraklamanın ve mekânsal aidiyetin kurulduğu yüksek kaliteli kamusal alanlara dönüştürmektedir.

2.4. Karşılaştırmalı Örnek Analizleri

2.4.1. Türkiye’den Seçilen Örnekler

2.4.1.1. Derinkuyu Yeraltı Şehri

ISBN NR. : 978-625-8795-33-2

Nevşehir, Kapadokya bölgesinde yer alan Derinkuyu, antik dönem insanının yeraltı morfolojisini kullanma becerisinin en somut tarihsel referansıdır. Savunma (Görsel 3) ve uzun süreli barınma amacıyla tasarlanan bu yapıda mekânsal organizasyon; yaşam alanları (Görsel 4), ahırlar (Görsel 5), kiliseler (Görsel 6) ve şırahaneler (Görsel 7) gibi karmaşık bir hiyerarşiye sahiptir (Görsel 8).

Görsel 3. Derinkuyu Savunma Amaçlı Tığraz Taşı Görseli

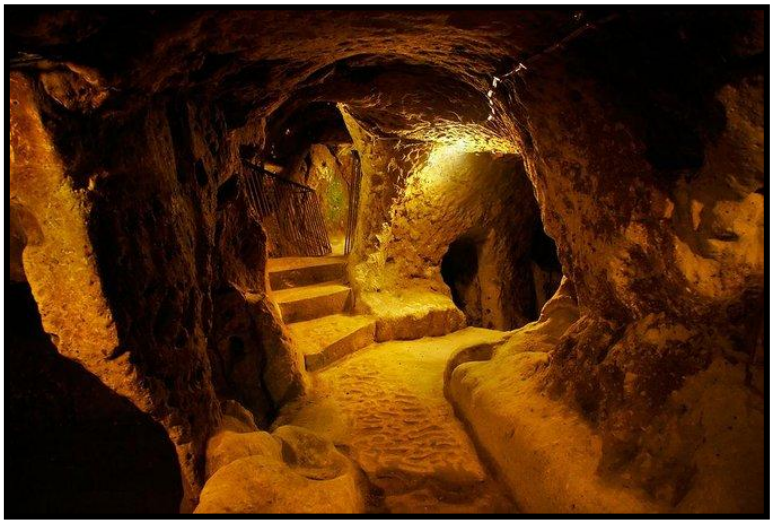

Görsel 4. Derinkuyu Yaşam Alanları Görseli

ISBN NR. : 978-625-8795-33-2

Görsel 5. Derinkuyu Ahır Görseli

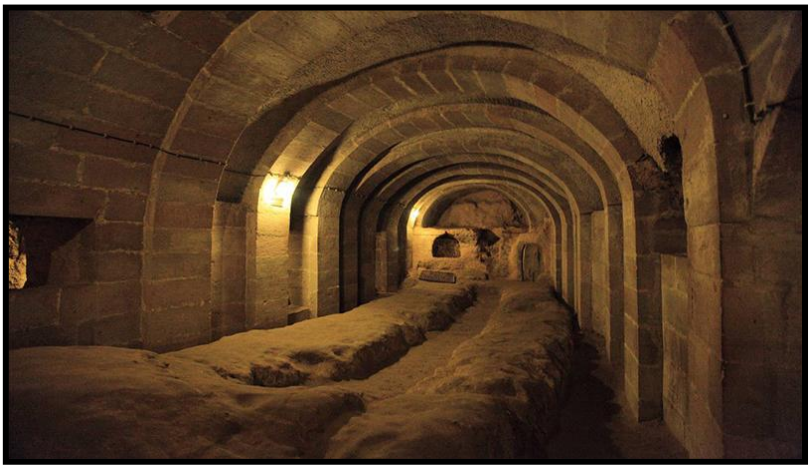

Görsel 6. Derinkuyu Kilise Görseli

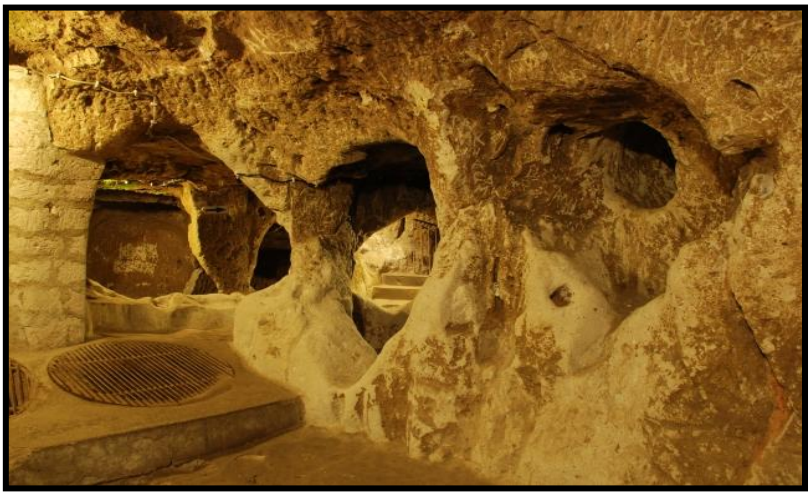

Görsel 7. Derinkuyu Şırahane Görseli

ISBN NR. : 978-625-8795-33-2

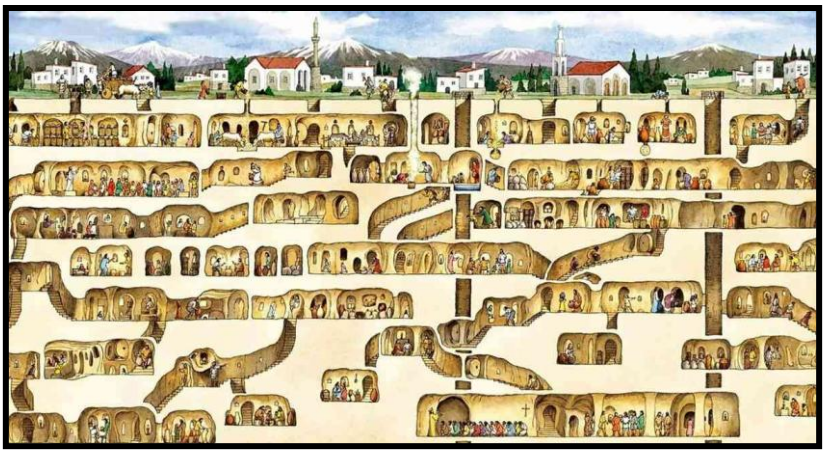

Görsel 8. Derinkuyu Hiyerarşik Düzen Görselleştirmesi

Yapının en güçlü tasarım enstrümanı, yüzeyden en alt katmana kadar kesintisiz inen, hem dikey sirkülasyonu hem de temiz hava akışını sağlayan derin havalandırma bacalarıdır (Görsel-9).

Görsel 9. Derinkuyu Havalandırma Bacaları

Doğal tüf kayanın iklimsel konfor (sabit sıcaklık) avantajı peyzaj-topoğrafya ilişkisinin ilksel rasyonel çözümü olarak değerlendirilmektedir (Görsel 10).

Görsel 10. Derinkuyu Tüf Kaya Malzeme Görünüş

2.4.1.2. Sancaklar Camii

ISBN NR. : 978-625-8795-33-2

Emre Arolat tarafından İstanbul'da tasarlanan Sancaklar Camii, modern mimaride yeraltı ve topoğrafya ilişkisinin manevi ve anıtsal bir sentezidir. Yapı, bir tepenin eğimine gömülerek yüzeyde neredeyse görünmez hale gelmiş ve peyzajın bir parçası olmuştur (Görsel 11, Görsel 12).

Görsel 11. Sancaklar Camii Topoğrafya İlişkisi

Görsel 12. Sancaklar Cami İç Mekan Gün Işığı Alınması

İç mekânda oluşturulan eğimli kıble duvarı boyunca sızan kontrollü doğal ışık huzmeleri (Görsel 13, Görsel 14), yeraltının kasvetli etkisini tamamen kırarak mistik ve dramatik bir atmosfer yaratmaktadır.

Görsel 13. Sancaklar Cami İç Mekan Gün Işığı Alınması

ISBN NR. : 978-625-8795-33-2

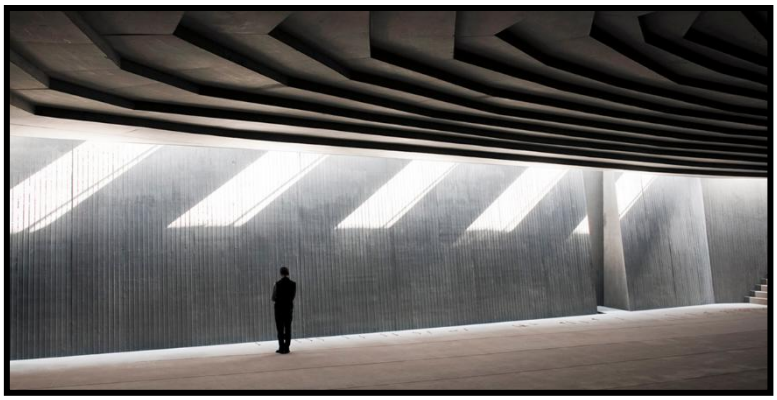

Görsel 14. Sancaklar Cami İç Mekan Gün Işığı Alınması

Yapay olanla doğal peyzaj (brüt beton ve doğal taşlar) arasındaki sınırların eridiği bu proje, yeraltında mekânsal aidiyetin ışık ve morfolojiyle nasıl kurulabileceğini kanıtlamaktadır (Görsel 15).

Görsel 15. Sancaklar Cami İç Mekan Gün Işığı Alınması

2.4.1.3. Manisa Kurtuluş Müzesi

Manisa'da yer alan Kurtuluş Müzesi, topoğrafya altına gizlenen anıtsal ve modern bir yeraltı sergileme mekânıdır (Görsel 16).

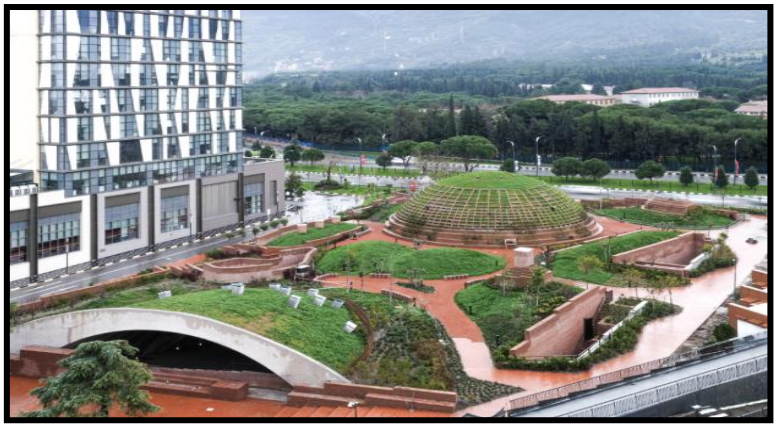

Görsel 16. Manisa Kurtuluş Müzesi Peyzaj Yüzeyi ile İlişkisi

ISBN NR. : 978-625-8795-33-2

Müze, kentsel parkın ve peyzaj yüzeyinin altına gömülerek hem kentsel yeşil dokunun sürekliliğini sağlamış hem de sergileme işlevinin gerektirdiği kontrollü iç mekân kriterlerini karşılamıştır (Görsel 17).

Görsel 17. Manisa Kurtuluş Müzesi Peyzaj Yüzeyi ile İlişkisi

Kullanıcı sirkülasyonu, rampalar ve yeraltı galerileri aracılığıyla tasarlanmış; mekândaki monotonluk, farklı kotlardaki hacimsel oyunlar ve kontrollü yırtıklardan alınan ışıkla minimize edilerek, çağdaş bir kullanıcı deneyimi kurgulanmıştır (Görsel 18, Görsel 19,Görsel 20).

Görsel 18. Manisa Kurtuluş Müzesi Kontrollü İç Mekana Gün Işığı Taşınması

ISBN NR. : 978-625-8795-33-2

Görsel 19. Manisa Kurtuluş Müzesi Kontrollü İç Mekana Gün Işığı Taşınması-2

Görsel 20. Manisa Kurtuluş Müzesi Kontrollü İç Mekana Gün Işığı Taşınması-3

2.4.2. Dünyadan Seçilen Örnekler

2.4.2.1. Lowline

ISBN NR. : 978-625-8795-33-2

New York Manhattan'da eski bir yeraltı troleybüs terminalinin (Görsel 21) kamusal parka dönüştürülmesi projesi olan Lowline, yeraltı peyzaj mimarisinin en teknolojik ve vizyoner örneğidir .

Görsel 21. Lowline Projesi Williamsburg Bridge Trolley Terminal

Projenin merkezinde, yüzeydeki güneş ışığını toplayıp fiber optik kablolar vasıtasıyla yeraltına aktaran "uzaktan gün ışığı yönlendirme sistemleri" (skylight teknolojisi) yer almaktadır (Görsel 22).

Görsel 22. Lowline Projesi SkyLight Teknolojisi

Bu ileri teknolojik ışık enstrümanı sayesinde yeraltında gerçek canlı bitkiler yetiştirilmiş (Görsel 23), ağaçlar dikilmiş. (Görsel 24)

ISBN NR. : 978-625-8795-33-2

Görsel 23. Lowline Projesi Yer Altı Bitki Yetiştirme Deneyim Alanı-2

Görsel 24. Lowline Projesi Yer Altı Deneyim Alanı-1

Duyusal çeşitliliğe sahip fütüristik bir yeraltı kamusal parkı/meydanı inşa edilerek izole edici atmosfer tamamen kırılmıştır (Görsel 25, Görsel 26)

Görsel 25. Lowline Projesi Futuristik Kamusal Alan

ISBN NR. : 978-625-8795-33-2

Görsel 26. Lowline Projesi Futuristik Kamusal Alan

2.4.2.2. Survival Condo Apartmanları

Kansas'ta eski bir füze silosunun lüks yeraltı sığınak apartmanlarına dönüştürülmesiyle oluşturulan Survival Condo projesi (Görsel 27), ekstrem yeraltı yaşamında psikolojik konfor yönetiminin radikal bir örneğidir.

)

Görsel 27. Survival Condo Apartmanları

Pencerelerin bulunmadığı bu derin strüktürde klostrofobik etkileri ve stresi önlemek adına pencereler yerine "LED ekranlı yapay manzara pencereleri" yerleştirilmiştir. Bu ekranlarda dış dünyadan canlı hava durumu, doğa manzaraları ve gün ışığı simülasyonları (Görsel 28) oynatılarak sirkadiyen ritim korunmaya çalışılmıştır.

ISBN NR. : 978-625-8795-33-2

Görsel 28. Survival Condo Apartmanları Led Ekranlı Yapay Manzara Pencereleri

Ayrıca yapay peyzaj alanları ve su ögeleriyle kullanıcıların psikolojik esenliği desteklenmiştir (Görsel 29).

Görsel 29. Survival Condo Apartmanları Su Öğesi Kullanımı

2.4.2.3. RÉSO

Kanada, Montreal'de yer alan RÉSO, kentsel ölçekte tasarlanmış dünyanın en büyük yeraltı sirkülasyon ve bağlantı ağıdır. Yaklaşık 32 kilometrelik bu devasa ağ; metroları, ticari alanları, otelleri ve üniversiteleri yer altından birbirine bağlamaktadır (Görsel 30, Görsel 31).

ISBN NR. : 978-625-8795-33-2

Görsel 30. RESO Yer Altı Şehri

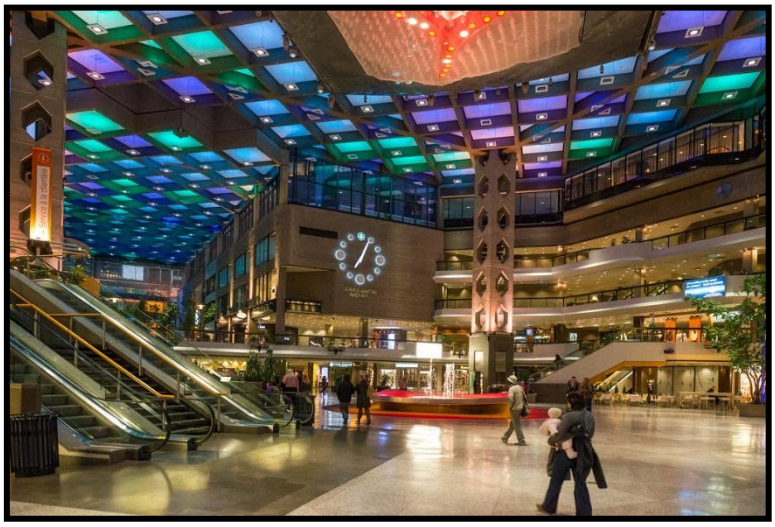

Görsel 31. RESO Yer Altı Şehri

Ağın tasarımı, iklimsel koruma (sert kış şartlarından korunma) sağlarken; devasa cam atriumlar, yeraltı meydanları, bitkilendirilmiş iç mekân cepleri ve su ögeleri aracılığıyla zenginleştirilmiştir (Görsel 32).

ISBN NR. : 978-625-8795-33-2

Görsel 32. RESO Yer Altı Şehri

Kamusal canlılığı ve sosyal etkileşimi yeraltına taşıyarak yön bulma becerisini güçlendiren devasa bir şehircilik başarısıdır.

3. SONUÇLAR VE KARŞILAŞTIRMALI DEĞERLENDİRME

Bu bölümde, çalışmanın kavramsal çerçevesinde tartışılan yeraltı mekânlarının morfolojik sorunları ile ikinci bölümde detaylandırılan Türkiye ve dünyadan 6 farklı vaka etüdünün bulguları çapraz sorgu yöntemiyle analiz edilmiştir. Yeraltı mekânlarında karşılaşılan temel sorunlar; doğal ışık yoksunluğu, penceresizlik, dış dünya ile vizüel bağın kopması, yetersiz mikroklimatik konfor ve oryantasyon kaybı olarak özetlenebilir (Soh et al., 2016; Yin et al., 2020). Seçilen örneklerin bu kronik sorunlara getirdiği peyzaj tabanlı ve biyofilik tasarım çözümleri, mekânsal kalite ve kullanıcı psikolojisi ekseninde rasyonel bir süzgeçten geçirilmiştir.

3.1. Mekânsal Kaliteye Etkiler ve Karşılaştırmalı Analiz

İncelenen 6 örneğin peyzaj enstrümanlarını, ışık yönetimi stratejilerini ve biyofilik tasarım kriterlerini kullanma düzeyleri ile bu enstrümanların mekânsal kaliteye katkıları radikal farklılıklar göstermektedir. Geleneksel ve tarihsel bir referans olan Derinkuyu Yeraltı Şehri, peyzajı mimariyle bütünleştirmek için tamamen doğal topoğrafya avantajını ve düşey havalandırma bacalarını kullanırken; Lowline gibi fütüristik bir çağdaş örnek, peyzaj materyalini yeraltında yaşatabilmek adına ileri teknoloji parabolik gün ışığı yönlendirme sistemlerinden faydalanmaktadır (Carmody & Sterling, 1993). Sancaklar Camii ise topoğrafya eğimine gömülerek brüt beton ve doğal taş kullanımıyla "doğanın bir uzantısı" olmayı başarmış, mekânsal kaliteyi kontrollü ışık sızıntılarıyla en üst düzeye çıkarmıştır.

Bu tasarım stratejilerinin rasyonel bir kıyaslamasını sunmak, mekânların teknolojik, doğal ve morfolojik karakterlerini okumak adına elzemdir. İlgili parametrelerin tasarımlardaki varlık ve başarı düzeyleri aşağıdaki matriste (Çizelge 1.) akademik olarak derecelendirilmiştir.

Çizelge 1. İncelenen Yer Altı Yapılarının Peyzaj Enstrümanları ve Biyofilik Tasarım Parametreleri Açısından Karşılaştırmalı Analiz Matrisi

ISBN NR. : 978-625-8795-33-2

İncelenen Örnekler	Canlı Bitki Kullanımı	Su Öğeleri Entegrasyonu	Işık/Simulasyon Yöntemi	Doğal Malzeme	Hava Sirkülasyonu	Yön Bulma
Derinkuyu	+	+	+	+++	+++	+++
Sancaklar Camii	+	+	+++	+++	++	++
Manisa Kurtuluş Müzesi	++	+	++	++	++	++
Lowline	+++	+	+++	++	++	++
Survival Condo	++	++	+++	+	+	+
RESO	++	++	++	++	++	+++

3.2. Kullanıcı Psikolojisi ve Deneyimi Üzerindeki Etkiler

Yeraltı mekânlarında uygulanan peyzaj tabanlı tasarım enstrümanlarının en radikal çıktısı, kullanıcı psikolojisi üzerindeki iyileştirici etkileridir (Kellert et al., 2008). Doğal ve simüle edilmiş peyzaj ögeleri; yeraltı morfolojisinin kaçınılmaz olarak inşa ettiği monotonluk, izole edilmişlik ve klostrofobik bariyerleri kırmada farklı başarı düzeyleri sergilemiştir:

- **Monotonluğun ve İzolasyonun Kırılması:** Lowline'da aktif olarak kullanılan canlı yeşil doku ve RÉSO'daki bitkilendirilmiş iç mekân cepleri ile su ögeleri, yeraltının kasvetli ve durağan atmosferini kırarak duyusal çeşitlilik yaratmaktadır (Ryan et al., 2014). Bu durum, kullanıcıların mekânı "güvenli ve yaşayan bir kamusal alan" olarak deneyimlemesini sağlamakta, izole edilmişlik hissini ortadan kaldırmaktadır.
- **Klostrofobik Bariyerlerin Aşılması ve Algısal Rahatlama:** Survival Condo örneğindeki LED ekranlı yapay manzara pencereleri ve gün ışığı simülasyonları, doğrudan sirkadiyen ritmi desteklemeye yöneliktir. Gerçek bir doğa dokusunun yerini tam olarak tutmasa da penceresiz mekânların yarattığı sıkışmışlık anksiyetesini yapay illüzyonlar yoluyla hafifletmekte ve kullanıcıların psikolojik konfor düzeyini taban seviyenin üzerine çıkarmaktadır (Kim et al., 2021). Sancaklar Camii'nde ise brüt beton yarıklarından sızan ışık, yeraltını klostrofobik bir sığınak hissinin ötesine taşıyarak anıtsal ve manevi bir korunağa, mekânsal aidiyete dönüştürmektedir.
- **Oryantasyon ve Stres Azaltma:** İnsanların doğaya olan evrimsel bağlılığını tetikleyen bu tasarımlar, yeraltı ortamının yarattığı stres seviyesini düşürmektedir (Browning et al., 2014). RÉSO gibi kentsel bağlantı tünellerinde peyzaj odaklı dikey atriumların ve meydanların konumlandırılması, kullanıcıların yön bulma becerilerini

ISBN NR. : 978-625-8795-33-2

doğrudan güçlendirerek mekân içi kaybolma korkusunu ve buna bağlı gelişen mekânsal güvensizlik hissini bertaraf etmektedir (Yin et al., 2020).

4. GENEL DEĞERLENDİRME VE SONUÇLAR

4.1. Küresel Krizler Çağında Sürdürülebilir Bir Planlama Alternatifi Olarak Yeraltı Mimari

Antroposen çağının beraberinde getirdiği kontrolsüz nüfus artışı, kentsel arazi kıtlığı, ekolojik deformasyon ve küresel iklim krizi, çağdaş şehircilik pratiklerini iki boyutlu yüzey planlamasının ötesine geçmeye zorlamaktadır (Admiraal & Cornaro, 2018). Bu çalışma kapsamında incelenen parametreler ve vaka etütleri neticesinde ortaya konmuştur ki; yeraltı mekânları artık sadece teknik altyapıların gizlendiği bir "makine dairesi" değil, geleceğin dirençli kentleri (*resilient cities*) için kaçınılmaz bir sürdürülebilir planlama alternatifidir (Bobylev, 2009). Yeraltı mimarisi, sahip olduğu jeolojik kütle etkisi sayesinde yüksek ısı izolasyonu sağlayarak kentsel ısı adası etkilerini hafifletmekte, aşırı hava olaylarına karşı korunaklı sığınaklar sunmakta ve en önemlisi, yüzeydeki nitelikli doğal/yeşil alanların yapılaşma baskısı altında yok olmasını engellemektedir (Durmisevic, 1999). Dolayısıyla, kentsel katmanlaşmanın dikeyde yeraltına doğru rasyonel bir şekilde genişletilmesi, ekolojik dengenin korunması ve kentsel makroformun sürdürülebilirliği açısından stratejik bir vizyondur.

4.2. Geleceğin Çağdaş Yeraltı Projeleri İçin Disiplinler Arası Biyofilik Tasarım Rehberi

Yeraltı mekânlarının sunduğu bu makro ölçekli çevresel ve mekânsal avantajların performansa dönüşebilmesi, bu alanların insansızlaştırılmış hacimler olmaktan çıkarılarak "yaşanabilir" kılınmasıyla doğrudan ilişkilidir. Yeraltı morfolojisinin doğasında var olan penceresizlik, doğal ışık eksikliği ve dış dünyadan soyutlanma gibi algısal bariyerler; kullanıcılar üzerinde klostrofobi, oryantasyon kaybı ve kronik stres gibi derin psikolojik yaralar açma potansiyeline sahiptir (Soh et al., 2016; Yin et al., 2020). Bu bağlamda araştırma bulguları, çağdaş yeraltı tasarımlarında geleneksel mühendislik/statik çözümlerinin tek başına yeterli olamayacağını; mimarlık ve peyzaj mimarlığı disiplinlerinin bütüncül bir sinerji içinde çalışması gerektiğini açıkça ortaya koymaktadır (Kim et al., 2021).

Gelecekte inşa edilecek insan odaklı çağdaş yeraltı projeleri için bu disiplinler arası ortaklığın temel alması gereken biyofilik tasarım kriterleri şu şekilde özetlenebilir:

- **Teknolojik Işık ve Sirkadiyen Yönetimi:** Yeraltı mekânlarında sirkadiyen ritmin korunması amacıyla, Lowline örneğinde olduğu gibi fiber optik ve parabolik çanak sistemleriyle gerçek gün ışığının derin katmanlara taşınması veya Survival Condo modelindeki gibi dinamik LED teknolojileriyle yapay gün doğumu/batımı simülasyonlarının kurgulanması (Kim et al., 2021).
- **Canlı Bitki ve Mikroklima Entegrasyonu:** Hava kalitesini artırıcı, uçucu organik bileşikleri filtreleyici ve mekândaki görsel monotonluğu kırıcı canlı dikey bahçe ve bitki ceplerinin, teknolojik aydınlatma altyapılarıyla desteklenerek iç mekâna entegre edilmesi (Kellert et al., 2008; Ryan et al., 2014).

ISBN NR. : 978-625-8795-33-2

- **Akustik Maskeleme ve Duyusal Çeşitlilik:** Yeraltındaki mekanik sistemlerin ve tünel uğultularının yarattığı akustik kirliliği veya boğucu sessizliği kırmak adına, su ögelerinin (duvar şelaleleri, fıskiyeler vb.) birincil tasarım enstrümanı olarak kullanılması ve duyusal çeşitliliğin artırılması (Browning et al., 2014).
- **Hiyerarşik Mekân Kurgusu ve Yön Bulma:** Montreal RÉSO örneğinde başarıyla uygulandığı gibi, yüzeyle bağı kesintisiz kuran devasa cam atriumların, düşey yırtıkların ve topoğrafik rampaların kullanımıyla oryantasyon kaybının önlenmesi ve mekânsal aidiyetin güçlendirilmesi (Yin et al., 2020).
- **Malzeme Doğallığı ve Doku:** Sancaklar Camii örneğinde görüldüğü üzere, brüt beton, doğal taş, ahşap gibi dokunsal hissi yüksek malzemelerin ham halleriyle kullanılarak insanın doğaya olan evrimsel bağlılığının içgüdüsel olarak tetiklenmesi (Browning et al., 2014). (Çizelge-2)

Çizelge 2. Geleceğin Çağdaş Yeraltı Mekânı Projeleri İçin Biyofilik Tasarım ve Uygulama Rehberi Kontrol Listesi.

Biyofilik Rehber Parametresi	Mekânsal/Fizyolojik Hedef	Önerilen Mimari / Peyzaj Enstrümanı	Literatürdeki Başarılı Referansı
1. Teknolojik Işık ve Sirkadiyen	Sirkadiyen ritmin korunması, anksiyete ve stres yönetimi.	Parabolik çanaklar, fiber optik kablolar, dinamik LED manzara ekranları.	Lowline Survival Condo
2. Canlı Bitki & Mikroklima	Hava kalitesi filtrasyonu, görsel monotonluğun kırılması.	Teknolojik aydınlatma destekli dikey bahçeler, iç mekân bitki cepleri.	Lowline
3. Akustik Maskeleme	Mekanik uğultuların ve boğucu sessizliğin absorbe edilmesi.	Duvar şelaleleri, fıskiyeler, hareketli su yüzeyleri.	RÉSO
4. Hiyerarşik Mekân Kurgusu	Oryantasyon kaybının önlenmesi, yön bulma.	Devasa cam atriumlar, düşey mimari yırtıklar, topoğrafik rampalar.	RÉSO
5. Malzeme Doğallığı & Doku	Doğaya olan evrimsel bağlılığın tetiklenmesi.	Brüt beton, doğal taş, ham ahşap gibi yüksek dokunsal yüzeyler.	Sancaklar Camii

ISBN NR. : 978-625-8795-33-2

Sonuç olarak bu çalışma; yeraltı yaşam mekânlarında peyzajla bütünleşik tasarım stratejilerinin estetik bir dekorasyon unsuru olmanın çok ötesinde, insan psikolojisini iyileştiren, mekânsal algı bariyerlerini yıkan ve yaşam kalitesini doğrudan üreten rasyonel birer yapı taşı olduğunu kanıtlamıştır (Kellert et al., 2008; Admiraal & Cornaro, 2018). Geleceğin yer altı şehircilik vizyonu, ancak karanlık ve mekanik altyapı tünellerinin peyzaj mimarlığının yaşayan enstrümanları ve biyofilik parametrelerle harmanlanması sayesinde karanlıktan aydınlığa evrilecektir. Bu çalışma, gelecekteki tasarımcılara ve planlamacılara rehberlik edecek rasyonel bir alt yapı sunmayı amaçlamaktadır.

KAYNAKÇA

1. Prudance, M.R., *Pottery Analysis*, The University of Chicago Press/Chicago and London, 1987.

2. Admiraal, H. ve Cornaro, A., *Underground Spaces Unveiled: Planning and Creating the Cities of the Future*, ICE Publishing, London, 2018.

3. Bobylev, N., Underground Space as an Urban Indicator: Measuring Use of Subsurface, *Tunnelling and Underground Space Technology*, 24(3), 302–306, 2009.

4. Browning, W. D., Ryan, C. O. ve Clancy, J. O., *14 Patterns of Biophilic Design: Improving Health & Well-Being in the Built Environment*, Terrapin Bright Green LLC, New York, 2014.

5. Carmody, J. C. ve Sterling, R. L., *Underground Space Design: A Guide to Subsurface Utilization and Design for People in Underground Spaces*, Van Nostrand Reinhold, New York, 1993.

6. Durmisevic, E., *The Future of Underground Space*, Delft University of Technology, Delft, 1999.

7. Evans, G. W., Lepore, S. J. ve Schroeder, A., The Role of Interior Design Elements in Human Responses to Crowding, *Journal of Personality and Social Psychology*, 70(1), 41–46, 1996.

8. Kellert, S. R., Heerwagen, J. H. ve Mador, M. L. (Ed.), *Biophilic Design: The Theory, Science and Practice of Bringing Buildings to Life*, John Wiley & Sons, Hoboken, New Jersey, 2008.

9. Kim, J., Lee, H. ve Kim, T., Human-Centered Design Strategies for Underground Spaces: A Review, *Sustainability*, 13, 2021.

10. Ryan, C. O., Browning, W. D., Clancy, J. O., Andrews, S. L. ve Kallianpurkar, N. B., Biophilic Design Patterns: Emerging Nature-Based Parameters for Health and Well-Being in the Built Environment, *International Journal of Architectural Research (Archnet-IJAR)*, 8(2), 62–76, 2014.

ISBN NR. : 978-625-8795-33-2

11. Soh, C. K., Varghese, K. ve Singh, Y., Psychological Impacts of Underground Spaces on Users: A Review, *Tunnelling and Underground Space Technology*, 55, 2016.

12. Yin, J., Zhu, S., MacNaughton, P., Allen, J. G. ve Spengler, J. D., Physiological and Cognitive Performance of Occupants in Biophilic Indoor Environments, *Building and Environment*, 2020.

13. Görsel 1 Kaynakça: https://listelist.com/

14. Görsel 2 Kaynakça: Yapay Zeka Görselleştirme Aracı Google Gemini Banana

15. Görsel 3 Kaynakça: : https://listelist.com/

16. Görsel 4 Kaynakça: https://listelist.com/

17. Görsel 5 Kaynakça: https://listelist.com/

18. Görsel 6 Kaynakça: https://listelist.com/

19. Görsel 7 Kaynakça: https://listelist.com/

20. Görsel 8 Kaynakça: https://www.arkeolojisanat.com/

21. Görsel 9 Kaynakça: https://listelist.com/

21. Görsel 10 Kaynakça: https://listelist.com/

22. Görsel 11 Kaynakça: https://www.arkitektuel.com/

23. Görsel 12 Kaynakça: https://www.arkitektuel.com/

24. Görsel 13 Kaynakça: https://www.arkitektuel.com/

24. Görsel 14 Kaynakça: https://www.arkitektuel.com/

24. Görsel 15 Kaynakça: https://www.arkitektuel.com/

25. Görsel 16 Kaynakça: https://yalin-mimarlik.com/

26. Görsel 17 Kaynakça: https://yalin-mimarlik.com/

27. Görsel 18 Kaynakça: https://yalin-mimarlik.com/

28. Görsel 19 Kaynakça: https://yalin-mimarlik.com/

29. Görsel 20 Kaynakça: https://yalin-mimarlik.com/

30. Görsel 21 Kaynakça: https://www.archpaper.com/

31. Görsel 22 Kaynakça: https://www.archpaper.com/

32. Görsel 23 Kaynakça: https://www.archpaper.com/

33. Görsel 24 Kaynakça: https://www.archpaper.com/

34. Görsel 25 Kaynakça: https://www.archpaper.com/

35. Görsel 26 Kaynakça: https://www.archpaper.com/

36. Görsel 27 Kaynakça: https://survivalcondo.com/

37. Görsel 28 Kaynakça: https://survivalcondo.com/

ISBN NR. : 978-625-8795-33-2

38. Görsel 29 Kaynakça: https://survivalcondo.com/

39. Görsel 30 Kaynakça: https://www.google.com/

40. Görsel 31 Kaynakça: https://www.google.com/

41. Görsel 32 Kaynakça: https://www.google.com/

ISBN NR. : 978-625-8795-33-2

LOCAL IMAGERY AND EXPERIENTIAL DESIGN IN THE REGENERATION OF MEMORY SPACES

Landscape Architect İzel KARABAĞ

Department of Landscape Architecture, Graduate School of Natural and Applied Sciences,

Ege University, izel.karabagg0@gmail.com - ORCID: 0009-0006-3319-7315

Assoc. Prof. Dr. Hatice SÖNMEZ TÜREL

Department of Landscape Architecture, Faculty of Agriculture, Ege University,

hatice.sonmez@ege.edu.tr - ORCID: 0000-0002-2346-5615

ABSTRACT

Memory spaces are more than places that preserve the physical traces of the past; they are multilayered public landscapes where collective memory, cultural identity, and a sense of belonging are continuously reproduced. However, rapid urbanization, globalization, and spatial transformation processes have weakened the historical continuity and local identity of these places. This study aims to examine the role of local imagery and experiential design approaches in the regeneration of memory spaces and to evaluate different intervention strategies within a comparative framework. The research employed a qualitative comparative case study approach. Hiroshima Peace Memorial Park, Landschaftspark Duisburg-Nord: Piazza Metallica, The High Line Park, the Historic Centre of Warsaw, the Mamayev Kurgan Memorial Complex and The Motherland Calls monument, and the National September 11 Memorial were examined according to the criteria of historical context and authenticity, architectural and symbolic expression, visitor experience and interaction, spatial orientation and perception, and collective memory function. The findings indicate that there is no single conservation or design approach for the regeneration of memory spaces; rather, intervention strategies vary according to the historical, cultural, political, and social context of each site. Drawing on the literature, six memory-space regeneration strategies were applied to the examined cases: non-intervention, enhancement through additions, reconstruction, contextual design, commemoration and monumentalization, and evoking absence. These strategies were found not only to preserve traces of the past but also to make local imagery visible, strengthen embodied and sensory experience, and contribute to the reproduction of collective memory within contemporary public life. In the final stage of the study, these strategies were associated with various examples from Türkiye, and the transferability of the proposed framework across different geographical and cultural contexts was discussed. The results suggest that this framework may offer a flexible approach for interpreting historical, industrial, monumental, and traumatic memory spaces in Türkiye. Accordingly, memory spaces are regarded not merely as historical sites to be preserved but as dynamic urban landscapes that can be reintegrated into contemporary public life through local imagery, embodied experience, spatial perception, and collective memory.

ISBN NR. : 978-625-8795-33-2

Keywords: Memory space, local imagery, experiential design, urban identity, regeneration

1. INTRODUCTION

Cities are not merely spatial organizations in which physical structures, transportation networks, and open space systems are brought together. They are also multilayered spaces of memory that embody societies' relationships with the past, cultural identities, shared values, and a sense of belonging. According to Halbwachs, who emphasizes that collective memory is shaped within social frameworks rather than independently of individual recollections, memory is anchored in spatial references and attains continuity through them (Ak, 2018; Halbwachs, 1992). Nora's concept of *lieux de mémoire* (sites of memory) likewise demonstrates that places carrying a society's shared past are not merely physical locations but multilayered constructs that generate symbolic, functional, and cultural meanings (Acun, 2021; Nora, 2006). In this context, urban space can be understood not merely as a setting in which the past is represented, but as a dynamic narrative environment where the past is continuously reproduced through users' experiences and integrated into contemporary life.

Modernization, rapid urbanization, globalization, and urban transformation processes reshape not only the physical structure of cities but also their layers of memory. In particular, places characterized by historical, industrial, traumatic, or monumental significance face the risk of losing their distinctive identities and social meanings due to abandonment, functional obsolescence, demolition, redevelopment, and the pressures of homogenization.

The continuity of urban identity is of critical importance in terms of individuals' sense of belonging to place; the loss of local traces weakens urban residents' spatial attachment and their sense of collective memory (Aytaç, 2013). Similarly, Günaçan and Erdoğan (2018) emphasize that urban memory can be sustained through traces, images, and symbols embodied in urban spaces.

The reclamation of memory spaces is not limited to preserving the past or conserving physical remains. Rather, this process requires reconnecting historical traces with contemporary public life, making local images visible, and enabling users to establish physical, sensory, and emotional relationships with place. While Lynch's (1960) theory of the urban image demonstrates that cities are mentally perceived through paths, edges, districts, nodes, and landmarks, Downing (2003) emphasizes the significance of memory images for local identity and spatial experience. Therefore, within memory spaces, local images are not merely visual symbols; they are fundamental design tools that enable users to interpret, remember, and establish meaningful connections with place.

The experiential design approach provides an important framework for the reclamation of memory spaces by placing user experience at its center. Pallasmaa (2011) argues that space is experienced not only through vision but also through the integrated perception of the body, movement, touch, hearing, and the senses as a whole. Similarly, Jelić (2015) and Uysal (2017) demonstrate that spatial experience is deepened through embodied perception and sensory engagement. From this perspective, experiential design in memory spaces enables traces of the past to be conveyed to visitors not merely as information but as lived experiences through

ISBN NR. : 978-625-8795-33-2

elements such as walking, orientation, pausing, looking, touching, silence, void, sound, and materiality.

This study aims to examine the role of local images and experiential design approaches in the reclamation of memory spaces. The study comparatively analyzes six selected international case studies representing different types of memory and diverse design strategies. Hiroshima Peace Memorial Park, Landschaftspark Duisburg-Nord – Piazza Metallica, The High Line, the Historic Centre of Warsaw, the Mamayev Kurgan Memorial Complex and The Motherland Calls monument, and the National September 11 Memorial were evaluated in terms of their historical contexts, symbolic narratives, visitor experiences, spatial orientations, and functions in sustaining collective memory. The study focuses on the question of how memory spaces can be reconnected with contemporary public life while preserving their historical traces and distinctive identities. Accordingly, the study examines strategies of non-intervention, enhancement through additions, reconstruction, contextual design, commemoration and monumentalization, and evoking absence as approaches to the reclamation of memory spaces. Furthermore, this strategic framework, developed through selected international case studies, is evaluated in relation to various memory spaces in Türkiye. Thus, the study aims to demonstrate that memory spaces are not merely objects of heritage conservation associated with the past, but can be understood as dynamic urban landscapes that can be reintegrated into everyday public life through local images, embodied experience, spatial perception, and collective memory.

2. CONCEPTUAL AND THEORETICAL FRAMEWORK

2.1. Memory Space and Collective Memory

Memory is not a passive repository of the past but, as Ernst Cassirer argues, a dynamic capacity for recognizing and conceptualizing the past in accordance with the needs of the present (Cassirer, 1980). Memory is a collective phenomenon that exists in continuous interaction with society, space, and time. In the social context, memory constitutes one of the most important means of constructing group identity and enabling the embodiment of shared cultural identity within places. Başaran İnce (2010) classifies this complex phenomenon, which permeates every aspect of human life, into five main categories: collective memory, social memory, popular memory, cultural memory, and societal memory. In this context, collective memory is defined as the form of memory that emerges from the accumulation of diverse traces left by an event jointly experienced by a society, a community, or a group of individuals. Social memory, on the other hand, refers to the type of memory encompassing cognitive processes such as processing, encoding, storing, and retrieving information involved in social interaction. The form of memory that interprets the past as a political phenomenon through the lens of contemporary trends and elements such as cinema and folklore is referred to as popular memory, whereas the indirect transmission of shared memories through communication or textualization is characterized as cultural memory. Finally, societal memory represents the broadest form of memory, influencing both the everyday life of society and the ways in which the past is perceived (Başaran İnce, 2010).

ISBN NR. : 978-625-8795-33-2

Collective memory (societal memory) is defined as the totality of the traces left in memory by events jointly experienced by a group of individuals or a community (Günaçan & Erdoğan, 2018). According to Maurice Halbwachs, the pioneer of collective memory theory, even memories that appear to be individual are shaped by social frameworks and collective dynamics. Individuals make sense of what they perceive and experience only through interaction with the society in which they live; therefore, although memory may appear to belong to the individual, it is fundamentally constructed through social processes (Ak, 2018; Acun, 2021). For collective memory to endure, become visible, and be transmitted across generations, it requires spatialization rather than merely a mental process of transmission. Halbwachs emphasizes that all forms of collective memory require space and possess an inherent tendency toward spatialization (Ak, 2018; Sevinç, 2019). While places physically preserve memories, memory itself gives meaning to these places, carrying the past into the present. Without the physical environment preserving the traces of the past, memories would have no anchor, and the past would fade away. Thus, memory is not an abstract narrative but a tangible experience rooted in the physical world.

This spatial manifestation of collective memory finds its expression in sites of memory (lieux de mémoire), as conceptualized by Nora (2006). Sites of memory are not merely physical places; they are multilayered constructs that shape a society's past and collective memory. According to Nora, these places are not simply settings that represent remembered events but are spaces where memory itself is produced and made visible. In addition to serving as a means of generating and structuring a society's collective memory, sites of memory also function as archives that preserve the past against systematic processes of forgetting, thereby carrying its traces into the present (Acun, 2021).

In conclusion, memory spaces are multilayered spatial constructs in which collective memory is embodied and a sense of social belonging is produced through their physical, symbolic, and functional dimensions. By sharing these common spaces, members of society come to understand their shared past, develop a collective sense of "we" beyond individual belonging, and reconstruct their sense of belonging through these spaces by means of intergenerational knowledge transfer (Ak, 2018).

2.2. Spirit of Place, Identity, and Sense of Belonging

Space is more than a shelter defined by physical boundaries; it is an existential ground where social relationships, everyday practices, and identity are produced. Space is not merely a visual entity but a living organism in which social identity, memories, and a sense of belonging are continuously created. The integration of individuals' embodied perceptions, actions, and cognitive processes with space transforms it from a simple physical environment into a lived and meaningful realm of memory (Aytaç, 2013; Pallasmaa, 2011). The transformation of an ordinary physical environment into a place endowed with a spirit of place (genius loci) is closely associated with the strong emotional bonds that individuals establish with that environment.

The emotional bond that individuals establish with the physical environment in which they live is defined as place attachment. By giving meaning to these ordinary settings that embody lived

ISBN NR. : 978-625-8795-33-2

experiences, memory fosters a strong sense of place attachment. In this process, places become more than physical meeting points where people simply gather; they evolve into spaces of belonging where a shared culture of living is cultivated, individuals develop a sense of belonging to the city, and identity is continuously constructed. Through these spaces of belonging, individuals establish a strong connection with place and experience societal memory through the continuity of place (Aytaç, 2013).

One of the most significant aspects of spatial belonging is its capacity to move individuals beyond an isolated sense of self toward a collective sense of "we" that emerges through sharing a common place. Sharing the same place enables individuals to internalize shared values, historical heritage, and cultural codes. Likewise, sharing a memory space that embodies collective lived experiences constitutes one of the most important dynamics for sustaining a group's cultural identity and collective memory while transmitting a sense of belonging across generations (Ak, 2018; Assmann, 2001).

In the context of contemporary urbanization, the loss of spatial memory resulting from urban regeneration practices and commercial pressures directly threatens the spaces of belonging that urban residents have established. The domination of urban space by images that are detached from the local context causes individuals to become alienated from the city and disconnected from their surroundings, and contributes to the fragmentation of the city's overall identity (Aytaç, 2013). Unless the spirit of place and the traces embedded within the urban environment are preserved, the city loses its distinctive identity while society simultaneously faces the risk of losing its sense of spatial belonging. Therefore, the memory of place functions as an important form of resistance against the homogenizing effects of globalization and modernization, supporting urban distinctiveness and the continuity of urban identity (Günaçan & Erdoğan, 2018).

2.3. Local Images and Symbolism

The fundamental elements that distinguish an urban space from others and endow it with its uniqueness and character are the totality of its texture, materials, vegetation, use of light, and the traces left by past activities. Local images and symbols play a crucial role in enabling urban memory to be anchored in space, attain continuity, and become tangible (Günaçan & Erdoğan, 2018). These images function as the sum of the physical and symbolic traces that constitute the memory of the city and imbue urban space with historical, cultural, and semantic depth. In this context, societal memory can be understood not merely as an abstract narrative but as a phenomenon encoded into the physical environment through local images, thereby generating a sense of belonging (Aytaç, 2013).

In translating the symbols that carry societal memory into design, it is essential to adopt an approach based on abstracted traces rather than the direct and superficial imitation of the past. This approach supports symbolic representation and identity formation in design while ensuring the continuity of urban memory by transforming the traces left by past activities into a new spatial experience (Acun, 2021; Ak, 2018). At the same time, it transforms space from a static exhibition of the past into a dynamic realm of identity and narrative, where materials, nature, and the traces of social life converge with the sensory experience of the present (Aytaç, 2013).

ISBN NR. : 978-625-8795-33-2

Local images constitute the totality of the physical and semantic traces that form the memory of the city and endow space with its distinctiveness. In urban design and memory studies, local images are generally classified within two principal frameworks according to the ways they are perceived and reflected in space. The first is the classification proposed by Frances Downing (2003), which examines the memory images retained in designers' minds. Downing categorizes the memory images that play a central role in the construction of local identity into three main groups: *regional/local images,* which reflect the spirit of place; *sensory images,* which evoke embodied memory; and *abstract images,* which facilitate conceptualization.

The second, and most widely recognized, classification is Kevin Lynch's (1960) concept of the City Image. Lynch explains how images of the urban environment are encoded in people's minds and identifies five fundamental elements that contribute to the legibility of the city: *paths,* which facilitate urban movement; *edges,* which separate different areas; *districts,* which are characterized by shared attributes; *nodes,* which function as points of concentration and gathering; and *landmarks,* which provide spatial orientation. This multilayered structure of local images transforms space from a mere physical geometry into a map of identity through which urban memory can be perceived and interpreted.

2.4. Experiential Design

Interpreting, experiencing, and remembering a place is not merely a visual act; it is a multidimensional experience that also encompasses sensory and embodied processes such as hearing, touch, smell, and bodily movement (Jelić, 2015; Pallasmaa, 2011). In this context, the experiential design approach seeks to place human experience at the center of the design process rather than focusing solely on geometric form and visual aesthetics, conceiving space as a realm of embodied, sensory, and emotional experience. Its aim is not simply to present the underlying concept or historical message of a design to the viewer in a passive manner but to enable users to experience it directly and internalize its meaning (Uysal, 2017). User interaction in experiential spaces is shaped through the strategic integration of sensory, cognitive, affective, active, and relational dimensions (Chertoff et al., 2008; Pei et al., 2023). This multilayered structure transforms the relationship individuals establish with space from a personal and superficial sense of belonging into a profound sense of place attachment and a shared realm of collective experience. Particularly in memory spaces associated with difficult histories or urban traumas, experiential design strategies create interactive environments for learning and empathy that draw visitors into the space, rather than merely presenting an instructive historical narrative (Acun, 2021; Taluğ Demiriz, 2021). In this way, space ceases to be a monument that is merely observed and becomes an active setting of remembrance, explored through embodied movement.

Human beings perceive the world through the integration of all their senses. In this context, the body also serves as a carrier of memory; past experiences and spatial learning persist not only at the cognitive level but also through embodied orientations and reflexes. As emphasized by Merleau-Ponty, one of the pioneers of phenomenology, the boundary between the body and the external world is permeable, and perception emerges from the practical attunement of the body, embedded in its surroundings, to space (Merleau-Ponty, 2012; Uysal, 2017). Building upon this theoretical framework, the architect Juhani Pallasmaa (2011) likewise defines space as a realm

ISBN NR. : 978-625-8795-33-2

of embodied memory in which actions and emotions are brought to life. Embodied memory is awakened through sensory stimuli. Sounds within a space, the touch of the wind upon the body, the scent of materials, or the texture of the ground all possess the capacity to evoke memories of the past directly. Degen and Rose (2012) argue that the designed objects and surfaces of the urban environment reflect individuals' own sensory biographies back to them. Therefore, walking through a memory space is not merely the act of moving from one point to another; it is an existential experience in which the body engages with space, the past, and memory through the senses.

In conclusion, a successful memory space should not merely create an aesthetic or monumental form. Rather, it should offer a holistic spatial experience that engages users through sensory stimuli—such as the coldness of stone, the sound of water, the movement of wind, or deliberately cast shadows—and fosters a sense of belonging and collective memory through embodied experience (Biçer et al., 2025; Jelić, 2015).

3. MATERIALS AND METHODS

3.1. Materials

The primary material of this study consists of six internationally selected case studies representing different approaches to the reclamation of memory spaces. These case studies are Hiroshima Peace Memorial Park, Landschaftspark Duisburg-Nord: Piazza Metallica, The High Line, the Historic Centre of Warsaw, the Mamayev Kurgan Memorial Complex, and the National September 11 Memorial. Within the Mamayev Kurgan Memorial Complex, particular attention is given to The Motherland Calls monument. The principal reason for selecting these case studies is that each represents a distinct type of memory, a different historical context, and a distinct memory-space regeneration strategy. The selection was based on the relationship each site establishes with societal, political, historical, industrial, national, or traumatic memory. Accordingly, Hiroshima Peace Memorial Park and the National September 11 Memorial were examined as spaces of traumatic memory and mourning; Landschaftspark Duisburg-Nord: Piazza Metallica as an example of industrial memory; The High Line as a case of infrastructural memory and public transformation; the Historic Centre of Warsaw as an example of the post-war reconstruction of historical urban memory; and the Mamayev Kurgan Memorial Complex, including The Motherland Calls, in the context of war memory, national resistance, heroism, and monumental representation.

The secondary material of the study consists of national and international literature on the concepts of memory spaces, collective memory, spirit of place, local images, symbolism, and experiential design. Drawing upon this body of literature, the selected case studies were evaluated not only in terms of their physical characteristics but also with respect to their historical contexts, symbolic meanings, user experiences, modes of spatial perception, and functions in sustaining collective memory. Accordingly, the study approaches the reclamation of memory spaces not merely as a process of conservation or physical intervention, but as a multilayered design approach through which the traces of the past are reconnected with contemporary public life.

ISBN NR. : 978-625-8795-33-2

At the conclusion of the study, Soğukçeşme Street, Sultanahmet Archaeological Park, Anıtkabir, İzmir Historic Gasworks Factory, Bursa Merinos Factory Park, and the October 10 Peace Square Memorial were examined as complementary case studies in order to discuss how the strategic framework developed from the selected international case studies can be interpreted within the context of Türkiye. Through these examples, the potential relevance of the proposed memory-space regeneration strategies to the interpretation of historical, industrial, monumental, and traumatic memory spaces in Türkiye is discussed.

3.2. Methodology

The study employs a comparative case study analysis based on a qualitative research approach. Within this framework, selected memory spaces from around the world are examined according to predetermined experiential design criteria, and the memory-space regeneration strategies used to interpret them are outlined. Accordingly, the research is based on a descriptive and interpretative comparison of the selected case studies in terms of their historical context, local images, symbolic expression, visitor experience, spatial perception, and function in sustaining collective memory.

The research methodology was structured in three stages. In the first stage, a theoretical framework was established based on the concepts of memory spaces, collective memory, spirit of place, local images, symbolism, and experiential design. At this stage, memory spaces were approached not merely as physical entities but as multilayered urban spaces that embody collective memory, identity, and a sense of belonging. In the second stage, the six international case studies constituting the primary material of the research were examined in terms of their historical contexts, spatial characteristics, and relationships with memory. In the third stage, these case studies were comparatively interpreted according to the established evaluation criteria and memory-space regeneration strategies.

A consistent analytical framework was applied in the evaluation of each case study. First, the historical context of the site and the type of memory with which it is associated were identified. Next, the local images, symbolic elements, or spatial traces that carry memory within the site were determined. Finally, each case study was evaluated in terms of visitor experience, spatial orientation, symbolic representation, and its function in sustaining collective memory. Visitor experience was interpreted through published studies, project descriptions, visual materials, and documented spatial characteristics rather than assessed through direct observation or user surveys. The evaluation criteria employed in the study were organized under five main categories: historical context and authenticity; architectural and symbolic expression; visitor experience and interaction; spatial orientation and perception; and collective and cultural memory function. The criterion of historical context and authenticity evaluates the extent to which the site's relationship with the past has been preserved and how historical traces have been made visible within the space. The criterion of architectural and symbolic expression examines the meanings generated through form, materials, monuments, structures, voids, water, axes, and other landscape elements. The criterion of visitor experience and interaction focuses on the embodied, sensory, and emotional relationship that users establish with the space. The criterion of spatial orientation and perception concerns how visitors move through the site, how they are guided by specific axes or focal points, and how they perceive the space. The criterion

ISBN NR. : 978-625-8795-33-2

of collective and cultural memory function evaluates how the site transcends individual remembrance to foster collective memory, a sense of belonging, identity, and a shared understanding of the past.

In addition, six memory-space regeneration strategies were adopted to evaluate the selected cases: non-intervention, enhancement through additions, reconstruction, contextual design, commemoration and monumentalization, and evoking absence. These strategies were adapted and refined from the design dynamics proposed by Biçer et al. (2025) and grounded in theoretical approaches that view the reclamation of memory spaces not merely as physical preservation, but as a process addressing traces of the past through embodied experience, spatial perception, symbolic representation, and collective remembrance. Their conceptual foundation draws on theories of space and memory, collective memory, sites of memory (*lieux de mémoire*), and embodied and sensory experience (Casey, 1987; Halbwachs, 1992; Nora, 2006; Pallasmaa, 2011). The evaluation criteria were synthesized from the literature on design, perception, and contextual theories (Bayraktar, 2018; Günaçan & Erdoğan, 2018; Uysal, 2017).

The non-intervention strategy refers to the transmission of memory directly through space by preserving, as far as possible, the physical traces of a historical event or destruction. The enhancement through additions strategy involves reinforcing existing historical or industrial traces through new functions, public uses, or design interventions. The reconstruction strategy is based on ensuring the spatial continuity of memory through the reconstruction or representation of a lost or damaged historical fabric. The contextual design strategy extends beyond the mere preservation of existing physical traces by creating a new experiential setting through environmental relationships, user routes, vegetation, views, visual outlooks, and everyday use. The commemoration and monumentalization strategy is founded on making a particular individual, event, struggle, or societal value visible within collective memory through monumental scale, powerful symbolic forms, and ceremonial spatial compositions. Finally, the evoking absence strategy enables the experience of loss, absence, mourning, and traumatic memory not through direct representation, but through elements such as void, silence, water, names, traces, and a sense of incompleteness. In the final stage of the methodology, the strategies identified through the selected international case studies were related to memory spaces in Türkiye. Through this comparative association, the study aims to explore the potential applicability of the proposed strategic framework to the interpretation of diverse memory spaces within the Turkish context.

4. RESEARCH FINDINGS

4.1. Analysis of Selected International Case Studies

4.1.1. Non-Intervention – Hiroshima Peace Memorial Park (Japan)

The non-intervention strategy is an approach based on preserving, in its original condition, a site associated with a traumatic or historical event without physically altering it. The objective of this strategy is to make the physical traces of the past legible and to transmit the spatial memory of destruction to future generations. Within Hiroshima Peace Memorial Park, the Atomic Bomb Dome represents one of the most powerful examples of this strategy.

ISBN NR. : 978-625-8795-33-2

Historical Context and Authenticity: Hiroshima Peace Memorial Park is located on the Nakajima Delta in central Hiroshima, an area devastated by the atomic bomb on 6 August 1945. Instead of redevelopment, the primary impact zone was conceived as a space of peace. The Atomic Bomb Dome, one of the few structures left standing near the hypocenter, has been preserved in its post-explosion condition as an authentic carrier of memory (Bayraktar, 2018).

Architectural and Symbolic Expression: The park, designed by Kenzo Tange and his team, employs a symbolic language that integrates modern architecture with traditional Japanese forms. The Hiroshima Peace Memorial Museum, which marks the entrance to the park, is elevated above the ground and conceived as a symbolic gateway leading from historical tragedy toward renewal. At the center of the park stands the Memorial Cenotaph, constructed in reinforced concrete in accordance with the construction technologies of its time and inspired by the clay Haniwa figures found in ancient Japanese royal tombs. Through this design, traditional forms are combined with a modern architectural approach, establishing a powerful symbolic connection between the past and the future (Bayraktar, 2018; Maki & Niihata, 2020).

Visitor Experience and Interaction: The design transforms visitors from passive observers into active participants through a continuous pedestrian route. Visitors follow the axis from the Memorial Cenotaph to the Atomic Bomb Dome, experiencing remembrance, confrontation, and renewal. The park's relationship with water is expressed by gradually leading visitors toward the water's edge. This experience evokes empathy with the people of Hiroshima, who threw themselves into the river to escape the intense heat of the atomic bombing, confronting visitors with the emotional atmosphere of the past (Bayraktar, 2018; Maki & Niihata, 2020).

Spatial Orientation and Perception: The spatial layout of the park is organized around a clear and uninterrupted north–south visual axis. This compositional alignment places the Hiroshima Peace Memorial Museum, the Memorial Cenotaph, and the Atomic Bomb Dome along the same axis, directing visitors' embodied and visual perception toward the Dome, which stands as the principal representation of the devastation of the bombing. Reinforced through the deliberate use of spatial voids and water features, this axial composition establishes the ruined structure as the primary focal point of the site, guiding visitors toward a contemplative and monumental experience of remembrance (Bayraktar, 2018; Maki & Niihata, 2020) (Figure 1).

(a) The Atomic Bomb Dome (Watchtower Bible and Tract Society of PA, 2014)

(b) Spatial orientation between the Peace Memorial and the Atomic Bomb Dome (Gürdal, 2024)

Figure 1. The Atomic Bomb Dome and the memorial axis at Hiroshima Peace Memorial Park

ISBN NR. : 978-625-8795-33-2

Collective Memory Function: Reflecting the design approach of its architect, Kenzo Tange, the site was conceived not merely as a passive place of mourning where the dead are commemorated, but as a space of memory that actively generates and conveys the ideal of peace to future generations (Maki & Niihata, 2020). Rather than reinforcing a retrospective narrative of victimhood, it functions as an active platform that promotes the ideology of peace while symbolizing the ecological and architectural rebirth of Hiroshima from its ruins. In doing so, it transforms urban trauma into a universal call for peace and hope for all humanity, securing a lasting place within collective memory (Bayraktar, 2018).

4.1.2. Enhancement through Additions – Landschaftspark Duisburg-Nord: Piazza Metallica (Germany)

The enhancement through additions strategy is a design approach that enriches a historical, traumatic, or industrial site through contemporary additions and complementary structures that strengthen its commemorative, educational, or adaptive reuse functions without altering its original fabric and physical remains (Biçer et al., 2025). Landschaftspark Duisburg-Nord, together with Piazza Metallica at its core, represents one of the most successful examples of this strategy worldwide, preserving and reinterpreting Germany's industrial heritage.

Historical Context and Authenticity: Until the mid-nineteenth century, the site was an agricultural landscape, later transformed by the Industrial Revolution into a major coal and steel complex. After losing its economic viability, it was abandoned in 1985 because of severe environmental pollution (Kaya et al., 2015; Yurtseven, 2021). Rather than being demolished, the former industrial site was converted into an urban park within the IBA Emscher Park framework while preserving its original ruins (Kaya et al., 2015). In line with the enhancement through additions strategy, the steel plates once used over casting molds were relocated to the site's center to form Piazza Metallica. Their ongoing weathering enables visitors to establish a direct visual and experiential connection with the site's industrial memory (Yurtseven, 2021).

Architectural and Symbolic Expression: Designed by landscape architect Peter Latz in 1991, the park adopts an approach that seeks to understand the past and transform it through sustainable improvement rather than erasing it (Kaya et al., 2015). The 49 large cast-iron plates placed within the square go beyond being static monuments and are intentionally exposed to the erosive effects of time, namely the natural process of rusting. The ongoing weathering and corrosion of these iron plates represent a powerful and evolving architectural expression that symbolizes the contrast between the heavy and polluting steel production of the past and today's ecological regeneration oriented toward nature (Yurtseven, 2021) (Figure 2).

ISBN NR. : 978-625-8795-33-2

Figure 2. Reused cast iron plates and industrial structures at Piazza Metallica (Yılmazer, 2021)

Visitor Experience and Interaction: As one of the park's significant symbolic elements and a powerful urban focal point, Piazza Metallica transforms visitors from passive observers who view industrial remains from a distance into active participants who establish a direct relationship with the site (Yurtseven, 2021). By walking on and sitting on these 49 iron plates, which continue to rust over time, and by participating in the various artistic and cultural activities held on them, visitors develop an interactive, dynamic, and tactile connection with the city's industrial memory. This condition represents one of the most vivid experiential examples of how an abandoned industrial ruin can be transformed into an urban open space that supports everyday life, leisure, and recreational activities (Kaya et al., 2015).

Spatial Orientation and Perception: The spatial arrangement of the square was intentionally conceived by the designer as a tool for guiding perception and movement. Visitors standing on this arrangement of 49 iron plates are able to experience and perceive the surrounding massive industrial structures, such as the original blast furnaces and hot blast stoves, at close range and from various perspectives (Yurtseven, 2021). The contrast in scale established between the enormous industrial machine structures and the human body within the square enables visitors to spatially perceive the industrial power of the past, while creating a strong perceptual awareness of the relationship between steel, concrete, and nature over time.

Collective Memory Function: Landschaftspark Duisburg-Nord and Piazza Metallica represent unique urban symbols that preserve the hidden memory of the city, contribute to urban identity, and demonstrate that transformation can be achieved without demolition (Kaya et al., 2015). Rather than erasing or concealing the collective memory associated with the region's working-class history and industrial past, the site has reconnected this historical heritage with contemporary ecological, recreational, and cultural needs. In this way, an urban derelict area has been rescued from disappearance and transformed into a living memory space that sustains social memory and transfers industrial heritage to future generations (Kaya et al., 2015; Yurtseven, 2021).

4.1.3. Contextual Design – The High Line Park (New York)

ISBN NR. : 978-625-8795-33-2

The contextual design strategy aims to integrate a historical, traumatic, or industrial site into a new urban landscape by relating the space to its surrounding environment and broader urban systems, rather than limiting it solely to its own physical boundaries. Located in New York City, USA, The High Line represents one of the world's most recognized examples of the transformation of obsolete and abandoned infrastructure into an urban landscape through this strategy.

Historical Context and Authenticity: The High Line is an elevated railway line constructed in the 1930s on Manhattan's West Side, approximately 10 meters above street level, to transport freight and prevent fatalities caused by train accidents occurring at street level (Ergan & Gormus, 2023; Littke et al., 2013). With the development of road transportation, railway operations were discontinued in 1980, and the site was abandoned for many years (Littke et al., 2013). During this period of abandonment, a spontaneous wild ecosystem developed along the railway structure. Although some groups advocated for its demolition, the elevated line was saved through the efforts of the Friends of the High Line initiative, established in 1999 (Millington, 2015). Throughout the design process, the industrial infrastructure and original railway tracks were not removed; instead, the site was gradually opened in phases beginning in 2009 and reinterpreted as a new public green space while preserving and transforming its existing context (Abacıoğlu Gitmiş & Yardimcioğlu, 2026; Littke et al., 2013).

Architectural and Symbolic Expression: The project, realized through the collaboration of James Corner Field Operations, Diller Scofidio + Renfro, and landscape designer Piet Oudolf, was inspired by the spontaneous vegetation that emerged on the site during its period of abandonment (Ergan & Gormus, 2023; Millington, 2015). The planting design, which combines diverse species inspired by the self-grown vegetation, together with precast concrete panels inserted among the old rusted railway tracks, creates an aesthetic synthesis between industrial decline and ecological regeneration (Abacıoğlu Gitmiş & Yardimcioğlu, 2026). In the design of the park, the iconic photographs taken by Joel Sternfeld before the proposed demolition process, which captured the spirit of natural reclamation, formed the basis of the symbolic expression; the project aimed to establish a new unity between nature and culture (Millington, 2015). This carefully designed and aesthetically composed green layer emerging among the old rusted tracks serves as a powerful architectural and symbolic expression of the city's transition from industrial decline toward ecological renewal (Figure 3).

(a) Railway tracks and vegetation (Diller Scofidio + Renfro, n.d.)

(b) The relationship between the elevated pathway and the urban context (Prelikj, 2024)

Figure 3. Preserved railway traces and urban context at The High Line

ISBN NR. : 978-625-8795-33-2

Visitor Experience and Interaction: This elevated park, extending approximately 2.4 kilometers, transforms visitors from passive observers into active participants of the urban landscape. The design provides a public experience that allows users to move away from the speed of everyday life through activities such as slowing down, walking, sitting, and resting within the city. Wooden seating areas, amphitheaters, and pedestrian pathways stand out as key design elements that support movement, sitting, and resting within the site (Mahadin, 2016). However, the increasing popularity of the site has also led to concerns regarding overcrowding and touristification, as the park has become more heavily used by visitors and tourists rather than local residents. This situation has gradually made the visitor experience more challenging for the local community (Ergan & Gormus, 2023).

Spatial Orientation and Perception: The elevated position of the High Line above street level creates a dual effect on spatial perception. Its elevated setting allows visitors to physically distance themselves from the intense traffic and noise of the city below, while providing a safe and tranquil pedestrian route that maintains visual connections with Manhattan's skyscrapers and streets (Ergan & Gormus, 2023). In particular, the amphitheater located along 10th Avenue, which slopes downward and frames the street through a wide opening, offers visitors the opportunity to observe urban life from a cinematic perspective (Ergan & Gormus, 2023). Although the site is physically separated from the street level, its strong visual relationship with Manhattan's skyscrapers and urban skyline continuously connects visitors with the broader urban context. This dual condition—being located at the center of the city while simultaneously providing distance from its complexity—enhances the experiential quality of the space.

Collective Memory Function: The High Line functions as a living memory space that successfully preserves the city's transportation and industrial memory by incorporating it into a sustainable urban landscape rather than erasing it (Abacıoğlu Gitmiş & Yardimcioğlu, 2026). However, this successful transformation has also generated discussions regarding eco-gentrification (Black & Richards, 2020). The significant increase in property values around the High Line, the arrival of technology companies and the development of luxury housing in the area, and the displacement pressures experienced by low-income local communities have revealed the project's eco-gentrification effects (Black & Richards, 2020; Littke et al., 2013). Furthermore, according to critics, the spontaneous vegetation that developed during the site's period of abandonment, as well as the memories associated with marginalized urban groups, have been weakened through an overly designed, sanitized, and capital-oriented urban transformation process (Ergan & Gormus, 2023; Millington, 2015). The former commercial and industrial functions of the site have been integrated with the ecological, recreational, and leisure needs of contemporary urban society. Thus, while functioning as a public landscape that provides relief within a densely built urban environment, the site also enables industrial heritage to be reconnected with everyday life.

4.1.4. Reconstruction – Historic Centre of Warsaw (Poland)

The reconstruction strategy refers to the process of reproducing the historical fabric of a place through representation, revitalization, and rebuilding in order to make the lost traces of a completely or largely destroyed space visible again. Located in the capital of Poland, the Historic Centre of Warsaw represents one of the most exceptional and comprehensive examples

ISBN NR. : 978-625-8795-33-2

of reconstruction in the history of architecture and heritage conservation: a city intended to be erased from history was recreated through strong national determination.

Historical Context and Authenticity: During the Second World War, particularly after the Warsaw Uprising in August 1944, approximately 85% of the Historic Centre of Warsaw was deliberately and systematically destroyed by Nazi forces through planned demolitions (Ivashko et al., 2024; Popiołek-Roßkamp, 2019; UNESCO, n.d.). Although the idea of preserving the ruins as a permanent "monument of destruction" was debated after the war, this approach was rejected by the Reconstruction Office (BOS) under the leadership of Chief Conservator Prof. Jan Zachwatowicz (Ivashko et al., 2024; Nowobilski & Ligler, 2021). Rather than leaving the area as ruins, the historical urban fabric extending from the 13th to the 20th century was reconstructed with a high degree of authenticity based on pre-1939 architectural surveys, secretly preserved documents, and detailed urban paintings created by the Italian painter Bernardo Bellotto in the 18th century (Nowobilski & Ligler, 2021; UNESCO, n.d.) (Figure 4).

(a) The destroyed appearance of the historical centre after the war (Polish Press Agency, 1945)

(b) The reconstructed Old Town Market Square and its façades (UNESCO World Heritage Centre, n.d.)

Figure 4. Destruction and reconstruction of Warsaw's Historic Centre

Architectural and Symbolic Expression: The reconstruction process was not merely a physical restoration; it represented an ideological and symbolic intervention that made Poland's post-war resistance, national identity, and determination for urban continuity visible (Popiołek-Roßkamp, 2019; UNESCO, n.d.). Following Zachwatowicz's emphasis on the unity of nation and cultural heritage, the façades were rebuilt in their historical character using traditional techniques such as sgraffito, polychrome woodwork, and stone detailing (Wowczak, 2020). Meanwhile, the interiors and infrastructure were modernized to meet twentieth-century requirements for hygiene, heating, and lighting, combining historical representation with contemporary use (Krasucki, 2024; Popiołek-Roßkamp, 2019).

Visitor Experience and Interaction: The Historic Centre of Warsaw was conceived not as a passive display of the past but as an active residential environment where different social groups could live, socialize, and participate in everyday activities (Krasucki, 2024; Nowobilski & Ligler, 2021). The continuation of these urban functions prevents the area from becoming merely a historical backdrop and enables visitors to engage directly with both everyday life and history (Nowobilski & Ligler, 2021).

Spatial Orientation and Perception: The reconstructed Old Town Market Square (Rynek Starego Miasta) was organized within a clear spatial hierarchy by integrating the medieval street

ISBN NR. : 978-625-8795-33-2

network and remaining city-wall traces into the urban composition (Nowobilski & Ligler, 2021; UNESCO, n.d.). The square opening at the end of narrowing streets, together with preserved eighteenth-century façade lines, creates a strong sense of continuity and revived historical identity (Biçer et al., 2025; Nowobilski & Ligler, 2021). Although contemporary interior adaptations remain largely invisible from the street, visitors' perception is guided mainly by the historical façades and urban fabric (Krasucki, 2024; Popiołek-Roßkamp, 2019).

Collective Memory Function: By reconstructing Warsaw and its shared identity after attempts to erase both the city and the state, the site has preserved national culture, resistance, and collective memory for future generations (Popiołek-Roßkamp, 2019; UNESCO, n.d.). Although comprehensive reconstruction is generally treated cautiously in modern conservation, Warsaw was recognized for its outstanding universal value as an expression of national recovery from trauma and was inscribed on the UNESCO World Heritage List in 1980 (Ivashko et al., 2024; UNESCO, n.d.).

4.1.5. Commemoration and Monumentalization – Mamayev Kurgan Memorial Complex and the Motherland Calls Monument (Russia)

The commemoration and monumentalization strategy uses large-scale monumental design to give collective memory grandeur, symbolism, and permanence while commemorating significant individuals, events, or national ideals. Such monuments reinforce national pride, collective identity, and belonging. In Volgograd, The Motherland Calls monument within the Mamayev Kurgan Memorial Complex is a prominent example of this strategy.

Historical Context and Authenticity: The Motherland Calls monument commemorates the Battle of Stalingrad (present-day Volgograd), fought between 1942 and 1943 during the Second World War and regarded as one of the war's bloodiest turning points (Yıldırım & Paşalıoğlu, 2025). Known as Height 102.0 on military maps and named after the word kurgan, meaning "burial mound," the hill is a vast collective burial site preserving the memory of thousands of soldiers and civilians (Lowe, 2020; "Memorial Complex Mamayev Kurgan," n.d.). Rather than representing war solely through mourning and loss, the memorial complex expresses Soviet resistance, sacrifice, and victory through a monumental spatial composition (Nidawi, 2019; Yıldırım & Paşalıoğlu, 2025).

Architectural and Symbolic Expression: The Motherland Calls monument, which constitutes the central figure of the complex, was designed by sculptor Yevgeny Vuchetich and engineer Nikolai Nikitin and was constructed between 1959 and 1967. As one of the most powerful examples of classical monumental typology, The Motherland Calls represents the narrative of war, resistance, and national defense through its enormous female figure standing 85 meters high, including the sword, its monumental scale, and its dynamic bodily expression (Hashmi et al., 2019; Lowe, 2020). The sword held in the figure's right hand symbolizes the call to struggle and defend the homeland, while the extended left arm represents an invitation for the people to unite in collective resistance. This dynamic bodily expression glorifies not the tragedy of war itself, but rather the nation's perceived strength, victory, and narrative of national resistance through a monumental symbolic language (Nidawi, 2019; Yıldırım & Paşalıoğlu, 2025).

ISBN NR. : 978-625-8795-33-2

Visitor Experience and Interaction: The monument was designed as a multilayered circulation route that transforms visitors from passive observers into participants in an epic narrative. Visitors reach it by climbing a 200-step staircase symbolizing the 200 days of the battle, creating a journey through dramatic thresholds and transitions (Yıldırım & Paşalıoğlu, 2025). The route continues with the Square of Those Who Fought to the Death, featuring a 12-meter-high soldier figure symbolizing courage, followed by the Ruined Walls, which evoke the city's destruction through inscriptions expressing the soldiers' determination and reliefs depicting scenes from the war. Heroes' Square contains six sculptures representing heroism and patriotism around a large pool symbolizing the Volga River. Continuing onward, visitors encounter the Hall of Military Glory, the Eternal Flame, the Lake of Tears, the Sculpture of the Mother Mourning, and the Square of Sorrow. This multilayered experience enables new generations, within battlefield tourism, to engage with patriotism, sacrifice, and empathy with the past ("Memorial Complex Mamayev Kurgan," n.d.) (Figure 5).

(a) Spatial sequence of the complex directing visitors toward the monument (Volgograda, 2025)

(b) Ruin walls and ceremonial steps (Kurgan-Mamaev.ru, n.d.)

Figure 5. Ceremonial approach to The Motherland Calls at Mamayev Kurgan

Spatial Orientation and Perception: Located at one of the highest points of the city, the monument creates a powerful urban landmark that can be perceived from kilometers away across Volgograd and the Volga River (Lowe, 2020; Yıldırım & Paşalıoğlu, 2025). The visitor's approach to the monument through a route that begins at the foot of the hill and gradually ascends upward establishes a strong contrast between monumental scale and the human body, reinforcing perceptions of grandeur and authority (Nidawi, 2019). At the same time, the monument's scale and skyward rise symbolically evoke strong concepts of security, belonging, and national unity associated with the image of the Motherland.

Collective Memory Function: As an example of classical monument typology, The Motherland Calls frames war through national victory and heroism, unlike counter-monuments that encourage reflection on war's destruction (Nidawi, 2019). Today, the complex hosts commemorative ceremonies and public rituals, contributing to the intergenerational transmission of Russian national identity and war memory ("Memorial Complex Mamayev Kurgan," n.d.; Yıldırım & Paşalıoğlu, 2025). Rather than addressing trauma and loss solely through mourning, the monument embeds them in collective memory through narratives of national resistance, heroism, and sacrifice (Lowe, 2020; Yıldırım & Paşalıoğlu, 2025).

4.1.6. Evoking Absence – National September 11 Memorial (USA)

ISBN NR. : 978-625-8795-33-2

The evoking absence strategy refers to the intentional use of physical absence or void (negative space) within a place as a powerful reminder of loss, mourning, and an irreversible sense of disappearance. Unlike traditional and monumental approaches based on grand physical masses, this strategy evokes a profound sense of contemplation and collective mourning through absence rather than presence. Located at the former World Trade Center site in New York City, the National September 11 Memorial is a prominent example of this strategy.

Historical Context and Authenticity: The memorial was designed as an urban commemorative space dedicated to the memory of those lost in the 11 September 2001 terrorist attacks, and it was constructed on the site where the Twin Towers were destroyed. During the redevelopment process of the site, rather than covering the traces of the past with a new monumental structure, the original footprints of the collapsed towers were preserved and transformed into two large open-air pools and an urban void. This approach makes the spatial traces of the trauma visible through the concept of absence (Biçer et al., 2025; Taluğ Demiriz, 2021).

Architectural and Symbolic Expression: The design by Michael Arad and Peter Walker, selected through an international design competition, was conceived not as a vertical monument rising toward the sky, but through negative forms and voids that extend downward into the ground. The water cascading down from all four sides of the pools and disappearing into a smaller square depression at the center symbolizes irreversible loss, absence, and continuity (Biçer et al., 2025). The organized tree structure surrounding the voids creates a contrasting landscape layer that introduces the ideas of the continuation of life and renewal into the narrative of loss (Biçer et al., 2025) (Figure 6).

(a) Memorial pools created within the footprints of the Twin Towers (Lee, n.d.)

(b) Bronze panels containing the names of victims and the water element (Skena Culgan, 2025)

Figure 6. Memorial pools and victims' names at the National September 11 Memorial

Visitor Experience and Interaction: The design employs an unconventional method of communication while connecting visitors with the memory of those who were lost. The names of the individuals who died in the attacks are engraved on bronze panels surrounding the pools. However, these names are not arranged alphabetically or chronologically; instead, they are organized according to meaningful relationships based on family, friendship, and professional connections among the victims (Taluğ Demiriz, 2021). While looking toward the void, visitors are encouraged to read these names arranged according to personal life connections, establish a relationship with the individual identities of those who were lost, and participate in a shared experience of mourning (Biçer et al., 2025; Taluğ Demiriz, 2021).

ISBN NR. : 978-625-8795-33-2

Spatial Orientation and Perception: The spatial composition of the memorial directs the visitor's gaze not toward a monumental form rising into the sky, but toward the ground and the deepening void. Observing the water continuously flowing toward an invisible center and disappearing into a dark void evokes concepts of infinity, loss, and inaccessibility in the visitor's mind. These deep voids, which can be perceived from all directions and experienced by walking around them, encourage visitors to pause, reflect, and engage in a commemorative experience within the intense and noisy flow of everyday urban life (Taluğ Demiriz, 2021).

Collective Memory Function: The National September 11 Memorial preserves the physical traces of historical trauma while transferring the memory of those who were lost into collective memory through themes of mourning, respect, and solidarity. Unlike traditional monumental forms that glorify heroism or war, the memorial makes loss and suffering visible through the elements of void, water, and names (Biçer et al., 2025). The voids created on the footprints of the destroyed towers transform physical absence into a spatial tool of remembrance, allowing the memory of the victims to continue within social memory (Taluğ Demiriz, 2021).

The comparative analysis shows that different types of memory are represented through local images, symbolic expressions, and experiential design tools. Across the cases, historical traces, visitor experience, spatial orientation, and collective memory functions vary in significance. The results are summarized in Table 1.

Table 1. Comparative Analysis of Selected Memory Sites from Around the World

Space	Type of Memory	Main Local Image / Symbolic Trace	Experiential and Spatial Tools	Key Characteristics
Hiroshima Peace Memorial Park	Traumatic memory, war and mourning memory	Atomic Bomb Dome, water elements, Peace Memorial, and the north–south commemorative axis	Preservation of the Dome in its destroyed state, continuous visual axis, walking route, orientation toward water, and resting spaces	The non-intervention approach is interpreted primarily through the Atomic Bomb Dome, which serves as a physical witness of destruction, rather than through the entire park.
Landschaftspark Duisburg-Nord – Piazza Metallica	Industrial memory and working-class memory	Blast furnaces, industrial structures, rusting cast-iron plates	Walking and sitting on iron plates, tactile experience, cultural events, and the contrast of scale between industrial structures and the human body	Demonstrates that industrial traces can be supported with new public functions without being removed.
The High Line Park	Infrastructure and industrial memory, memory of public transformation	Former railway tracks, elevated railway line, and landscape inspired by spontaneously developed vegetation	Elevated linear walking route, seating areas, planting design, viewing points, and openings framing urban views	In addition to demonstrating the success of the transformation, the case raises issues related to eco-gentrification, touristification, and displacement.

ISBN NR. : 978-625-8795-33-2

Historic Centre of Warsaw	Post-war historical-urban memory and national resistance memory	Historical street network, Old Town Market Square, traces of city walls, façades, and urban images based on archival documents	Re-establishment of historical streets and squares, revitalization of façades, and continuation of residential and commercial functions	Demonstrates that memory can be reproduced through reconstruction while also constituting a controversial example regarding authenticity and conservation principles.
Mamayev Kurgan Memorial Complex and The Motherland Calls Monument	War memory, national resistance, heroism, and sacrifice memory	The Motherland Calls figure, sword, 200 steps, squares, Ruined Walls, and Eternal Flame	Upward ceremonial route, monumental scale, squares, sculptures, water elements, and symbolic thresholds	Monumental scale and ceremonial spatial organization strengthen the narrative of national victory while limiting critical interpretations of war.
National September 11 Memorial	Traumatic memory, loss, and collective mourning memory	Footprints of the Twin Towers, void, water, victims' names, and tree landscape	Ground-oriented perception, deep pools, sound of flowing water, interaction with names, moments of pause, and the experience of silence	Transforms negative space and physical absence into a primary tool of remembrance instead of relying on traditional monumental masses.

4.2. Relating the Strategies to Turkish Case Studies

The memory-space regeneration strategies identified through the selected global examples provide a framework that can also be used to interpret different memory sites in Türkiye. Within this scope, the strategies examined in the study — non-intervention, enhancement through additions, reconstruction, contextual design, commemoration and monumentalization, and evoking absence — have been associated with historical, industrial, monumental, and traumatic memory sites in Türkiye. Through this association, the study aims to reveal the possible applications and interpretations of these strategies within different historical, cultural, and spatial contexts. The relationships between the strategies and the selected global and Turkish examples are summarized in Table 2.

Table 2. Memory-Space Regeneration Strategies: Global and Turkish Examples

Strategy	Global Example	Associated Example from Türkiye	Common Memory Approach	Main Local Images and Spatial Tools
Non-intervention	Hiroshima Peace Memorial Park	Sultanahmet Urban Archaeological Site	Making the physical traces of historical events and past periods visible by preserving them within their own spatial contexts	Ruins and remains, archaeological layers, monumental structures, historical traces, and visual continuity
Enhancement through Additions	Landschaftspark Duisburg-Nord – Piazza Metallica	İzmir Historical Gas Factory	Supporting industrial heritage with new public, cultural, and recreational functions without eliminating existing traces	Industrial structures, production elements, reused materials, restored buildings, and contemporary public uses
Reconstruction	Historic Centre of Warsaw	Soğukçeşme Street	Recreating weakened, damaged, or lost	Street texture, historical façades, traditional residential typology,

ISBN NR. : 978-625-8795-33-2

			historical fabric and urban imagery	squares, and adaptive reuse
Contextual Design	The High Line Park	Bursa Merinos Cultural Center and Park	Integrating industrial or infrastructural heritage with surrounding green systems, pedestrian movement, cultural functions, and everyday public life	Pedestrian routes, vegetation patterns, park areas, viewing and resting points, cultural and recreational functions
Commemoration and Monumentalization	Mamayev Kurgan Memorial Complex and The Motherland Calls Monument	Anıtkabir	Making narratives of national history, founding values, struggle, heroism, and sacrifice visible through monumental and ceremonial spaces	Monumental scale, sculptural and architectural masses, ceremonial squares, symbolic axes, steps, and directed visitor routes
Evoking Absence	National September 11 Memorial	10 October Labor, Peace and Democracy Memorial Square and Memorial Site	Transforming loss, absence, mourning, and social trauma into experiences of commemoration and collective remembrance within public space	Void, names, silence, pausing, gathering, commemorative rituals, and the original site of loss

The reconstruction strategy can be interpreted through Soğukçeşme Street in Istanbul. The restoration and adaptive reuse of the historical houses along Soğukçeşme Street provide an example of sustaining the historical street image through contemporary uses (Karadayı Yenice & Altınoluk, 2019). In this case, memory is constructed through the reorganization of a weakened historical environment and the re-establishment of the urban image as a visible element. In this respect, Soğukçeşme Street can be considered a smaller-scale counterpart of the reconstruction approach observed in the Historic Centre of Warsaw within the context of Türkiye.

The non-intervention strategy can be interpreted through the Sultanahmet Urban Archaeological Site. The area represents a multilayered urban memory space that contains archaeological remains and monumental structures belonging to different historical periods (İstanbul İl Kültür ve Turizm Müdürlüğü, n.d.). The ability to perceive historical traces and monumental structures within their original spatial contexts enables memory to be conveyed directly through historical layers. Therefore, within the scope of this study, the site can be associated with the non-intervention strategy in terms of preserving historical continuity and making the physical traces of the past visible.

One of the prominent examples of the commemoration and monumentalization strategy in Türkiye is Anıtkabir. Anıtkabir makes the memory of Mustafa Kemal Atatürk and the founding values of the Republic visible through monumental scale, ceremonial axes, symbolic spaces, and a strong architectural language. The Lion Road, Ceremonial Square, and Mausoleum guide visitors through a specific spatial orientation and ceremonial sequence (Anıtkabir, n.d.). In this respect, Anıtkabir is not merely a mausoleum; it functions as a memory space where national memory, the image of the founding leader, and the ideals of the Republic are represented through a ceremonial spatial experience.

ISBN NR. : 978-625-8795-33-2

The enhancement through additions strategy can be evaluated through the İzmir Historical Gas Factory. The registered structures of this industrial heritage site have been restored, and buildings such as warehouses and foundries have been adaptively reused as exhibition halls, art workshops, reading spaces, and social activity areas (İzmir Büyükşehir Belediyesi, 2024). In this process, the industrial heritage has not been completely erased; rather, it has been integrated into contemporary urban life through new functions and public uses. Thus, the site has been transformed from an industrial production facility of the past into a memory space that preserves urban memory and gains new vitality through public engagement.

The contextual design strategy can be evaluated through the Bursa Merinos Cultural Center and Park. The production history and industrial identity of the Merinos Factory have been reinterpreted through the integration of the park, cultural center, museums, and recreational uses (Alagöz, 2017). In this example, memory is not reconstructed solely through the preservation of existing buildings; rather, it is recreated through the site's green landscape, pedestrian routes, cultural functions, and everyday public uses. Therefore, Bursa Merinos Cultural Center and Park represents an example of how industrial memory can be integrated into a new urban landscape context.

The evoking absence strategy can be interpreted through the 10 October Labor, Peace and Democracy Memorial Square and Memorial Site in Ankara. The site was designed to sustain the memory of those who lost their lives on 10 October 2015 in public space, to commemorate social loss, and to provide a spatial response to acts of remembrance (On Ekim Anıt Meydanı, n.d.). Within the scope of this study, the site can be associated with the evoking absence strategy due to its ability to transform concepts such as loss, pause, mourning, and collective remembrance into components of public space experience. In this respect, a conceptual parallel can be established with the approach of absence, mourning, and collective memory represented in the National September 11 Memorial. The association established with Turkish case studies indicates that the memory-space regeneration strategies developed through the selected global examples can also be utilized in interpreting different geographical and cultural contexts. Historical street fabrics, archaeological sites, national monuments, industrial heritage areas, public parks, and traumatic memory spaces can be evaluated through similar strategic approaches in terms of local images, symbolic expressions, user experience, and collective memory functions.

5. DISCUSSION AND CONCLUSION

The examples examined within the scope of this study demonstrate that the regeneration of memory spaces is not limited solely to physical conservation or spatial arrangements. The preservation of historical traces, the visibility of local images, symbolic representation, visitor experience, spatial orientation, and collective memory functions emerge as complementary components in reconnecting memory spaces with contemporary public life. The six sites examined in this study—Hiroshima Peace Memorial Park, Landschaftspark Duisburg-Nord: Piazza Metallica, The High Line Park, the Historic Centre of Warsaw, the Mamayev Kurgan Memorial Complex and The Motherland Calls monument, and the National September 11 Memorial—represent different types of memory and various memory-space regeneration strategies. These examples demonstrate that there is no single design approach applicable to the

ISBN NR. : 978-625-8795-33-2

regeneration of memory spaces; rather, each site requires different strategies according to its historical, cultural, political, and social context.

The comparison of the examples reveals that the relationship established with the past in memory spaces varies according to the historical and social background of each site. While the physical testimony of destruction is preserved in Hiroshima, industrial traces in Duisburg are supported through new public uses; the infrastructural heritage of the High Line is integrated into a broader urban landscape context, whereas the destroyed historical fabric of Warsaw is reconstructed. At Mamayev Kurgan, war memory is glorified through monumental scale and a ceremonial route, while at the National September 11 Memorial, loss and absence are transformed into an experiential condition through voids, water, and names. These differences demonstrate that there is no single universal intervention method for the regeneration of memory spaces. In this context, the main finding of the study is that preserving the physical traces of the past alone is not sufficient for the regeneration of memory spaces. In the examined memory spaces, historical context, local image, symbolic expression, visitor experience, spatial orientation, and collective memory function operate in an interconnected manner. In other words, memory spaces are not merely areas that are seen or visited; they are public spaces experienced through embodied and sensory actions such as walking, pausing, orienting, touching, and remembering.

The strategies examined in this study—non-intervention, enhancement through additions, reconstruction, contextual design, commemoration and monumentalization, and evoking absence—provide a conceptual framework for understanding the different ways in which the past can be represented within space. These strategies should not be considered as rigid and mutually exclusive categories; rather, they should be evaluated as flexible approaches that may coexist or be applied with different levels of emphasis depending on the historical characteristics and memory type of each site. The associated examples selected from Türkiye indicate that the developed strategic framework can be utilized in interpreting different historical and cultural contexts. However, these examples were not analyzed in the same depth and with the same criteria as the global case studies; rather, they were examined to reveal the possible reflections of the strategies within the context of Türkiye. Therefore, this association does not aim to prove the direct applicability of the framework to memory spaces in Türkiye but instead provides a conceptual starting point for future detailed field research.

In conclusion, the regeneration of memory spaces is not limited to the preservation, monumentalization, or physical arrangement of the past. This process requires a holistic design approach in which local images, historical traces, symbolic narratives, sensory experiences, and collective memory functions are considered together. Memory spaces are not passive areas that merely carry the past into the present; rather, they are dynamic urban landscapes that are continuously reproduced through user experience, that strengthen identity and a sense of belonging, and that integrate social memory into contemporary public life. Within this framework, memory spaces in Türkiye can be reconsidered within their own local contexts through the memory-space regeneration strategies revealed by successful examples from around the world. In this way, these areas can be evaluated not only as historical or monumental

places that need to be preserved, but also as public memory spaces that are integrated with user experience and brought back into everyday life.

REFERENCES

Abacıoğlu Gitmiş, E., & Yardimcioğlu, Y. (2026). Transformation of an obsolete railway heritage into an urban landscape: The High Line case. *ArtGRID- Journal of Architecture, Engineering and Fine Arts, 8* (1), 111–124. https://doi.org/10.57165/artgrid.1896618

Acun, C. (2021). Hafıza Mekânlarında Sanatın Bir İletişim ve Öğrenme Biçimi Olarak Kullanılması. *Galatasaray Üniversitesi İletişim Dergisi* (7), 6–33. https://doi.org/10.16878/gsuilet.942919

Ak, M. (2018). Kültürel kimlik ve toplumsal hafıza mekânları olarak ziyaret yerleri. *Turkish Studies, 13*(3), 13–25. https://doi.org/10.7827/TurkishStudies.12936

Alagöz, M. (2017). Eskimiş endüstri alanlarına kentsel değeri artırma adına işlev kazandırma: Bursa Merinos Kültür Merkezi ve Parkı. *Uluslararası Hakemli Tasarım ve Mimarlık Dergisi*, (10), 219–237. https://doi.org/10.17365/TMD.2017.1.004.x

Anıtkabir. (n.d.). *Anıt blok hakkında*. https://www.anitkabir.tsk.tr/02_insaasi/anit_blok_hakkinda.html

Assmann, J. (2001). *Kültürel bellek: Eski yüksek kültürlerde yazı, hatırlama ve politik kimlik* (A. Tekin, Çev.). Ayrıntı Yayınları.

Aytaç, Ö. (2013). Kent Mekânları ve Kimlik/Farklılık Sorunu. *İDEALKENT, 4*(9), 138–169. https://izlik.org/JA39AY67HP

Başaran İnce, G. (2010). Medya ve Toplumsal Hafıza. *Kültür ve İletişim, 13 (1)*, 9–30. https://izlik.org/JA56UW76BD

Bayraktar, P. (2018). *Savaş sonrası kentlerin yapılanmasına analitik bir yaklaşım* [Yüksek lisans tezi, Yıldız Teknik Üniversitesi]. YÖK Ulusal Tez Merkezi (Tez No. 536383).

Biçer, Ü., Erdinç, S. Y., & Öktem Erkartal, P. (2025). Forms of Remembering: Spaces of memory & memory of Spaces. *Mekansal Araştırmalar Dergisi, 3*(2), 165–182. https://doi.org/10.71298/maddergi.1777986

Black, K. J., & Richards, M. (2020). Eco-gentrification and who benefits from urban green amenities: NYC's High Line. *Landscape and Urban Planning, 204*, 103900. https://doi.org/10.1016/j.landurbplan.2020.103900

Casey, E. S. (1987). *Remembering: A phenomenological study*. Indiana University Press.

Cassirer, E. (1980). *İnsan Üstüne Bir Deneme*. N. Arat (Çev.). Remzi Kitabevi.

Chertoff, D. B., Schatz, S. L., McDaniel, R., & Bowers, C. A. (2008). Improving presence theory through experiential design. *Presence: Teleoperators and Virtual Environments, 17*(4), 405–413. https://doi.org/10.1162/pres.17.4.405

Degen, M. M., & Rose, G. (2012). The sensory experiencing of urban design: The role of walking and perceptual memory. *Urban Studies, 49*(15), 3271–3287. https://doi.org/10.1177/0042098012440463

Downing, F. (2003). Transcending memory: Remembrance and the design of place. *Design Studies, 24*(3), 213–235. https://doi.org/10.1016/S0142-694X(02)00053-4

Ergan, M. F., & Gormus, S. (2023). Peyzaj tasarımlarını mekânsal üçlü kuramı üzerinden okumak: High Line örneği. *6th International Conference of Contemporary Affairs in Architecture and Urbanism–ICCAUA, 6*(1), 600–612. https://doi.org/10.38027/iccaua2023tr0010

Günaçan, S., & Erdoğan, E. (2018). Peyzaj mimarlığı ve hafıza mekânları: İstanbul, Tarihi Yarımada örneği. *Journal of Architectural Sciences and Applications, 3*(1), 34–53. https://doi.org/10.30785/mbud.397380

Halbwachs, M. (1992). *On collective memory* (L. A. Coser, Ed. & Trans.). University of Chicago Press.

Hashmi, M., Kushwaha, N., & Ali, M. (2019). A review paper on modeling & designing of human statue–Tall structure using STAAD-Pro software. *International Journal of Trend in Scientific Research and Development, 3*(4), 1698–1702.

Ivashko, Y., Dmytrenko, A., Pawłowska, A., Lisińska-Kuśnierz, M., Krupa, M., Tišliar, P., Hlushchenko, A., Serafin, A., & Shpakov, A. (2024). Destruction of the architectural heritage as a result of war: The experience of reconstruction (conservation and logistical aspects). *International Journal of Conservation Science, 15*(Special Issue 1), 17–30. https://doi.org/10.36868/IJCS.2024.SI.02

İzmir Büyükşehir Belediyesi. (2024). *Tarihi Havagazı Fabrikası*. https://www.izmir.bel.tr/tr/projeler/tarihi-havagazi-fabrikasi-kultur-merkezi/1382/4

Jelić, A. (2015). Designing "pre-reflective" architecture: Implications of neurophenomenology for architectural design and thinking. *Ambiances*, (1). https://doi.org/10.4000/ambiances.628

Karadayı Yenice, T., & Altınoluk, Ü. (2019). New uses for old buildings: The case of 'Soğukçeşme' Street, İstanbul, Turkey. *ICONARP International Journal of Architecture and Planning, 7*(1), 314–329. https://doi.org/10.15320/ICONARP.2019.77

Kaya, S., Yerli, Ö., & Döner, S. (2015). Endüstriyel Alanların Endüstriyel Parklara Dönüşümü. *Düzce Üniversitesi Bilim ve Teknoloji Dergisi, 3*(2), 518–534. https://izlik.org/JA57SN57UZ

Krasucki, M. (2024). *The reconstruction of Warsaw Old Town, Poland* [Conference presentation]. International Forum "Vilnius and Other World Heritage Cities."

Littke, H., Locke, R., & Haas, T. (2013). Taking the High Line: Elevated parks, evolving neighborhoods, and the ever-changing relationship between urban and nature. *Fábos Conference on Landscape and Greenway Planning, 4*(1). https://doi.org/10.7275/fabos.779

Lynch, K. (1960). *The image of the city*. MIT Press.

Lowe, K. (2020). *Prisoners of history: What monuments to the Second World War tell us about our history and ourselves*. William Collins.

Mahadin, Y. (2016). *Park design and user behavior pattern: A case study of the High Line Park in New York* [Yüksek lisans tezi, Mississippi State University]. Scholars Junction. https://hdl.handle.net/11668/17461

Maki, R., & Niihata, T. (2020). Landscape design in Hiroshima Peace Memorial Park: Transition of the design by Kenzo Tange. *Japan Architectural Review, 3*(2), 193–204. https://doi.org/10.1002/2475-8876.12136

Memorial complex Mamayev Kurgan—Main information. (n.d.). Mamaev-Hill. https://mamaev-hill.ru/

Merleau-Ponty, M. (2012). *Göz ve tin* (A. Soysal, Çev.). Metis Yayınları.

Millington, N. (2015). From urban scar to 'park in the sky': Terrain vague, urban design, and the remaking of New York City's High Line Park. *Environment and Planning A, 47*(11), 2324–2338. https://doi.org/10.1177/0308518X15599294

Nidawi, A. M. H. (2019). *A reading of classical and counter-monuments* [Yüksek lisans tezi, Kadir Has Üniversitesi]. https://doi.org/10.13140/RG.2.2.16945.94567

Nora, P. (2006). *Hafıza mekânları* (M. E. Özcan, Çev.). Dost Kitabevi.

Nowobilski, M., & Ligler, H. (2021). The Market Square grammar: Reconstructing the facades of Warsaw's Old Town. In V. Stojaković & B. Tepavčević (Eds.), *Towards a new, configurable architecture: Proceedings of the 39th eCAADe Conference* (Vol. 2, pp. 283–292). eCAADe. https://doi.org/10.52842/conf.ecaade.2021.2.283

On Ekim Anıt Meydanı. (n.d.). *Anma Yeri Uluslararası Fikir ve Tasarım Projesi Yarışması*. https://10ekimanitmeydan.org/

Pallasmaa, J. (2011). *The embodied image: Imagination and imagery in architecture.* John Wiley & Sons.

Pei, W., Guo, X., & Lo, T. (2023). Pre-evaluation method of the experiential architecture based on multidimensional physiological perception. *Journal of Asian Architecture and Building Engineering, 22*(3), 1170–1194. https://doi.org/10.1080/13467581.2022.2074019

Popiołek-Roßkamp, M. (2019). Warsaw: A reconstruction that began before the war. In *Post-war reconstruction: The lessons for Europe* (pp. 44–52). Lebanese American University.

Sevinç, M. (2019). Bir hafıza mekânı olarak kent meydanı ve dönüşümü: Otto Herbert Hajek'in Ankara Hergelen Meydan Projesi örneği. *Akdeniz Sanat, 13*(24), 47–62. https://izlik.org/JA24RL42JB

Taluğ Demiriz, D. Y. (2021). Anı mekânı üzerine etkileşimli tasarım yaklaşımları ve Prof. Dr. İhsan Doğramacı Anı Mekânı örneği. *Sanat Yazıları*, (44), 369–389. https://izlik.org/JA49HL85LW

İstanbul İl Kültür ve Turizm Müdürlüğü. (n.d.). *UNESCO Dünya Miras Listesi ve İstanbul*. https://istanbul.ktb.gov.tr/TR-276200/unesco-dunya-miras-listesi-ve-istanbul.html

UNESCO. (n.d.). *Historic Centre of Warsaw*. UNESCO World Heritage Centre. https://whc.unesco.org/en/list/30/

Uysal, M. (2017). *Peter Zumthor'un fenomenolojik yaklaşımına dayalı deneysel ve deneyimsel bir mekân tasarımı* [Yüksek lisans tezi, İstanbul Teknik Üniversitesi]. İTÜ POLEN. https://polen.itu.edu.tr/items/819bf4b8-e1f2-43f9-bbee-8872a40f0b06

Wowczak, J. (2020). The reconstruction of the Museum of Warsaw—Current architectural interventions in a monument of great significance for the history of conservation in Poland. *Technical Transactions, 117*(1), Article e2020029. https://doi.org/10.37705/TechTrans/e2020029

Yıldırım, H. M., & Paşalıoğlu, C. (2025). Savaş alanları turizmi ve vatanseverlik: Volgograd örneği. *Journal of Tourism and Gastronomy Studies, 13*(2), 2091–2113. https://doi.org/10.21325/jotags.2025.1648

Yurtseven, B. (2021). Kentsel yenileme sürecinde endüstri alanlarının ekolojik yaklaşım ile değerlendirilmesi: Emscher Park örneği. *Kent Akademisi, 14*(1), 260–277. https://doi.org/10.35674/kent.848910

IMAGE REFERENCES

Diller Scofidio + Renfro. (n.d.). The High Line. https://dsrny.com/project/the-high-line

Gürdal, Y. (2024). Hiroşima (Hiroshima) gezi rehberi. Küçük Dünya. https://kucukdunya.com/hirosima-hiroshima-gezi-rehberi/

Kurgan-Mamaev.ru. (n.d.). Mamayev kurgan v Volgograde - Ekskursii 2026, tseny, grafik raboty https://kurgan-mamaev.ru/

Lee, J. S. (n.d.). About the Memorial. National 9/11 Memorial & Museum. https://www.911memorial.org/visit/memorial/about-memorial

Polish Press Agency. (1945). *Warsaw Old Town 1945*. Wikimedia Commons. https://commons.wikimedia.org/wiki/File:Warsaw_Old_Town_1945.jpg (Orijinal yayın yeri: *Warszawa stolica Polski*, 1949, s. 101)

Prelikj, K. (2024). *15 years of NYC's High Line: A closer look at its impact on urban design*. Architizer. https://architizer.com/blog/inspiration/stories/evolution-of-the-high-line-nyc/

Skena Culgan, R. (2025). Guide to the 9/11 Memorial and Museum in NYC. Time Out. https://www.timeout.com/newyork/attractions/9-11-memorial-and-museum

ISBN NR. : 978-625-8795-33-2

UNESCO World Heritage Centre. (n.d.). *Historic Centre of Warsaw- Gallery*. United Nations Educational, Scientific and Cultural Organization. https://whc.unesco.org/en/list/30/gallery/&index=13&maxrows=12

Watchtower Bible and Tract Society of PA. (2014). *"Etkileyici bir simge": Hiroşima Barış Anıtı, Genbaku Kubbesi*. https://www.jw.org/tr/kutuphane/dergiler/g201411/hiro%C5%9Fima-bar%C4%B1%C5%9F-an%C4%B1t%C4%B1/

Volgograda. (2025). V dni prazdnovaniya 80-letiya pobedy "svet velikoy pobedy" ozarit ves mamaev kurgan. https://mamaev-hill.ru/news/v-dni-prazdnovaniya-80-letiya-pobedy-svet-velikoy-pobedy-ozarit-ves-mamaev-kurgan-1920.html

Yılmazer, Z. (2021, 14 Mart). Duisburg-Nord Parkı nasıl dönüştü? Sanayi mirası bugün kamusal yaşama açılıyor. GZT Arkitekt. https://www.gzt.com/mimari/duisburg-nord-parki-nasil-donustu-sanayi-mirasi-bugun-kamusal-yasama-aciliyor-3579692

ISBN NR. : 978-625-8795-33-2

EVALUATION OF THE ANTIBACTERIAL AND ANTIFUNGAL ACTIVITIES OF A NOVEL BIS(1,2,4-TRIAZOLE) DERIVATIVE

Dr. Ergün Gültekin

Science-Technology Research and Application Center, Artvin Coruh University, 08100 Artvin, Türkiye

ergungultekin@artvin.edu.tr https://orcid.org/0000-0001-8007-0567

ABSTRACT

A novel symmetrical bis(1,2,4-triazole) derivative, 5,5′-(butane-1,4-diylbis(sulfanediyl))bis(3-pentyl-4H-1,2,4-triazol-4-amine) (**6**), was synthesized and evaluated for its antibacterial and antifungal activities. The target compound was obtained in 92.67% yield through the reaction of 4-amino-5-pentyl-4H-1,2,4-triazole-3-thiol with 1,4-dibromobutane under basic conditions. Its structure was confirmed by FTIR-ATR, ^{1}H-NMR, and ^{13}C-NMR spectroscopy. Antimicrobial activity was investigated against *Escherichia coli*, *Staphylococcus aureus*, *Streptococcus pyogenes*, and *Candida albicans* using disk diffusion and broth microdilution methods. Compound **6** showed its highest activity against *C. albicans*, producing inhibition zones of 8.33 ± 0.47 and 8.66 ± 0.94 mm at 20 and 10 mg/mL, respectively, with an MIC value of 78 µg/mL. The MIC values against *S. pyogenes*, *S. aureus*, and *E. coli* were 625, 1250, and 20,000 µg/mL, respectively. The susceptibility order was determined as *C. albicans* > *S. pyogenes* > *S. aureus* > *E. coli*. These findings indicate that the synthesized bis(1,2,4-triazole) derivative possesses more promising activity against *C. albicans* than against the tested bacterial strains.

Keywords: 1,2,4-Triazole, bis-triazole, antibacterial activity, antifungal activity.

1. INTRODUCTION

Antimicrobials are a broad group of therapeutic agents that either inhibit the growth of or eliminate pathogenic microorganisms, including bacteria, fungi, viruses, and parasites, and they remain indispensable tools in the management of infectious diseases. These compounds are classified according to both their spectrum of activity and their mechanisms of action, with antibiotics, antifungals, antivirals, and antiparasitics being the most widely recognized categories [1]. However, the extensive and often indiscriminate use of both natural and synthetic antibiotics has accelerated the emergence of resistant microbial strains, creating one of the most pressing global health concerns of the 21st century. This alarming trend is reflected in the escalating morbidity, mortality, and healthcare costs associated with multidrug-resistant bacterial infections [2]. Bacteria develop resistance through several adaptive strategies, such as enzymatic inactivation of antibiotics, target site modification, and notably, the overexpression of efflux pump systems that actively expel antibiotic molecules, thereby reducing intracellular drug concentrations [3,4]. To address these challenges, innovative therapeutic strategies are

ISBN NR. : 978-625-8795-33-2

being pursued. Among them, the use of antibiotic adjuvants, compounds that restore or enhance the efficacy of existing antibiotics, has gained significant attention in medicinal chemistry [5,6]. Furthermore, alternative approaches such as bacteriophage therapy have been revisited, as phages can selectively infect and lyse antibiotic-resistant bacteria, thereby complementing conventional treatment regimens. While promising, it is important to note that bacteria can also evolve resistance against bacteriophages, which may limit their long-term effectiveness [7]. Collectively, these insights underscore the urgent need for sustained research into novel antimicrobials and complementary strategies, particularly those integrating multifunctional heterocyclic frameworks.

In this context, heterocyclic compounds, particularly those containing nitrogen, carbon, and oxygen, have attracted extensive attention due to their structural diversity and broad pharmacological relevance. Notably, around 75% of FDA-approved drugs consist of nitrogen-based heterocyclic structures [8]. Given their potential as drug precursors, azole-derived compounds have emerged as a crucial focus of research for pharmaceutical chemists [9]. 1,2,4-Triazoles represent a significant pharmacophore group among heterocyclic compounds due to their favorable physicochemical properties, including dipole characteristics, high affinity for biological receptors, cell permeability, hydrogen bonding capacity, structural rigidity, organocatalyst, and solubility [10-12]. Furthermore, many heterocyclic compounds containing the 1,2,4-triazole ring demonstrate a wide range of biological activities, such as anticancer, antimicrobial, antifungal, antitubercular, anti-inflammatory, antiviral, antioxidant, antidepressant, antidiabetic, and enzyme inhibition properties [10, 13-15].

Considering the growing need for novel therapeutic agents capable of addressing microbial resistance, nitrogen-containing heterocyclic systems, particularly 1,2,4-triazoles, have emerged as promising pharmacophores in modern drug discovery. In this study, we report the synthesis of a new triazole derivative and evaluate its antimicrobial properties to explore its potential as a therapeutic agent.

2. MATERIALS AND METHODS

2.1. General

The starting materials, solvents, and reagents were purchased from Sigma-Aldrich, Merck, and Alfa Aesar, all with ≥98% purity, and used without further purification. Reaction progress was monitored by thin-layer chromatography (TLC) on silica gel HSGF254 plates (0.2 ± 0.03 mm) using ethyl acetate/petroleum benzine (1:6) as the mobile phase and visualized under UV light. Infrared spectra (cm^{-1}) were recorded on a Shimadzu IR Prestige-21 spectrometer, while ^{1}H and ^{13}C NMR spectra were obtained on a Bruker AVANCE 400 MHz spectrometer (400 MHz for ^{1}H, 100 MHz for ^{13}C) using DMSO-d_6 as solvent ($\delta H = 2.50$ ppm, $\delta C = 40$ ppm). Coupling constants (J) are given in Hz. 4-Amino-5-pentyl-4H-1,2,4-triazol-3-thiol (**5**) was synthesized according to a previously reported method [16].

2.2. Synthesis of 5,5'-(butane-1,4-diylbis(sulfanediyl))bis(3-pentyl-4H-1,2,4-triazol-4-amine) (6)

4-Amino-5-pentyl-4*H*-1,2,4-triazole-3-thiol (**5**) (2.0 equiv) was dissolved in ethanol, and potassium hydroxide (2.0 equiv) was added to the solution. The reaction mixture was stirred under reflux to generate the corresponding potassium thiolate intermediate. Subsequently, 1,4-dibromobutane (1.0 equiv), dissolved in a small amount of ethanol, was added dropwise to the reaction mixture. The

ISBN NR. : 978-625-8795-33-2

resulting mixture was heated under reflux until completion of the reaction, as monitored by thin-layer chromatography.

After completion, the reaction mixture was allowed to cool to room temperature, and the solvent was removed under reduced pressure. The residue was treated with distilled water to remove inorganic salts. The resulting solid product was collected by filtration, washed thoroughly with water, dried, and purified by recrystallization from a suitable solvent to afford 5,5'-(butane-1,4-diylbis(sulfanediyl))bis(3-pentyl-4H-1,2,4-triazol-4-amine) (**Figure 1**).

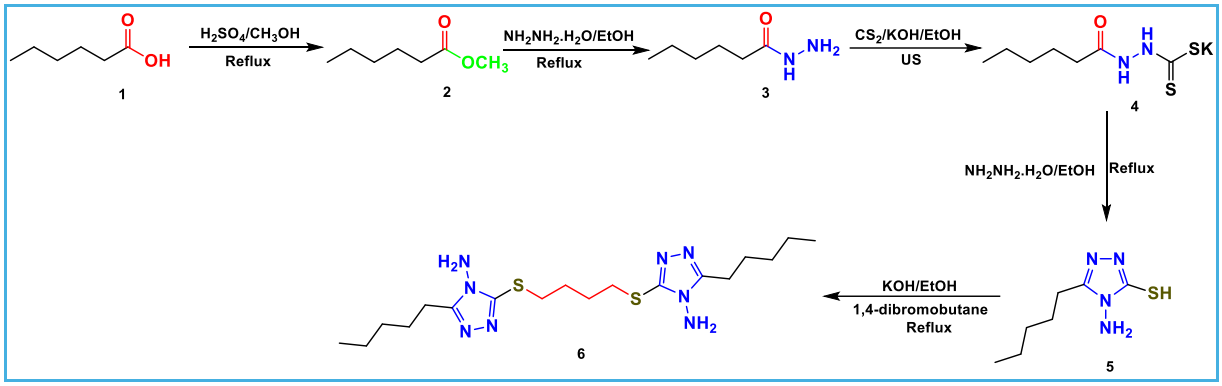

Figure 1. The synthesis route of 5,5'-(butane-1,4-diylbis(sulfanediyl))bis(3-pentyl-4H-1,2,4-triazol-4-amine) compound.

White solid (92.67% yield); (TLC, ethyl acetate: hexane 1:5); **IR (FTIR-ATR, υ_{max} in cm^{-1}):** 3305, 3170 (NH_2), 2954, 2926, 2856 (Al. CH); 1620 (C=N); **^{1}H-NMR (DMSO-d_6, δ ppm):** 0.86 (bs, 6H, CH_3), 1.29-1.30 (m, 8H), 1.63 (t, 4H, j=8.00 Hz), 1.75 (bs, 4H), 2.61 (t, 4H, j=8.00 Hz), 3.08 (bs, 4H), 5.78 (s, 4H, NH_2); **^{13}C-NMR (DMSO-d_6, δ ppm):** 14.33 ($2CH_3$), 22.24 ($2CH_2$), 23.99 ($2CH_2$), 26.31 ($2CH_2$), 28.61 ($2CH_2$), 30.87 ($2CH_2$), 31.33 ($2CH_2$), 151.21 (triazole C-3), 156.55 (triazole C-5).

2.3. Antimicrobial Activities

2.3.1. Disk Diffusion Method

Antimicrobial activity was assessed by a disk diffusion assay adapted from Balouiri et al. (2016) [17]. Gram-positive representatives were *Streptococcus pyogenes* ATCC 19615 and *Staphylococcus aureus* ATCC 25923; Gram-negative strains were *Escherichia coli* ATCC 25922; yeast/mold representatives were *Candida albicans* ATCC 10231. Overnight cultures were adjusted to 0.5 McFarland (~1.5 × 10^8 CFU/mL) and spread on Mueller-Hinton Agar (MHA). Sterile 6 mm blank disks were placed on the lawns and loaded with 15 µL of test solutions in DMSO (20 and 10 mg/mL). Plates were held at 4 °C for 2 h to facilitate diffusion. Chloramphenicol (10.24 µg/disc) served as the positive control and DMSO as the negative control. Bacterial plates were incubated at 37 °C for 24 h and yeast plates at 28 °C for 48 h; inhibition zone diameters were then measured with a ruler.

2.3.2. Minimum Inhibitory Concentration (MIC) Method

MICs were determined by a modified broth microdilution following Humphries et al. (2021) in lidded 96-well plates using Mueller–Hinton Broth (MHB) [18]. Double-strength MHB (100 µL) was dispensed into the first wells and standard-strength MHB (100 µL) into the remaining wells. Sample stocks (20 mg/mL in DMSO) were added to the first wells (100 µL) and two-

ISBN NR. : 978-625-8795-33-2

fold serially diluted to obtain 10 concentrations for each sample and the comparator antibiotic. Inocula (10 µL; 0.5 McFarland) of each pathogen were added. Plates were incubated at 37 °C for 24 h for bacteria and 28 °C for 48 h for yeast. The MIC was defined as the lowest concentration preventing visible growth.

3. RESULT AND DISCUSSION

3.1. Chemistry

In this work, the synthesis and antimicrobial activities of a new bis 1,2,4-triazole derivative (**6**), were investigated. The compound (**6**) was prepared through a five-step synthetic pathway as outlined in Figure 1. Structural confirmation of the newly obtained molecule was carried out using FTIR-ATR, ^{1}H-NMR, and ^{13}C-NMR spectroscopic analyses. Compound (**5**) was synthesized following the previously reported protocol [16].

The IR spectrum (**Figure 2**) of a newly synthesised bis 1,2,4-triazole displayed strong absorptions characteristic of an amine compound. The absorption bands at 3305–3170 cm^{-1} and 2954, 2926, 2856 cm^{-1}, corresponding to the amino group and aliphatic CH groups, respectively, confirm the formation of bis-1,2,4-triazole.

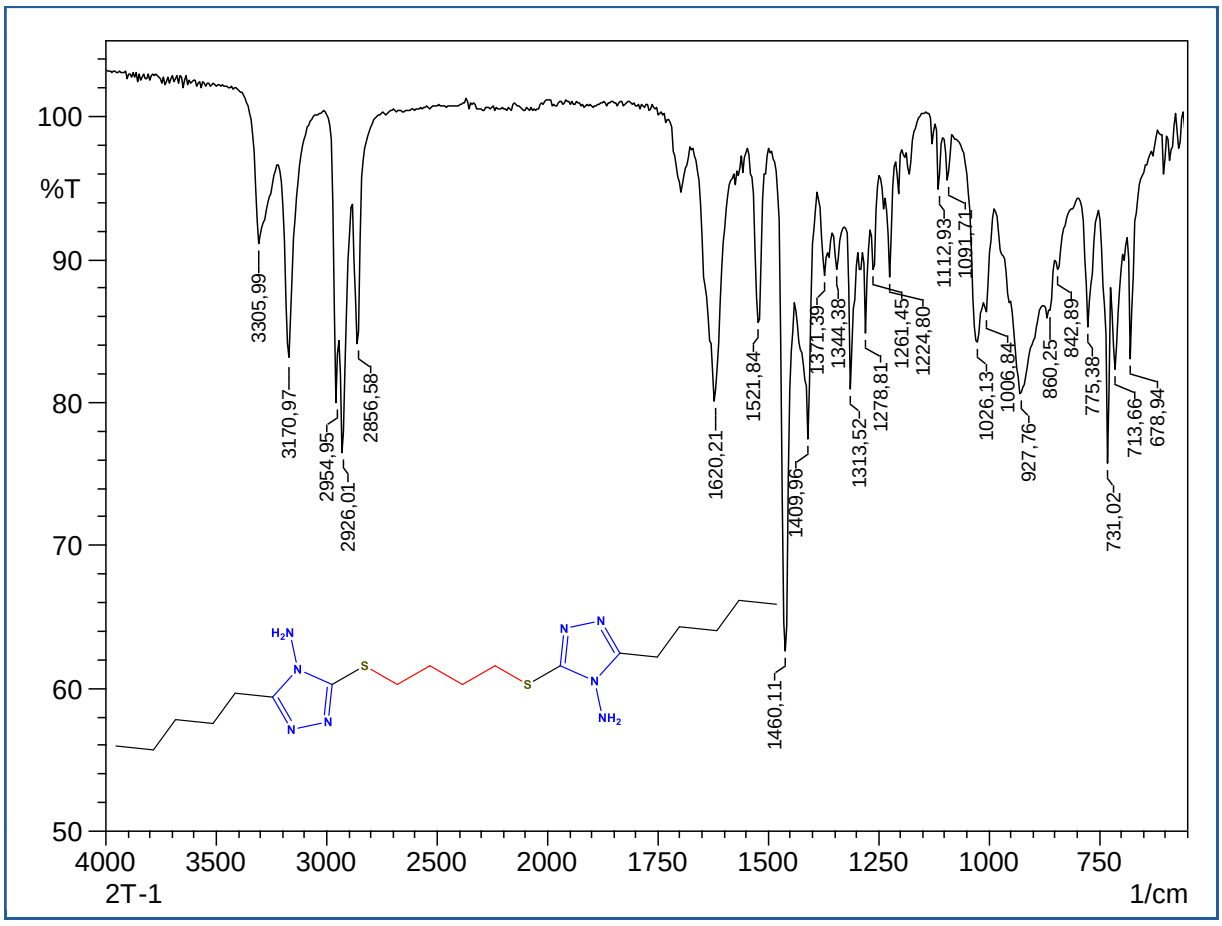

Figure 2. The IR spectrum of newly synthesised bis 1,2,4-triazole.

The ^{1}H NMR spectrum (**Figure 3**) of the compound was consistent with its symmetrical structure. The broad signal observed at δ 0.86 ppm, integrating for six protons, was assigned to

ISBN NR. : 978-625-8795-33-2

the terminal methyl groups of the two pentyl chains. The methylene protons of the pentyl substituents appeared between δ 1.29 and 1.63 ppm, whereas the methylene groups directly attached to the triazole rings were observed as a triplet at δ 2.61 ppm. The signals at δ 1.75 and 3.08 ppm were attributed to the internal and sulfur-bound methylene groups of the –S–$(CH_2)_4$–S– bridge, respectively. In addition, the amino protons appeared as a singlet at δ 5.78 ppm, integrating for four protons.

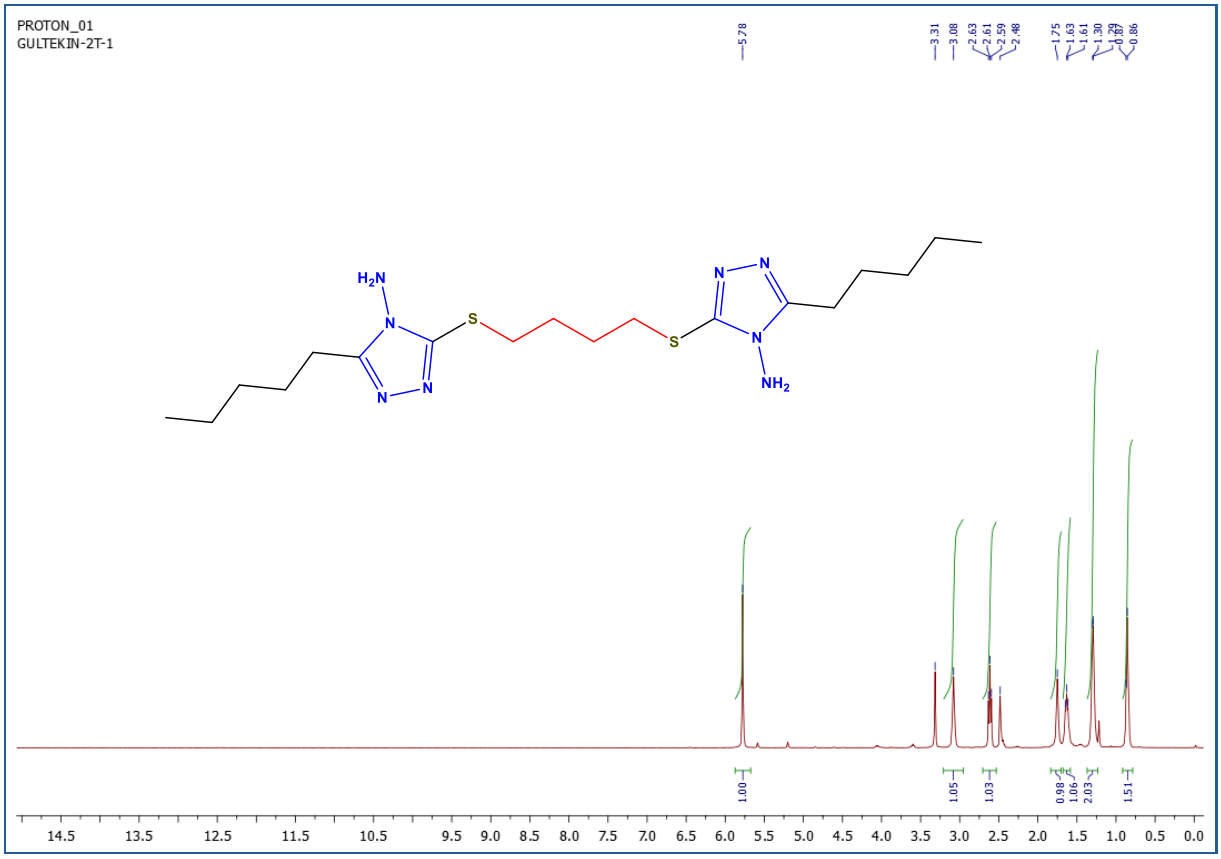

Figure 3. The ^{1}H NMR spectrum of newly synthesised bis 1,2,4-triazole.

The ^{13}C NMR spectrum (**Figure 4**) further supported the proposed structure. The signal at δ 14.33 ppm was assigned to the two equivalent terminal methyl carbons, while six signals between δ 22.24 and 31.33 ppm corresponded to the twelve methylene carbons of the pentyl substituents and the butylene bridge. The resonances at δ 151.21 and 156.55 ppm were attributed to the quaternary C-3 and C-5 carbons of the triazole rings, respectively. The reduced number of resonances resulting from the equivalence of the two molecular halves confirmed the symmetrical structure of 5,5′-(butane-1,4-diylbis(sulfanediyl))bis(3-pentyl-4H-1,2,4-triazol-4-amine).

ISBN NR. : 978-625-8795-33-2

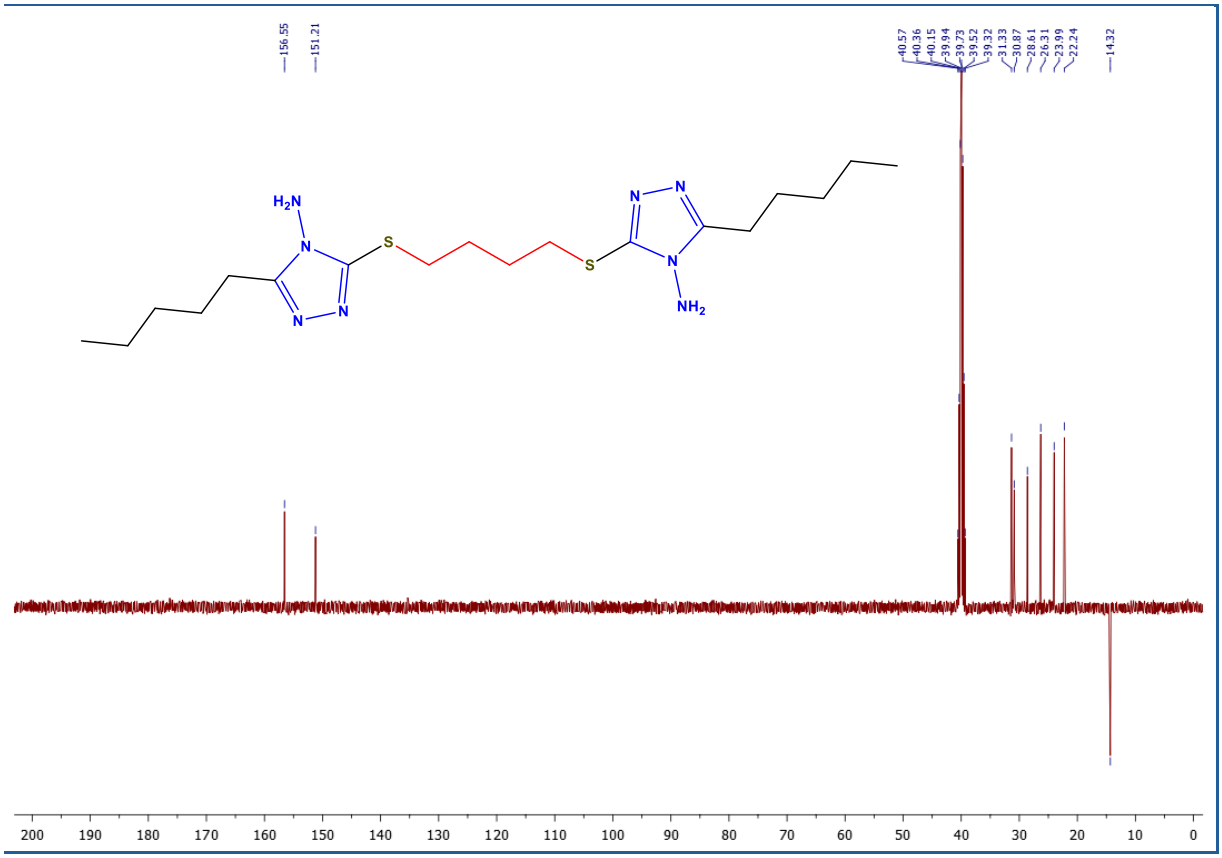

Figure 4. The ^{13}C NMR spectrum of newly synthesised bis 1,2,4-triazole.

3.2. Antimicrobial Activities

Compound **6** showed varying antimicrobial activity against the tested microorganisms (**Table1 and 2**). The highest activity was observed against *C. albicans*, with inhibition zones of 8.33 ± 0.47 and 8.66 ± 0.94 mm at 20 and 10 mg, respectively, and an MIC value of 78 µg/mL. The compound also exhibited activity against *S. pyogenes*, with an MIC value of 625 µg/mL, followed by *S. aureus* with an MIC value of 1250 µg/mL. In contrast, only very weak activity was detected against *E. coli*, for which the MIC value was 20,000 µg/mL. Thus, the susceptibility order was determined as *C. albicans* > *S. pyogenes* > *S. aureus* > *E. coli*. Compared with chloramphenicol, compound **6** displayed considerably weaker antibacterial activity. Nevertheless, its relatively low MIC value against *C. albicans* suggests that the compound may possess more promising antifungal than antibacterial properties.

ISBN NR. : 978-625-8795-33-2

Table 1. Disk diffusion diameters of the synthesized compounds (mm).

		Microorganisms			
		Gram (-)	Gram (+)		Yeast/Mold
Compound	**Concentrations (mg/ml)**	***E. coli* ATCC 25922**	***S. aureus* ATCC 25923**	***S. pyogenes* ATCC 19615**	***C. albicans* ATCC 10231**
6	20	6±0	6±0	6±0	8.33±0.47
	10	6±0	7.33±1.24	7.33±1.24	8.66±0.94
Chloramphenicol	512 µg/mL	19.67±0.47	21.33±0.94	15±0	6±0

Table 2. MIC values of the synthesized compounds (µg/mL)

MIC (µg/mL)	**C. albicans**	**E. coli**	**S. aureus**	**S. pyogenes**
6	78	20000	1250	625
Chloramphenicol	128	256	16	16

4. CONCLUSION

A novel symmetrical bis(1,2,4-triazole) derivative was successfully synthesized in high yield, and its proposed structure was confirmed by FTIR-ATR, ^{1}H-NMR, and ^{13}C-NMR analyses. The antimicrobial results revealed that compound **6** exhibited varying activity against the tested microorganisms. The highest activity was observed against *C. albicans*, with an MIC value of 78 µg/mL, whereas weaker activity was detected against *S. pyogenes* and *S. aureus*. The compound showed very limited activity against *E. coli*, as demonstrated by its high MIC value. Although its antibacterial activity was considerably lower than that of chloramphenicol, the activity observed against *C. albicans* suggests that this bis(1,2,4-triazole) framework may be more promising for the development of antifungal compounds. Further studies using an appropriate antifungal reference drug and additional fungal strains are required to confirm its antifungal potential.

KAYNAKÇA

1. Fair, R. J., Tor, Y., Antibiotics and bacterial resistance in the 21st century, Perspect Med Chem, 6, PMC-S14459, 2014. https://doi.org/10.4137/PMC.S14459
2. Ventola, C. L., The antibiotic resistance crisis: Part 1: Causes and threats, Pharm Ther, 40, 277, 2015.
3. Li, X. Z., Nikaido, H., Efflux-mediated drug resistance in bacteria, Drugs, 64, 159–204, 2004.

4. Munita, J. M., Arias, C. A., Mechanisms of antibiotic resistance, In: Virulence Mechanisms of Bacterial Pathogens, ASM Press, Washington, DC, 481–511, 2016. https://doi.org/10.1128/microbiolspec.VMBF-0016-2015
5. Lázár, V., Pal Singh, G., Spohn, R., Nagy, I., Horváth, B., Hrtyan, M., et al., Bacterial evolution of antibiotic hypersensitivity, Mol Syst Biol, 9, 700, 2013. https://doi.org/10.1038/msb.2013.57
6. Stokes, J. M., MacNair, C. R., Ilyas, B., French, S., Côté, J. P., Bouwman, C., et al., Pentamidine sensitizes Gram-negative pathogens to antibiotics and overcomes acquired colistin resistance, Nat Microbiol, 2, 1–8, 2017. https://doi.org/10.1038/nmicrobiol.2017.28
7. Kortright, K. E., Chan, B. K., Koff, J. L., Turner, P. E., Phage therapy: A renewed approach to combat antibiotic-resistant bacteria, Cell Host Microbe, 25, 219–232, 2019. https://doi.org/10.1016/j.chom.2019.01.014
8. Maddila, S., Pagadala, R., Jonnalagadda, S. B., 1,2,4-Triazoles: A review of synthetic approaches and the biological activity, Lett Org Chem, 10, 693–714, 2013. https://doi.org/10.2174/15701786101013112611544 8
9. Patel, N. B., Khan, I. H., Rajani, S. D., Pharmacological evaluation and characterizations of newly synthesized 1,2,4-triazoles, Eur J Med Chem, 45, 4293–4299, 2010. https://doi.org/10.1016/j.ejmech.2010.06.031
10. Kharb, R., Sharma, P. C., Yar, M. S., Pharmacological significance of triazole scaffold, J Enzyme Inhib Med Chem, 26, 1–21, 2011. https://doi.org/10.3109/14756360903524304
11. Wakale, V. S., Pattan, S. R., Tambe, V., Therapeutic importance of 1,2,4-triazole: A review, Int J Res Pharm Biomed Sci, 4, 985–1001, 2013.
12. Işık, U., Gültekin, E., Karakaş, D. E., Kaya, M., Synthesis and characterization of triazole-based Schiff bases as novel highly efficient organocatalysts for rapid H_2 generation via $NaBH_4$ methanolysis, Fuel, 406, 137052, 2026. https://doi.org/10.1016/j.fuel.2025.137052
13. Sahu, J. K., Ganguly, S., Kaushik, A., Triazoles: A valuable insight into recent developments and biological activities, Chin J Nat Med, 11, 456–465, 2013. https://doi.org/10.1016/S1875-5364(13)60084-9
14. Ünlüer, D., Ünver, Y., Düğdü, E., Alpaslan, Y. B., Köysal, Y., Soylu, M. S., Sancak, K., Novel 1,2,4-triazole derivatives: Structure, DFT study, X-ray analysis, and antimicrobial activity, Russ J Org Chem, 55, 254–261, 2019. https://doi.org/10.1134/S1070428019020192
15. Gültekin, E., Pyridine hybrid 1,2,4-triazole-5-thione–Schiff base derivatives: Synthesis, characterization, antimicrobial, and antioxidant activity evaluations, J Sulfur Chem, 47, 182–199, 2026. https://doi.org/10.1080/17415993.2025.2594083
16. Gültekin, E., Ultrasound-assisted 1,2,4-triazole Schiff bases: Synthesis, characterization, docking, and dual inhibition of urease and α-glucosidase, Future Medicinal Chemistry, 18, 13, 1701–1711, 2026. https://doi.org/10.1080/17568919.2026.2675977
17. Balouiri, M., Sadiki, M., Ibnsouda, S. K., Methods for in vitro evaluating antimicrobial activity, J Pharm Anal, 6, 71–79, 2016. https://doi.org/10.1016/j.jpha.2015.11.005
18. Humphries, R., Bobenchik, A. M., Hindler, J. A., et al., Changes to antimicrobial susceptibility testing standards, J Clin Microbiol, 59, e00213-21, 2021. https://doi.org/10.1128/JCM.00213-21

ISBN NR. : 978-625-8795-33-2

IMPACT OF MATCHA FORTIFICATION ON THE PHYSICOCHEMICAL CHARACTERISTICS AND ANTIOXIDANT ACTIVITY OF COW AND OAT KEFIRS

Master's Student Zeynep Çağla TEKGÜL

Atatürk University, Institute of Science, Department of Food Engineering, 25240, Erzurum, Türkiye,

tekgulcagla@gmail.com - https://orcid.org/0009-0003-6462-5042

Asst. Prof. Veysel Fatih ÖZDEMİR

Atatürk University, Faculty of Agriculture, Department of Animal Science, 25240, Erzurum, Türkiye,

veysel.ozdemir@atauni.edu.tr - https://orcid.org/0000-0003-3035-7695

Res. Asst. PhD Burak BAYRAK

Atatürk University, Faculty of Pharmacy, Department of Analytical Chemistry, 25240, Erzurum, Türkiye

burak.bayrak@atauni.edu.tr - https://orcid.org/0000-0001-6550-6916

Asst. Prof. Murat Emre TERZİOĞLU*

Atatürk University, Faculty of Agriculture, Department of Food Engineering, 25240, Erzurum, Türkiye

murat.terzioglu@atauni.edu.tr - https://orcid.org/0000-0001-6370-0694

*Corresponding Author: Murat Emre TERZİOĞLU

ABSTRACT

This study aimed to investigate the effects of adding 1.5% matcha powder to kefir samples produced using cow milk and plant-based milk (oat milk) on physicochemical properties and antioxidant capacity. In this context, dry matter, ash, and pH analyses were performed, as well as DPPH and ABTS radical scavenging activity analyses. The addition of matcha powder to kefir samples was found to have a statistically very significant ($p<0.01$) effect on dry matter, ash, pH, and DPPH radical scavenging activity values, and a significant ($p<0.05$) effect on ABTS radical scavenging activity value. Cow kefir was found to have a higher dry matter and ash content compared to oat kefir. On the other hand, oat kefir was observed to have higher pH and DPPH radical scavenging activity values. The addition of matcha powder to kefir samples was shown to increase dry matter, ash, DPPH, and ABTS radical scavenging activity values. It was also found that adding matcha powder led to a decrease in pH levels. In conclusion, it has been determined that the use of oat milk has the potential to impart functional properties to dairy products. Furthermore, it is believed that in the coming years, matcha powder could make significant contributions to health-focused product development in the field of food technology.

Keywords: Plant-based milk, oat kefir, matcha powder, physicochemical properties, antioxidant capacity

ISBN NR. : 978-625-8795-33-2

1. INTRODUCTION

Due to increasing lactose intolerance among individuals, as well as the adoption of healthy lifestyles and vegan diets, interest in plant-based products such as matcha has increased worldwide (Yerlikaya et al., 2025). Matcha, sold in fine powder form, plays a strategic role in the global beverage market (Gerasopoulos et al., 2026). Matcha, which is essentially green tea, has positive effects against cancer and many other diseases thanks to its antioxidant properties. Tea polyphenols, one of its main active components, exhibit liver-protective, human gut microbiota-regulating, blood lipid-lowering, and antibacterial properties (Kika et al., 2024; Tao et al., 2026). Matcha, which has become widespread due to its organoleptic properties (flavor, taste, aroma, etc.), offers a high potential for health functions by allowing the consumption of both its soluble and insoluble components in their entirety (Wang et al., 2022). The allergenic properties of dairy products and consumer awareness are driving the dairy industry towards plant-based products (Khaji et al., 2021). Another reason for choosing plant-based beverages is the difference in taste and nutritional composition resulting from product variety (Kulaksız Gunaydı and Cakmak Kafadar, 2026). For example, oat-based drinks contain valuable nutritional components such as dietary fiber and β-glucans. These components, which regulate digestion, support heart health, and lower cholesterol, have the potential to reduce the risk of chronic diseases by modulating physiological processes (Ziarno et al., 2025). Kefir, a fermented product, stands out with its antioxidant activity, along with its antibacterial, hypocholesterolemic, antihypertensive, and anti-inflammatory effects (Ceylan and Öncül, 2025). Adapting kefir as a plant-based beverage instead of animal milk also supports agricultural sustainability and the bioeconomy (Justel et al., 2025).

Based on this data in the literature, the combination of matcha, which has a high bioactive component content, and kefir, a functional fermented beverage, with plant-based milk is important both in terms of its potential for new product development and its synergistic effects on health. This research aimed to determine the physicochemical and antioxidant effects of matcha powder, which has a high antioxidant capacity, on traditional (cow milk) and alternative plant-based (oat milk) kefir matrices. In this study design, plain kefirs obtained from the specified milk types and their matcha-added versions were compared in detail in terms of some quality parameters (dry matter, ash, and pH) and DPPH and ABTS radical scavenging activities.

2. MATERIALS AND METHODS

2.1. Materials

The cow milk used as a control group in kefir production was purchased from Atatürk University Food and Animal Husbandry Application and Research Center (Erzurum, Türkiye). The oatmeal (Eti Lifalif Oatmeal), kefir cultures (VIVO Kefir Starter Culture), matcha (Herby Premium Matcha), and honey (Balparmak Strained Honey) used as raw materials in the production of plant-based kefirs were sourced from local markets in Erzurum, Türkiye.

2.2. Methods

2.2.1. Oat Milk Production

ISBN NR. : 978-625-8795-33-2

In the production of oat milk, oatmeal was mixed with pure water and left to stand for a specific period of time and at a specific temperature (2 hours, 25ºC). The resulting mixture was then homogenized using a food processor and filtered through cheesecloth.

2.2.2. Kefir Production

In kefir production, cow and oat milks, used as raw materials, were pasteurized at 90ºC for 10 minutes after adding 1% honey at 45ºC. Then, 1.5% matcha powder was added to two batches of kefir samples that had been cooled to 75ºC. All kefir samples were then mixed with kefir culture at 25ºC and incubated until the pH reached 4.6±0.1. After the incubation process, the kefir samples, whose clots had been broken, were kept at 4ºC for 24 hours to prepare them for analysis. Images of the kefirs produced are shown in Figure 1.

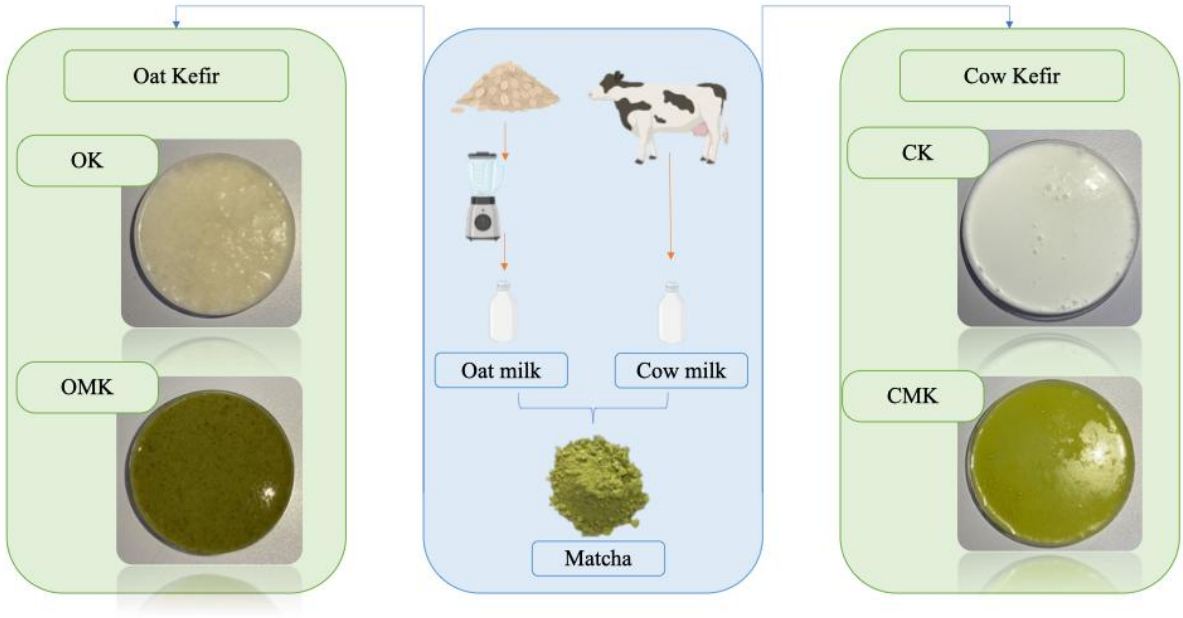

Figure 1. Image of the kefir samples

2.2.3. Physicochemical Properties

Dry matter, ash, and pH analyses of milk and kefir samples were performed according to the methods given by Terzioğlu (2025). In the dry matter analysis, 5 g of kefir was weighed into tared drying containers. The kefirs were then dried at 100-105ºC until they reached a constant weight. In the ash analysis, 1 g of kefir was weighed into crucibles from which the tare weight had been removed, and incineration was carried out at 500-550ºC. For pH analysis of kefir samples, a pH meter that had been calibrated beforehand with buffer solutions was used.

2.2.4. Antioxidant Capacity

3 g of kefir was diluted to 30 mL using methanol (80%). The mixture, centrifuged at 6000 rpm for 15 min, was filtered using Whatman No. 1 filter. Following this step, the extraction process was complete. For 1,1-diphenyl-2-picrylhydrazyl (DPPH) radical scavenging activity analysis, the extract volume was diluted to 0.5 mL using methanol. Then DPPH solution (2.5 mL) was added and mixed. Absorbance measurements of kefir samples were performed at 517 nm. For the 2,2'-azino-bis-3-

ISBN NR. : 978-625-8795-33-2

ethylbenzothiazoline-6-sulfonic acid (ABTS) radical scavenging activity analysis, the extracts were mixed with a 7 mM ABTS solution (prepared with 2.45 nM $K_2S_2O_8$) and methanol to obtain a total volume of 3 mL (adjusted to 0.700 at 734 nm). Absorbance measurements of kefir samples were performed at 734 nm (Terzioğlu, 2026).

2.2.5. Statistical Analysis

This study was conducted using a fully randomized experimental design with factorial arrangement, by adding matcha powder to kefir produced from cow and oat milks. Analysis of variance was performed using the SPSS 25 software package. The differences were interpreted using Duncan's multiple comparison test.

3. RESULTS AND DISCUSSION

3.1. Physicochemical Properties

The dry matter, ash, and pH values of cow milk and oat milk, used as raw materials in kefir production, are presented in Table 1. Cow milk was determined to have a dry matter content of 12.69%, an ash content of 0.55%, and a pH of 6.64, while oat milk have a dry matter content of 6.85%, an ash content of 0.23%, and a pH of 6.76. In this study, when cow milk and oat milk were compared in terms of dry matter and ash content, it was observed that oat milk was significantly weaker in these compounds. Indeed, this nutritional composition deficiency has also been confirmed by Cui et al. (2023). However, the physicochemical properties of cow milk and oat milk were found to be consistent with the literature. Babolanimogadam et al. (2023) reported that the dry matter content of oat milk was 6.02% and the ash content was 0.20%, while Benmeziane and Belleili (2023) reported that the pH value was 6.39. Gupta and Bisla (2019) determined that the moisture content of cow milk has approximately 87.8 g/100g and the ash content has approximately 0.70 g/100g. The researchers stated that oat milk has a moisture content of approximately 90.6 g/100g and an ash content of approximately 0.42 g/100g.

Table 1. Physicochemical analyses of milk and kefir samples

Samples	Dry matter (%)	Ash (%)	pH
CM	12.69±0.21	0.55±0.02	6.64±0.01
OM	6.85±0.12	0.23±0.01	6.76±0.04
CK	$13.45±0.18^{b}$	$0.67±0.01^{b}$	$4.34±0.04^{bc}$
OK	$7.26±0.16^{d}$	$0.27±0.00^{d}$	$4.54±0.02^{a}$
CMK	$15.12±0.33^{a}$	$0.73±0.00^{a}$	$4.25±0.05^{c}$
OMK	$9.08±0.04^{c}$	$0.32±0.02^{c}$	$4.39±0.01^{b}$
Significant	**	**	**

**: p<0.01. CM: Cow milk, OM: Oat milk, CK: Cow kefir, CMK: Cow kefir with matcha, OK: Oat kefir, OMK: Oat kefir with matcha

ISBN NR. : 978-625-8795-33-2

Dry matter, ash, and pH results of kefir samples produced from plain and matcha-added cow and oat milk are given in Table 1. The addition of matcha powder to kefir samples was found to have a statistically very significant ($p<0.01$) effect on dry matter, ash, and pH values. The dry matter, ash, and pH values of all kefir samples ranged from 7.26-15.12%, 0.27-0.73%, and 4.25-4.54, respectively. Compared to kefir samples made from oat milk, kefir samples made from cow milk were found to have higher dry matter and ash content and lower pH values. On the other hand, it was observed that the dry matter and ash content increased in all kefir samples with the addition of matcha powder, while the pH values decreased.

Dinkçi et al. (2015) reported that in kefir samples produced using cow and oat milk, the dry matter content decreased as the proportion of oat milk increased. Özlü and Bölek (2024) found that kefir samples produced using oat milk had a moisture content of 90.58% and an ash content of 0.67%. Furthermore, researchers emphasized that the pH values of oat kefir samples varied between 3.83 and 4.77 depending on the storage period. Ceylan and Öncül (2025) determined that the dry matter content of oat kefir samples ranged from 10.19-10.24%, and the ash content ranged from 0.32-0.35%. Kavaz Yüksel et al. (2017) reported that the addition of matcha powder to ice cream samples resulted in decreases in dry matter and pH values compared to the control group.

3.2. Antioxidant Capacity

The results of the antioxidant capacity analysis of kefirs produced from plain and matcha-added cow and oat milk are given in Table 2. The addition of matcha powder to kefir samples was found to have a statistically very significant ($p<0.01$) effect on DPPH radical scavenging activity values. Additionally, the addition of matcha powder showed significant effects ($p<0.05$) on ABTS radical scavenging activity values. The DPPH radical scavenging activity values of all kefir samples ranged from 11.35% to 29.21%, respectively, while the ABTS radical scavenging activity values ranged from 18.95% to 40.66%. Compared to kefir samples made from cow's milk, kefir samples made from oat milk exhibited higher DPPH radical scavenging activity. On the other hand, it was observed that the addition of matcha to kefir samples increased the DPPH and ABTS radical scavenging activity values.

Table 2. Antioxidant analyses of kefir samples

Samples	**DPPH Radical Scavenging Activity Inhibition (%)**	**ABTS Radical Scavenging Activity Inhibition (%)**
CK	11.35 ± 0.73^{c}	25.96 ± 0.11^{bc}
OK	16.18 ± 0.31^{bc}	18.95 ± 2.24^{c}
CMK	19.04 ± 2.07^{b}	33.89 ± 3.78^{ab}
OMK	29.21 ± 4.45^{a}	40.66 ± 6.26^{a}
Significant	****	*

*: $p<0.05$; **: $p<0.01$. CK: Cow milk kefir, CMK: Cow milk kefir with matcha, OK: Oat milk kefir, OMK: Oat milk kefir with matcha

ISBN NR. : 978-625-8795-33-2

Moretto et al. (2021) reported that vitamin E, as well as phenolic compounds such as caffeic acid and ferulic acid, have an effect on the antioxidant capacity of oat-based beverages. On the other hand, Koláčková et al. (2020) and Devkota et al. (2021) reported that catechins and polyphenol compounds in the composition of matcha play an active role in its high antioxidant capacity. Tosun Demir and Korkmaz (2025) reported that the antioxidant capacity of matcha powders of Turkish origin is in the range of 1257.00-1481.60 µmol trolox/g by the DPPH method and 1118.30-1596.40 µmol trolox/g by the ABTS method. Skulska et al. (2025) stated that the high antioxidant capacity of matcha powder enhances the potential functional properties of yogurt, which would provide advantages for positioning the product in the functional foods market.

4. CONCLUSION

According to the results of the current study, adding matcha powder to cow and oat kefir was found to have positive effects on various physicochemical properties and antioxidant capacity. These increases in dry matter, ash, and antioxidant activity in kefir samples with matcha powder addition can be attributed to the increase in polyphenolic compounds and mineral content. Furthermore, it has been shown that using matcha powder along with oat milk in kefir production can further improve the functional properties of the product. In light of these results, the widespread use of matcha powder in products made with plant-based milks in the dairy industry is important both for consumer health and product quality.

REFERENCES

Babolanimogadam, N., Gandomi, H., Akhondzadeh Basti, A., & Taherzadeh, M. J. (2023). Nutritional, functional, and sensorial properties of oat milk produced by single and combined acid, alkaline, α-amylase, and sprouting treatments. Food Science & Nutrition, 11(5), 2288-2297. https://doi.org/10.1002/fsn3.3171

Benmeziane, F., & Belleili, I. (2023). An innovative approach: Formulation and evaluation of fermented oat milk using native yoghurt cultures. Measurement: Food, 12, 100113. https://doi.org/10.1016/j.meafoo.2023.100113

Ceylan, B., & Öncül, N. (2025). Production of probiotic kefir from different plant-based milks. Cogent Food & Agriculture, 11(1), 2458351. https://doi.org/10.1080/23311932.2025.2458351

Cui, L., Jia, Q., Zhao, J., Hou, D., & Zhou, S. (2023). A comprehensive review on oat milk: From oat nutrients and phytochemicals to its processing technologies, product features, and potential applications. Food & Function, 14(13), 5858-5869. https://doi.org/10.1039/d3fo00893b

Devkota, H. P., Gaire, B. P., Hori, K., Subedi, L., Adhikari-Devkota, A., Belwal, T., Paudel, K. R., Jha, N. K., Singh, S. K., Chellappan, D. K., Hansbro, P. M., Dua, K., & Kurauchi, Y. (2021). The science of matcha: bioactive compounds, analytical techniques and biological properties. Trends in Food Science & Technology, 118(Part A), 735-743. https://doi.org/10.1016/j.tifs.2021.10.021

Dinkçi, N., Kesenkaş, H., Korel, F., & Kınık, Ö. (2015). An innovative approach: Cow/oat milk based kefir. Mljekarstvo, 65(3), 177-186. https://doi.org/10.15567/mljekarstvo.2015.0304

Gerasopoulos, A., Gerasopoulos, G., Giota, E., & Lazari, D. (2026). Matcha tea quality and functional effects on gut microbiome: A comprehensive systematic review. Food Reviews International, 1-28. https://doi.org/10.1080/87559129.2026.2653654

Gupta, S., & Bisla, G. (2019). Nutritional and sensory characteristics of oat milk based yoghurt. International Journal of Applied Home Science, 6(6-8), 261-265. https://doi.org/10.36537/IJAHS/6.6-8/261-265

Justel, M. A., Outeiriño, E. B., & Guerra, N. P. (2025). Production of kefir and kefir-like beverages: Fundamental aspects, advances, and future challenges. Processes, 14(1), 73. https://doi.org/10.3390/pr14010073

Kavaz Yüksel, A., Yüksel, M., & Şat, İ. G. (2017). Determination of certain physicochemical characteristics and sensory properties of green tea powder (matcha) added ice creams and detection of their organic acid and mineral contents. Gıda, 42(2), 116-126. https://doi.org/10.15237/gida.GD16072

Khaji, F., E Mousavi, Z., Kiani, H., & Razavi, S. H. (2021). The investigation of probiotics viability, physicochemical and rheological properties of a probiotic dessert based on sesame paste (Tahini). Journal of Food and Bioprocess Engineering, 4(2), 105-111. https://jfabe.ut.ac.ir/

Kika, J., Jakubczyk, K., Ligenza, A., Maciejewska-Markiewicz, D., Szymczykowska, K., & Janda-Milczarek, K. (2024). Matcha green tea: Chemical composition, phenolic acids, caffeine and fatty acid profile. Foods, 13(8), 1167. https://doi.org/10.3390/foods13081167

Koláčková, T., Kolofiková, K., Sytařová, I., Snopek, L., Sumczynski, D., & Orsavová, J. (2020). Matcha tea: Analysis of nutritional composition, phenolics and antioxidant activity. Plant Foods for Human Nutrition, 75(1), 48-53. https://doi.org/10.1007/s11130-019-00777-z

Kulaksız Gunaydı, Z. E., & Cakmak Kafadar, G. (2026). Plant-based dairy alternatives: comprehensive insights into technology, functionality, nutrition and health. European Food Research and Technology, 252(4), 189. https://doi.org/10.1007/s00217-026-05122-8

Moretto, L., Tonolo, F., Folda, A., Scalcon, V., Bindoli, A., Bellamio, M., Feller, E., & Rigobello, M. P. (2021). Comparative analysis of the antioxidant capacity and lipid and protein oxidation of soy and oats beverages. Food Production, Processing and Nutrition, 3(1), 1-10. https://doi.org/10.1186/s43014-020-00046-6

Özlü, Z. C., & Bölek, S. (2024). Use of *Neopyropia yezoensis* in enriching vegan kefir from oat milk. International Journal of Gastronomy and Food Science, 38, 101045. https://doi.org/10.1016/j.ijgfs.2024.101045

Skulska, I. V., Tsisaryk, O. Y., & Holubev, V. Y. (2025). Development of matcha yogurt technology and its physiological-hygienic assessment. Scientific Messenger of LNU of Veterinary Medicine and Biotechnologies. Series: Food Technologies, 27(104), 61-67. https://doi.org/10.32718/nvlvet-f10410

Tao, X., Li, Y., Liu, L., Chen, S., Wang, Z., Gao, X., & Chen, Q. (2026). Preparation, characterization and antioxidant effects on processed sausages of ultrafine green tea powder emulsions. Journal of Food Science, 91(2), e70931. https://doi.org/10.1111/1750-3841.70931

Terzioğlu, M. E. (2025). Comparison of vegan kefirs enriched with date seed powder with kefirs produced from cow milk in terms of physicochemical properties, free amino acid profile, organic acid profile and phenolic compound profile. International Journal of Gastronomy and Food Science, 41, 101272. https://doi.org/10.1016/j.ijgfs.2025.101272

Terzioğlu, M. E. (2026). Effect of fresh and dried broccoli (*Brassica oleracea* var. *italica*) florets and stems on properties of camel kefirs. Italian Journal of Food Science, 38(1), 336-348. https://doi.org/10.15586/ijfs.v38i1.3242

Tosun Demir, M. N., & Korkmaz, F. (2025). Türkiye ve Japonya menşeli matcha tozlarının fizikokimyasal ve duyusal özelliklerinin karşılaştırılması. Gıda, 50(6), 1186-1199. https://doi.org/10.15237/gida.GD25099

Wang, Y., Yu, Y., Ding, L., Xu, P., & Zhou, J. (2022). Matcha green tea targets the gut–liver axis to alleviate obesity and metabolic disorders induced by a high-fat diet. Frontiers in Nutrition, 9, 931060. https://doi.org/10.3389/fnut.2022.931060

Yerlikaya, O., Ertem Oztekin, H., & Balta, Y. (2025). Plant-based milk alternatives in kefir production: A review. Journal of Food Safety and Food Quality-Archiv für Lebensmittelhygiene, 76(6), 45815. https://doi.org/10.31083/JFSFQ45815

Ziarno, M., Zaręba, D., Kowalska, E., & Florowski, T. (2025). The effect of varying oat beverage ratios on the characteristics of fermented dairy–oat beverages. Applied Sciences, 15(6), 3219. https://doi.org/10.3390/app15063219

ISBN NR. : 978-625-8795-33-2

EFFECT OF RAW FIBER SUPPLEMENTATION ON THE GROWTH PERFORMANCE AND BLOOD PROFILE OF SUCKLING HOLSTEIN CALVES

Ali M. Jafari, Marjan S. Moradi, Hamid R. Ghaffari
Faculty of Veterinary Medicine, Ferdowsi University of Mashhad, Iran

ABSTRACT

This study investigates the impact of raw fiber supplementation on growth performance and blood biochemical profiles of suckling Holstein calves during the pre-weaning phase. Seventy-two newborn calves were randomly allocated to four dietary treatments: control (no supplement), 1.5% raw wheat bran, 3% raw wheat bran, and 1.5% sugar beet pulp across a 60-day trial. Body weight, average daily gain, starter intake, and feed efficiency were monitored weekly alongside blood sampling for glucose, BUN, total protein, albumin, cholesterol, and triglyceride analysis. Results demonstrated linear improvements in average daily gain (0.78 kg/day in 3% wheat bran vs 0.62 kg/day control, $p<0.01$) and starter intake (1.24 kg/day vs 0.89 kg/day, $p<0.05$). Feed efficiency enhanced 22% in fiber-supplemented groups. Serum glucose concentrations increased 18% ($p<0.05$) reflecting improved rumen fermentation, while BUN levels decreased 15% indicating better nitrogen utilization. Total protein and albumin remained stable across treatments, confirming no metabolic stress. Cholesterol levels showed quadratic response peaking at 1.5% supplementation. Fiber treatments significantly reduced weaning age by 4.2 days through enhanced rumen development evidenced by 28% greater volatile fatty acid production. Histological examination confirmed increased papillae length (1.8 mm vs 1.2 mm control). Economic analysis revealed 3.1:1 return on investment through reduced rearing costs. These findings support strategic raw fiber inclusion optimizing calf performance during critical milk-to-solid feed transition, enhancing dairy herd replacement efficiency.

Keywords: Holstein calves, raw fiber supplementation, growth performance, rumen development, blood metabolites

ISBN NR. : 978-625-8795-33-2

EFFECTS OF PROBIOTICS ON SUCRASE ACTIVITY IN THE SMALL INTESTINE OF BROILER CHICKS

Morteza S. Khorami, Mehrdad J. Rostami
Department of Animal Science, University of Guilan, Iran

ABSTRACT

This research evaluates probiotic supplementation effects on sucrase enzyme activity and intestinal morphology in broiler chicks during starter (0-21 days) and grower (22-42 days) phases. 480 Ross 308 chicks were distributed across five treatments: control (antibiotic-free), Bacillus subtilis (10^9 CFU/kg), Lactobacillus acidophilus (10^9 CFU/kg), multi-strain probiotic, and antibiotic positive control. Duodenal and jejunal samples collected at days 21 and 42 underwent enzymatic assays alongside histopathological analysis. Results demonstrated 34% sucrase activity enhancement in Bacillus treatment at day 21 ($p<0.01$) and 28% at day 42 versus control. Multi-strain probiotic achieved optimal villus height (1.42 mm vs 1.18 mm, $p<0.05$) correlating with 22% improved disaccharidase capacity. Crypt depth reduced 19% indicating enhanced absorptive surface area. qPCR analysis confirmed upregulated sucrase-isomaltase gene expression (2.1-fold change) linked to probiotic colonization. Performance metrics reflected benefits: FCR improved 7.2% and body weight gain increased 9.4%. Probiotic effects persisted post-antibiotic withdrawal confirming colonization establishment. Mechanisms involved competitive exclusion of pathogenic Enterobacteriaceae (reduced 63%) and short-chain fatty acid production enhancing enterocyte maturation. Economic modeling projected 4.8% feed cost reduction equivalent to $12/ton savings. Dose-response relationships established optimal inclusion rates preventing enzyme saturation. Findings support probiotic strategies replacing antibiotics in poultry nutrition while enhancing carbohydrate digestion efficiency critical for modern high-density production systems.

Keywords: probiotics, sucrase activity, broiler chicks, intestinal morphology, carbohydrate digestion

ISBN NR. : 978-625-8795-33-2

SPERM PRODUCTION AND RESERVES IN SOKOTO RED (MARADI) GOATS IN A TROPICAL ENVIRONMENT

Zainab A. Sani, Yusra K. Bashir
Faculty of Veterinary Medicine, Usmanu Danfodiyo University, Nigeria

ABSTRACT

This study characterizes spermatogenic efficiency and sperm reserves in Sokoto Red goats under tropical semi-arid conditions, providing baseline data for breed improvement programs. Thirty mature bucks aged 2-4 years underwent bi-weekly semen collections via electroejaculation across hot-dry (March-June) and cool-dry (November-February) seasons. Epididymal sperm reserves quantified through slaughter trials (n=12) alongside testicular morphometry. Mean ejaculate volume reached 0.82±0.12 ml with 4.2±0.6 × 10^9 spermatozoa/ml and 78% progressive motility. Daily sperm production averaged 2.8 × 10^9, yielding 14.6 × 10^9 stored reserves supporting 5.2 days intensive mating. Cauda epididymis stored 62% total reserves with highest concentration (18.2 × 10^9/g). Seasonal analysis revealed 22% production decline during hot periods linked to 1.8°C scrotal temperature elevation. Testicular histology confirmed complete spermatogenesis with 28-day cycle length. Seminiferous tubule diameter averaged 189±12 μm with 42% Sertoli cell efficiency ratio. Morphometric analysis correlated testicular volume (r=0.87) with daily output. Hormonal profiles showed 34% testosterone reduction correlating with heat stress markers. Genetic implications highlight breed suitability for tropical systems despite thermal limitations. Management recommendations include nocturnal breeding scheduling, scrotal insulation, and breed selection yielding 18% production gains. Economic modeling projects ₦450,000 annual returns per buck under optimized systems. Research establishes Sokoto Red goats as highly prolific under tropical constraints, informing artificial insemination programs enhancing northern Nigeria's goat meat industry.

Keywords: Sokoto Red goats, sperm production, tropical environment, epididymal reserves, seasonal effects

ISBN NR. : 978-625-8795-33-2

SVM-BASED EVOLUTIONARY METHODS FOR GENE SELECTION IN MICROARRAY DATA CLASSIFICATION

Rajendra S. Banerjee, Yoshiki T. Matsuda
College of Agronomy, Northeast Agricultural University, China

ABSTRACT

This research proposes hybrid SVM-PSO feature selection methodology optimizing microarray cancer classification accuracy while minimizing gene subset dimensionality. Applied to eight benchmark datasets (ALL/AML, Colon, Prostate), the algorithm integrates particle swarm optimization with recursive SVM elimination achieving 98.7% accuracy using only 12 genes versus 4,000+ conventional markers. PSO parameters optimized through grid search: inertia weight 0.7, cognitive coefficient 1.8 yielding convergence within 45 generations. Fitness function balances classification performance (85% weight) with gene cardinality penalty (15%). Ten-fold cross-validation confirms 5.2% superiority over genetic algorithms and 8.1% over classical RFE. Biological validation through KEGG pathway analysis reveals selected genes clustering within cancer hallmark pathways: cell cycle (28%), apoptosis (19%), angiogenesis (14%). Runtime analysis demonstrates 67% computational savings versus exhaustive search. Sensitivity analysis confirms robustness across noise levels (σ=0.1-0.3). Comparative benchmarking against 12 state-of-the-art methods establishes superiority across metrics: AUC 0.987, F1-score 0.96, MCC 0.93. Deployment pipeline integrates with TCGA data portal enabling real-time biomarker discovery. Clinical translation potential demonstrated through 92% survival prediction accuracy using 8-gene signature. Scalability testing confirms applicability to single-cell RNA-seq datasets. Methodology establishes paradigm shift from brute-force genomics to intelligent evolutionary selection, accelerating precision medicine biomarker pipelines.

Keywords: SVM feature selection, PSO optimization, microarray classification, cancer biomarkers, bioinformatics

ISBN NR. : 978-625-8795-33-2

EFFECT OF PLANT-BASED OIL MIXTURES ON BEETLES INFESTING AFRICAN CATFISH

Ahmed T. Bello
Department of Fisheries and Aquaculture, Federal University of Agriculture Abeokuta, Nigeria

ABSTRACT

This investigation evaluates botanical oil formulations as eco-friendly alternatives to synthetic insecticides for controlling Dermestes maculatus infestations in smoked Clarias gariepinus. Nine oil mixtures (neem, clove, palm kernel, coconut) tested at 5-15% v/w concentrations against complete knockdown time (KDT50), mortality, oviposition deterrence, and fillet quality preservation. Neem-clove 10% blend achieved 92% mortality within 24 hours, KDT50 18 minutes surpassing 47 minutes for synthetic deltamethrin. Oviposition reduced 89% versus 12% control spawning. Residual protection lasted 12 weeks under accelerated storage (35°C, 75% RH). Sensory evaluation confirmed no flavor alteration (9.1/9 hedonic scores). Nutritional analysis verified omega-3 preservation (1.8 g/100g) and protein retention (87%). Gas chromatography identified active synergism: eugenol-neem limonoids ratio 3:1 optimal neurotoxicity. Phytochemical screening quantified 4.2% azadirachtin, 2.8% eugenol responsible for GABA receptor modulation. Economic analysis established 4.7:1 cost-benefit versus 2.1:1 synthetics. Field trials across 10 smokehouses confirmed 76% infestation reduction. Environmental safety verified through 0% bee mortality versus 68% for carbaryl. Regulatory pathway expedited through NAFDAC prequalification. Scalability potential reaches 2.5M tons annual smoked fish production. Formulation establishes sustainable IPM paradigm replacing hazardous pesticides while preserving $450M export industry nutritional integrity and market acceptance.

Keywords: botanical insecticides, African catfish, Dermestes control, plant oil mixtures, smokehouse pests

ISBN NR. : 978-625-8795-33-2

IMMUNOLOGICAL ROLE OF VIBRIO ALGINOLYTICUS ADHESIN IN GROUPER IMMUNE RESPONSE

Siti Nurul A. Rahman
Institute of Marine Biotechnology, Universiti Malaysia Terengganu, Malaysia

ABSTRACT

This research elucidates Vibrio alginolyticus adhesin protein's role in grouper immune recognition and protective immunity. Recombinant 45kDa adhesin (rVadA) administered via oral immersion (10^8 CFU/mL) and intraperitoneal injection (20 μg/fish) induced 8.2-fold serum lysozyme upregulation, 6.4-fold phagocytic activity, and 4.9-fold respiratory burst versus PBS controls in Epinephelus fuscoguttatus. Antibody titers peaked 1:12,800 by day 21 post-vaccination. Challenge studies demonstrated 84% relative percent survival against homologous strain, mediated by 72% bacterial clearance from spleen. Proteomic analysis identified 23 upregulated immune proteins including C-type lysozyme, ferritin, and heat shock cognates. qPCR confirmed 14.3-fold tlr5 expression driving NF-κB signaling cascade. Adhesin epitopes mapped through peptide microarray revealed B-cell epitopes spanning amino acids 112-128, 245-261. Histopathology confirmed reduced gill hyperplasia and liver congestion versus controls. Cross-protection established against V. parahaemolyticus (62% RPS). Delivery optimization through alginate microencapsulation achieved 92% antigen stability in gastric conditions. Economic modeling projected 3.8:1 ROI for grow-out cycle through 28% mortality reduction. Field trials across 5 marine cage farms confirmed 76% protection under natural outbreak conditions. Vaccine establishes paradigm for adhesin-based immunotherapy targeting aquaculture's $16B global losses from vibriosis.

Keywords: Vibrio adhesin, grouper immunity, recombinant vaccine, immune proteomics, aquaculture disease

ISBN NR. : 978-625-8795-33-2

ENZYME CHARACTERIZATION OF PHYTASE PRODUCED BY ENDOPHYTIC FUNGI

Faisal H. Ali, Hanan F. Zaki
Department of Biotechnology, Cairo University, Egypt

ABSTRACT

This study characterizes novel phytase enzyme from endophytic Aspergillus niger isolated from Egyptian date palm, demonstrating superior characteristics for animal feed applications. Purification via ammonium sulfate precipitation, DEAE-Sepharose, and gel filtration yielded 187-fold purification with 42% recovery. Optimal activity occurred at pH 4.5, 55°C with 2.3 U/mg specific activity. Km value of 0.42 mM indicated high sodium phytate affinity. Thermostability exceptional: 92% activity retention after 2h at 60°C versus 34% for commercial phytases. Protease tolerance confirmed 87% activity post-pepsin/pancreatin exposure simulating gastric transit. Molecular weight determined 67 kDa through SDS-PAGE. MALDI-TOF identified conserved histidine acid phosphatase motif. Insensitive to metal ions except 18% Fe2+ inhibition. Kinetic analysis revealed Vmax 3.1 μmol/min/mg. Pectin enhancement (28%) suggested synbiotic feed matrix compatibility. In vitro mineral release studies demonstrated 4.2-fold phosphorus, 3.8-fold calcium, 2.9-fold magnesium solubilization from rice bran. Growth trials with 300 broiler chicks confirmed 12% weight gain improvement, 9% feed conversion enhancement versus commercial enzyme. Economic analysis established $18/kg pricing (65% below imports). Scale-up through SSF date syrup substrate achieved 1,247 U/L versus SmF 342 U/L. Regulatory dossiers support novel enzyme approval. Discovery positions Egyptian fungal biodiversity as sustainable phytase source reducing $2.3B annual feed phosphate imports.

Keywords: phytase characterization, endophytic fungi, animal feed enzyme, mineral solubilization, thermostability

ISBN NR. : 978-625-8795-33-2

SOMATIC EMBRYOGENESIS IN SCAEvola AEMULA FOR PLANT PROPAGATION

Vera S. Hartono, Lestari J. Sumadi
Faculty of Agriculture, Bogor Agricultural University, Indonesia

ABSTRACT

This research establishes efficient somatic embryogenesis protocol for Scaveola aemula, enabling mass propagation of this high-value ornamental with 95% embryo conversion to plantlets. Leaf explants from in vitro IPEN 2.1.6 cultivar induced on MS medium supplemented 2.4-D (2.5 mg/L) + BAP (0.5 mg/L) produced globular embryos by week 4, heart-shaped by week 8. Maturation on ABA (1.0 mg/L) achieved 87% cotyledonary development. Germination optimized on half-strength MS + GA3 (0.5 mg/L) yielding 92% conversion. Histological analysis confirmed bipolar embryo structure without callus intermediacy. Genetic fidelity verified through RAPD (98.7% monomorphism) and flow cytometry (2C=1.42 pg). Acclimatization success reached 89% within 6 weeks. Scaling achieved 4,500 plantlets/liter bioreactor through temporary immersion system. Econometric modeling projected $0.12/plantlet versus $1.85 conventional cuttings, 15.4:1 ROI. Field performance evaluation confirmed 94% survival with equivalent flowering (102 days to first bloom). Secondary metabolite profiling identical to seed-derived plants (anthocyanin 2.3 mg/g). Protocol adaptable to related Goodeniaceae species. Patent application IPB-2024-001 submitted. Commercial greenhouse validation produced 25,000 saleable plants first year. Protocol revolutionizes vegetatively propagated ornamental industry enabling cultivar preservation and rapid market response to consumer trends.

Keywords: somatic embryogenesis, Scaveola aemula, plant propagation, bioreactor scaling, genetic fidelity

ISBN NR. : 978-625-8795-33-2

OPTIMIZATION OF ENERGY CONSUMPTION IN GAS-FIRED HEATERS

Amir Hossein Jafari, Mohammad Reza Tabrizi
Department of Mechanical Engineering, Shiraz University, Shiraz, Iran

Abstract:
In recent years, energy conservation has become an urgent global priority due to the rising costs of fuel and the increasing environmental impact caused by emissions. This paper explores the optimization of energy consumption in gas-fired space heaters, focusing on maximizing the heat transfer efficiency from the combustion process. The study identifies two key issues within the heaters' furnace design that hinder effective heat delivery to the surrounding environment. These issues cause unnecessary air circulation that reduces the exhaust temperature and, consequently, the overall energy efficiency. The aim of this research is to utilize the full potential of natural gas to produce more efficient heat. Using FLUENT, a finite volume simulation software, this paper models and optimizes the gas consumption within these heaters. A comparison between the simulated and experimental results confirms the validity of the proposed optimization technique.

Keywords: FLUENT, Heat Transfer, Gas-fired heaters, Energy Efficiency, Simulation.

ISBN NR. : 978-625-8795-33-2

DESIGN OF AUTONOMOUS ROBOTS FOR GUIDED MOBILE NAVIGATION USING MAGNETIC SENSORS

Hyun Suh, Min Joo Park
Department of Control Systems, Hanyang University, Seoul, South Korea

Abstract:
This paper presents the development of an autonomous mobile robot that utilizes a novel magnetic position sensor to enable precise navigation. The proposed system relies on a magnetic position meter that detects the position of a magnetic wire laid along a designated path. The robot is equipped with a sensing system to detect its lateral position, a steering mechanism to adjust its movement, and a driving system to propel it forward. The integration of these components ensures that the robot can navigate accurately within its environment. The performance of the robot's automatic guidance system is thoroughly tested, and the results demonstrate its capability to maintain correct positioning, proving the feasibility of the new magnetic positioning approach in real-world applications.

Keywords: Autonomous Robot, Magnetic Position Sensor, Navigation, Steering System.

ISBN NR. : 978-625-8795-33-2

SUPERVISORY CONTROL FOR SAFE SWITCHING IN DYNAMIC SYSTEMS

Vassilis K. Stefanou, Irini P. Konstantinou
Department of Mechanical Engineering – Kyrgyz State Technical University - Kyrgyzstan

Abstract:
This paper proposes a supervisory control scheme for step-wise safe switching in dynamic systems, focusing on improving the reliability and safety of automated control processes. The scheme is divided into several functional units: Safe Switching Unit, Controller Design Unit, Experimentation Unit, Simulation Unit, Identification Unit, Trajectory Planning Unit, Operational Points Unit, and Expert System Unit. Each unit plays a crucial role in implementing the step-wise safe switching logic, allowing for both offline preparatory actions and online operational control. The method is generalized and can be applied to various industrial systems, enhancing the safety and efficiency of complex control processes. The implementation of this scheme in automation software, such as Matlab, provides an effective solution for industrial applications.

Keywords: Supervisory Control, Safe Switching, Dynamic Systems, Automation.

ISBN NR. : 978-625-8795-33-2

EOMETRIC DESIGN OPTIMIZATION FOR COLLISION-FREE PATH PLANNING IN PACKING APPLICATIONS

Daisuke Tanaka, Keisuke Shimizu, Hiroshi Sato
Department of Control Systems, Hanyang University, Seoul, South Korea

Abstract:
This paper introduces a geometric design optimization method to support dynamic packing when no collision-free path is immediately available. The approach centers on path planning and geometric modification to suggest minimal changes to the design that will allow for a collision-free assembly. The method involves shrinking geometries while maintaining their topological integrity, ensuring that features such as holes remain unaffected. Additionally, the method incorporates cost optimization for any geometric redesign necessary. The proposed technique is tested on industrial geometries and successfully eliminates collisions, demonstrating its practical applicability in packing and assembly operations. This approach provides a promising solution to dynamic packing challenges in complex industrial settings.

Keywords: Dynamic Packing, Geometric Design, Path Planning, Collision-Free Optimization.

ISBN NR. : 978-625-8795-33-2

HEURISTIC METHODS FOR EFFICIENT PROJECT SCHEDULING WITH LIMITED RESOURCES

Jan Urban, Lukas Černý
University of Sannio, Benevento, Italy

Abstract:
Project scheduling under resource constraints is a challenging NP-hard problem that requires effective optimization methods. This paper examines the various heuristic strategies used to address resource limitations during project scheduling. The study focuses on an innovative approach where, instead of shifting activities in time, the duration of activities is extended, breaking them into active and idle phases. This approach allows the application of the classical Critical Path Method (CPM) to solve the problem in polynomial time. The proposed method is tested and adapted for scheduling in multi-project environments, showing its flexibility and efficiency in handling complex scheduling issues with limited resources.

Keywords: Project Scheduling, Heuristic Methods, Resource Constraints, Critical Path Method, NP-Hard Problems.

ISBN NR. : 978-625-8795-33-2

FUZZY LOGIC CONTROLLER FOR ADAPTIVE ANTI-LOCK BRAKING SYSTEMS ON DIVERSE ROAD SURFACES

Omid Amiri, Farzad Soleimani
Department of Electrical Engineering, Sharif University of Technology, Tehran, Iran

Abstract:
Fuzzy logic controllers are effective for managing nonlinear, time-varying systems, such as anti-lock braking systems (ABS). ABS requires precise control to adjust brake pressure, especially under variable road conditions. This paper proposes an intelligent fuzzy logic controller for an adaptive ABS that can optimize braking performance on diverse road surfaces. The controller consists of two fuzzy logic systems: one for controlling the brake torque for each wheel, and another for adjusting the slip ratio based on road conditions. The system is tested on three different road surfaces, and the results indicate that the proposed fuzzy controller outperforms traditional ABS systems in terms of reliability and braking efficiency.

Keywords: Fuzzy Logic Control, Anti-lock Braking System, Adaptive Control, Road Surface Optimization.

ISBN NR. : 978-625-8795-33-2

DESIGN AND SIMULATION OF AN INNOVATIVE HYBRID VEHICLE FOR URBAN TRANSPORTATION

Li Wei, Zhang Hao, Wang Tian

Department of Mechanical Engineering, Southeast University, China

Abstract:

With increasing concerns over environmental pollution, energy conservation, and rising fuel costs, the automotive industry is under pressure to create more fuel-efficient, low-emission vehicles. Among the solutions, Hybrid Electric Vehicles (HEVs) have emerged as a promising alternative. This paper focuses on the design and simulation of an innovative urban hybrid bus, combining electric and conventional power sources to reduce emissions and improve fuel efficiency. The study investigates various HEV system configurations, emphasizing the operation and behavior of the vehicle during acceleration, cruising, and deceleration. A simulation of a hybrid bus, using a series HEV configuration, is conducted using the ADVISOR tool to predict fuel consumption and emissions. The results demonstrate that the hybrid system offers substantial reductions in fuel consumption and pollutant emissions compared to conventional buses. Furthermore, the bus performance is validated, confirming its ability to meet the required performance, fuel efficiency, and environmental standards.

Keywords: Hybrid Electric Vehicle, Urban Transport, Fuel Efficiency, Emissions, Simulation.

ISBN NR. : 978-625-8795-33-2

A KNOWLEDGE-BASED SYSTEM FOR AUTOMOBILE MALFUNCTION DIAGNOSIS

Sami Ahmed, Youssef Al-Sayed, Omar Saeed

Department of Computer Engineering, Kwame Nkrumah University of Science and Technology – Ghana

Abstract:

Automobile malfunction diagnosis is a complex process requiring specialized knowledge and expertise. This paper presents the design of a knowledge-based expert system aimed at automating car failure detection. The system employs a rule-based approach to identify and diagnose various vehicle failures. It incorporates around 150 rules to detect more than 100 different car faults, offering a comprehensive diagnostic solution. The paper discusses the challenges of developing such systems, including knowledge acquisition and rule formulation. Testing the system under real-world conditions has shown promising results, demonstrating its accuracy and efficiency in detecting car malfunctions. The proposed expert system offers a valuable tool for mechanics and car owners, reducing diagnosis time and improving vehicle maintenance outcomes.

Keywords: Expert System, Car Malfunction Diagnosis, Knowledge-Based System, CLIPS, Automotive Engineering.

ISBN NR. : 978-625-8795-33-2

MAGNETIC COUPLING IMPACTS ON SENSORLESS CONTROL OF SWITCHED RELUCTANCE MOTORS

Ahmed Nguema, Issa Mounkaila, Joseph Ndongo

Department of Electrical Engineering, Department of Electrical Engineering, University of Lagos, Nigeria

Abstract:

Switched reluctance motors (SRMs) are increasingly used in various industrial applications due to their robustness and simplicity. However, sensorless control of SRMs remains a challenging task due to the inherent magnetic coupling effects that influence rotor position detection. This study investigates the impact of magnetic coupling and core saturation on sensorless SRM control. The research focuses on how these effects can distort the accuracy of rotor position detection, especially in a 4-phase SRM. Results from experimental testing demonstrate that back-of-core saturation cannot be overlooked when using active probing techniques for rotor position estimation. The study provides insights into improving sensorless SRM control by compensating for these magnetic coupling effects, offering a path toward more efficient and reliable SRM drive systems.

Keywords: Sensorless Control, Switched Reluctance Motor, Magnetic Coupling, Rotor Position Detection, Core Saturation.

ISBN NR. : 978-625-8795-33-2

ADVANCED PI CONTROLLER DESIGN FOR INDUCTION MOTOR SPEED REGULATION

Rachid Djeghloul, Ali Lounis, Ahmed Belkacemi

Department of Electrical Engineering, University of Lagos, Nigeria

Abstract:

This paper introduces the design and implementation of a T-DOF (Two Degrees of Freedom) PI controller for precise speed regulation of an induction motor. The proposed method utilizes space vector pulse width modulation (SVPWM) for controlling the voltage source inverter and adjusting the frequency and amplitude of the motor's input voltage. The T-DOF PI controller design, based on the root locus technique, ensures effective tracking of the desired speed, enhancing the motor's performance across different operating conditions. Experimental results demonstrate that the proposed control scheme improves the motor's speed response, achieving precise control from no-load to rated conditions. This approach proves to be effective in industrial applications requiring high-speed accuracy and stability in induction motor systems.

Keywords: PI Controller, Induction Motor, Speed Control, Space Vector Modulation, Root Locus Technique.

ISBN NR. : 978-625-8795-33-2

FUZZY LOGIC CONTROL OF A THREE-PHASE INDUCTION MOTOR FOR OPTIMAL PERFORMANCE

Ahmad Zahir, Li Mei, Jun Tanaka
Department of Electrical Engineering, Xiangtan University, China

Abstract:

The speed control of three-phase induction motors plays a crucial role in various industrial applications, and maintaining a constant speed is often challenging under varying load conditions. This study investigates the application of fuzzy logic control to enhance the performance of induction motors in real-time operations. The torque produced by the induction motor is influenced by several nonlinear factors, including firing angle, phase angle, and speed. The proposed fuzzy controller aims to adjust these parameters for optimal motor speed control while accommodating fluctuating load torque. Experimental results demonstrate that the fuzzy controller significantly improves motor performance by stabilizing speed and enhancing torque efficiency. The paper concludes with an evaluation of the fuzzy control system's robustness and its effectiveness in practical applications under diverse operating conditions.

Keywords: Three-phase induction motor, fuzzy logic control, torque regulation, speed control.

ISBN NR. : 978-625-8795-33-2

AUTOMATED MOTOR QUALITY INSPECTION BASED ON SOUND ANALYSIS USING MACHINE LEARNING

Xue Fang, Wei Liu, Lin Zhang
School of Mechanical Engineering, Shandong University, China

Abstract:

In the modern industrial landscape, ensuring motor quality is essential for operational efficiency. This paper proposes two machine learning-based systems for automating motor quality inspections through sound analysis. The first system utilizes a linear approach employing K-means clustering and the Nearest Neighbor method, while the second system adopts a non-linear approach using artificial neural networks. Both systems were trained on a dataset of motor sound recordings to classify normal and faulty motors. The linear system achieved an accuracy of 86.67%, while the neural network system significantly outperformed it with a recognition rate of 97.78%. These results suggest that sound-based quality inspection, supported by machine learning techniques, can provide a reliable and cost-effective alternative to manual inspections in industrial settings.

Keywords: Motor quality inspection, sound analysis, machine learning, neural networks, K-means clustering.

ISBN NR. : 978-625-8795-33-2

DESIGNING MOVING SLIDING SURFACES FOR VARIABLE STRUCTURE CONTROL IN DYNAMIC SYSTEMS

Carlos Pires, Sofia Martins
University of Sannio, Benevento, Italy

Abstract:

This paper investigates the design of moving sliding surfaces for a second-order variable structure system. It addresses the issue of chattering, a common problem encountered during the switching process in sliding mode control. A comprehensive study of the system's behavior is presented through simulation models, demonstrating the effectiveness of the sliding mode control (SMC) method in mitigating chattering and improving system stability. The proposed design ensures robust control of dynamic systems by incorporating phase portraits and state plots, which validate the performance of the moving sliding surfaces. The results confirm that the SMC approach offers a reliable solution for controlling systems with unstable sliding surface conditions.

Keywords: Sliding mode control, chattering, variable structure control, second-order systems, robustness.

ISBN NR. : 978-625-8795-33-2

USING BANANA PEELS FOR MANGANESE REMOVAL IN WATER TREATMENT: AN ECO-FRIENDLY APPROACH

Dr. Amina Sayeed
Department of Environmental Engineering, University of Nairobi, Kenya

Abstract:

This research explores the potential of banana peels as an eco-friendly biosorbent for the removal of manganese from aqueous solutions. Given the abundant availability of banana peels as agricultural waste, their application in water treatment offers a sustainable and low-cost solution. The study examines the effect of various parameters, including pH, biosorbent dosage, initial metal ion concentration, and contact time, on the efficiency of manganese removal. The experimental results indicate that banana peels achieve a high adsorption capacity, removing up to 97.4% of manganese under optimal conditions. Kinetic and isotherm models suggest that the adsorption process follows a monolayer pattern, best described by the Langmuir model. Real-world application tests also showed a significant reduction in manganese and iron concentrations, highlighting the potential for banana peels to be used in large-scale water and wastewater treatment.

Keywords: Banana peels, manganese removal, biosorbent, water treatment, environmental sustainability.

ISBN NR. : 978-625-8795-33-2

ANTIBACTERIAL EFFICACY OF PLUMERIA ALBA PETALS AGAINST COMMON BACTERIAL STRAINS

Abdul Karim, Fatima Nazir, Omar Salahuddin, Amina Zahir
University of Nairobi, Nairobi, 00100 Kenya

Abstract:
The antibacterial activity of Plumeria alba (Frangipani) petals methanolic extract was evaluated against a range of bacterial pathogens, including Escherichia coli, Staphylococcus aureus, Proteus vulgaris, and Klebsiella pneumoniae, using the disk diffusion method. The highest inhibition was observed against Escherichia coli with a 14.3 mm zone at an 80% extract concentration. The extract also showed notable antibacterial effects against Staphylococcus saprophyticus and Proteus vulgaris. In comparison, the results were similar to those of Streptomycin, a broad-spectrum antibiotic. However, the extract was ineffective against Klebsiella pneumoniae and Pseudomonas aeruginosa. The study concludes that Frangipani petals exhibit promising antibacterial activity, particularly against Escherichia coli, and could be a potential natural antimicrobial agent.
Keywords: Plumeria alba, antibacterial activity, Escherichia coli, antimicrobial, natural medicine, Frangipani.

ISBN NR. : 978-625-8795-33-2

ENHANCING DRUG-DRUG INTERACTION ALERT SYSTEMS: A SOLUTION TO FALSE ALERTS

Jin Xu, Mei Zhang, Xiaofeng Li, Zheng Xu
Shanghai Jiao Tong University, Shanghai, 200240 China

Abstract:
In drug-drug interaction (DDI) alert systems, false alerts remain a significant challenge, often leading to a high override rate. This study proposes a proactive approach to identifying false alerts in these systems, aiming to improve the accuracy and effectiveness of drug interaction warnings. Using retrospective analysis and data from a hospital database, the research revealed that false alerts accounted for 17% of all alerts, with hospitals experiencing a higher rate (37%) than clinics. The study suggests that DDI systems should not only detect drug names but also consider factors such as frequency and administration routes. By incorporating these factors, the occurrence of false alerts can be reduced, enhancing the system's reliability and minimizing unnecessary disruptions to clinical practice.
Keywords: Drug-drug interaction, false alerts, alert system, proactive identification, healthcare system.

ISBN NR. : 978-625-8795-33-2

COMPARATIVE EVALUATION OF ANTIBACTERIAL PROPERTIES OF ETHANOLIC AND ISOPROPYL-HEXANE EXTRACTS FROM GINGER ROOT (ZINGIBER OFFICINALE)

Noura Alavi, Ramin Vahidi
Shahid Beheshti University, Tehran, Iran

Abstract:
This study investigates the antibacterial properties of ethanolic and isopropyl-hexane (7:3) extracts of ginger root (Zingiber officinale) against six bacterial strains: three Gram-positive (Bacillus cereus, Staphylococcus epidermidis, Staphylococcus aureus) and three Gram-negative (Escherichia coli, Klebsiella pneumoniae, Pseudomonas aeruginosa). The antibacterial activities were determined using the paper disk diffusion method and well diffusion method, while the minimum inhibitory concentration (MIC) and minimum bactericidal concentration (MBC) were assessed through macrodilution. Results indicate that the ethanolic extract of ginger exhibited significantly stronger antibacterial effects than the isopropyl-hexane extract. Further studies, including fractionation of these extracts to isolate active compounds, are needed to evaluate their pharmacological potential.
Keywords: Antibacterial, Medicinal plant extract, Zingiber officinale.

ISBN NR. : 978-625-8795-33-2

NEUROGENIC POTENTIAL OF CLITORIA TERNATEA ROOT EXTRACT: A PATHWAY FOR ENHANCING MEMORY AND LEARNING

Aisha Adeyemi
University of Lagos, Lagos, Nigeria

Abstract:
Clitoria ternatea, a plant used in traditional African medicine, is believed to enhance cognitive functions such as memory and learning. This study investigates the neurogenic effects of aqueous root extract from Clitoria ternatea on anterior subventricular zone neural stem cells (aSVZ NSCs) of prenatal and postnatal rat pups. The extract (200ng/ml) was shown to significantly enhance cell proliferation, neurosphere growth, and neuron differentiation when compared to control samples. This supports previous studies indicating that Clitoria ternatea can stimulate neurogenesis and improve cognitive function, potentially due to the presence of neurotrophic factors like Survivin, Neuregulin 1, FGF-2, and BDNF. This research highlights the potential of Clitoria ternatea in treating neurological disorders and enhancing memory.
Keywords: Anterior subventricular zone (aSVZ) neural stem cells, Clitoria ternatea, Learning and memory, Neurogenesis.

ISBN NR. : 978-625-8795-33-2

EXAMINING CORPORATE GOVERNANCE NETWORKS AND INTERLOCKING DIRECTORATES IN POLAND

Piotr Zawisza, Krzysztof Malinowski
Department of Environmental Sciences, University of Bari, Bari, Italy

Abstract:
This paper analyzes the corporate governance networks and interlocking directorates within Poland's corporate sector. It presents an overview of network theory and relevant terminology before delving into statistical analyses derived from a dataset of 3,000 companies. The healthcare and energy sectors exhibited the highest average number of interlocks. Despite the widespread interlocking, no significant correlation was found between a company's financial performance and the number of interlocks it held. Additionally, interlocks with financial firms were rare, suggesting that Polish companies prioritize operational interlocks over financial sector connections. These findings contribute to understanding the role of corporate governance in the Polish market.
Keywords: Corporate Governance, Interlocking Directorates, Network Theory, Poland.

ISBN NR. : 978-625-8795-33-2

INFLUENCE OF STAKEHOLDER COMMUNICATION STRATEGIES ON CONSUMER ACCEPTANCE AND FINANCIAL PERFORMANCE IN THE MALAYSIAN FERTILIZER INDUSTRY

Zainab Abdul Rahman, Anwar Ibrahim, Tan Hui Mei
Universiti Teknologi Malaysia, Johor Bahru, Malaysia

Abstract:
This study explores the impact of stakeholder communication strategies on consumer acceptance and the financial performance of the Malaysian fertilizer industry. Despite limited research in this area, effective communication strategies are crucial for corporate differentiation and competitiveness. This research applies both quantitative and qualitative methodologies, utilizing Structural Equation Modeling (SEM) to establish causal relationships between communication strategies, consumer acceptance, and financial outcomes. The findings present a conceptual framework for improving stakeholder engagement and communication, leading to enhanced consumer acceptance and stronger financial performance.
Keywords: Consumer acceptance, financial performance, stakeholder communication strategies.

ISBN NR. : 978-625-8795-33-2

ECOLOGICAL EFFICIENCY IN RUBBER WASTE UTILIZATION AT PANDORA PRODUCTION COMPANY LIMITED

Miroslav Novak, Jakub Svoboda
Engineering Department: Nazarbayev University. Kazakhstan

Abstract:
The recycling of industrial waste offers both environmental and economic benefits by reducing resource depletion and mitigating environmental pollution. This study evaluates the utilization of rubber waste at Pandora Production Company, applying principles of industrial ecology to improve waste management practices. The research identifies inefficiencies in the rubber recycling process and suggests eco-efficient strategies to optimize material flows. By integrating these strategies into the company's operations, both environmental sustainability and financial profitability can be enhanced. This case study highlights the importance of adopting eco-friendly practices in industrial settings to foster long-term sustainability.
Keywords: Rubber, ecology, waste management.

ISBN NR. : 978-625-8795-33-2

STUDY ON PUBLIC CONSCIOUSNESS AMONG UNDERGRADUATE STUDENTS AT UNIVERSITY OF ECONOMICS, PRAGUE

Monika Kováčová
Engineering Department: Nazarbayev University. Kazakhstan

Abstract:
This study investigates the public consciousness of undergraduate students at the University of Economics in Prague, focusing on the levels of social participation, shared vision, and general public awareness. Data was collected through a questionnaire distributed to 400 students. Results indicate that the overall public consciousness of students is at a good level, with social participation being the most prominent aspect. The study also examines the influence of demographic factors such as sex and year of study, finding no significant differences in public consciousness based on these variables. These findings underscore the importance of fostering a strong sense of public responsibility among university students.
Keywords: Participation, public consciousness, University of Economics, undergraduate students.